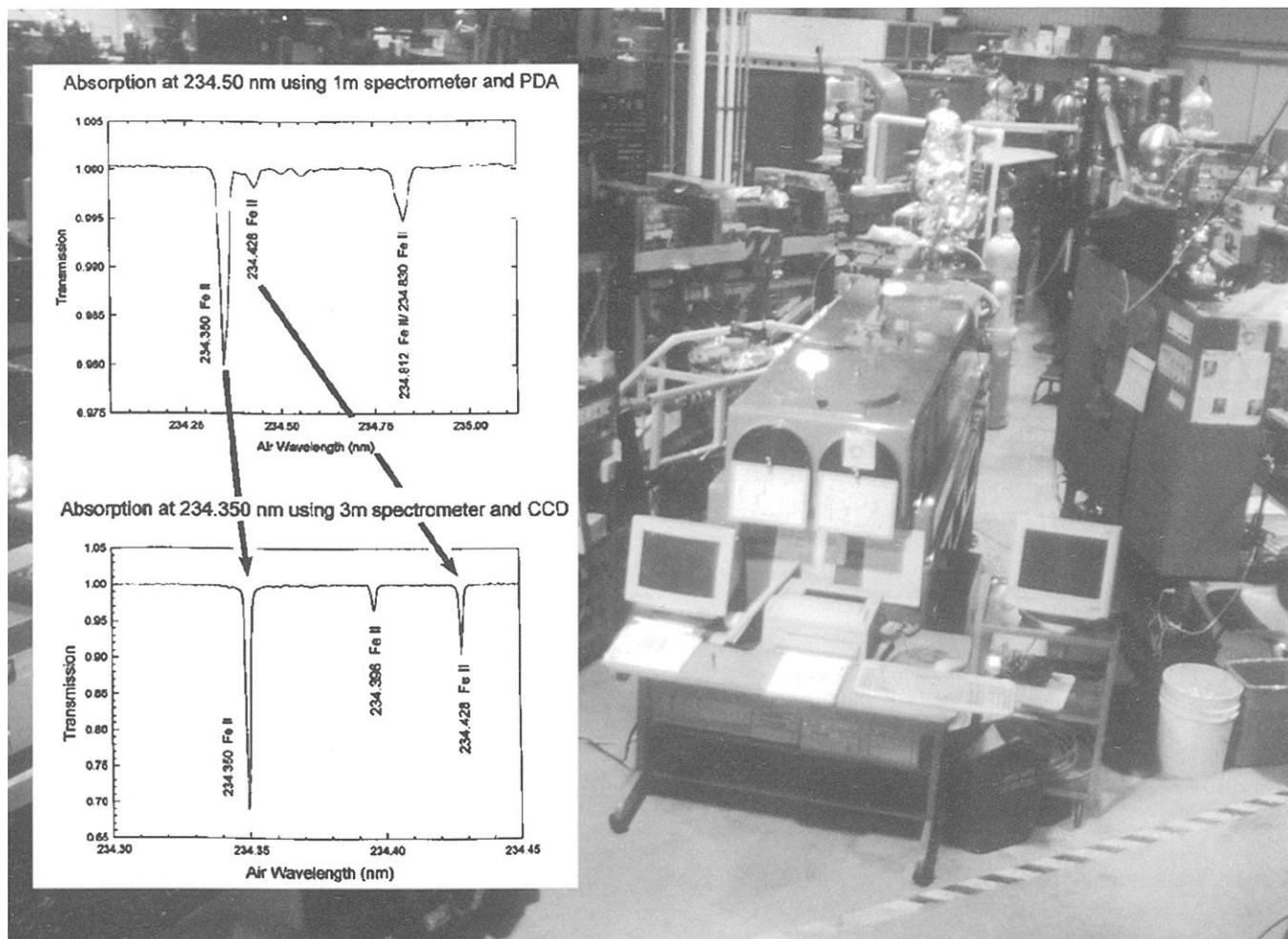


# BULLETIN

OF THE AMERICAN PHYSICAL SOCIETY



**Program of the 50<sup>th</sup> Annual  
Gaseous Electronics Conference**

**October 6–9, 1997  
Madison, Wisconsin**

**October 1997  
Volume 42, No. 8**

# BULLETIN

OF THE AMERICAN PHYSICAL SOCIETY

Coden BAPSA6  
Series II, Vol. 42, No. 8

ISSN: 0003-0503  
October 1997

## APS COUNCIL 1997

### President

D. Allan Bromley, *Yale University*

### President-Elect

Andrew M. Sessler, *Lawrence Berkeley Laboratory*

### Vice-President

Jerome Friedman, *Massachusetts Institute of Technology*

### Executive Officer

Judy R. Franz, *University of Alabama, Huntsville*

### Treasurer

Thomas McIlrath, *University of Maryland*

### Editor-in-Chief

Martin Blume, *Brookhaven National Laboratory*

### Past-President

Robert Schrieffer, *Florida State University*

### General Councillors

Daniel Auerbach, Kevin Aylesworth, Virginia R. Brown, Jennifer Cohen, Charles Duke, Elsa Garmire, S. James Gates, Donald Hamann, William Happer, Anthony M. Johnson, Zachary Levine, Paul Peercy, Susan Seestrom, Virginia Trimble, Ronald Walsworth, Sau Lan Wu

### Chair, Nominating Committee

Gerald Crawley

### Chair, Panel on Public Affairs

Robert M. White

### Division and Forum Councillors

Frank C. Jones (*Astrophysics*), Eric Heller, Gordon Dunn (*Atomic, Molecular, and Optical*), Robert Callender (*Biological*), Stephen Leone (*Chemical*), Joe D. Thompson, David Aspnes, Lu J. Sham, Zachary Fisk (*Condensed Matter*), Warren Pickett (*Computational*), Guenter Ahlers (*Fluid Dynamics*), James Wynne (*Forum on Education*), Albert Wattenberg (*Forum on History of Physics*), Ernest Henley (*Forum on International Physics*), Dietrich Schroerer (*Forum on Physics and Society*), Andrew Lovinger (*High Polymer*), Matt Richter (*Forum on Industrial and Applied Physics*), Daniel Grischkowsky (*Laser Science*), Howard Birnbaum (*Materials*), John Schiffer, Peter Paul (*Nuclear*), Henry Frisch, George Trilling (*Particles and Fields*), Hermann Grunder (*Physics of Beams*), Roy Gould, William Krueer (*Plasma*)

## COUNCIL ADVISORS

### Sectional Representatives

John Pribram, *New England*; Peter Lesser, *New York*; Perry P. Yaney, *Ohio*; Joseph Hamilton, *Southeastern*; Stephen Baker, *Texas*

### Representatives from Other Societies

Ronald Edge, *AAPT*; Marc Brodsky, *AIP*

## Editor: Barrett H. Ripin

Meeting Publications Coordinator: Danita Boonchaisri

### APS MEETINGS DEPARTMENT

#### One Physics Ellipse

College Park, MD 20740-3844

Telephone: (301) 209-3200

FAX: (301) 209-0866

Donna Baudrau, *Meetings Manager*

Tammany Buckwalter, *Assistant Meetings Manager*

Adrienne Vincent, *Publications Specialist*

Desiree Atherly, *Assistant to the Meetings Manager*

Don Wise, *Registrar*

### Staff Representatives

Barrett Ripin, *Associate Executive Officer*; Irving Lerch, *Director of International Affairs*; Robert L. Park, *Director, Public Information*; Michael Lubell, *Director, Public Affairs*; Stanley Brown, *Administrative Editor*; Reid Terwilliger, *Director of Editorial Office Services*; Michael Stephens, *Controller and Assistant Treasurer*

The *Bulletin of The American Physical Society* is published 12X in 1997, March, April, May, June, July, August, October (2X), November (3X), and December, by The American Physical Society, through the American Institute of Physics. It contains advance information about meetings of the Society, including abstracts of papers to be presented, as well as transactions of past meetings. Reprints of papers can be obtained only by writing directly to the authors.

The *Bulletin* is delivered, on subscription, by Periodicals mail. Complete volumes are also available on microfilm.

**APS Members** may subscribe to individual issues, or for the entire year. **Nonmembers** may subscribe to the *Bulletin* at the following rates: Domestic \$410; Foreign Surface \$430; Air Freight \$455. Information on prices, as well as subscription orders, renewals, and address changes, should be addressed as follows: **For APS Members**—Membership Department, The American Physical Society, One Physics Ellipse, College Park, MD 20740-3844. **For Nonmembers**—Circulation and Fulfillment Division, The American Institute of Physics, 500 Sunnyside Blvd., Woodbury, NY 11797. Allow at least 6 weeks advance notice. For address changes, please send both the old and new addresses, and, if possible, include a mailing label from a recent issue. Requests from subscribers for missing issues will be honored without charge only if received within 6 months of the issue's actual date of publication.

Periodicals postage paid at Woodbury, NY 11797, and additional mailing offices. Postmaster: Send address changes to *Bulletin of The American Physical Society*, Membership Department, The American Physical Society, One Physics Ellipse, College Park, MD 20740-3844

**On The Cover:** Plasma Spectroscopy using Synchrotron Radiation.



# BULLETIN

OF THE AMERICAN PHYSICAL SOCIETY

Vol. 42, No. 8, October 1997

## TABLE OF CONTENTS

### 50<sup>th</sup> Annual Gaseous Electronics Conference

General Information .....	iii
GEC History Exhibit .....	iii
GEC Student Award for Excellence .....	iii
Conference Headquarters/Registration .....	iv
Presentations .....	iv
Posters .....	iv
Vendor Exhibits .....	iv
Travel Information .....	iv
Hotels .....	iv
Dining Options .....	iv
Banquet .....	v
GEC Executive Committee .....	v
Please Note .....	v
Civilian Time to Military Time Conversion .....	v
University and Downtown Area Map .....	vi
Memorial Union Meeting Facilities Floor Plan .....	vii
Epitome .....	viii
Main Text .....	1699
<i>Monday</i> .....	1699
<i>Tuesday</i> .....	1721
<i>Wednesday</i> .....	1738
<i>Thursday</i> .....	1762

**Author Index** ..... 1773

**Condensed Epitome** ..... **Back Covers**

---

---

# 50th Annual Gaseous Electronics Conference October 6–9, 1997; Madison, Wisconsin

---

---

## GENERAL INFORMATION

Welcome to the 50th Annual Gaseous Electronics Conference (GEC), a topical conference of the American Physical Society. The GEC'97 program includes a special plenary session to recognize the 50th Anniversary of the founding of the GEC, a "Foundation Talk", the initiation of a new student award, and a number of sessions of both contributed and invited papers.

The plenary session will include presentations by:

**John F. Waymouth** - *Forty Years of Overlap: Electric Discharge Light Source R&D and the GEC.*

**Alexander Dalgarno** - *Electron Collisions in Astrophysical Plasmas.*

**Gerry Hays** - *Gas-Phase Lasers - a Historical Perspective in Relation to the GEC.*

**Art Phelps** - *Comments on the Kinetics of Swarms and Discharges from Models of Experiments.*

The Foundation Talk, a new feature this year, is the presentation of a review paper aimed at educating students and individuals working outside the immediate field. The Talk, presented by Alan Gallagher, entitled, *Gas Phase Processes in Low-pressure Silicon Deposition Plasmas*, will take a dispassionate and broad view of the on-going work on this subject.

Other topics to be addressed include:

- Electron-Atom Collisions
- Electron-Molecule Collisions
- Electron and Positron Scattering
- Heavy Particle Collisions
- Environmental Applications
- Light Sources
- Future Processing Trends
- Surface Processes
- Inductively Coupled Plasmas
- Propulsion and Space Plasmas
- Plasma Display Panels

- Cold Collisions and Recombination
- Diagnostics
- Modeling
- Helicon and Surface Wave Plasmas

In addition to the scientific program, there will be a Town Hall Meeting on Monday night, October 6, at 7:30 p.m., to discuss the future organization of the GEC, including the possibility of forming a Topical Group on Gaseous Electronics within the American Physical Society. A number of options exist that will be presented at the meeting. Further input from the conference attendees will be solicited at the business meeting to be held at noon on Tuesday, October 7.

## GEC HISTORY EXHIBIT

In recognition of the 50th anniversary of the GEC, there will be an historical exhibit on the achievements of Irving Langmuir. It was Langmuir who first coined the word "plasma" to describe the bulk region of certain laboratory discharges. He more-or-less started the science of surface reaction processes and catalysis work which was recognized with a Nobel prize in 1932. Langmuir's efforts led him to significant technological advances, such as the mercury diffusion vacuum pump, the gas-filled incandescent lamp, the thoriated electrode, and the high-vacuum electron tube diode and amplifier. His impact on gaseous electronics might be measured by our own modern terminology: Langmuir's film theory of heat convection, Langmuir waves, and Langmuir probes. The exhibit will be on display throughout the conference.

## GEC STUDENT AWARD FOR EXCELLENCE

In an effort to recognize and encourage the outstanding contributions of students to the Gaseous Electronics Conference, the GEC has established an award for the

best paper presented by a student. The title of the award is *GEC Student Award for Excellence*. The prize will be \$500. The award winner will be selected by a subcommittee of the GEC Executive Committee. The following students are finalists for the award, and will give oral presentations at the conference:

**John B. Boffard** (University of Wisconsin-Madison) [PR1.04] *Measurement of electron impact excitation cross sections out of the metastable levels of argon.*

**H. K. Chung** (University of Wisconsin-Madison) [BM2.09] *Opacity Effects on Line Broadening in Electron Density Analysis of Transient Plasmas.*

**M.V. Malyshev** (Princeton University) [IT2.03] *Determination of Electron Temperature, Plasma Density and Cl<sub>2</sub> Percent Dissociation by Optical Emission Spectroscopy.*

**Louis-Philippe Masse** (Universite de Montreal) [PR2.05] *Development of a surface-wave magnetoplasma sputtering source for the elemental analysis of solid samples.*

**Steven Shannon** (University of Michigan) [NW2.04] *RIE Glow Discharge Tomography.*

**M. van de Grift** (Eindhoven University of Technology) [RR2.02] *Transport of argon ions in the presheath of an ICP.*

## CONFERENCE HEADQUARTERS/ REGISTRATION

Headquarters for the conference is the Memorial Union. Registration and the opening reception will be held there from 7:00 p.m. to 9:00 p.m. on Sunday, October 5. Registration will also be open near the meeting rooms in the Union each day of the conference. Registration fees are \$175 (\$225 after September 5), and \$100 for students and retirees. Participants are required to register and wear their name tags to all scientific sessions and social events.

## PRESENTATIONS

Papers that have been accepted for presentation are listed in the daily schedule of technical sessions. Additional postdeadline papers will be distributed at the meeting. Oral contributed presentations are allotted 12

minutes, with an additional 3 minutes for discussion. Invited papers are 25 minutes in length, with 5 minutes for discussion. Standard overhead projectors are available for the presentations. Other audio/visual needs should be arranged with the conference secretary.

## POSTERS

The poster boards for poster presentations are 4 ft. high by 6 ft. wide.

## VENDOR EXHIBITS

An area in Great Hall has been set aside for vendor exhibits. The vendors being represented this year include NorCal, Spectra International, Scientific Systems, VAT, Alcatel, EVAC International, Surface Interface, and Delatech.

## TRAVEL INFORMATION

Dane County International Airport is a short taxi ride (approximately \$12) from the University of Wisconsin campus and the conference hotels, and is served by a number of shuttle flights from Chicago-O'Hare, Minneapolis, Detroit, Milwaukee, and Cincinnati. There are frequent shuttle buses from O'Hare (Van Galder Bus Company, 800-747-0994) and Milwaukee (Badger Bus Company, 608-255-6771) airports.

## HOTELS

A number of hotels have reserved rooms for the GEC, all within walking distance of the Memorial Union. For information on housing, contact Maureen Sundell (608-252-5514, FAX 608-262-8516, email [sundell@admin.uwex.edu](mailto:sundell@admin.uwex.edu)).

## DINING OPTIONS

An extensive outdoor mall on State Street offering a wide variety of restaurants is located a few blocks from the conference center.



## BANQUET

The conference banquet will be held Tuesday, October 7, beginning with a reception at 6:30 p.m. The speaker will be Alan Garsgadden, who will speak on *Celebrities of the Gaseous Electronics Conference*.

## GEC EXECUTIVE COMMITTEE

**M. J. Kushner**, Chair, University of Illinois

**T. G. Walker**, Secretary, University of Wisconsin

**J. N. Bardsley**, Past-Chair, Lawrence Livermore National Laboratory

**G. A. Hebner**, Treasurer, Sandia National Laboratory

**M. A. Dillon**, Past-Secretary, Argonne National Laboratory

**C. B. Fleddermann**, Secretary-Elect, University of New Mexico

**P. Loewenhardt**, Applied Materials Inc.

**J. W. McConkey**, University of Windsor

**S. Samukawa**, NEC Corporation

**T. J. Sommerer**, General Electric R&D Center

For further information contact:

Thad G. Walker

University of Wisconsin-Madison

Department of Physics

1150 University Ave.

Madison, WI 53706 USA

(608) 262-4093 FAX (608) 265-2334

Email: walker@uwnuc0.physics.wisc.edu

## CIVILIAN TIME TO MILITARY TIME CONVERSION

The meeting is run at military time. For the convenience of meeting attendees, below is a guide for the conversion of civilian to military time.

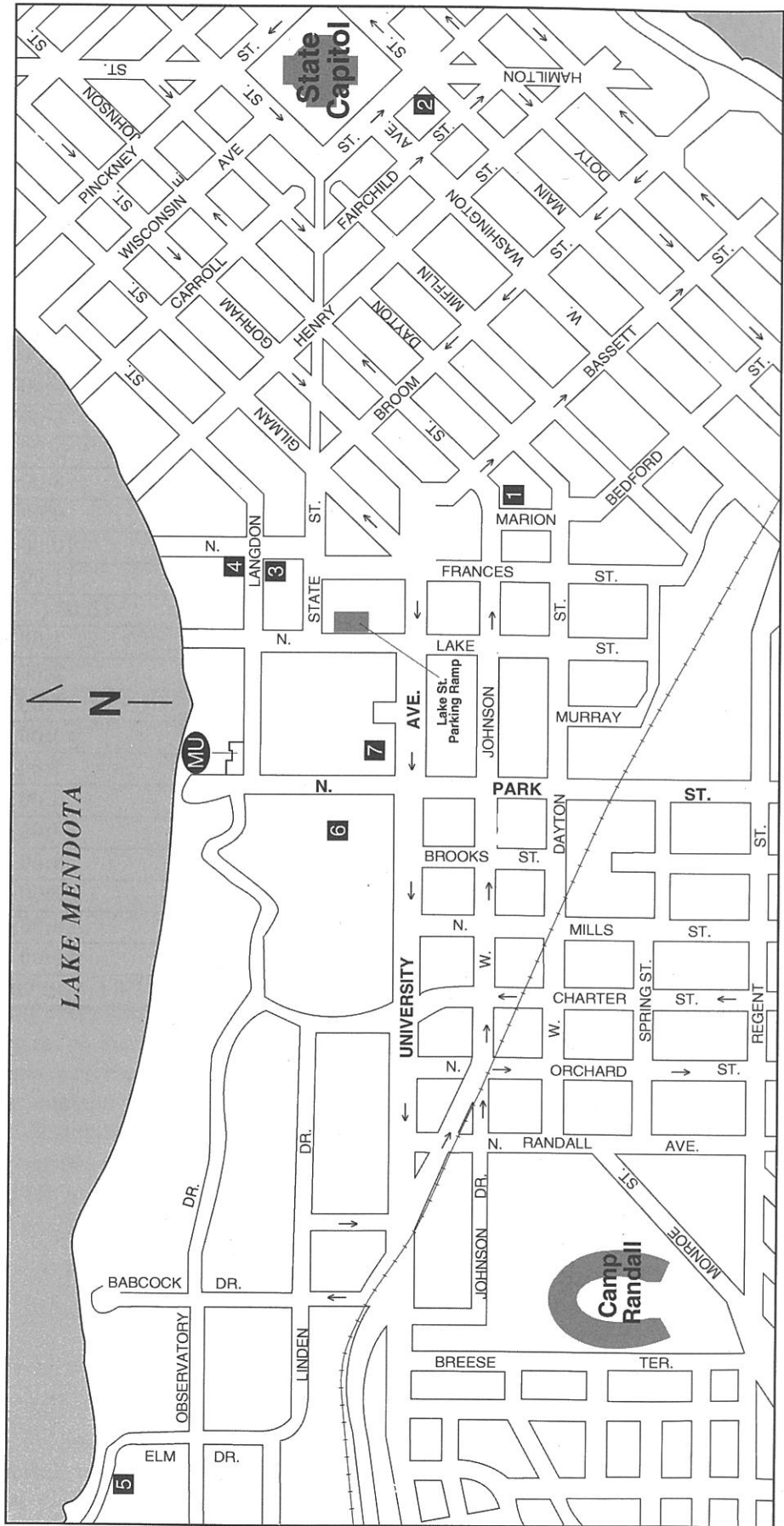
CIVILIAN TIME	MILITARY TIME
1:00 (AM)	1:00
2:00 (AM)	2:00
3:00 (AM)	3:00
4:00 (AM)	4:00
5:00 (AM)	5:00
6:00 (AM)	6:00
7:00 (AM)	7:00
8:00 (AM)	8:00
9:00 (AM)	9:00
10:00 (AM)	10:00
11:00 (AM)	11:00
<b>12:00 (NOON)</b>	<b>12:00</b>
<b>1:00 (PM)</b>	<b>13:00</b>
<b>2:00 (PM)</b>	<b>14:00</b>
<b>3:00 (PM)</b>	<b>15:00</b>
<b>4:00 (PM)</b>	<b>16:00</b>
<b>5:00 (PM)</b>	<b>17:00</b>
<b>6:00 (PM)</b>	<b>18:00</b>
<b>7:00 (PM)</b>	<b>19:00</b>
<b>8:00 (PM)</b>	<b>20:00</b>
<b>9:00 (PM)</b>	<b>21:00</b>
<b>10:00 (PM)</b>	<b>22:00</b>
<b>11:00 (PM)</b>	<b>23:00</b>
<b>12:00 (MIDNIGHT)</b>	<b>24:00</b>

## PLEASE NOTE

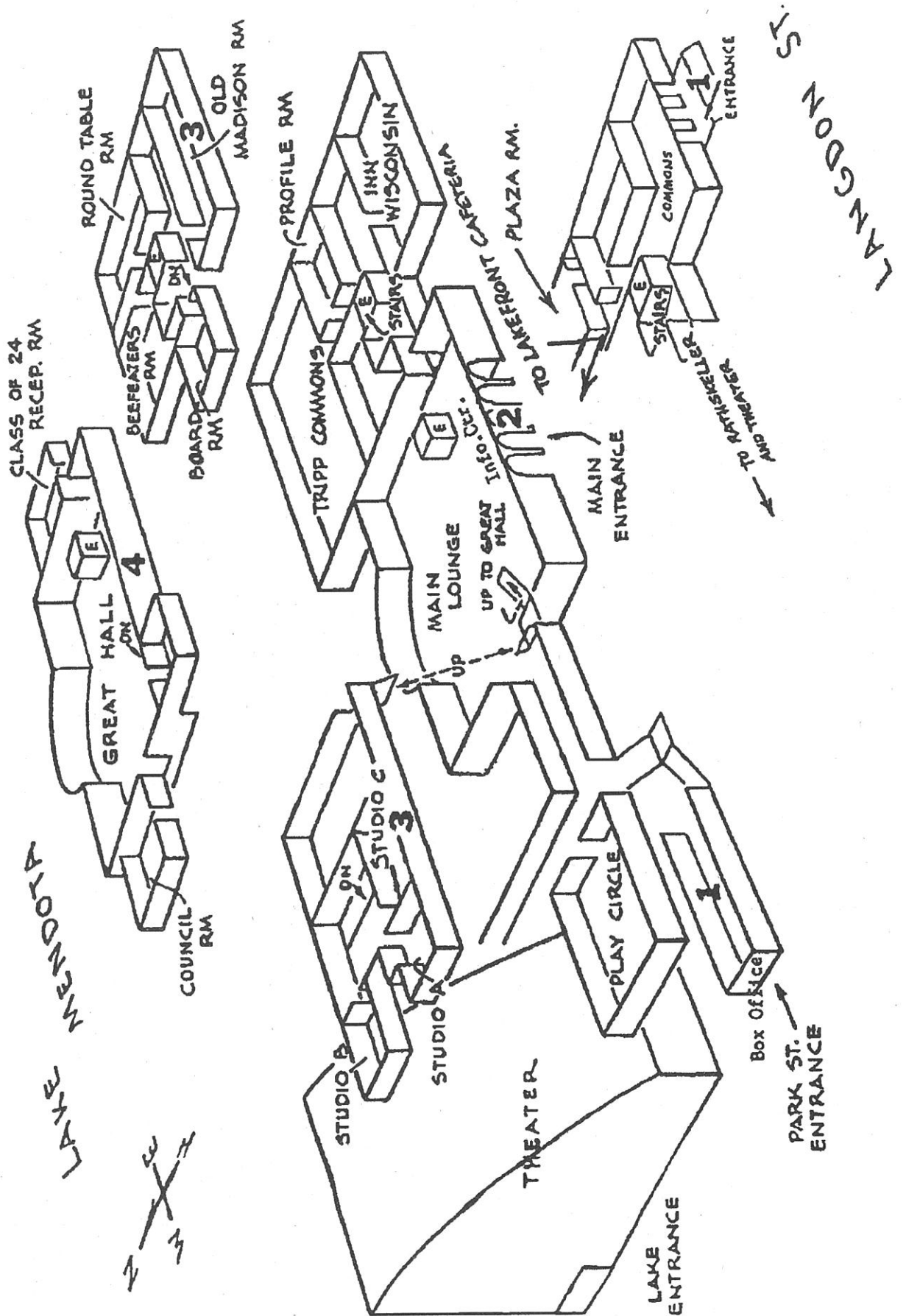
The APS has made every effort to provide accurate and complete information in this *Bulletin*. However, changes or corrections may occasionally be necessary and may be made without notice after the date of publication. To ensure that you receive the most up-to-date information, please check the meeting Corrigenda distributed with this *Bulletin*.

# University and Downtown Area

- MU** Memorial Union  
800 Langdon St.
- 1** Howard Johnson's  
525 W. Johnson St.  
(608) 251-5511
- 2** Inn on the Park  
22 S. Carroll St.  
(608) 257-8811
- 3** Madison Inn  
601 Langdon St.  
(608) 257-4391
- 4** Wis. Center  
Guest House  
(Lowell Hall)  
610 Langdon St.  
(608) 256-2621
- 5** J. F. Friedrich  
Center  
1950 Willow Dr.  
(608) 231-1341
- 6** Music Hall
- 7** Mills Concert  
Hall
- Humanities  
Building



# MEMORIAL UNION MEETING FACILITIES



# EPITOME OF THE 50th ANNUAL GASEOUS ELECTRONICS CONFERENCE

---

## MONDAY MORNING 6 OCTOBER

---

8:00

AM1            **Heavy Particle Collisions**  
*Armentrout*  
Class of '24 Reception Room

AM2            **Environmental Applications**  
*Yousfi, Rosocha, Green*  
Tripp Commons

---

## MONDAY MORNING 6 OCTOBER

---

10:15

BM1            **Light Sources**  
*Neiger, Doughty*  
Class of '24 Reception Room

BM2            **Pulsed Plasma**  
Tripp Commons

---

## MONDAY AFTERNOON 6 OCTOBER

---

13:30

CM1            **Glows, Swarms and  
General Discharge Physics**  
Class of '24 Reception Room

CM2            **Future Processing Trends**  
*Ikegami, McNevin, Brueck*  
Tripp Commons

---

## MONDAY AFTERNOON 6 OCTOBER

---

16:00

DMP1           **Poster Session:  
Electron-Molecule Collisions**  
Great Hall

DMP2           **Poster Session:  
Environmental Applications**  
Great Hall

DMP3

**Poster Session:  
Pulsed Plasmas (Processing)**  
Great Hall

DMP4

**Poster Session: Glows**  
Great Hall

DMP5

**Poster Session: Lighting**  
Great Hall

---

## MONDAY EVENING 6 OCTOBER

---

19:30

EM            **Town Hall Meeting on  
Topical Group**  
Union Theater

---

## TUESDAY MORNING 7 OCTOBER

---

8:00

FT            **Plenary**  
*Waymouth, Dalgarno, Hays, Phelps*  
Music Hall

---

## TUESDAY MORNING 7 OCTOBER

---

11:00

GT            **Foundations of Gaseous  
Electronics**  
*Gallagher*  
Music Hall

---

## TUESDAY MORNING 7 OCTOBER

---

11:45

HT            **GEC Business Meeting**  
Music Hall



---

**TUESDAY AFTERNOON  
7 OCTOBER**

---

13:30

IT1            **Surface Processes**  
*Niwano, Blain*  
Class of '24 Reception Room

IT2            **Inductively Coupled Plasmas I**  
*Holland, Samukawa*  
Tripp Commons

---

**TUESDAY AFTERNOON  
7 OCTOBER**

---

16:00

JTP1           **Poster Session: Electron Collision  
Cross Sections**  
Great Hall

JTP2           **Poster Session: Photoabsorption**  
Great Hall

JTP3           **Poster Session: RF Glow  
Discharges**  
Great Hall

JTP4           **Poster Session: Propulsion and  
Space Plasmas**  
Great Hall

JTP5           **Poster Session: Flat Panel and  
Large Area Plasmas**  
Great Hall

---

**TUESDAY AFTERNOON  
7 OCTOBER**

---

18:30

KT            **Reception and Banquet**  
Lowell Hall

---

**WEDNESDAY MORNING  
8 OCTOBER**

---

8:00

LW1           **Positron and Electron Scattering**  
*Kaupilla, Stauffer*  
Class of '24 Reception Room

LW2

**Propulsion and Space Plasmas/  
Microdischarges and Plasma  
Display Panels**  
*Lawler, Beattie*  
Great Hall

---

**WEDNESDAY MORNING  
8 OCTOBER**

---

10:15

MW1           **Cold Collisions and  
Recombination.**  
*Walker, Julienne, Flannery.*  
Class of '24 Reception Room

MW2

**Diagnostics I**  
*Steffens*  
Tripp Commons

---

**WEDNESDAY AFTERNOON  
8 OCTOBER**

---

13:30

NW1           **Modeling**  
*Jones, Boyd, Hitchon*  
Class of '24 Reception Room

NW2

**Etching**  
Tripp Commons

---

**WEDNESDAY AFTERNOON  
8 OCTOBER**

---

16:00

OWP1           **Poster Session: Ionization**  
Great Hall

OWP2           **Poster Session: High Density  
Plasmas for Processing**  
Great Hall

OWP3           **Poster Session: Extreme  
Submicron Processing**  
Great Hall

OWP4           **Poster Session: Diagnostics and  
Sensors**  
Great Hall

---

**THURSDAY MORNING**  
**9 OCTOBER**

---

**8:00**

PR1            **Electron-Atom Collisions**  
*Madison, Buckman*  
Class of '24 Reception Room

PR2            **Magnetized Plasmas**  
Tripp Commons

---

**THURSDAY MORNING**  
**9 OCTOBER**

---

**10:15**

QR1            **Electron-Molecule Collisions**  
*Hatano, Huo, Rescigno*  
Class of '24 Reception Room

QR2

**Helicon and Surface Wave  
Plasmas**  
*Margot*  
Tripp Commons

---

**THURSDAY AFTERNOON**  
**9 OCTOBER**

---

**13:30**

RR1            **Diagnostics II**  
*Graham*  
Class of '24 Reception Room

RR2            **Inductively Coupled Plasmas II**  
*Berry, Nanbu, Makabe*  
Tripp Commons

## SESSION AM1: HEAVY PARTICLE COLLISIONS

Monday morning, 6 October 1997; Class of '24 Reception Room, Memorial Union at 8:00; Paul Burrow, University of Nebraska, presiding

### Invited Paper

8:00

#### AM1 1 The kinetic energy dependence of ion-molecule reactions.

P. B. ARMENTROUT, *Chemistry Department, University of Utah*

Over the past several years, we have examined the kinetic energy dependence of a wide array of ion-molecule reactions, many of which are related to plasma chemistry. These studies involve the use of a guided ion beam tandem mass spectrometer which is capable of measuring absolute reaction cross sections as a function of ion kinetic energy ranging from thermal (0.05 eV) to hundreds of electron volts. While a few of these reactions follow theoretically predicted behavior, most do not. The talk will try to elucidate different examples of the kinetic energy behavior of ion-molecule reactions, drawing primarily from studies of charge transfer, dissociative charge transfer, and reactive collisions related to plasma chemistry. The ability to extract thermodynamic information from this work will also be highlighted.

### Contributed Papers

8:30

**AM1 2 Photoassociation of Hg-Hg Pairs in the Ultraviolet** \* Z. G. FIGEN, *University of Illinois at Urbana-Champaign* V. S. ZUEV, *Lebedev Physical Institute, Moscow* J. G. EDEN, *University of Illinois at Urbana-Champaign* Bound-free transitions (photoassociation) of Hg-Hg pairs has been studied in the mid-UV ( $270 \leq \lambda \leq 290$  nm) with a frequency-doubled, pulsed dye laser. Production of Hg<sub>2</sub> in the excited D1<sub>u</sub> state was detected by pumping the GO<sub>u</sub><sup>+</sup> ← AO<sub>g</sub><sup>+</sup> transition and monitoring GO<sub>u</sub><sup>+</sup> → XO<sub>g</sub><sup>+</sup> emission in the 210–240 nm region. Structure in the photoassociation spectrum that is associated with more than 20 D1<sub>u</sub> vibrational states has been observed and analysis of the spectrum has yielded several spectroscopic constants for the D1<sub>u</sub> and XO<sub>g</sub><sup>+</sup> states.

\*Supported by AFOSR and US National Research Council.

8:45

**AM1 3 Collisional Quenching of Hg<sub>2</sub> (AO<sub>g</sub><sup>+</sup>)** \* Z. G. FIGEN, *University of Illinois at Urbana-Champaign* J. G. EDEN, *University of Illinois at Urbana-Champaign* The rate constants for quenching of the AO<sub>g</sub><sup>+</sup> state of Hg<sub>2</sub> have been measured by a pump-probe laser induced fluorescence technique. The metastable Hg<sub>2</sub> (AO<sub>g</sub><sup>+</sup>) species was produced by photoassociating Hg-Hg pairs at 266 nm which excites the Hg (D1<sub>u</sub>) level. Subsequent collisional relaxation populates the metastable AO<sub>g</sub><sup>+</sup> state. The temporal history of the population was monitored by driving the AO<sub>g</sub><sup>+</sup> → GO<sub>u</sub><sup>+</sup> transition in the yellow ( $\lambda \sim 564$  nm) and observing the GO<sub>u</sub><sup>+</sup> → XO<sub>g</sub><sup>+</sup> emission in the UV ( $\lambda \sim 210$ –240 nm). The rate constants for quenching of Hg<sub>2</sub> (AO<sub>g</sub><sup>+</sup>) in two and three body collisions with background Hg atoms have been measured to be  $1.1 \pm 0.2 \times 10^{-14}$  cm<sup>3</sup>-s<sup>-1</sup> and  $9.9 \pm 2.5 \times 10^{-34}$  cm<sup>6</sup>-s<sup>-1</sup>.

\*Supported by AFOSR.

9:00

**AM1 4 Reaction Kinetics of Gas-Phase Transition Metal Cations** \* D. RITTER, *Southeast Missouri State U* We have begun studies of reactions of transition metal ions with small hydrocarbons in the gas phase at moderate 1 Torr pressures. We have

constructed a new source for production of metal ions in a fast-flow reactor. We quantitatively identify the ions produced by the metal ion source. We have completed several preliminary studies to characterize the source and examine reactions of various transition metal ions with small hydrocarbons. We have tested various metals and found the discharge source to be a prolific source for V<sup>+</sup>, Fe<sup>+</sup>, Co<sup>+</sup>, Ni<sup>+</sup>, Cu<sup>+</sup>, and Nb<sup>+</sup> ions. Interestingly, we have been unable to discern Ti<sup>+</sup> with a Ti cathode. We have also been unable to unambiguously identify M2<sup>+</sup> ions from any of the metals studied thus far. The mechanism for the removal of metal from the cathode surface and ionization is not certain at this time.

\*Funded by ACS-PRF 27625-GB3 and Research Corp Cottrell grants

9:15

**AM1 5 Collision Induced Dissociation and Proton Transfer for Low Energy Collisions Involving CH<sub>4</sub><sup>+</sup>** BRIAN L. PEKO, ILYA V. DYAKOV, ROY L. CHAMPION, *College of William and Mary, Williamsburg, VA 23187* In an attempt to provide a database for use in modeling discharges such as CF<sub>4</sub>, CH<sub>4</sub>, and H<sub>2</sub>, cross sections have been measured for various ion-molecule reactions occurring in these discharges. Absolute cross section for collision induced dissociation, proton abstraction, and electron transfer will be presented for the reactants CH<sub>4</sub><sup>+</sup> + H<sub>2</sub>, Ar and CH<sub>4</sub>, and isotopic variants, for the laboratory energies ranging from a few up to 400 eV. In addition, the role of internal energy in the product and parent ions and, in particular, its role in proton abstraction will be discussed. The importance and implications of these and previous measurements for modeling discharges will be addressed. This work was supported in part by the Division of Chemical Sciences, Office of Basic Energy of the U. S. Department of Energy.

9:30

**AM1 6 Absolute Emission Spectroscopy of Electronically Excited Products of Dissociative Recombination** M. P. SKRZYPKOWSKI, T. GOUGOUSI, M. F. GOLDE, R. JOHNSON, *University of Pittsburgh, Pittsburgh, PA* \* We have employed spatially-resolved optical emission spectroscopy in a flowing afterglow plasma to investigate radiations in the 200–400 nm range

resulting from electron-ion dissociative recombination. Calibrated emission data combined with Langmuir probe electron-density measurements are analyzed to obtain branching ratios for electronically excited recombination products. In particular, we will report absolute yields of  $CO(a^3\Pi)$  resulting from recombining  $CO_2^+$  ions,  $NO(B^2\Pi)$  from  $N_2O^+$ ,  $OH(A^2\Sigma^+)$  from  $HCO_2^+$ , as well as  $NH(A^3\Pi_i)$ , and  $OH(A^2\Sigma^+)$  from the recombination of  $N_2OH^+$  ions.

\*This work was supported by NASA

9:45

**AM1 7 Kinetic Energies of Ions Produced by Electron Impact on Propane** \* V. GRILL, H.U. POLL, T.D. MAERK, *Universitaet Innsbruck, Austria* N. ABRAMZON, K. BECKER, *Stevens Institute of Technology, USA* Mass spectrometric techniques in conjunction with the ion deflection method have been used to

measure kinetic energy spectra of a variety of ions produced by electron-impact ionization of propane,  $C_3H_8$ . The larger ions  $C_3H_i^+$  ( $i=8-0$ ) are almost exclusively formed with quasi-thermal energies. The spectra of the  $C_2H_i^+$  ( $i=5-0$ ) ions show a quasi-thermal peak and several peaks at higher kinetic energies. This indicates that a fraction of the ions results from processes favoring the formation of energetic, non-thermal ions. The spectra of the  $CH_i^+$  fragment ions ( $i=3-0$ ) are dominated by the presence of energetic, non-thermal ions with kinetic energies of up to 4 eV per fragment ion and with only small contributions from quasi-thermal ions. Possible mechanisms for the formation of all ions will be discussed on the basis of the measured kinetic energy spectra and appearance energies of the various ions.

\*Work supported by FWF, OENB, OEAW, BMWVK, Austria and NASA

## SESSION AM2: ENVIRONMENTAL APPLICATIONS

Monday morning, 6 October 1997; Tripp Commons, Memorial Union at 8:00; Shirshak Dhali, Southern Illinois University, presiding

### Contributed Paper

8:00

**AM2 1 Elimination of global warming concerns from DCVD chamber cleans.** RAOUX SEBASTIEN, TANAKA TOMI, BAHN MOHAN, KELKAR MUKUL, PONNEKANTI HARI, SILVETTI DAVE, CHEUNG DAVID, FAIRBAIRN KEVIN, *APPLIED MATERIALS Inc.* JONHSON ANDY, *AIR PRODUCTS & CHEMICALS Inc.* The semiconductor industry uses a large amount of PerFluoroCompounds (PFCs) and their impact on global warming has become a major environmental concern. On DCVD (Dielectric Chemical Vapor Deposition) systems, PFCs are used to periodically clean the deposits on the chamber walls. With a conventional parallel plate RF reactor, the PFC gas utilization is

incomplete (<20%) and a large fraction of the PFC gas is unreacted and emitted in the atmosphere. We developed a microwave plasma source that provides >95% gas utilization and abatement during chamber cleans, using NF<sub>3</sub> as a source gas. This technology brings the GWP (Global Warming Potential) of a chamber clean to negligible levels and also provides improvement in the chamber clean efficiency and throughput. Here we review the requirements for the manufacturability of a plasma abatement process. We use gaseous FTIR (Fourier Transform InfraRed) and QMS (Quadrupole Mass Spectroscopy) techniques to characterize the NF<sub>3</sub> destruction process during a SiO<sub>2</sub> deposition chamber clean. Finally, we analyze the functionality and efficiency of plasma abatement devices compared to other abatement techniques.

### Invited Papers

8:15

**AM2 2 Boltzmann Equation Analysis Of Electron Swarms For Non Thermal Flue Gas Discharge Modeling.**  
M. YOUSFI, *CPAT-Universite Paul Sabatier-Toulouse-France*

The aim of this presentation is to give an overview on the electron swarm development in the flue gas mixture discharges involving N<sub>2</sub>, O<sub>2</sub>, H<sub>2</sub>O and CO<sub>2</sub>. The corresponding electron basic data needed for the non thermal plasma device for pollution control are given in typical flue gases from Boltzmann equation solution including the dominant collision processes (elastic, inelastic and super-elastic). These data are first the electron-molecule collision cross sections for each gas of the mixture and then the transport and reaction coefficients of electron swarms in the gas mixture. The strong coupling between this electron swarm model with the different models used for the non thermal plasma device of our interest are emphasized. This concerns the electron Boltzmann equation coupled with the charged particle (or electrical) model, the gas dynamics and also the chemical kinetics models. Some illustrative results of this coupling are then given.

8:45

**AM2 3 Nonthermal Plasma Processing of VOCs with Electric Discharges: Gaseous Electronics and Plasma Chemistry Considerations.**  
LOUIS A. ROSOCHA, *Los Alamos National Laboratory* \*

Electrical discharges in gases can be used to create nonthermal (or nonequilibrium) plasmas having energetic electrons (order few to several eV) at near-ambient background gas temperature. These low-temperature plasmas are an excellent source of free radicals and other active species useful for chemical conversion and synthesis: O(<sup>3</sup>P), OH, N, H, NH, CH, O<sub>3</sub>, O<sub>2</sub>(<sup>1</sup>Δ), plasma electrons. Interactions of the active species with chemical pollutants such as volatile organic compounds (VOCs) are characterized by high reaction-rate constants for decomposition of the VOCs. The yields of the



active species depend on the gaseous electronics properties of the discharge (e.g.,  $E/N$ ,  $v_d$ ), while the decomposition pathways depend on the plasma chemistry. In this talk, we will concentrate on two example nonthermal plasma reactors based upon electric-discharge streamers - pulsed corona and dielectric-barrier devices. The connections between the gaseous electronics of the discharge and the plasma chemistry will be discussed. Examples of VOC decomposition based on different processes (e.g., radical-initiated attack vs dissociative electron attachment) will be discussed, as well as representative practical pollution-control applications for the technology.

\*Thanks to other members of the Los Alamos team - Graydon Anderson, John Coogan, Zoran Falkenstein, Richard Korzekwa and Hans Snyder - for their contributions to this field.

9:15

**AM2 4 Database needs for processing of VOCs.**

DAVID S. GREEN, *NIST, Gaithersburg, MD 20899* \*

Databases and models are required to evaluate the applicability of non-thermal plasma-based methods (electron beam irradiation or electrical discharge techniques) for the abatement of volatile organic compounds (VOCs) in contaminated humid air gas streams. Data needs are also driven by the desire to design, optimize, and control these methods. Much of the existing information on the energy efficiency of VOC destruction and the nature of byproducts is empirical and the processes are so complicated that it is essential that predictive models and simulations be improved. The general data types needed include transport, thermodynamic, kinetic, and electron interactions. The amount of data needed is very large, and in part the nature of this data is dependent upon the concentration, pressure, temperature and degree of ionization. Chemical conversion initiated by electron-impact dissociation and ionization of molecules involves the competition between a variety of neutral radical and ion-molecule reactions. The abatement efficiency will depend critically upon the electron excitation/dissociation/attachment cross-section, ion mobility, proton affinity and ionization potential of the particular class of VOCs and byproducts under consideration. The range of classes of VOCs include ketones, alcohols, unsaturated hydrocarbons, aromatics and halocarbons. Modeling of dense streams or modeling to provide detailed analysis of results may need more data on excitation, energy transfer and reactions of excited states (vibrational and electronic) than dilute streams. Neutral and ion-molecule kinetics modified for moderate temperatures and ambient pressure will be discussed. Progress made at NIST to supply an evaluated database for the humid air plasma as the basis for addition of any mixture of VOCs will be highlighted. Preliminary data on selected VOC systems such as toluene-air shall be presented. The development of minimized kinetic mechanisms with evaluated data that may be used as input to more sophisticated reactor and electric field models shall be examined.

\*This work was performed in collaboration with Wayne Sieck and John Herron

*Contributed Paper*

9:45

**AM2 5 Plasma Catalysis of Methane Decomposition in Pulse Microwave Discharge**

B. POTAPKIN, V. RUSANOV, V. JIVOTOV, A. BABARITSKI, S. POTECHIN, *RRC Kurchatov Institute, 123182 Moscow, Russia* C. ETIEVANT, *CIEE, 78 000 Versailles, France* Investigation of plasma catalysis effects in various chemical reactions, such as  $\text{SO}_2$  and hydrocarbons oxidation, ammonia and nitrogen oxides synthesis, has been of interest for many decades. Present work describes the first experimental observation and theoretical analysis of plasma catalysis effects in the case of endothermic methane decomposition into molecular hydrogen and carbon black. Process energy requirements are covered mainly by low potential gas thermal energy while plasma is

used for acceleration of chemical reactions via active species generation. The experiments were done as follows: (i) methane was preheated in a conventional heat exchanger up to about 40-65 °C where thermal methane decomposition is limited by process kinetics, (ii) methane was passed through a non-equilibrium pulse microwave discharge (9.04 GHz, pulse duration 1  $\mu\text{s}$ ). Experiments have shown a strong catalytic effect of plasma on methane decomposition. The degree of conversion after discharge increased drastically, despite gas cooling, because of heat absorption in the methane decomposition reaction. Theoretical analysis of process kinetics and energy balance gave clear evidence of the catalytic effect of plasma under experimental conditions. The estimated chain length was about 300. The possible mechanism of plasma catalysis, the ion-molecular chain Winchester mechanism, is proposed and described.

---

**SESSION BMI: LIGHT SOURCES**

Monday morning, 6 October 1997; Class of '24 Reception Room, Memorial Union at 10:15; Paul N. Barnes, Wright Laboratory, presiding

*Invited Papers*

10:15

**BMI 1 Recent Results on the Radiation Mechanism of Cluster Lamps.**

MANFRED NEIGER, *University of Karlsruhe, LTI (Germany)*

Cluster lamps are high pressure discharge lamps operated in vapors of metal halides, metal oxides or metal oxi-halides at vapor pressures high enough to enable condensation of small metal clusters (nm-size) to take place within hot regions

of the lamp plasma. These hot particles emit incandescent radiation corresponding to their temperature, which is the local plasma temperature where condensation takes place, e.g. 3500 K for tungsten clusters or 4500 K for rhenium clusters. This is the reason why the dominant characteristic of cluster lamps is a nearly continuous spectrum. Recent results show that nearly all halides, oxo-halides or oxides of transition metals show a continuous spectrum characteristic of incandescent radiation, superimposed by some atomic and molecular radiation in the blue part of the spectrum. The paper presented discusses operating principles of cluster lamps and different radiation mechanisms contributing to the emission spectrum of these lamps.

10:45

**BM1 2 Discharge Paths to Mercury-Free Lighting.\***

DOUGLAS A. DOUGHTY, *GE Corporate Research and Development*

This talk will begin with a review of where and why mercury is used in various light sources, and why there is a desire to eliminate mercury from these sources. Emphasis will be given to replacing existing mercury-based fluorescent technology, as this sector uses the largest fraction of mercury in the lighting industry. The criteria that need to be satisfied by candidate mercury replacement materials will be considered and a list of possible strategies will emerge. These strategies broadly divide into ultraviolet generation (to be coupled with a phosphor) and direct visible generation. Ultraviolet sources can be further divided into atomic versus molecular discharges. Rare-gas replacements for mercury, such as xenon, satisfy many of the necessary criteria, but place a significant burden on phosphor development. Results from a characterization of the ultraviolet properties of xenon plasmas, both electrodeless and electrodeless, will be presented. A low pressure sulfur discharge is a potential molecular-based candidate, but measurements on the UV efficiency of such plasmas are not encouraging. Dielectric barrier discharges, in which excimer radiation is produced, will also be considered as a molecular UV source. Finally, direct-visible strategies to replace fluorescent lamps will be discussed. This might involve a low-pressure metal-halide discharge to reproduce the low surface brightness properties of fluorescent lighting, or perhaps a centralized high pressure metal halide light source with appropriate light distribution systems.

\*Work supported in part by the US National Institute of Standards and Technology under the Advanced Technology Program

*Contributed Papers*

11:15

**BM1 3 Excimer Emission from Direct Current Microhollow Cathode Discharges\***

R. H. STARK, A. EL-HABACHI, W. SHI, K. H. SCHOENBACH, *Physical Electronics Research Institute, Old Dominion University, Norfolk, VA 23529* Reducing the dimensions of the cathode hole to less than 200 micrometer has allowed us to operate argon discharges in a hollow cathode discharge mode, dc, up to pressures of one atmosphere. Spectral measurements in the VUV have shown that the microdischarges are strong sources of argon excimer radiation at 128 nm. This points to a nonthermal electron energy distribution where a considerable part of the electrons have energies exceeding the ionization potential of argon. Whereas the discharges in argon were dc up to atmospheric pressure, discharges in xenon became unstable at pressures exceeding 300 Torr, and current spikes were observed. The xenon excimer emission at 172 nm, however, was found to increase, independent of the mode, dc or pulsed, when the pressure was increased to one atmosphere. The microdischarges have resistive current-voltage characteristics. This has allowed us to generate simple arrays of these discharges, with possible applications as flat panel excimer lamps.

\*This work is supported by DOE, Advanced Energy Division, and by AFOSR

11:30

**BM1 4 Analysis of the near-cathode region in high-pressure discharge lamps**

M. S. BENILOV, R. M. S. ALMEIDA, *Departamento de Física, Universidade da Madeira, Largo do Município, 9000 Funchal, Portugal* Physics of the near-cathode plasma layer in high-pressure arc lamps is considered. Hierarchy of macroscopic length scales and various mean free paths has been analyzed. According to this hierarchy, current transfer through the near-cathode plasma layer in the considered range of the plasma pressures and temperatures may occur in two physically different

regimes, one of them being a regime of a weakly ionized plasma with the electron temperature close to the heavy-particle temperature, and another being a regime of a moderately to strongly ionized plasma with the electron temperature essentially higher than the heavy-particle temperature. Estimates for both regimes have been made by means of appropriate models. It has been shown that regimes of a weakly ionized plasma are unlikely to realize in the range of current densities typical for high-pressure arc lamps. Regimes with moderately and strongly ionized plasmas can realize, regimes with moderately ionized plasmas being associated with modes of a diffuse current transfer to cathodes of arc lamps and regimes with strongly ionized plasmas being associated with the hot-spot modes.

11:45

**BM1 5 Radiometric Efficiency of Barium Discharge Plasmas\***

HEIDI M. ANDERSON, J. MACDONAGH-DUMLER, J. J. CURRY, J. E. LAWLER, *University of Wisconsin-Madison* Barium has a number of characteristics that indicate it may be a good atomic radiator in a glow discharge. 1) At practical operating temperatures Ba has a vapor pressure in the mTorr range (5 mTorr at 585°C). 2) The excitation energy of the primary radiating level in Ba is less than half of the ionization energy. 3) The wavelength of the resonance transition is suitable for direct use as a visible light source. At 553 nm, this radiation lies at the peak of the photopic eye sensitivity curve. For these reasons, a Ba glow discharge may prove to be of interest to the lighting industry for use in a novel, efficient light source. Progress in experimental determinations of the radiometric efficiency of a dc glow discharge and of an rf discharge and progress in modeling the radiometric efficiency of Ba glow discharges will be reported.

\*supported by the NSF

12:00

**BM1 6 Efficient Bright UV and VUV Light Sources** D. E. MURNICK, H. DAHI, *Rutgers University, Newark NJ 07102* A. ULRICH, J. WIESER, *Fakultät für Physik, Technische Universität München Germany* Electron beams at around 20keV transmitted through thin ceramic foils into high pressure gas cells yield efficient bright uv and vuv light sources. With pure rare gases, excimer bands have been observed with 40% efficiency.<sup>1</sup> Using gas mixtures, narrow excimer halide radiation and vuv line emission has also been produced. A particularly interesting system enhances transfer from neon excimers to n=3D2 hydrogen, producing essentially monochromatic Lyman- $\alpha$  light at 121nm. The systems are small, run continuously and may be engineered, with pulsed electrons, to produce short wavelength excimer lasers with very high beam quality.

<sup>1</sup>J. Wieser, D. E. Murnick, A. Ulrich, H. A. Huggins, A. Liddle, and W. L. Brown *Rev. Sci. Instrum.* 68, 1360 (1997).

12:15

**BM1 7 Coulomb-Collision implemented PIC Simulation of High-Density Plasmas for X-Ray Laser Systems** S. YONEMURA, K. NANBU, *Institute of Fluid Science, Tohoku University* The particle-in-cell simulation is carried out for the expansion of multi-charged dense plasmas for X-ray laser systems. All Coulomb collisions among charged particles are considered because they play an important role on dense plasma. Recently Nanbu found an accurate theory of Coulomb collisions. The essence of his theory is in grouping of many successive small-angle collisions into a unique binary collision with a large scattering angle. His theory is applied to this simulation, extending it to the case when the weight assigned to a sample particle varies from particle to particle. Effects of Coulomb collisions on the expanding plasmas are studied in detail. First, Coulomb collisions greatly recover the translational equilibrium, splitting of temperature components being largely reduced during the expansion. Secondly, temperature components hardly vary over the region from the shrinking dense plasma core to the expanding low density corona. Also, density fluctuations near the wave front of the expanding corona are vanished. Thirdly, the plasma core shrinks more slowly because of Coulomb collisions. These features are quite different if the Coulomb collisions are disregarded.

capacitor and this depends on the ion density and mobility. The power reflected from the matching network decreases on time scales associated with the formation of stable sheaths on the powered and earthed electrodes. At low pressures below 1 mTorr, the ionization probability is greatly decreased and the time necessary for breakdown can increase by orders of magnitude to hundreds of microseconds. Experimental results will be presented showing the breakdown characteristics and their relationship to the Paschen curve. Implications for plasma processing will be discussed.

10:30

**BM2 2 Step and Pulsed Responses of RF Discharges** JING YANG, *Hokkaido University* P.L.G. VENTZEK, Y. SAKAI, *Hokkaido University* K. KITAMORI, H. TAGASHIRA, *Hokkaido Institute of Technology* M. MEYYAPPAN, *NASA Ames Research Center* Simulations of the periodic steady state plasma dynamics in rf capacitively coupled discharges (CCPs) are at a mature level. The modelling capability for pulsed discharges and transient capacitively coupled discharges is at a less mature level. We present the results of 1 dimensional fluid simulations of rf CCP discharges in argon, chlorine and silane. We find that when dimensionality is considered, the transients often take 10s of thousands of cycles to re-stabilize. This in itself has important implications for the simulation of pulsed sources. Often, a transient can result in a near extinguishing of the plasma. We interpret the observed transients in terms of both transport and chemistry and illustrate how this interpretation may be used to reduce the dimensionality of a model resulting in simulations which can capture long time-scale pulsed discharge pulse-periodic steady states.

BM2 3

WITHDRAWN

---

## SESSION BM2: PULSED PLASMA

Monday morning, 6 October 1997

Tripp Commons, Memorial Union at 10:15

Larry Overzet, Univ. of Texas/Dallas, presiding

10:15

**BM2 1 Time delays in rapidly pulsed capacitive discharges** R.W. BOSWELL, *RSPHysSE, Australian National University, Canberra, ACT 0200, Australia* C. CHARLES, *RSPHysSE, Australian National University, Canberra, ACT 0200, Australia* In rapidly pulsed rf parallel plate systems there are two time periods which define the initial stages of the discharge. The first is the time necessary for the gas between the electrodes to break down and for the debye length to enter the system. At typical operating pressures of around 50 mTorr, this time is of the order of 100's of nanoseconds (a few rf cycles) and the ions created during the avalanche ionization do not have time to diffuse to the walls of the system. The second is the time necessary to charge the blocking or tune

10:45

**BM2 4 Simulation of Inductively-Coupled Pulsed Plasmas.** D.P. LYMBEROPOULOS, *Applied Materials* V.I. KOLOBOV, D.J. ECONOMOU, *University of Houston* \* Pulsed plasmas offer opportunities for charge-free etching, better selectivity and uniformity, and reduced particle formation. We have developed a self-consistent fluid simulation tool for inductively coupled plasmas in which the power source is pulsed with a period of 10-500 ms. The substrate electrode is biased by a separate power supply of variable frequency. Both electropositive (argon) and electronegative (chlorine) discharges have been examined with special emphasis



on phenomena occurring in the afterglow. The thin sheath is resolved in the simulation allowing detailed studies of the effect of substrate bias on fluxes and energy distributions of charged particles bombarding the substrate. Also, the complex thinning and thickening of the sheath as a function of time can be followed. Results will be presented on the important spatiotemporal dynamics of the plasma as a function of pulse period, duty cycle, and frequency of substrate bias. The implications of these results for charge-free processing will be discussed in combination with relevant experimental observations.

\*Work at the University of Houston supported by NSF and Sandia/SEMATECH

11:00

**BM2 5 Pulsed plasma discharges in a magnetically confined inductively coupled plasma source** M. HARPER, *ERC for Plasm-Aided Manufacturing, University of Wisconsin-Madison* M. SARFATY, P. SANDSTROM, N. HERSHKOWITZ, *ERC for Plasm-Aided Manufacturing, University of Wisconsin-Madison* Initial pulse time-modulated plasma discharges are conducted to study the benefits over conventional continuous wave plasmas. A single and triple Langmuir probe measurements have been made with argon and chlorine plasmas operated at a pulse rate of 5kHz and duty cycle of 50%. During the afterglow the electron temperature decreases rapidly, within a few microseconds, relative to the order of magnitude longer decay time of the ion density. The presence of negative ions in Cl<sub>2</sub> afterglow has been detected by a Langmuir probe. The ratio of electron to ion saturation currents is more than 100 times lower in the afterglow. This is an indication that the electrons are almost completely replaced in the afterglow by negative ions. Time averaged optical emission spectra of CF<sub>4</sub> and argon plasmas using pulse rates of 50 kHz and 50% duty cycle show that pulsing the plasma affects only the fluorine line emission and not the argon lines. This suggests that pulsed plasmas can be used to tailor species concentrations to obtain a desired etch selectivity.

11:15

**BM2 6 Determination of Electron Temperature in a Pulsed Inductively Coupled RF Plasma** A. BROCKHAUS, ST. BEHLE, A. GEORG, V. WINGSCH, J. ENGEMANN, *fnt, University of Wuppertal* We studied a pulsed inductively-coupled plasma generated by 13.56 MHz radiofrequency waves. Pulse frequencies range from DC to 20 kHz. Argon, helium and pure oxygen were used as feedstock gases. Electron densities and energy distribution functions were obtained by RF-filtered Langmuir probes. Characteristics could be reconstructed from time-resolved current traces sampled at different bias voltages. Results show that the effective electron temperature exhibits a pronounced peak at the beginning of the discharge. This effect is attributed to efficient electron heating when the density is relatively low. Electrical diagnostics were complemented by optical emission spectroscopic measurements of selected atomic lines. We determined the time-resolved excitation temperatures from several line intensity ratios and compared them to the results obtained by probes assuming the applicability of the Corona model. Correlation of both methods is discussed<sup>1</sup>.

<sup>1</sup>Work in part supported by Deutsche Forschungsgemeinschaft DFG.

11:30

**BM2 7 Simulation of Unsteady-State Expansion of a Chlorine Plasma into Vacuum** SATOSHI TANAKA, *Hokkaido University* SATOSHI UCHIDA, P.L.G. VENTZEK, Y. SAKAI, *Hokkaido University* K. KITAMORI, H. TAGASHIRA, *Hokkaido Institute of Technology* Good neutral beam sources are characterized by strong beam anisotropy and high directed particle energies. Laser ablation of frozen chlorine may provide such beam characteristics. While experiments by other investigators have proven encouraging, laser ablation, at present, appears to be unable to supply the efficiency (energy, and particle flux) needed for this approach to advance. Sparking the laser ablation plume may do two things: enhance the radical content, introduce a controllable charge content. We are investigating these issues with a Monte Carlo simulation of the early stages of the expanding plasma/gas since it is then, when the plume is collisional, that most of the chemistry and plume directionality is frozen-in. Trends for beam directionality, plume dissociation fraction and charged particle content will be presented as a function of laser fluence and beam spot size.

11:45

**BM2 8 Ion-Ion Plasmas.** \* D.J. ECONOMOU, V.I. KOLOBOV, *University of Houston* Ion-ion plasmas are formed in the late afterglow of pulsed discharges in electronegative gases (e.g., chlorine). In the power-off fraction of the cycle, electrons cool down and attach to form negative ions or are lost to the walls of the container, leaving behind an ion-ion plasma. The fundamentals of ion-ion plasma formation and dynamics will be discussed with emphasis on: (a) the transition from electron-ion to ion-ion plasma, (b) the spatiotemporal dynamics and decay of ion-ion plasmas, and (c) extraction of negative ions from ion-ion plasmas by biasing the substrate electrode. It is shown that these unconventional plasmas possess rich physicochemical characteristics, yet they are of critical practical importance for charge-free semiconductor processing.

\*Supported by NSF and Sandia/SEMATECH

12:00

**BM2 9 Opacity Effects on Line Broadening in Electron Density Analysis of Transient Plasmas** H.K. CHUNG, D.H. COHEN, J.J. MACFARLANE, G.A. MOSES, *University of Wisconsin-Madison* Electron densities in plasmas are often determined from measured line widths by assuming that lines are broadened by Stark and instrumental broadening. Measured lines, however, can be further broadened when they are optically thick. It is found that taking opacity effects into account modifies the shapes as well as the relative intensities of the lines. We have developed a line-fitting program in which the shapes and intensities of several lines are fitted simultaneously in a  $\chi^2$  minimization scheme. We have applied this program to analyze Ar II spectra from transient argon plasmas produced by a high-energy lithium ion beam. Our fitting results show that electron densities can be overestimated by a factor of 2 or 3 depending on line optical depths when they are compared with the case of Stark broadening only. Here, we present details of fitting program and results from Ar II line width analysis.



**SESSION CM1: GLOWS, SWARMS AND GENERAL DISCHARGE PHYSICS**

Monday afternoon, 6 October 1997

Class of '24 Reception Room, Memorial Union at 13:30

Hiroyuki Date, Hokkaido University, presiding

13:30

**CM1 1 Study of Plasma Transport Around Dust Particles with Complex Shapes** \* ERIC R. KEITER, MARK J. KUSHNER, *University of Illinois - Urbana/Champaign* Dust particles in reactive ion etching (RIE) tools often form large agglomerates having complex shapes. Simulations addressing interactions between these agglomerates have been based on simplifying assumptions for the electrostatic field around the particles. These assumptions include that the agglomerate can be represented as a cluster of spherical particles each of which has the charge of an isolated particle and that the electrostatic field around the cluster is the superposition of the plasma shielded electrostatic fields generated by each of the spheres <sup>1</sup>. In this paper we present results from a numerical investigation to test the accuracy of these approximations. An implicit solution of Poisson's equation, and fluid equations for electrons and ions is performed on a nonstructured mesh which is capable of closely approximating the typical shape of agglomerates. The electrostatic field is self consistently generated by solving Poisson's equation while including both plasma space charge and charge collected on the surface of the agglomerate. Trajectories of test particles in the vicinity of the agglomerate are used to compare the electrostatic fields generated by the superposition approximation, and the direct solution.

\*Work supported by SRC, NSF, ARPA/NCSU and the U of Wisc. ERC

<sup>1</sup>F. Huang and M.J. Kushner, *J. Appl. Phys.*, 81 (9) 1. May 1997

13:45

**CM1 2 Collective sheaths around dust ensembles in a helium glow discharge** B.N. GANGULY, A. GARSCADDEN, P. BLETZINGER, P.D. HAALAND, *Wright Laboratory, WPAFB, OH* Light scattering and plasma induced emission measurements were made in a dusty plasma produced in a low frequency 1 to 2 Torr helium discharge with asymmetric graphite electrodes. These show that when the dust density growth creates a thin layer of dust all around the edge of the large electrode sheath, the latter expands. This result indicates an increase in potential drop which is also observed in the V-I measurements. Similarly, a thick sheath appears on the side of the dust layer facing the large electrode. The thickness of the dust sheath on the plasma side is much smaller. The disk of dust acts like a suspended insulator that is charged to different potentials on its two sides, thus creating two double layers. The estimates of the electric field gradient inside the dust layers yield self-consistent values of the trapped space-charge. Also in other geometries, the measured (using a telecentric lens) correlated counter-streaming charged particle motions reveal the existence of triple layers at the boundaries of the self-organized dusts. The triple layer barrier heights are estimated to be about 0.1 eV from the kinetic energies of the trapped particles.

14:00

**CM1 3 Electron Transport in CF<sub>4</sub> by using DNP of the Boltzmann equation** M. KURIHARA, N. NAKANO, T. MAKABE, *Keio University Yokohama, Japan* Negative ion plasma in CF<sub>4</sub> is extensively used for dry etching of semiconductor devices. We

first recompiled a set of cross-sections for e+CF<sub>4</sub> from the original results of Nakamura <sup>1</sup> by considering the recent cross-sections for neutral dissociations <sup>2</sup> and partial ionizations. It's primarily important to investigate the electron transport in CF<sub>4</sub> in RF field. The electron velocity distribution function under density gradient expansion and the corresponding swarm parameters in CF<sub>4</sub> are calculated by using a direct numerical procedure(DNP) <sup>3</sup> of the Boltzmann equation in DC field and a wide range of AC frequency (100kHz ≤ f ≤ 1GHz). In RF field, the time averaged value of the electron energy ⟨ε⟩<sub>DC</sub> and the longitudinal diffusion coefficient ND<sub>LDC</sub> have the peaks as a function of frequency. The drift velocity v<sub>d</sub>(t) shows an overshoot just after the zero crossing of the field, due to the presence of negative differential conductivity in a DC field. In high frequency, ND<sub>L</sub> shows the anomalous property which satisfies ND<sub>L</sub> ≥ ND<sub>T</sub> at a certain phase. It depends on the relation among the frequency ω, energy and momentum relaxation times, τ<sub>ε</sub> and τ<sub>m</sub>.

<sup>1</sup>Y. Nakamura, unpublished.

<sup>2</sup>T. Nakano and H. Sugai, *Contrib. Plasma Phys.*, 35, 415-20 (1992)

<sup>3</sup>K. Maeda, T. Makabe, N. Nakano, S. Bzenic and Z. Lj. Petrovic, *Phys. Rev. E* 55, 5901-8 (1997)

14:15

**CM1 4 Boundary Effects on Arrival-Time-Spectra (ATS) Measurements of Electron Swarms** HIROYUKI DATE, *Hokkaido University* P.L.G. VENTZEK, *Hokkaido University* K. KONDO, *Anan College of Technology* H. HASEGAWA, *Tomakomai National College of Technology* M. SHIMOZUMA, *Hokkaido University* H. TAGASHIRA, *Hokkaido University* We present results from a Monte Carlo simulation of arrival-time-spectra (ATS) measurements of electron swarms. In ATS measurements, arrival-time spectra of electrons from a source up-stream are obtained from a signal proportional to the electron flux adjacent to the anode surface using shutter electrodes in a drift tube. In our simulation, the effect of the anode boundary on the electron density and the flux near the anode is examined. It is likely that the anode itself could interfere with the accurate estimation of the density and flux of electrons because electrons which are absorbed may not back-diffuse into the bulk and that ATS theory is based upon the isolated electron swarm theory (boundary free). Our results show that although there is an exponential decay of electron density by the anode; the flux does not change in its spatial distribution. Consequently, we feel the interpretation of double-shutter ATS experiments using boundary free theory is appropriate.

14:30

**CM1 5 Spatio-Temporal Development of Electron Swarms in Gases** HIROTAKA SUGAWARA, Y. SAKAI, *Hokkaido University* H. TAGASHIRA, K. KITAMORI, *Hokkaido Institute of Technology* In time-of-flight experiments for obtaining electron transport coefficients, the spatial distribution of electrons, p(x), is often approximated as a Gaussian distribution. The validity of this approximation is theoretically confirmed in the present work. The spatio-temporal development of electron swarms under a uniform electric field is described in terms of series of moment equations. When a sufficient number of spatial moments are calculated, p(x) is derived from their instantaneous values using a Hermite polynomial expansion technique. The weight of the n-th order Hermite component is represented by orders (≤ n) of the electron diffusion coefficients D<sub>n</sub>. Their representations indicate that the normalized form of p(x) tends to a Gaussian distribution through relaxation processes. A time constant τ = D<sub>3</sub><sup>2</sup>/D<sub>L</sub><sup>3</sup> is introduced to evaluate the speed of convergence of p(x) to a Gaussian distribution. Here, D<sub>L</sub>

and  $D_3$  are the second and third order longitudinal diffusion coefficients.  $p(x)$  can be regarded as a Gaussian distribution when  $\sqrt{\pi}t \ll 1$ . As an example, an electron swarm in  $\text{SF}_6$  at  $E/N = 1414$  Td is simulated using a propagator method. Electron transport coefficients and  $p(x)$  obtained by the propagator method agree well with the results from a Monte Carlo simulation.

14:45

**CM1 6 Kinetic description of large-scale low pressure glow discharges** UWE KORTSHAGEN, BRIAN HEIL, *University of Minnesota, Dept. of Mech. Engineering* In recent years the so called "nonlocal approximation" to the solution of the electron Boltzmann equation has attracted considerable attention as an extremely efficient method for the kinetic modeling of low pressure discharges. However, it appears that modern discharges, which are optimized to provide large-scale plasma uniformity, are explicitly designed to work in a regime, in which the nonlocal approximation is no longer strictly valid. In the presentation we discuss results of a hybrid model, which is based on the natural division of the electron distribution function into a nonlocal body, which is determined by elastic collisions only, and a high energy part which requires a more complete treatment due to the action of inelastic collisions and wall losses of electrons. The method is applied to an inductively coupled low pressure discharge. We discuss the transition from plasma density profiles maximal on the discharge axis to plasma density profiles with off-center maxima, which has been observed in experiments. A positive feedback mechanism involved in this transition is pointed out.

15:00

**CM1 7 The self-separation of the multi-component plasma into regions with different ion composition** I.D. KAGANOVICH, *University Bochum, Germany* L.D. TSENDIN, *St. Petersburg Technical State University, Russia* The study of multi-species plasma properties are important for practically all modern plasma applications. It is obtained that stratification of such a plasma into the regions with different ion composition is its universal property. The detailed analysis of the transport problems for multi-species non-isothermal plasma was performed for discharges in electronegative gases. The obtained profiles of ion densities consisted of two regions of different ion composition. The first one is situated near the discharge boundary; negative ion density is small here compared with electron and positive ion densities. The second region is situated in the discharge center where values of electron density are small here compared with ion ones. These regions are divided by narrow transition region where ion density profiles have a very steep slope; practically ion density shocks are formed in this region. The derived formalism is applied for the analysis of spatial structures of a positive column and of a RF discharge with negative ions.

15:15

**CM1 8 Fully self-consistent kinetic Convected Scheme simulation of a positive column discharge** G. J. PARKER, *Lawrence Livermore National Laboratory* W. N. G. HITCHON, *University of Wisconsin-Madison* The Convected Scheme (CS) provides a solution of the Boltzmann equation by using a phase-space computational mesh on which particle densities are iterated in time by use of Green's functions or "propagators." A new propagator to describe the collisionless radial motion in an arbitrary radial potential is presented and discussed. This propagator continuously launches moving cells from a fixed phase space mesh. After a finite amount of time, each of these moving cells are emptied by collisions and are no longer followed. The new CS is used to calculate electron and ion transport in positive column discharges

over a range of neutral pressures. The axial electric field is adjusted to give a specified axial current while the radial fields are found self-consistently via Poisson's equation. Results are compared to other simulations when available.

15:30

**CM1 9 A Self-Consistent Energy-Resolved Model of the D. C. Positive Column** EDWARD A. RICHLEY, *Xerox PARC* A method for generating a self-consistent determination of the electron energy distribution function in the D. C. positive column is necessary for a thorough understanding of the fundamental physics of these discharges. This talk will describe such a model in which the 2-term spherical harmonic expansion of the EEDF is solved simultaneously with the ion equations of motion and Poisson's equation in order to produce a complete solution based on fundamental transport properties. The solution technique is based on techniques developed for time-dependent simulations of two-dimensional reactive flow. Emphasis will be on the numerical methods employed, and on the peculiarities involved in their application to such a complicated and unusual problem. Some results for a practical situation will be discussed.

15:45

**CM1 10 Nonequilibrium Positive Column.** J. H. INGOLD, *One Bratenahl Place #610, Bratenahl, OH 44108* The DC positive column is modeled with a system of moment equations that ensure conservation of the following quantities: electron and ion densities, electron momentum and energy, and ion momentum. Moment equations for electron properties are derived from equations for  $f_0(\mathbf{r}, \mathbf{v})$  and  $f_1(r, v)$  based on the two term Legendre expansion of the EEDF. Ion temperature is assumed to be zero. In nonequilibrium, it is assumed that electron transport coefficients and collision frequencies bear the same relation to average energy as they do in equilibrium—according to a 0-D Boltzmann solution. Model results in the nonequilibrium regime agree closely with published results of a numerical solution of the 1-D Boltzmann equation, including results for radial heat flow in the electron gas with radially varying average energy. The nonequilibrium model transitions smoothly to the traditional equilibrium model at sufficiently high pressure. A criterion for validity of the equilibrium model is derived, showing that pressure-radius product  $PR$  must be in the range 50-100 Torr-cm for equilibrium to prevail in a neon positive column.

---

## SESSION CM2: FUTURE PROCESSING TRENDS

Monday afternoon, 6 October 1997

Tripp Commons, Memorial Union at 13:30

Tom Ni, Lam Research, presiding

### Contributed Paper

13:30

**CM2 1 Evolving Window Factor Analysis (EWFA) and Multiple Curve Resolution (MCR): New Techniques for Endpoint and Fault Detection in HDP Oxide Etching** HAROLD M. ANDERSON, *University of New Mexico* RAY FORRISTER, *University of New Mexico* ENLIAN LU, QINGYUN YANG, *SEMATECH* ION C. ABRAHAM, *UW-Madison Plasma ERC* R. CLAUDE WOODS, *UW-Madison Plasma ERC* Analytic techniques are needed for real time monitoring of the complex chemistry of HDP oxide etching. EWFA and MCR are two multivariate

analysis techniques that allow one to dynamically track the principal components of the oxide etch process. The techniques are applied in this study to OES and downstream FTIR spectral data gathered from an AMAT 5300 HDP oxide etcher. EWFA analysis, in combination with either OES or FTIR, is shown to be a useful tool for endpoint detection for wafers with exposed oxide areas as low as 0.1%. EWFA is also shown to be useful for automatic fault detection. MCR is used to depict the dynamic rate of formation (or

depletion) of the principal chemical species in the plasma during the etch. For the case of contact hole etching, the principal components display an unexpected accelerated growth and decay cycle around endpoint. These findings have implications for feature scale modeling, as well as endpoint and fault detection.<sup>1</sup>

<sup>1</sup>This work has been supported by SEMATECH

### *Invited Papers*

13:45

#### **CM2 2 Ultrahigh-Aspect-Ratio Contact Hole Etching.**

NAOKATSU Ikegami, *VLSI R and D Center, Oki Electric Ind. Co., Ltd.*

An ultrasmall, 60nm-diameter, 2um-deep contact hole pattern of BPSG film was successfully fabricated using a poly-Si mask and a magnetically enhanced reactive-ion-etching system. Significantly weaker dependence of etch rate on aspect ratio (AR) was obtained up to AR=30, showing that the energetic ions (and/or neutralized molecules) with a sufficient flux for etching reaction are supplied onto the hole bottom even in such an extremely fine feature. On the other hand, neutral supply of polymer precursors onto the hole bottom (Si substrate) is not sufficient for polymerization in holes with aspect ratios greater than 10, where several energetic particles reach the hole bottoms and contribute to the etching reaction with Si substrates. For features with dimensions below 100nm, processing of vertical profiles is extremely difficult, and problems in the form of bowing at the sidewalls of the holes can occur. The shape of the etched feature and the occurrence of etch stops were shown to be in a trade-off relationship. However, vertical profiles were successfully obtained with diameters greater than 100nm without etch stops. It is possible that ion flux is significantly influenced (reduced) when ions pass through the poly-Si mask, rather than through the BPSG hole. The bowing is associated with bending of the incident ion trajectories, where the first stage of the trajectory change occurs at the mask, and subsequent multiple scattering of ions at the sidewall of the hole can occur. Other factors include sidewall protection by redeposited Si that was sputtered from the poly-Si mask and/or the deposited fluorocarbon polymers, and the effects of ion flux and energy bombarding these deposited materials. In the future, it will be necessary to clarify the details of the mechanisms of these phenomena and to establish technologies to control them.

14:15

#### **CM2 3 Contact Etch Scaling with Contact Dimension.**

SUSAN MCNEVIN, *Bell Labs, Lucent Technologies*\*

It is known that the contact etch rate decreases with decreasing diameter. Etch depth measurements for deep sub-micron contacts will be shown to depend linearly on (1/contact diameter). This experimental dependence will then be compared to that predicted for various theoretical models of the contact etching. One way in which these models differ is the species which is assumed to be rate limiting, ions or neutrals. Another difference is the interaction of neutrals with the contact sidewalls. In some models the walls are infinitely reflective, while in others they are infinitely reactive. The models also differ in the effect of the contact sidewalls on the ion trajectory. All of the models predict a decreasing etch depth as a function of contact diameter. However, some of the models more accurately predict the observed (1/contact diameter) dependence of the measured etch depth. It will be suggested that elements of the various theoretical models be combined. In particular, contact etching probably depends on both the ions and neutrals. Accurate models would therefore take into account the different aspect ratio dependences of these charged and uncharged species. It is also urged that modeling should address not only the etch depth at a given etch time, but also as a function of the etch time. The models should also include calculations for the side wall angle and the curvature of the etching front in the oxide.

\*M. Cerullo and J.T.C.Lee

14:45

#### **CM2 4 Interferometric Lithography for Nanoscale Fabrication.\***

S. R. J. BRUECK, *Center for High Technology Materials, University of New Mexico*

The Si industry is maintaining and even accelerating the historical rate of decrease in the critical dimension (CD - smallest printed feature size) of ULSI circuits. The current industry roadmap calls for introduction of 180-nm features in manufacturing in 1999 for logic circuits (relaxed line:space ratio) and in 2000 for memory products (1:1 line:space ratio). Succeeding generations (130 nm and 100 nm, etc.) follow at three year intervals. This rapid pace of change has implications not only for the lithography community, but for all related manufacturing processes including etching and deposition. An overview of the current status of potential future generation lithographic techniques and of the implications for gaseous electronic processing will be presented. As just one example, the limits in depth-of-field and photoresist mechanical properties will likely lead to thinner resist layers, demanding increased selectivity during etching. Interferometric lithography is a newly developed optical technique that allows fabrication of the next several CD generations with currently available sources and photoresist systems, enabling immediate development of the necessary etch and deposi-



tion tools - before the availability of a complete lithographic solution. Process development results for 180-nm features at I-line (365-nm wavelength) will be presented illustrating the effects of surface tension in limiting the resist thickness. Imaging interferometric lithography is a newly developed technique providing a true integration of imaging optical and interferometric techniques that offers the potential of extending optical lithography to beyond 70 nm. The current status of this technology will be discussed.

\*Supported by DARPA and SEMATECH

### Contributed Papers

15:15

**CM2 5 Process Development for Deposition of Chromium Oxide Using Plasma Source Ion Implantation** SHAMIM MALIK, *University of Wisconsin-Madison* In Plasma Source Ion Implantation (PSII)1,2 a substrate is immersed in a plasma and pulse biased to a high negative voltage ( 50kV). Ions are injected into the near surface of substrate material under the influence of the electric field. In order to produce Energetic Ion Assisted Mixing And Deposition (EIAMAD) of films in PSII, materials of interest are sputtered (using DC and RF power to the sputter target) onto a substrate and simultaneously negative bias pulses of upto 15 kV are applied to the substrate itself. We have performed deposition of chromium oxide inside hollow cylinder and on planar geometry. Chromium oxide forms various oxides with different colors and atomic composition. The process characteristics, plasma parameters, and deposition rates have been evaluated. Analysis of these results will be presented. \*This work was supported by NSF. No DMI-9528746, US-Army No. DAALH 03-94-G-0283 IJ. R. Conrad, *et al.* J. Appl. Phys.62, 4951 (1987). 2M.M. Shamim *et al.*, J. Vac. Sci. Technol. 12(2), 843 (1994).

15:30

**CM2 6 Simulation of Plasma Enhanced CVD with Irregular Substrate Geometry** DA ZHANG, *University of Illinois - Urbana/Champaign* MANOJ DALVIE, *Becton Dickinson Research Center* MARK J. KUSHNER, *University of Illinois - Urbana/Champaign* \* The desire to replace glass vials and tubes with plastic has motivated investigation of the deposition of barrier coatings of SiO<sub>2</sub> by plasma enhanced chemical vapor deposition (PECVD) in low pressure rf discharges. The economics of the process requires that many pieces be simultaneously processed, for example, an array of vertically standing containers on the powered electrode. The uniformity of deposition is then determined by the plasma properties generated by the interaction of closely spaced arrays of rf powered posts. These discharge conditions were investigated using the Hybrid Plasma Equipment Model (HPEM). We found that the uniformity of reactive species (ions, radicals) incident on the verticle and horizontal surfaces of the tubes was strongly affected by the spacing between tubes and the depth of the plasma above the tubes. Hollow cathode behavior was observed for critical pd (pressure-distance) arrangements of the tubes, as was segmentation of the plasma into distinct regions, particularly with attaching gas mixtures. Comparisons to experimental data for deposition uniformity will be presented.

\*Work supported by Becton Dickinson, National Science Foundation, and the U of Wisconsin ERC

15:45

**CM2 7 Simulations of Remote Ar/O<sub>2</sub> and Ar/N<sub>2</sub>O Plasmas for Oxide Growth and Interface Treatments\*** RON KINDER, MARK J. KUSHNER, *University of Illinois-Urbana/Champaign* Remote plasma reactors are being developed for treating surfaces between layers in MOS (metal-oxide-semiconductor) stacks, and for depositing (or growing) the SiO<sub>2</sub> layer. Systematic differ-

ences in the properties of oxide layers produced in remote plasma reactors have been observed when using different source gases for the oxygen precursors, presumably resulting from variations in the deposition precursors. In this work the two-dimensional Hybrid Plasma Equipment Model (HPEM) has been applied to investigating remote plasma reactors operating in Ar/O<sub>2</sub> and Ar/N<sub>2</sub>O mixtures. A statistical design of experiments is used to analyze reactant fluxes (ions, oxygen radicals and molecular excited states) to the substrate over a large parameter space in pressure (10s to 100s mTorr) and power deposition (a few to 100 W). Comparison to experimental measurements are used to correlate reactant fluxes with film properties.

\*Research supported by ARPA/NCSU, SRC and NSF (ECS94-04133, CTS 94-12565).

---

### SESSION DMP1: POSTER SESSION: ELECTRON-MOLECULE COLLISIONS

Monday afternoon, 6 October 1997

Great Hall, Memorial Union at 16:00

Elizabeth A. Den Hartog, Univ. of Wisc., presiding

**DMP1 1 Isotope effects in O(<sup>1</sup>S) production following electron impact on H<sub>2</sub>O and D<sub>2</sub>O.** \* JOSEPH DERBYSHIRE, WLADYSLAW KEDZIERSKI, WILLIAM McCONKEY, *University of Windsor* A special xenon-matrix detector which is selectively sensitive to O(<sup>1</sup>S) atoms has been used to monitor the dissociation of normal and heavy water into this fragment over an incident energy range from threshold to 400 eV. By pulsing the electron beam and using time-of-flight techniques, the fragment energies have been measured. These coupled with measurements of production thresholds have enabled specific dissociation channels to be identified. Cross sections have been made absolute using the production of O(<sup>1</sup>S) from CO<sub>2</sub> as a secondary standard. Significant isotope effects between the two targets have been quantified.

\*Research supported by the Natural Sciences and Engineering Research Council of Canada

**DMP1 2 OH(X) production following electron impact on H<sub>2</sub>O\*** TAREK HARB, WLADYSLAW KEDZIERSKI, WILLIAM McCONKEY, *University of Windsor* Using a magnetically-collimated electron beam crossed with a pulsed supersonic gas beam, the break-up of water into ground state OH fragments has been probed using LIF techniques. By varying the delay between the electron and YAG/dye laser pulses, separation between the slow and fast fragments can be achieved. Particular attention is paid to the near threshold region to seek to distinguish between the various dissociation mechanisms which can occur.

\*Research supported by the Natural Sciences and Engineering Research Council of Canada

**DMP1 3 Non-Local Theory of Dissociative Electron Attachment to H<sub>2</sub> and HF Molecules** \* I.I. FABRIKANT, G.A. GALLUP, Y. XU, *Univ. of Nebraska* The process of the dissociative electron attachment is governed by the non-local dynamics describing the nuclear motion of the intermediate negative ion.<sup>1</sup> We present an approach which combines *ab initio* calculations of the energy and the width of the intermediate resonance state with a quasi-classical treatment of the non-local nuclear dynamics. The wave function of the diabatic negative ion state is calculated using a Gaussian basis. The interaction with the electron continuum is included using the Fano-Feshbach projection operator approach. At the second stage we solve the nuclear dynamics for non-local complex potential using the quasi-classical approach.<sup>2</sup> Our results for the dissociative attachment to H<sub>2</sub> and HF agree well with previous non-local calculations and with experiment. For HF we investigate how our results depend on inclusion of the long-range interaction in calculation of the continuum wave function.

\*Supported by the National Science Foundation

<sup>1</sup>W. Domcke, *Phys. Rep.* **208**, 97 (1991).

<sup>2</sup>S.A. Kalin and A.K. Kazansky, *J. Phys. B* **23**, 4377 (1990)

**DMP1 4 Dissociative Attachment in Chloroalkanes and the Correlation with Vertical Attachment Energies** \* K. AFLATOONI, G. A. GALLUP, P. D. BURROW, *University of Nebraska, Lincoln* In monochloroalkanes, the peak cross sections for dissociative electron attachment decline exponentially<sup>1</sup> with increasing vertical attachment energies (VAE), that is, with the energies required to form the temporary negative ion states. The latter are observed using electron transmission spectroscopy<sup>2</sup>. In the present work, we have expanded our measurements to include a series of dichloroalkanes. We find that the same exponential dependence continues to still lower VAE, with only one significant exception thus far. Including both sets of molecules, the measured peak cross sections decline exponentially by a factor of 10<sup>5</sup> as the VAE increases from 1.4 eV to 3.5 eV. This behavior is attributed in part to the nearly linear increase in the widths over the resonances over this energy range.

\*Supported by NSF.

<sup>1</sup>D. M. Pearl and P. D. Burrow, *J. Chem. Phys.* **101**, 2940 (1994).

<sup>2</sup>L. Sanche and G. J. Schulz, *Phys. Rev. A* **5**, 1672 (1972).

**DMP1 5 Electron Collisions with C<sub>2</sub>F<sub>6</sub> and *c*-C<sub>4</sub>F<sub>8</sub>** C. WINSTEAD, C.-H. LEE, V. MCKOY, *Caltech* We have used the Schwinger multichannel method to calculate elastic and inelastic cross sections for low-energy electrons colliding with the fluorocarbon gases C<sub>2</sub>F<sub>6</sub> and *c*-C<sub>4</sub>F<sub>8</sub>, which are used extensively in plasma etching of semiconductors. Elastic cross sections show multiple shape resonances that can be classified by symmetry on the basis of the present calculations. Together with studies of excited-state potential energy surfaces, the inelastic cross sections provide information on the dissociation of these molecules following electron-impact excitation. We analyze the relation between our results and available measurements of the elastic, total, ionization, and neutral-dissociation cross sections.

**DMP1 6 Electron Collisions with CF<sub>2</sub>, CHF, and CF<sub>3</sub> Radicals** C.-H. LEE, C. WINSTEAD, V. MCKOY, *Caltech* We have calculated electronically elastic and inelastic cross sections for collisions of low-energy electrons with the fluorocarbon radicals CF<sub>3</sub>, CF<sub>2</sub> and CHF. Cross sections for such radicals are needed in modelling semiconductor etching plasmas and are difficult to obtain experimentally. Elastic calculations included an accurate represen-

tation of polarization effects, which strongly influence the cross section at the lowest energies. Inelastic calculations were carried out for the lowest singlet and triplet excited states, and the dissociation behavior of these states was studied by conventional electronic structure calculations.

**DMP1 7 Electron Attachment to BCl<sub>3</sub>** W.L. MORGAN, *Kinema Research and Software, Monument, CO 80132* \* I have used a numerical optimization algorithm<sup>1</sup> to derive low energy electron attachment cross sections for BCl<sub>3</sub> from published attachment rate coefficient data. The low energy cross section peaks at about 10 square Angstroms between 0.1 and 0.2 eV. The energy is in agreement with Olthoff's<sup>2</sup> unpublished relative measurements. Due to the size of this cross section, its position relative to the BCl<sub>3</sub> vibrational excitation thresholds, and to the Ramsauer minimum in the Ar momentum transfer cross section, its effects on the drift velocities measured<sup>3</sup> in Ar/BCl<sub>3</sub> mixtures is expected to be significant. This will be discussed using Boltzmann calculations of the drift velocities in such mixtures.

\*Supported by NSF through a grant to ITAMP at Harvard University and the Smithsonian Astrophysical Observatory.

<sup>1</sup>W.L. Morgan, *Phys. Rev. A* **44**, 1677 (1991); *J. Phys. D* **26**, 209 (1993).

<sup>2</sup>J.K. Olthoff, Ph.D. Dissertation, University of Maryland (1985).

<sup>3</sup>D.L. Mosteller, Jr., *et al.*, *J. Appl. Phys.* **74**, 2247 (1993).

**DMP1 8 Electron Attachment to Electronically Excited Molecules** R. B. SIEGEL, J. K. OLTHOFF, L. G. CHRISTOPHOROU, *NIST* Few measurements of absolute electron attachment cross sections to molecules in electronic excited states exist in spite of evidence that the attachment cross section to an electronically excited molecule may be orders of magnitude larger than the corresponding cross section for the target molecule in its ground state.<sup>1,2</sup> Because of the importance of this process and the lack of measurements, we have designed and built an apparatus capable of measuring absolute electron attachment cross sections to electronically excited molecules under single collision conditions. We use a laser-excited effusive beam crossed by a monoenergetic electron beam produced by a trochoidal electron monochromator, and detect the resulting negative ions with a quadrupole mass spectrometer. Quantitative cross sections are determined by measuring the fraction of electronically excited molecules in the target beam using a monochromator-PMT combination. Results of SIMION calculations to determine the performance of the instrument and preliminary results for SO<sub>2</sub> will be presented.

<sup>1</sup>L. G. Christophorou *et al.*, in *Linking the Gaseous and Condensed Phases of Matter*, Plenum Press, New York, 1994, p. 415

<sup>2</sup>T. Jaffke *et al.*, *Chem. Phys. Lett.* **203**, 21 (1993)

**DMP1 9 Hydrogen Balmer and Lyman Line Emissions Produced by Electron Impact on TMS, TEOS, and HMDSO** \* K.E. MARTUS, *William Paterson College, Wayne, NJ* P. KURUNCZI, K. BECKER, *Stevens Institute of Technology, Hoboken, NJ* The Si-organic compounds tetramethylsilane (TMS), tetraethoxysilane (TEOS), and hexamethyldisiloxane (HMDSO) are frequently used in gas mixtures in plasmas for plasma-assisted polymerization and deposition applications. Optical emission spectroscopy (OES) and mass spectrometry are routinely used to monitor species concentrations in these plasmas. OES is the only suitable method to monitor hydrogen concentrations. The quantitative interpretation of OES data requires information about the absolute photoemission cross sections of the relevant emission features that are moni-

tored. We report absolute photoemission cross sections and appearance energies for the H Balmer and Lyman line emissions produced by controlled single electron impact on TMS, TEOS, and HMDSO. These measurements complement earlier studies of Si and CH emissions (P. Kurunczi *et al.*, *Contrib. Plasma Phys.* 36 (1996) 723).

\*Work supported by NSF

**DMP1 10 Electron-Impact Induced Fluorescence Cross Sections of Atomic Oxygen Important to Astrophysics** C. NOREN, I. KANIK, G.K. JAMES, J.M. AJELLO, *Jet Propulsion Laboratory, California Institute of Technology, Pasadena, CA 91109, USA* There is a severe lack of available experimental cross section data, especially in the low energy regime, for electron-atom collisions involving neutral species such as OI, NI, CI, etc. This situation is in imbalance with the wealth of observational data currently available from UV spectrographs (IUE, HST, Copernicus, Voyager etc.). One cannot overstate the importance of ultraviolet (UV) lines of neutral oxygen, which is the third most abundant element within normal stars. In this poster we present the preliminary measurements of the emission cross sections of the atomic oxygen 1304-Å EUV triplet lines resulting from low energy electron impact. A high density atomic oxygen beam, created by a microwave discharge source, was intersected at a right angle by a magnetically focused electron beam. A 0.2m Acton spectrometer in tandem with a CsI coated channel electron multiplier was used to analyze the resulting EUV lines emitted perpendicular to both the atomic and electron beams.

**DMP1 11 Electron-Impact Excitation of Nitric Oxide** R. SCOTT SCHAPE, LINDSAY HALL, MARK WAWRZYNIAK, *Lake Forest College* We present electron-impact cross sections for the  $\beta$  system ( $B^2\Pi - X^2\Pi$ ) of nitric oxide for electron energies from threshold to 500 eV. We report emission cross sections measured using the optical method for vibrational transitions in the visible and near IR that do not significantly overlap with other bands.

**DMP1 12 Fluorination Effects in Electron-Polyatomic Molecule Collisions:  $CH_4, C_2H_4$  and  $C_2H_6$**  H TANAKA, T. MA-SAI, T SUZUKI, *Department of Physics, Sophia University, Tokyo, Japan* M. KIMURA, *Yamaguchi University, Yamaguchi 755, Japan* M. A. DILLON, *Argonne National Laboratory* The electron scattering properties of  $CH_3F, CH_2F_2, CHF_3$  and  $CF_4$  have been investigated by a combination of experimental and theoretical methods. Elastic differential cross sections (DCS) for the fluorinated series from  $CH_4$  to  $CF_4$  have been measured using crossed electron and molecular beams in the energy range from 1.5 to 100 eV over the angular range from 15 to 130 Deg. For comparison the continuum multiple-scattering (CMS) method was used to compute the DCS in the same dynamical range. The DCS reported show a few features relating to scattering dynamics and electronic structure: (i) at low energies below 10 eV, the DCS's for  $CH_3F, CH_2F_2$  and  $CHF_3$  increase sharply at a forward scattering angles, a typical characteristic of polar-molecules, and (ii) above 20eV, a shoulder begins to appear in the DCS around 60 Deg as the number of F atoms in a molecule increases. We have carried out the similar studies for fluorinated ethane and ethylene.

---

## SESSION DMP2: POSTER SESSION: ENVIRONMENTAL APPLICATIONS

Monday afternoon, 6 October 1997

Great Hall, Memorial Union at 16:00

Elizabeth A. Den Hartog, Univ. of Wisc., presiding

**DMP2 1 Destruction of  $CH_2Cl_2$  Using a Glow Discharge Scheme** DENNIS MCCORKLE, CHENG-YU MA, LAL PINNADUWAGE, *Oak Ridge National Laboratory and the University of Tennessee, Knoxville* We will present preliminary results of a glow discharge technique for the destruction of volatile organic compounds. Destruction efficiencies for  $CH_2Cl_2$  in Ar/ $CH_2Cl_2$  mixtures were measured using both a continuous and a pulsed glow discharge. A gas chromatograph was used to monitor the destruction efficiency. The destruction efficiency was measured as a function of the total gas pressure. The relative destruction efficiencies for the two discharge techniques will also be presented. \* Work supported by the Environmental Science Management Program of the U.S. Department of Energy. The Oak Ridge National Laboratory is managed by Lockheed Martin Energy Research Corp. for the U. S. DOE under contract No. DE-AC05-96OR22464.

**DMP2 2 Laser Absorption and Fluorescence Spectroscopy of a Dielectric Barrier Discharge for Exhaust Gas Cleaning** M. SPAAN, D. LUGGENHÖLSCHER, V. SCHULZ-VON DER GATHEN, H.-F. DÖBELE, *Institut für Laser- und Plasmaphysik, Universität GH Essen, D-45117 Essen, Germany* Laser spectroscopic studies at a dielectric barrier discharge model reactor operated in the pressure range 0.5 - 1 bar are reported. The characteristic feature of this reactor is its very fast voltage rise to 20 kV in about 300 ns with a repetition rate up to 40 kHz. This steep voltage rise leads to a collective ignition of the discharge filaments in a time interval of about 50 ns. We report on laser absorption spectroscopy at NO molecule ( $\gamma(0,0)$  band) and on spatially resolved observation of the NO destruction close to the filaments which indicates the influence of photodissociation. Comparison with calculated rotational spectra allows to determine the gas temperature. Fluorescence spectroscopy yields relative density distributions of radical species important for the understanding of reaction kinetics. TALIF at 226 nm is applied to determine space and time resolved density distributions of atomic oxygen in the vicinity of the discharge channels. The gas composition at the reactor exit is diagnosed by FTIR spectroscopy.

**DMP2 3 Analysis of Optical Emission Spectroscopy from a Long Transferred Arc for Waste Remediation** \* J.L. GIULIANI, *Naval Research Laboratory* J.E. ROGERSON, R.W. CLARK, P. KEPPLER, V. SHAMAMIAN, B. SARTWELL, *Naval Research Laboratory* D. COUNTS, *Geo-Centers, Inc* The Naval Research Laboratory is investigating the application of plasma arc technology for the on-board remediation of waste material generated by sea faring ships. Part of the research component is to determine the plasma characteristics and radiation production in and near the arc under various operating conditions. In this work we present an analysis of the temperature profile in a 100 kW, 20cm long DC transferred arc for currents between 300 and 360Amps and air flow rates from 60 to 90slpm at atmospheric pressure. The working gas was seeded with hydrogen as a diagnostic. Assuming the temperature peaks at the center of the arc and LTE, the emission ratio  $H_\alpha/H_\beta$  should increase radially outward,



contrary to the observations. A collisional radiative equilibrium model for H and N was developed to calculate synthetic spectra. Comparison with the data using various temperature profiles indicates that photo-pumping from the hot core leads to non-LTE populations and an inversion in the emission ratio, similar to the observed data.

\*Supported by ONR and NSWC.

**DMP2 4 Development of Novel CF<sub>2</sub> Radical Source by Using Laser Ablation of PTFE** K. FUJITA, M. INAYOSHI, M. ITO, M. HORI, T. GOTO, *Quantum Engineering, Nagoya University, JAPAN* In SiO<sub>2</sub>/Si selective etching plasmas, fluorocarbon gas is generally employed. The production of fluorocarbon gas, however, will be restricted because of environmental problems in near future. Therefore, it is necessary to develop new feed gas or feed gas source for avoiding the environmental problems. In this study, we developed a new radical source where polytetrafluoroethylene (PTFE) was employed as a new gas source and ablated by a YAG laser. To characterize the gas component, CF<sub>x</sub> (x=1-3) radical densities were measured by infrared diode laser absorption spectroscopy (IRLAS). The YAG laser beam irradiated the surface of the PTFE target placed at a pressure of  $1 \times 10^{-5}$  Torr. The repetition rate of the YAG laser was 20 Hz. The PTFE target was ablated above energy density of 7 J/cm<sup>2</sup>. When the energy density of the YAG laser was 49.4 J/cm<sup>2</sup>, the pressure of reaction chamber rose to 2.6 mTorr. Under this condition, CF<sub>2</sub> radicals density was  $1.1 \times 10^{13}$  cm<sup>-3</sup>. On the other hand, both CF and CF<sub>3</sub> radical densities were less than  $1 \times 10^{11}$  cm<sup>-3</sup>. These results indicate that CF<sub>2</sub> radicals were efficiently generated and this technique will be applicable for the etching process. Therefore, it was found that PTFE ablation technique using a YAG laser has a great potential for CF<sub>2</sub> radical source.

**DMP2 5 Response of Atmospheric Pressure Arc to Time-Varying Transverse Magnetic Field** MAX KARASIK, L ROQUEMORE, S.J. ZWEBEN, *Princeton Plasma Physics Lab* G.A. WURDEN, *Los Alamos National Lab* Experiments on equilibrium and stability of atmospheric pressure arcs are underway at PPPL to understand and improve the performance of arc furnaces used for processing applications in metallurgy and hazardous waste treatment. In particular, arc deflection due to stray magnetic fields causes uneven melting and increased furnace wall erosion<sup>1</sup>. A 30kW, 500 Amp CW DC experimental arc furnace was constructed with a graphite cathode and a molten steel anode. The arc plasma is diagnosed with a fast-shutter digital camera, light detectors, and voltage and current monitors. A set of experiments on response of the arc to applied transverse DC and AC (up to 10kHz) magnetic field are carried out. Preliminary results indicate that the arc dynamics at low frequencies can be described by a simple fluid model.

<sup>1</sup>N. Ao and M.Nakai. SEASIS Quarterly. Oct. 94. p.20

**DMP2 6 Investigation of a Dielectric-Barrier Discharge for Plasma Processing at Atmospheric Pressure** SHIRSHAK DHALI, JING LI, *Southern Illinois University* \* A dielectric-barrier discharge is an excellent source of plasma at atmospheric pressure. We report the experimental and simulation results of radical production in an air plasma at atmospheric pressure. The results indicate that the dielectric properties have little effect on radical production. We also discuss novel configurations for plasma production in air.

\*This work was partially supported by a grant from NSF

## SESSION DMP3: POSTER SESSION: PULSED PLASMAS (PROCESSING)

Monday afternoon, 6 October 1997

Great Hall, Memorial Union at 16:00

Elizabeth A. Den Hartog, Univ. of Wisc., presiding

**DMP3 1 Relaxation phenomena in pulsed discharges** K.-U. RIEMANN, P. MEYER, TH. DAUBE, *Theoretische Physik 1, Ruhr-Universität Bochum, D-44780 Bochum, Germany* The relaxation of the plasma boundary layer in front of a wall biased to a pulsed negative potential is investigated on the basis of fluid equations as well as by a particle simulation (PIC-MC) method. The electrons are assumed to be Boltzmann distributed, and the ions are dominated by charge exchange collisions. The electron Debye length is smaller than the ion mean free path. Results are presented for various frequencies and pulse forms. We demonstrate typical relaxation phenomena of the sheath and of the presheath on different time scales. For moderate frequencies the maximum ion energy at the wall is significantly smaller than the energy corresponding to the maximum sheath voltage. In the high frequency limit, the pulse form has only little influence and the results are similar to those in rf-discharges.

**DMP3 2 Ignition Phase of a Pulsed Microwave-excited Plasma in Oxygen** A. BROCKHAUS, ST. BEHLE, A. GEORG, V. WINGSCH, J. ENGEMANN, *fmt, University of Wuppertal* A pure oxygen plasma has been investigated for continuous mode as well as for pulsed power operation. Microwave power is fed to the plasma by an annular waveguide with 10 slot line radiators on the inner side (SLAN principle). Plasma diagnostics were performed using electrostatic probe methods, two-dimensional optical emission spectroscopy for excited oxygen mapping, and two-photon laser-induced fluorescence for the quantitative measurement of atomic oxygen. Time-resolved optical emission spectroscopy was possible with a fast gated CCD camera. The temporal and spatial density variation of excited atomic oxygen was monitored during the ignition phase of the discharge. A first signal is visible about 7 μs after power application. It is followed by an emission burst about 15 μs after gas breakdown which is localized nearby the quartz wall. End-on images from the camera prove that the plasma then expands mainly azimuthally. After 150 μs a symmetrical excitation zone with 10 emission maxima has formed and a homogeneous power coupling from all slot antennae is achieved<sup>1</sup>.

<sup>1</sup>Work supported by Bundesministerium für Bildung, Wissenschaft, Forschung und Technologie BMBF.

**DMP3 3 Afterglow Kinetics of Low Pressure Xe/I<sub>2</sub> Mixtures in Inductively Coupled RF Discharges** PAUL N. BARNES, *Wright Laboratory, WPAFB, OH.* An experimental investigation was conducted using absorption spectroscopy and emission spectroscopy of the afterglow from radio frequency inductively coupled discharges of Xe/I<sub>2</sub> mixtures. RF power at 11.5 MHz was supplied to coils surrounding a cylindrical discharge cell. The xenon partial pressures were between 0.5 Torr and 5.0 Torr and the iodine partial pressure was 0.3 Torr. Observations were made as a function of radius and time following the termination of the discharge. Previous results obtained from steady state discharges indicated that the XeI\* excimer is formed by highly excited I<sub>2</sub> and ground state Xe as opposed to the harpoon reaction. <sup>1</sup> Results presented here indicate that the same process occurs in the afterglow. Evidence is presented that ion-ion neutralization is a major precursor reaction

for the formation of other excited species present in the afterglow and not just for  $I^*(^2P_{3/2})$ .<sup>2</sup>

<sup>1</sup>Barnes and Kushner, *J. Appl. Phys.* 80, 5593 (1996).

<sup>2</sup>Barnes and Kushner, *J. Appl. Phys.* (in press).

**DMP3 4 Formation of Ion-Ion Plasma during the Pauses of Pulsed Negative-Ion Current Source** A.A. KUDRYAVTSEV, N.A. KHROMOV, *Institute of Physics, St. Petersburg State University, Russia* An interpretation is proposed of the effect, observed in the literature, of a relative increase in the negative-hydrogen-ion current upon switching to the pulsed power supply regime. It is connected with the escape of electrons from the volume in the initial stages of decay and formation of ion-ion plasma. The presence of negative ions has a substantial influence on the properties of a gas-discharge plasma, as is manifested, in particular, in the nature of the diffusion of its different components. For example<sup>1</sup>, it was found that the decay of such a plasma takes place in two stages. In the first step, one observes a smooth decrease of the positive-ion current to the wall in the almost complete absence of a negative-ion current. Then, after a certain time the negative-ion current suddenly increases and equalizes with positive-ion current. In our opinion, the effects observed in Refs<sup>2</sup> are analogous. On this basis, it is possible to propose an alternative explanations of the these experimental results, based on the particular features of the transport processes in a plasma of an electrically negative gas. This circumstance can have fundamental significance for our understanding of the physical mechanisms of ion sources and optimization of their operation.

<sup>1</sup>D. Smith, A. G. Dean, and N. G. Adams, *J. Phys. D* 7, 1944 (1974)

<sup>2</sup>M. B. Hopkins, M. Bacal, and W. G. Graham, *J. Appl. Phys.* 70, 2009 (1991)

**DMP3 5 Ignition of Pulsed Inductively Coupled Plasmas in the GEC Reference Reactor** \* BLAKE E. CHERRINGTON, LAWRENCE J. OVERZET, *University of Texas at Dallas* The mechanisms of plasma ignition in pulsed inductively coupled plasmas are important in determining the optimum pulse period and duty cycle, and how to efficiently deposit energy in the plasma. The spatial and temporal behavior of pulsed plasma ignition in a GEC reference reactor excited by a planar inductive coil have been studied. The primary diagnostic tool has been imaging of optical emission from the plasma using an electronically shuttered image intensified CCD camera capable of 5 nsec temporal resolution. Studies will be presented of plasma ignition in low pressure (25 microns and below) Argon discharges operating at 13.56 MHz with power levels of up to 300 Watts. Two stages of plasma ignition were found - a low optical emission intensity plasma beginning a few microseconds after the beginning of the RF pulse and a very rapid transition to a high emission intensity (inductive) discharge. The dependence of these stages on gas pressure and power will be shown. The influence of the matching network and details of coil excitation can also be seen.

\*This material is based upon work supported by the Texas Advanced Research Program under Grant No. 009741-043

**DMP3 6 Measurements of the transition to a positive ion - negative ion plasma** \* B. A. SMITH, L. J. OVERZET, B. E. CHERRINGTON, *The University of Texas at Dallas*. Pulsed discharges are of interest partly because they can produce negative ions. For the electronegative gases used in semiconductor processing, there can be a time during the pulse modulation period in

which only negative and positive ions are present, all the electrons having been lost to diffusion or attachment. We have observed this transition to an electron free plasma using a double probe in an inductively coupled SF<sub>6</sub> discharge. The 0.5 microsecond time-resolution of the probe allowed us to resolve the transition from changes in the current-voltage characteristic. The probe current is dominated by the interaction between ions and electrons while electrons are present, and by the flow of negative and positive ions once the electron density becomes small. The electron density can decrease rapidly in an SF<sub>6</sub> afterglow, becoming insignificant as soon as 1 microsecond after removing the rf excitation. The probe construction will be presented along with data indicating the changes to the I-V characteristic caused by the transition to an electron free plasma.

\*This material is based in part upon work supported by the Texas Advanced Research Program under Grant No. 009741-043 and by the National Science Foundation Young Investigator Award No. ECS-9257383.

**DMP3 7 Implantation of Ions from Solid Materials using a Compact Plasma Source** ANDRANIK SARKISSIAN, DENIS LAFRANCE, BARRY STANSFIELD, YVAN PELLETIER, *INRS-Energie et Materiaux, Varennes, Quebec, Canada* Plasma Source Ion Implantation has proved to be a promising technique for the implantation of ions into planar as well as non-planar surfaces. In this paper we will discuss a variant of PSII which we call Isotropic Ion Implantation or 4πII, and which has been found promising for implanting non-gaseous ions into the substrate. The technique uses a biased target inside of a concentric grid, with a surface ECR plasma source localized outside of the grid. The ions are accelerated through the grid toward the target, so that the system resembles an ion source surrounding the target. The ion trajectories are thus determined by the electric potential in the target-grid region. Metallic ions have been produced from a sputtering source located outside the grid, while phosphorus ions have been produced from thermal evaporation. Depth profiles of implanted phosphorus will be shown, along with simulated profiles, which indicate that the main ionic species produced in the source is P<sub>2</sub><sup>+</sup>.

**DMP3 8 Plasma-assisted Recoil Implantation for Shallow Boron Doping in Silicon** \* H.L. LIU, *University of Wisconsin-Madison* S.S. GEARHART, *University of Wisconsin-Madison* J.H. BOOSKE, *University of Wisconsin-Madison* W. WANG, *University of Wisconsin-Madison* An ion beam mixing technique is used to fabricate ultra-shallow p+/n junctions for the application of sub-micron CMOS source/drain formation. In this method, a thin boron layer is first sputtered onto the Si wafer. Then -3kV argon Plasma Source Ion Implantation (PSII) drives the boron atoms into the Si substrate by means of ion beam mixing. This process avoids the hazardous toxic gases, undesirable F co-implantation and F etching effects. Sub-100nm deep p+/n junctions have been formed with this method. Numerical simulations were performed to predict the recoiled boron profiles, which are in agreement with the experimental data. The boron sputter deposition process has been optimized. Auger electron spectroscopy (AES) confirms high purity of the deposited boron films. Numerical Simulations show that the B films with thickness ranging from 5nm to 10nm result in very similar recoiled B profiles. The thickness of 7.5nm is chosen for the deposited B layer to make the entire process more reproducible. Moreover, a part of the implantation damage will be contained in the B layer, which will be removed prior to the annealing step. This should help to alleviate the transient enhanced B diffu-

sion. The research for the recoil implantation of 7.5nm thick B layer is currently underway.

\*Funded by NSF under grant number EEC-8721545

**DMP3 9 Contamination Effects in PSII Fabricated Diodes** \* K. BROWN, *Univ. of Wisconsin* J.L. SHOHET, *Univ. of Wisconsin* J. SHOTT, *Stanford Univ.* P. RISSMAN, *Hewlett-Packard*. Plasma Source Ion Implantation (PSII) can play a key role in microelectronic fabrication, in particular ultra shallow junctions. PSII has many advantages over ion beam implantation including low-energy large-area high dose rastering, beam extraction and focusing. However, it lacks mass selection; so ions can be implanted due to sputtering from the wall or fixtures. Though pn junction diodes have been fabricated using PSII and their performance characterized, previous studies did not vary contamination in a controlled manner. To do this, prime Si wafers were implanted with Al and B in an effort to determine the critical ratio of Al to B at which the diodes no longer function adequately. Al was selected since it is often used in PSII systems. Initial studies showed that diodes, with Al:B ratios of 1:10, had ideality factors below 1.05. To ensure that this effect is not process dependent, the arrays are being fabricated in another facility to determine a definitive value for maximum impurity levels for satisfactory performance.

\*Work supported in part by the NSF under grant EEC-8721545.

**DMP3 10 Role of the Matchbox in Pulsed Capacitively coupled rf discharges** R.W. BOSWELL, *RSPHysSE, Australian National University, Canberra, ACT 0200 Australia* H.B. SMITH, *RSPHysSE, Australian National University, Canberra, ACT 0200, Australia* C. CHARLES, *RSPHysSE, Australian National University, Canberra, ACT 0200, Australia* B. DICKSON, *RSPHysSE, Australian National University, Canberra, ACT 0200, Australia* A. BELINGER, *Balzars Process Systems, FL-9796 Balzers, Liechtenstein, Switzerland* L. DUBOST, *Balzars Process Systems, 5 rue Leon Blum, F.991124 Palaiseau, Cedex, France* J. SAVY, *Institut des Sciences et Techniques de Valenciennes (I.S.T.V) Universite de Valenciennes et du Hainaut Cambresis, B.P.311-59304 Valenciennes cedex France* Pulsed rf plasmas pose particular problems for the design and operation of the impedance matching network connecting the rf generator to the plasma electrode. Primarily, a decision has to be made as to what part of the pulse will have the best tuning, ie. the minimum reflected power. Generally long term (> 1 ms) steady state plasma conditions are used to establish the optimal tuning. However, this is not necessarily the best choice for very short pulse lengths, which are dominated by the breakdown and early evolution of the plasma. During this period parameters such as the plasma density, electron temperature and sheath widths are rapidly evolving, producing large variations in the plasma impedance, which can dramatically effect the resonance conditions with the external circuitry. To demonstrate the interaction between the evolving plasma and the matching network experimental measurements, analytical modelling and computer simulation of the coupled matchbox-plasma system will be presented, with emphasis on the first few microseconds of the discharge.

## SESSION DMP4: POSTER SESSION: GLOWS

Monday afternoon, 6 October 1997

Great Hall, Memorial Union at 16:00

Elizabeth A. Den Hartog, Univ. of Wisc., presiding

**DMP4 1 On the diagnostic of nanometer-sized contaminant particles using dust acoustic waves** UWE KORTSHAGEN, GURPRIT CHANDHOKE, *University of Minnesota, Dept. of Mechanical Engineering* In plasma enhanced chemical vapor deposition (PECVD) nanometer-sized contaminant particles can appear in high concentrations due to gas phase nucleation. The detection of these particles during the nucleation phase is extremely difficult. Particles with diameters of less than 20 nm are practically invisible to laser light scattering methods. In this contribution we discuss the possibility of using dust plasma acoustic waves for an inexpensive and accurate characterization of nanometer-sized dust particles. The dispersion relation of dust plasma sound waves under typical conditions found in PECVD plasmas is analyzed. It is shown that the dispersion characteristics of the sound waves depend sensitively on the particles size. The influence of momentum transfer to neutral gas atoms and of charge fluctuations of these small particles on the dissipation of the dust acoustic waves is discussed.

**DMP4 2 The Influence of Vibrational Excitation on Streamer-to-Arc Transition** A. KNIGNIK, A. FRIDMAN, B. POTAPKIN, *RRC Kurchatov Institute, 123182 Moscow, Russia* Streamer discharges are often applied in modern plasma chemistry. To utilize the non-equilibrium features of corona systems one should prevent discharge from spike formation. It is well known that the probability of streamer-to-arc transition is defined by the total energy release in the translational degree of freedom. Present work is concerned with investigation of the fast gas heating in the streamer channel due to the anharmonic vibrational-vibrational (V-V) exchange. V-V heating was analyzed taking into account the non-Boltzmann (Treanor effect) and the non-stationary character of the vibrational distribution function and eV pumping. It was shown that for gases of polar molecules, such as CO and CO<sub>2</sub>, vibrational kinetics develops relatively fast and anharmonic V-V heating is noticeable and should be taken into account. The second part of the present work is concerned with streamer dynamics and the determination of required energy consumption in the streamer channel for successful streamer-to-arc transition. Under certain assumptions (mainly the invariance of electric field in overlapped secondary streamer) a mathematical model of transition was developed, and analytical evolution dependences in the two limiting cases: 'thin' and 'thick' streamers, were obtained. The developed model was applied to analyze the effect of vibrational heating on streamer dynamics.

**DMP4 3 Electron Energy and Neutral Gas Temperature in a Glow Discharge**<sup>1</sup> S. POPOVIĆ, L. VUŠKOVIĆ, *Old Dominion University* We investigated nonlinear and dispersion effects of strong acoustic waves in weakly ionized gas generated by glow discharge. Direct current glow discharge between two hollow cylindrical electrodes in flowing gas is a convenient arrangement for this kind of study. One of the critical parameters is the ratio of electron mean energy and neutral gas temperature, both associated with characteristic wavespeed in ionized and neutral gas. Models usually assume this parameter to be equal to infinity ("cold ions") and the effects of finite gas kinetic temperature are not included.



We evaluated the axial and radial distributions of electron mean energy and gas temperature in negative glow and positive column of glow discharge in flowing Argon and Nitrogen in the pressure range of 1 to 100 Torr. These two gases are chosen because of their substantially different ionization mechanisms. The difference in discharge penetration depth into the hollow cathode, extent of the negative glow, high energy electron relaxation depth, and axial neutral transport in the two gases are obtained. Results of gas kinetic temperature are compared with reported experiments and calculations in Argon<sup>2</sup> and Nitrogen.<sup>3</sup>

<sup>1</sup>Supported by NASA Langley Research Center.

<sup>2</sup>M. Sato and S. Arima, *J. Phys. D: Appl. Phys.* **23**, 1302 (1990).

<sup>3</sup>H. Brunet and J. Rocca-Serra, *J. Appl. Phys.* **57**, 1574 (1985).

#### DMP4 4 Predictions of Microstreamer Properties in Dielectric Barrier Discharges\*

XUDONG XU, MARK J. KUSHNER, *University of Illinois-Urbana/Champaign* Dielectric Barrier Discharges (DBD) are being investigated for plasma remediation of toxic gases. The microstreamers in DBD's (10s - 100s  $\mu\text{m}$ 's diameter) are terminated by dielectric charging which removes voltage from the gap. The microstreamers grow by radial diffusion into regions of high electric field and subsequent avalanche. 1-d and 2-d plasma hydrodynamics models have been developed to investigate these processes in DBDs sustained in air, nonattaching gases (Ar, N<sub>2</sub>) and highly attaching gas mixtures (10s to 100s ppm of CCl<sub>4</sub>). We found that microstreamers continue to radially expand as long as there is sufficient applied voltage in the absence of dielectric charging in advance of the core of the microstreamer. This observation implies that there is a finite surface conductivity which allows radial flow of current and subsequent charging of the dielectric. Predictions for microstreamer radii using this process agree well with experiments.<sup>1</sup> We also found that in electronegative gases, voltage collapses in the core of the streamer results in cooling and rapid attachment of electrons, creating a core which is largely converted to a negative ion-positive ion plasma, surrounded by an avalanching shell of hot electrons.

\*Work supported by NSF (CTS 94-12565).

<sup>1</sup>J. Coogan, *Trans. Plasma Sci.* **24**, 91 (1996)

#### DMP4 5 Direct Current Hollow Cathode Discharge for a Proton Donor Production<sup>1</sup>

G. BROOKE, S. POPOVIĆ, L. VUŠKOVIĆ, *Old Dominion University* In the negative glow of a hollow cathode discharge, we produced proton donor molecules to be used in charge transfer reactions.<sup>2</sup> Our study involves the development of a hollow cathode discharge in argon mixed with water vapor to produce H<sub>3</sub>O<sup>+</sup> ions as proton donors. The voltage-current characteristics of the discharge were measured over pressures ranging from 0.1 to 1 Torr. The data was found to be in accordance with the mobility-limited model and was used to understand the two observed modes of the hollow cathode discharge. The presence of atomic hydrogen was found from Balmer lines in the visible spectrum emitted from the negative glow of argon-water mixture. We used the emission spectrum of the negative glow to monitor spatial distribution of charged and neutral particles. Results will be presented in the form of two-dimensional plots of proton donor concentration.

<sup>1</sup>Supported by Jeffress Foundation.

<sup>2</sup>D. Smith and N. G. Adams, *Adv. At. Mol. Phys.* **24**, 1 (1987).

**DMP4 6 Nonlocal Electron Kinetics in a Weakly Ionized Plasma\*** E. FURKAL, A.I. SMOLYAKOV, A. HIROSE, *Department of Physics and Engineering Physics, University of Saskatchewan, Saskatoon S7N 5E2 Canada* Electron kinetics in a weakly ionized plasma is analyzed under the condition such that the electron mean free path is not small compared to the characteristic length scale of electric field inhomogeneity. In this case the standard two-term approximation is not valid and higher order spherical harmonics in the perturbed electron distribution function have to be taken into account. The electron distribution function is represented by an infinite series of spherical functions. This results in an infinite hierarchy of coupled equations for the separate angular harmonics that can be reduced to an infinite continued fraction. Expression for the perturbed electron distribution function is found. The conductivity and the surface impedance are obtained for a semi infinite plasma when the Ramsauer effect is taken into consideration. The anomalous penetration of the electric field and heat deposition are analyzed.

\*Supported by NSERC of Canada

#### DMP4 7 Numerical simulation of streamer dynamics in N<sub>2</sub> and SF<sub>6</sub>

Z.S. KANZARI, M. YOUSFI, *CPAT* This work has been devoted to the numerical simulation of the streamer development and propagation in N<sub>2</sub> and SF<sub>6</sub> between plane parallel electrodes with 0.5cm of gap distance, at atmospheric pressure and 300K for gas temperature. This study is based on a discharge model using the transport equations for charged particles, already used in the literature, for streamer propagation i.e the equations of density and momentum conservation. This first order model is closed with the classical local electric field approximation. Due to the sharp gradients in the head of the streamer, this approximation is not necessarily the most appropriate. This is why we have developed a second order model involving also the equation of energy conservation and closed with the approximation of local energy. The results (electric field, densities, potential, etc.) obtained from these two models are analysed and compared thus emphasizing the usefulness of the present second order model.

#### DMP4 8 Ion and Fast-Atom Induced Electron Emission at the Cathode of Argon Discharges

A. V. PHELPS, *JILA, Univ. of Colorado and NIST*. We a) obtain consistency among published beam data for ion-induced and fast-atom-induced electron emission for Ar by separating results for "clean" and "dirty" surfaces and b) model the contributions of various electron production processes at the cathode at breakdown. Here cleaning means heating to  $\approx 2000$  K under good vacuum. For clean surfaces ion and fast-atom induced yields are very different at energies below 3000 eV, while for dirty surfaces, e.g., oxidized surfaces, yields for Ar ion and fast-atom beams are the same at all energies. The energy-independent (potential) ejection of electrons by Ar<sup>+</sup> is much smaller for dirty surfaces than for clean surfaces. The energy dependent (kinetic) ejection by ions and atoms is orders of magnitude larger for dirty surfaces than for clean surfaces. The effective electron yield per ion determined from electrical breakdown data for dirty surfaces increases approximately linearly with  $E/n$  at above 2000 Td. In order to model these effective yields we require much larger ion- and atom-induced electron yields than given by beam experiments. At  $E/n < 500$  Td the effective electron yield per ion calculated from breakdown data increases rapidly with decreasing  $E/n$  as we predict for photoelectron emission by Ar resonance photons. The model requires more than a factor of ten variation in photoelectric yield among experiments.

**DMP4 9 Investigation of the spectrally resolved emission during arc spot ignition on cold cathodes** MICHAEL SCHUMANN, DANIEL NANDELSTADT, ADAM KORBEL, JUERGEN MENTEL, *Ruhr-Universität Bochum, Germany* JOCHEN SCHEIN, *University of Minnesota, Minneapolis, MN, USA* The magnetic blowing of an arc against a third so called commutation electrode CE positioned perpendicularly to the discharge axis, in a distance of 1 mm behind a diaphragm with a hole in the center, allowed a reproducible interaction of the plasma with the electrode to be achieved. A side on view of the cathode surface is imaged onto the entrance of a spectrograph with the surface parallel to the slit. The optical spectrum is recorded with a CCD-camera equipped with a microchannel plate as an amplifier and a fast shutter allowing a minimum exposure time of 5 ns. Spectra are recorded of arc spot ignition on cathodes made of Au, Cu, W, Al, and graphite in atmospheric pressure Ar and H<sub>2</sub>. Two modes of arc spot ignition disclosed by high speed photography in correlation with different surface structures emit distinctly different spectra. The luminous layer preceding arc spot ignition on an inhomogeneous surface emits atomic and ionic lines of the electrode material and atomic lines of the filling gas. The plasma ball formed on a homogeneous cathode surface and the plasma channel bridging the gap between the bulk plasma and the CE at arc spot ignition emit the ionic spectrum of the filling gas argon.

**DMP4 10 Self-Consistent Particle Simulation of the Glow Discharge Plasma and the Background Gas** VLADIMIR SERIKOV, SHINJI KAWAMOTO, *Nippon Sheet Glass Co., Ltd., Japan* KENICHI NANBU, *Institute of Fluid Science, Tohoku University, Japan* A Particle-in-Cell/Direct Simulation Monte Carlo (PIC/DSMC) model has been developed to simulate a glow discharge self-consistently with the background gas flow field which can be affected by the discharge plasma and/or sputtered material atoms. In the model the charged particle motions are considered in a self-consistent electric field produced by the space charge distribution. The neutral background gas and sputtered atoms are treated by the DSMC approach which makes sense, since under the operating conditions characteristic of the plasma-assisted materials processing systems, nonlocal hence nonequilibrium effects are prevailing in the plasma and the neutral gas. To test the model, a one-dimensional DC sputtering discharge in Ar has been simulated wherein a pronounced background gas heating effect was predicted. The gas temperature was calculated readily from the sampled kinetic energy of argon atoms. The results obtained with the use of the developed PIC/DSMC model are compared with those predicted by the PIC/fluid simulation where the gas temperature was calculated by solving the heat conduction equation.

**DMP4 11 1-D TPMC Simulation of Electron Kinetics in a Parallel Plate Magnetron Ar Discharge** M.J. PINHEIRO, *Instituto Superior Tecnico, UTL, Lisboa, Portugal* We report a 1-D (along Pedersen axis) test particle Monte Carlo (TPMC) simulation of electrons behaviour in a parallel plate magnetron discharge, considering a complete set of electronic processes in Ar. The Lorentz's force system of equations is solved yielding the 3 components of the electron velocity for various electric (E) and crossed magnetic field (B) configurations. The main advantage is simplicity albeit phenomena related to the Hall current are not described. Simulation results are presented for various E and B profiles and strength. For a given ExB profile, it is shown that when B increases also increases the electronic density due to a higher confinement but decreases the electronic temperature. At least below 0.1 Torr, the value of pressure (p) at which occurs a maximization of ionizing and elastic collisions increases when B

decreases. It is shown that the direct current grows with p but can decrease with B, depending on the plasma sheath thickness near the cathode. It is analyzed the effect of anisotropic collisions (for both elastic and ionization processes) on the main plasma parameters as well as the conditions to have a more uniform plasma, suitable for surface treatment. Whenever available experimental data exists comparison is made with the simulation and general good agreement is attained.

#### DMP4 12

WITHDRAWN

**DMP4 13 Object Oriented Plasma Process Modelling I.** HORIE, *Hokkaido Institute of Technology* K. KITAMORI, U. OGAWA, *Hokkaido Institute of Technology* P.L.G. VENTZEK, *Hokkaido University* Models for multi-dimensional plasma source simulations are becoming more and more complex. Issues as important as the physics in the model or simulation are maintainability, portability, and adaptability. The ideal is that a simulation be able to access physics modules, geometry information or chemistry data, for example, through a seamless connection. Object oriented models address these needs. Moreover, for a much repeated process in a simulation, such as sampling in a Monte Carlo simulation, it is important to treat sampling as an object so that 1) it may be easily accessed and 2) engineered without threat to the integrity of the simulation. Object oriented languages like JAVA are well suited for these tasks. Using JAVA we illustrate the methodology of object oriented plasma simulation for Legendre Polynomial Weighted Sampling (LPWS) in a Monte Carlo simulation of an inductively coupled plasma (ICP) source as an example.

**DMP4 14 The Electrical Structure of Discharges Modified by Electron Beams** F.A. HAAS, N.ST.J. BRAITHWAITE, *Open University* Injection of an electron beam into a low pressure plasma modifies both the electrical structure and the distributions of charged particle energies. The electrical structure is investigated here in a one-dimensional model by representing the discharge as two collisionless sheaths with a monenergetic electron beam, linked by a quasi-neutral collisional region. The latter is modelled by fluid equations in which the beam current decreases with position. Since the electrodes are connected by an external conductor this implies through Kirchoff's laws that the thermal electron current must correspondingly increase with position. Given the



boundary conditions and beam input at the first electrode then the rest of the system is uniquely described. The model reveals the dependence of the sheath potentials at the emitting and absorbing surfaces on the beam current. The model is relevant to externally injected beams and to electron beams originating from secondary processes on surfaces exposed to the plasma.

**DMP4 15 Self-Consistent Treatment of the Neon Positive Column based on the Nonlocal Approximation** E. J. BENNETT, WM. F. BAILEY, *Air Force Institute of Technology* Characterization and understanding of plasma sources requires accurate yet efficient self-consistent solutions of the coupled electron and ion kinetic equations. A theory<sup>1</sup> has been developed which extends the nonlocal approximation<sup>2</sup> by coupling the solution of the Boltzmann equation for electrons with Poisson's equation and ion moment equations, enabling a self-consistent solution for the discharge parameters. This theory has been refined by incorporating a self-consistent calculation of electron wall losses. Comparison with experiment, which required a detailed treatment of the metastable population, revealed good agreement in contrast with the results of local theory. Monte Carlo calculations have been performed which further confirm the validity of the nonlocal approximation for the conditions considered.

<sup>1</sup>Bennett, E. J. and Wm. F. Bailey, "Determination of the Self-Consistent Space Charge Potential Using the Nonlocal Approach," *Bulletin of the American Physical Society*, 41(6):1344 (October 1996)

<sup>2</sup>Bernstein, I. B. and T. Holstein, "Electron Energy Distributions in Stationary Discharges," *Physical Review*, 94:1475-1482 (June 1954)

**DMP4 16 Suppression of the Glow-to-Arc Transition in Glow Discharges** \*E.E. KUNHARDT, K. BECKER, L. ARMORER, *Stevens Institute of Technology, Hoboken, NJ, USA* L. PALATINI, *University of Orleans, France* The operating regime of stable glow discharges is limited by instabilities, in particular by the well-known glow-to-arc-transition (GAT). The GAT arises in the cathode fall region of the glow discharge where the electric field is very high and causes a transition from a diffuse uniform glow and to a filamentary, high current arc discharge. While there have been previous efforts to stabilize glow discharges (see e.g. Akishev *et al.*, Proc. XX. ICPIG, Bochum, 1991) even at atmospheric pressures, the proposed concepts tend to be energy inefficient, cumbersome to implement, and lend themselves only to the generation of very small stable glow discharge volumes. We introduce a novel cathode design (patent pending) which allows us to generate and maintain stable, uniform glow discharges at pressures up to atmospheric pressure. The novel cathode design facilitates stabilization by actively limiting the current density in the cathode fall. Full details of the novel concept and experimental results will be presented and discussed at the Conference.

\*Work supported by AFOSR

**DMP4 17 A Boltzmann Equation Analysis of Electron Swarm Parameters in Xe/Ne Mixtures Considering Reactions of Excited Particles** SATOSHI UCHIDA, HIROTAKE SUGAWARA, P.L.G. VENTZEK, YOSUKE SAKAI, *Hokkaido University* Xe/Ne mixtures are important for plasma display panels and UV light sources. However, reactions of excited particles in the mixtures are so complicated that the influence of the excited particles on the discharge parameters is not understood well. In this work, taking account of reactions of excited particles, such as cumulative ionization, Penning ionization, radiation decay, and so on, the elec-

tron swarm parameters in Xe/Ne mixtures are calculated using the Boltzmann equation. The calculation is carried out under steady state Townsend conditions,  $E/N=3\sim 750$  Td,  $K(=N_{Xe}/N_{Ne+Xe})=0\sim 1$ ,  $n_e=10^3\sim 10^{11}$  cm<sup>-3</sup>. Values of  $\alpha/E$  agree with experimental data of Bhattacharya<sup>1</sup>. The  $\alpha/E$  in low  $E/N$  is shown to be brought through the excited particles. The influence of excited particles on other swarm parameters is also discussed.

<sup>1</sup>A.K.Bhattacharya, *Phys.Rev.A*, 13, 1219-25 (1976)

**DMP4 18 Plasma Ion Source Based on Ion-Sound Surface Wave Discharge** \*N.A. AZARENKO, A.A. BISYUKOV, A.V. GAPON, I.B. DENISENKO, *Department of Physics and Technology, Kharkiv State University, 310077 Kharkiv, Ukraine* A. I. SMOLYAKOV, *Department of Physics and Engineering Physics, University of Saskatchewan, Saskatoon S7N 5E2 Canada* A concept of a low-energy ( $\leq 300$ eV) ion-beam source based on the planar ion-sound surface wave discharge is proposed. The beam is formed in the vacuum gap between the plasma surface and the biased metal plate. Ions are extracted from plasma by externally applied DC field from the electrode and deflected by the field of the travelling surface wave. The spatial structure of the travelling ion-sound wave is determined. The ion trajectories in the vacuum gap are investigated, and the energy and angle distribution of the particle flux on the metal surface are obtained for different plasma parameters. It is shown that the angle distribution of the energy and momentum flux can be changed by controlling ion density, amplitude of the surface wave, width of vacuum gap and intensity of extracting DC field. It is shown that significant fraction of the particles have large incidence angles. Such ion beams can be used for the surface processing such as polishing and film deposition.

\*Supported by the Science and Technology Center of Ukraine and NSERC of Canada

**DMP4 19 Monte Carlo Analysis of Swarm Parameters in Magnetic Fields** SATORU NAKAMURA, *Hokkaido Polytechnic College* P.L.G. VENTZEK, *Hokkaido University* K. KITAMORI, H. TAGASHIRA, *Hokkaido Institute of Technology* In inductively coupled plasmas, magnetrons or MERIE's and magnetically confined plasma sources, the influence of magnetic fields on transport parameters is often simplified to scalings with the ratio of the cyclotron frequency to the collision frequency. In high density plasma sources, this simple scaling may be inadequate. We present the results of a Monte Carlo simulation of electron swarms in crossed and parallel dc electric and magnetic fields in an attempt to re-evaluate and investigate scaling parameters for transport coefficients for fluid simulations that may be useful for the consideration of magnetic fields in lower pressure high density plasmas. We consider two cases: methane and argon for pressures ranging from 10 mTorr to 1 Torr, E/P's ranging from 50-500 V/cm/Torr and magnetic fields up to 1kG. We find that the magnetic field influences swarm parameters like drift velocity more strongly than classical theory would predict. In addition, although drift velocities do increase for "low" magnetic fields in the direction of EXB, they ultimately also monotonically decrease for higher magnetic fields.

**DMP4 20 Excitation coefficients for atomic and ionic levels in argon** G.N. MALOVIĆ, J.V. BOŽIN, B.M. JELENKOVIĆ, Z.LJ. PETROVIĆ, *Institute of Physics, University of Belgrade, P.O.Box 57, 11001 Belgrade, Yugoslavia* By using Townsend discharges of Ar we have measured electron excitation coefficients for three

levels of Ar atom ( $3p_5$ ,  $3p_6$ , and  $3p_8$ ) and for four levels of Ar ion ( $^2P$ ,  $^2D$ ,  $^2F$ ,  $^4P$ ). The results are given for a wide range of E/N values, from 30 Td to 6 kTd for atomic transitions, and from 400 Td to 11 kTd for ionic transitions. Here E/N is electric field to gas density ratio, and  $1 \text{ Td} = 10^{-21} \text{ Vm}^2$ . The results for ionic transitions are the first absolute measurements of the excitation coefficients. The apparatus and the procedure for converting the optical emission near anode to the absolute value of the excitation coefficient are the same as in our measurements of excitation of  $2p$  levels of Ar<sup>1</sup>. The excitation coefficients for atomic  $3p$  levels show a maximum between 500 Td and 1 kTd, while for ionic transitions the maximum is between 2.2 and 3.5 kTd.

<sup>1</sup>Božin *et al.*, Phys. Rev. E **53**, 4007 (1996)

**DMP4 21 Spatially Resolved Analysis of Electron Energy Distribution and Transport Properties in Steady State** AKIHIDE TAKEDA, *Shikoku Univ.* NOBUAKI IKUTA, *Chiba Inst.Tech.* Most of electron transport properties have been measured in steady state or in its modulated situations. Exact analyses for the electron behavior in such situations have been expected to evaluate the accuracy and propriety of measurements. However, there have not been any reports on the practical steady state analyses since the electron behavior in the drift space necessarily include the non-equilibrium regions influenced by the initial and boundary conditions. Recently, an exact procedure to analyze the electron behavior in steady state, SST-FTI method, has been developed.<sup>1)</sup> The results of analysis in CF<sub>4</sub> are as below. The non-equilibrium region for electrons near the cathode necessarily appears as a path to reach equilibrium, and the non-equilibrium region in front of the anode is due to the absorption of electrons at the anode, as are well known. Transport properties in the equilibrium region are independent of initial and boundary conditions but dependent on the density gradient in it.<sup>2)</sup> Thus, the validity of this method is verified with the results naturally fitting with theoretical expectations. The possibility of analysis will be extended further to other purposes. For example, the net electron release rate from the cathode governed by the initial energy distribution, the reflection coefficient at the cathode, the reduced electric field and the thickness of gas will be calculated accurately. 1)A.Takeda and N.Ikuta: J.phys.Soc.Jpn.66(1997)1672. 2)H.Tagashira and Y.Sakai: J.Phys.D 10(1997)51.

**DMP4 22 Relation between Longitudinal and Transverse Diffusion Coefficients of Alkali Ions in Noble Gases** M.J. HOGAN, *Salem-Teikyo University* The relation between longitudinal and transverse diffusion coefficients of ions drifting in a neutral gas under the influence of an electric field has been investigated for alkali ions in noble gases. The 125 combinations of ions of Li, Na, K, Rb, and Cs in the neutral gases He, Ne, Ar, Kr, and Xe at gas temperatures of 100, 200, 300, 400 and 500 K were included in this study. Plots of the ratio of the longitudinal-to-transverse diffusion coefficients versus E/N exhibited similar variation in the values of the ratios. As the value of E/N increased from zero, the value of the ratio increased rapidly from one for all ion/neutral/temperature combinations. The ratio peaked at values mostly in the range of 1.2 to 2.5 at E/N values in the range of 20 to 120 Td. As E/N increased further, the ratio values decreased, at an ever lower rate, to values ranging from 0.8 to 1.2. These results suggest the existence of a single function relating the longitudinal and transverse diffusion coefficients.

**DMP4 23 Radially inhomogeneous electron velocity distribution in the positive column plasma** D. UHRLANDT, R. WINKLER, *Institute for Nonthermal-Plasmaphysics Greifswald, Germany* The radial structure of electron kinetic quantities in the positive column of cylindrical dc glow discharges is analysed to reveal the microscopic nature of the electron confinement by the radial space charge potential. To determine the radial alteration of the isotropic and anisotropic parts of the electron velocity distribution function the appropriate inhomogeneous kinetic equation considering the radial electric field action is solved. The kinetic description includes the self-consistent calculation of the excited gas atom densities and the accurate determination of the electron production in the volume. The required boundary conditions are discussed. Results are presented for the column plasma of inert gas discharges at different pressures where the electron kinetic behaviour changes from a distinctly nonlocal to a nearly local behaviour. Main emphasis is placed on the detailed analysis of the radial alteration of the electron particle and energy fluxes and of the spatially resolved electron energy budget in the column plasma.

**DMP4 24 Fluid Modeling of Low Pressure Discharges** \* A. I. SMOLYAKOV, E. FURKAL, *Department of Physics and Engineering Physics, University of Saskatchewan, Saskatoon S7N 5E2 Canada* Modern materials processing applications often require plasma sources operating in regimes of high electron density and low pressure of neutral gas. Under these conditions kinetic effects of the electron motion, such as collisionless wave-particle interactions, becomes important. We formulate fluid type model for description of such kinetic effects in the low collisional regimes. The model consists of moment equations for the electron density, velocity and energy. The kinetic effects are included with kinetic closures for the electron viscosity and heat flux in terms of the lower order moments and electromagnetic field. The kinetic closure are calculated from the linearized kinetic equation. This hybrid fluid/kinetic model reproduces exactly the linear kinetic response and allows calculation of the collisionless heating in the quasilinear approximation. Both fluctuations of the electric and magnetic field are included in the model.

\*Supported by NSERC of Canada

**DMP4 25 Barium Discharge Plasma Apparatus** \* JEFF MACDONAGH-DUMLER, HEIDI M. ANDERSON, J. E. LAWLER, *University of Wisconsin-Madison* Barium has a number of characteristics that indicate it may be a good atomic radiator in a glow discharge. However, its chemical reactivity and the relatively high temperature required to produce a few mTorr vapor pressure present some challenges in creating and observing a Ba glow discharge. At the temperature required for sufficient Ba vapor pressure, the hot Ba will darken most transparent discharge envelope materials. A novel design for a dc discharge apparatus will be described.

\*supported by the NSF and the Wisconsin/Hilldale Fellowship program

**DMP4 26 Electron transmission process in nitrogen** \* H. ITOH, N. IKUTA, *Chiba Institute of Technology* We have performed experiments in order to measure the transmission ratios TR of photoelectrons that moves across the parallel plane electrodes in nitrogen, argon and methane etc<sup>1</sup>. From our experiments in nitrogen, we found three features in the TR. First, the variations of TR against the reduced electric field at a constant gas pressure (0.1 ~ 500 Torr) depended on the electron drift velocity in nitrogen in a wide E/p<sub>0</sub> range for up to 10 V/cm·Torr. Second, if the applied

voltage between both of the electrodes was lower than approximately 0.1V, the TR were independent of the  $E/p_0$ , but were dependent only on the inverse of the gas pressure. Finally, the TR was saturated against  $E/p_0$  near 10 V/cm·Torr. The saturation current in nitrogen agreed with the photoelectric current in a vacuum. Recently, MCS calculations were carried out by us to reexamine the TR which obtained experimentally. The results show that the TR are dominated by the diffusion of electrons and the electron drift velocity. They are closely related to the non-equilibrium and the equilibrium of the electron energy. Detailed results will be shown at the conference.

<sup>1</sup>H.Itoh and N.Ikuta, Contributed Papers of ICPIG XVI, 72 (1983)

**DMP4 27 Radial Heat Flow Nonequilibrium Positive Column**  
J. H. INGOLD, *One Bratenahl Place #610, Bratenahl, OH 44108*  
Moment equations for electron properties in the nonequilibrium DC positive column are derived from equations for  $f_0(\mathbf{r},\mathbf{v})$  and  $f_1(r,v)$  based on the two term Legendre expansion of the EEDF. These equations predict large radial flow of electron energy in the nonequilibrium DC positive column. It is shown that this radial heat flow can be resolved into convective, conductive, and diffusive components. The convective component is small compared with the other two components, which generally flow in opposite directions and nearly cancel each other. It is pointed out that the diffusion component vanishes when  $f_0(\mathbf{r},\mathbf{v})$  is Maxwellian, resulting in little or no radial variation in average energy of electrons.

**DMP4 28 Helical Instabilities of DC Discharge Plasmas**  
XIAOGANG WANG, *University of Iowa*  
DC discharge plasmas have wide-range applications in many areas. Therefore, research for equilibria and helical magnetic instabilities of DC discharge plasmas is a very important subject in low temperature plasma physics. A DC discharge column can be unstable due to helical perturbations and the rotational symmetry of the equilibrium can be destroyed by those modes. An linear study for "slow" magnetic helical instabilities of DC discharges in a cylindrical plasma is developed. Based on a set of electrostatic MHD equations, we investigate "slow" helical modes with an external axial magnetic field. The stability analysis by the criterion obtained in this work shows that the "slow" resistive-viscous helical instabilities are linearly stable in both long wave-length and short wave-length limits. These results are in agreement with numerical results. The most dangerous instability has a wave-length of order of the length of a discharge arc. It is found that an external axial magnetic field can destabilize those helical modes. Those helical instabilities generated by an axial external field are indeed observed in recent experiments.

**DMP4 29 A Prototype Java Plasma Chemistry Database and Modeling Tool Located on the World Wide Web**  
W.K. TRAIL, W.L. MORGAN, *Kinema Research and Software, Monument, CO 80132* /thanksWork partially supported by SEMATECH under subcontract with the Caltech Dept. of Chemistry  
We are developing a database of atomic and molecular data, electron collision cross sections, and plasma chemistry data for use in modeling and simulation of plasma processing of microelectronics. The software is written in Java and resides as a collection of Java Applets on one or more of our sites on the World Wide Web (see theKinema URL). Going beyond providing merely a database, this approach allows us to provide platform independent computational and graphics programs for manipulating and visualizing the data and results. It also allows us to have parts of the database and associated programs distributed on different computers and ultimately to

have the database directly accessible as needed by modeling programs running on users' own desktop computers. We will demonstrate and discuss these developments and their relationship to the future of modeling in gaseous electronics.

**DMP4 30 Low Energy Electron Transport in CHF<sub>3</sub>** \* J.D. CLARK, B.W. WRIGHT, J.D. WRBANEK, *Physics Department, Wright State University*  
A GARSADDEN, *Plasma Research Group, Wright Laboratories, WPAFB*  
Electron transport measurements were made in CHF<sub>3</sub> and CHF<sub>3</sub>-Argon mixtures, using a pulsed Townsend type drift tube. Drift velocities were measured as a function of E/N in pure CHF<sub>3</sub> and mixtures ranging from 0.1 to 2 percent CHF<sub>3</sub> in Argon. The E/N range of 0.04 to 50 Td corresponds to average electron energies less than 10 eV. A two term Boltzmann transport code was used to unfolded a set of low energy electron scattering cross sections for CHF<sub>3</sub>. The dominate cross sections considered are the total momentum transfer and vibrational excitation. In addition electron attachment was observed. The attachment coefficient was measured to rise toward low electron energy. Comparison of experimental and calculated transport parameters will be presented.

\*Supported by Aero Propulsion and Power Directorate, WPAFB, through the Northeastern Center for Electrical Engineering Education.

**DMP4 31 Investigations of Nonlocal Kinetics within a Fully Self-Consistent Plasma Model** \* ERIC KEITER, W. N. G. HITCHON, *University of Wisconsin*  
MARK J. KUSHNER, *University of Illinois*  
In recent years, several models for nonlocal kinetics have appeared, which have not been integrated into fully self consistent plasma simulations. In particular, they have estimated parameters such as the electrostatic potential and have been generally applied to simple gases, such as argon. Here we describe a fully self consistent hybrid plasma model, which includes a nonlocal kinetics EEDF solver and module which solves a spatially dependent (2d-space) Boltzmann equation. We apply the model to analyzing plasmas which have a range of inelastic collisionality (Ar, Ar/N<sub>2</sub>, N<sub>2</sub>), for a variety of pressures and powers. Since the validity of the nonlocal model depends, in part, on the inelastic electron collision processes this range of parameters provides a severe test of the nonlocal approach. As the percentage of nitrogen in Ar/N<sub>2</sub> mixtures increases, the electron energy relaxation length decreases, thus lowering the maximum pressure for which the nonlocal model is valid.

\*Research supported by AFOSR/ARPA (F49620-95-1-0524), SRC, and the University of Wisconsin ERC

**DMP4 32 A DSMC Study of Low Pressure Argon Discharge**  
DAVID HASH, \* M. MEYYAPPAN, † *NASA Ames Research Center*  
Work toward a self-consistent plasma simulation using the DSMC method for examination of the flowfields of low-pressure high density plasma reactors is presented. Presently, DSMC simulations for these applications involve either treating the electrons as a fluid or imposing experimentally determined values for the electron number density profile. In either approach, the electrons themselves are not physically simulated. Self-consistent plasma DSMC simulations have been conducted for aerospace applications but at a severe computational cost due in part to the scalar architectures on which the codes were employed. The present work attempts to conduct such simulations at a more reasonable cost using a plasma version of the object-oriented parallel Cornell DSMC code, MONACO, on an IBM SP-2. Due the availability of experimental data, the GEC reference cell is chosen to conduct



preliminary investigations. An argon discharge is examined thus affording a simple chemistry set with eight gas-phase reactions and five species: Ar, Ar<sup>+</sup>, Ar\*, Ar<sub>2</sub>, and e where Ar\* is a metastable.

\*National Research Council Associate

†Project Manager, Device and Process Modeling Integrated Product Team

---

---

## SESSION DMP5: POSTER SESSION: LIGHTING

Monday afternoon, 6 October 1997

Great Hall, Memorial Union at 16:00

Elizabeth A. Den Hartog, Univ. of Wisc., presiding

**DMP5 1 Microwave Discharges in Sulfur** SCOTT A. ANDERSON, REX ANDERSON, M.L. BRAKE, *The University of Michigan* Optical emission of an argon/sulfur discharge generated in an Asmussen microwave resonant cavity has been observed. High purity sulfur powder was inserted into an 8 mm I.D. quartz tube which was oriented along the axis of the microwave cavity. The quartz discharge tube was back-filled with argon at pressures of 5-10 Torr. A very bright sulfur plasma was generated using a 2.45 GHz continuous source when the cavity was operated in the TM012 mode. A discharge was initiated using microwave power levels between 50 and 100 Watts. Optical emission spectroscopy observed S<sub>2</sub> (B<sup>3</sup>Σ-X<sup>3</sup>Σ) bands. The lighting industry is interested in electrodeless lights with high brightness, such as sulfur discharges.

**DMP5 2 Spherical Negative Glow-Thermionic Cathode Model for Low Pressure Discharges** YAN-MING LI, *OSRAM SYLVANIA INC., 71 Cherry Hill Dr., Beverly, MA 01915* The high density negative glow plasma maintained by the thermionic emitted beam electrons is an important ingredient in overall thermionic cathode operation. In this work, the planar negative glow ambipolar diffusion theory given by <sup>1</sup> is extended to the spherical case. Such modification accommodates the fact that the negative glow plasma often appears as a spherical ball of plasma centered at the cathode hot spot. In addition, the coupling between the thin ion free-fall sheath and the calculation of total ion current transport back to the hot spot becomes more accurate <sup>2, 3</sup>. Coupled with cathode power balance, the model enables the determination of hot spot temperature, cathode fall, plasma and electric field distributions for a given discharge current. The effect of gas convective-conduction cooling on cathode power balance, cathode fall and negative glow discharge characteristics will also be examined.

<sup>1</sup>J. H. Ingold, *Phys. Rev.*, vol. 43, p. 3093 (1991)

<sup>2</sup>R. C. Garner, Y. M. Li, *IEEE ICOPS Conf. record*, p.287 (1997)

<sup>3</sup>Y. M. Li, *ICPIG* (1997)

**DMP5 3 A Simulation of Xe Excimer Lamp Barrier Discharge - Influence of Charges on Dielectric Barriers -** AKINORI ODA, HIROTAKE SUGAWARA, P.L.G. VENTZEK, YOSUKE SAKAI, *Hokkaido University* HARUAKI AKASHI, *National Defense Academy* Dielectric barrier discharge-excited excimer lamp is important as a vacuum ultra-violet light source. The barrier is expected to avoid arc discharge formation which may bring decrease in the excimer production rate. For optimal design of the lamp, it is important to understand characteristics of the discharge

quantitatively. We report the influence of charges accumulated on the dielectric barriers on the discharge characteristics for various power frequencies and gas pressures in the framework of a 1-dimensional model. In this calculation, we examine power source frequencies between 50 kHz and 13.56 MHz, gas pressures between 10 Torr and 100 Torr. The high excimer density is obtained in vicinity of the electrodes, although the electron density in this regions is lower than that in the bulk. Dependence of the efficiency to produce excimers on the frequency and gas pressure is discussed.

## DMP5 4 Bulk Excitation in Radio Frequency Driven Plasmas

C.M.O. MAHONY, *Dept. of Physics, The Queens University of Belfast, Northern Ireland* P.G. STEEN, *Dept. of Physics, The Queens University of Belfast, Northern Ireland* J. MCFARLAND, *Dept. of Physics, The Queens University of Belfast, Northern Ireland* W.G. GRAHAM, *Dept. of Physics, The Queens University of Belfast, Northern Ireland* Spatially and temporally resolved optical emission spectroscopy (STROES) has been used to investigate bulk plasma excitation in a GEC reference reactor. Hydrogen, deuterium, helium and argon were used at pressures up to 1 Torr and plasma powers up to 100 W. STROES data was acquired using a 2 ns ICCD and excitation determined by deconvolution. This work continues previous studies correlating excitation with time varying plasma and electrode potentials <sup>1</sup>. Here we concentrate on the bulk excitation which is observed in all gases in capacitive rf discharges. For all data, contours of constant excitation plotted against time and distance from the driven electrode show a common form. The bulk excitation event starts when the driven electrode becomes negative with respect to the plasma. As time advances it fans out across the interelectrode gap at an angle markedly dependant on gas species. The slope is significantly steeper for H<sub>2</sub> and D<sub>2</sub> than for He and Ar. Spatially it rises within the sheath, peaks and then decays across the bulk plasma. We discuss the form of the excitation profile in terms of the elastic, excitation and ionising processes for electron-neutral collisions.

\*This work was funded by the Engineering and Physical Sciences Research Council

<sup>1</sup>C.M.O. Mahony, R. Al-Wazzan & W.G. Graham., *Appl. Phys. Lett* (to be published: Aug 1997)

## DMP5 5 High Pressure Microwave Powered UV Light Sources

M. CEKIC, *Fusion UV Systems, Gaithersburg, MD 20878* J.D. FRANK, *Fusion UV Systems, Gaithersburg, MD 20878* S. POPOVIC, *Old Dominion University, Norfolk, VA 23529* C.H. WOOD, *Fusion UV Systems, Gaithersburg, MD 20878* Industrial microwave powered (\*electrodeless\*) light sources have been limited to quiescent pressures of 300 Torr of buffer gas and metal-halide fills. Recently developed multi-atmospheric electronegative bulb fills (noble gas-halide excimers, metal halide) require electric fields for ionization that are often large multiples of the breakdown voltage for air. For these fills an auxiliary ignition system is necessary. The most successful scheme utilizes a high voltage pulse power supply and a novel field emission source. Acting together they create localized condition of pressure reduction and high free electron density. This allows the normal microwave fields to drive this small region into avalanche, ignite the bulb, and heat the plasma to its operating point. Standard diagnostic techniques of high density discharges are inapplicable to the excimer bulbs, because of the ionic molecular excited state structure and absence of self-absorption. The method for temperature determination is based on the equilibrium population of certain vibrational levels of excimer ionic excited states. Electron density was de-

terminated from the measurements of Stark profiles of  $H_{\beta}$  radiation from a small amount of hydrogen mixed with noble gas and halogens. At the present time, high pressure (Te 0.5eV, ne  $3 \times 10^{17} \text{ cm}^{-3}$ ) production bulbs produce over 900W of radiation in a 30nm band, centered at 30nm. Similarly, these prototypes when loaded with metal-halide bulb fills produce 1 kW of radiation in 30nm wide bands, centered about the wavelength of interest.

**DMP5 6 X-ray Absorption by Mercury Vapor in a High-Intensity Discharge Lamp** \* J.J. CURRY, M. SAKAI, J.E. LAWLER, *Department of Physics, University of Wisconsin* An x-ray absorption diagnostic possesses several advantages over its optical counterpart when high-pressure arcs are being investigated. For instance, the arc is not opaque to x-rays, as it is to optical resonance frequencies. The optical quality of the arc envelope is not a limiting factor for x-rays. And, there is no background of x-ray emission by the arc from which the absorption signal must be extracted. Due to the development of new technologies, x-ray techniques have rapidly become more flexible and useful in recent years than they have been in the past. One example is the phosphor storage plate technology which has superseded conventional x-ray film for many applications. Unlike film, this technology produces a digital image with 16-bit dynamic range. But most importantly, the phosphor response is linear over five orders of magnitude in x-ray flux. We will discuss our use of this technology to obtain spatially-resolved measurements of the absorption of x-rays by the mercury vapor in a high-intensity discharge lamp.

\*Supported by the National Science Foundation.

**DMP5 7 Tungsten Sputtering and Transport Measurements in High Intensity Discharge Lamps During Starting** A. LENEFF, W. MOSKOWITZ, J. OLSEN, *OSRAM SYLVANIA Products Inc.* Electrode sputtering during starting and subsequent tungsten deposition on the wall reduces life in high intensity discharge (HID)

lamps. Using arc tubes filled with Ar and saturated Hg vapor to simulate HID lamp starting conditions, we have measured sputtering rates from tungsten electrodes and approximate transport rates. Absolute spatially averaged time-dependent tungsten densities were measured using multi-wavelength UV absorption spectroscopy to deduce sputtering rates. Transport was measured by taking a sequence of time-delayed 2D-images of 4009Å tungsten emissions during starts using a monochromatic imaging technique<sup>1</sup> with a gated, intensified CCD camera. Results show the duration and rate of sputtering are strongly dependent on starting current. Images and density measurements show evidence for transport at rates much greater than expected for neutral tungsten diffusion. We discuss transport mechanisms, and the role of glow-to-arc transition time, ballast parameters, and transport on tungsten deposition, and the influence of the sheath on sputtering rates in these lamps.

<sup>1</sup>J. Olsen and W. Moskowitz, Abstracts of 1996 IEEE International Conference on Plasma Science (Boston, 3-5 June, 1996), p. 119.

**DMP5 8 Starting of Long Tube Discharges** R. KENNETH HUTCHERSON, RICHARD C. GARNER, *Osram Sylvania Products, INC.* Starting phenomena of long tube rare gas discharges have been investigated emphasizing the processes that slow the ionizing front which propagates from cathode to anode. Using current, voltage and imaging / spectroscopic measurement methods, spatial and temporal features of the cathode-to-glass wall ionized channel and the axially propagating ionizing front have been observed for a range of gas pressure (1 to 100 Torr neon), electrode spacing (0.1 to 10 cm) and driving voltage (0 to 1kV). Also, the ground plane surface area and its distance from the discharge tube have been varied in an attempt to investigate the influence of distributed capacitance on starting. The results of these measurements help describe the basic processes limiting ionizing front propagation in long tube discharges.



**SESSION FT: PLENARY**

Tuesday morning, 7 October 1997; Music Hall, University of Wisconsin campus at 8:00; C.C. Lin, Univ. of Wisconsin-Madison, presiding

**8:00****FT 1 Forty Years of Overlap: Electric Discharge Light Source R&D and the GEC.**JOHN F. WAYMOUTH, *Marblehead, MA*

For many years R&D targeting electric discharge light sources was reported at the GEC. These years will be reviewed from the perspective of the three major functions of a scientific conference for a researcher from industry. First, the opportunity to receive feedback from the world's leading experts on the presentation of one's work as formal papers. Second, the opportunity to obtain early warning of new developments in the field from hearing papers presented by others on their work, several years before final publication. Finally, the opportunity for education obtainable from attending sessions in related fields in the same gaseous electronics discipline. These three major functions are further subdivided and amplified through the opportunities for personal contacts: with one's competitors in the industry; with researchers from other industries and government laboratories in related fields; and with the large and vibrant university-research community. The success of the relationship between light source research and the GEC over the years is evaluated from a very personal perspective, using examples from my own recollection and files. I believe it has been mutually beneficial, although there are clearly missed opportunities on both sides. Unfortunately, in recent years participation in the GEC by light source researchers has been declining. Never more than 7% of the GEC, light source R&D papers have been increasingly diverted toward the triennial International Symposium on Science and Technology of Light Sources, and toward the International Conference on Plasma Science ("ICOPS") of the IEEE. Possible reasons for this migration, and its implications for the future of light source R&D at the GEC will be discussed.

**8:40****FT 2 Electron Collisions in Astrophysical Plasmas.**A. DALGARNO, *Harvard-Smithsonian Center for Astrophysics*

In many astronomical objects the emission spectra and the thermal and ionization structure are determined by electron collision processes. Electron collisions are critical also in the chemistry of astronomical environments. Developments in our recognition of the importance of electron collisions and their use as diagnostic probes of remote objects over the last 50 years will be reviewed.

**9:20****FT 3 Gas-Phase Lasers - a Historical Perspective in Relation to the GEC.**GERRY HAYS, *Sandia National Laboratories*

Understanding of gas-phase lasers inevitably involves an expertise in many of the specialties of the GEC community - especially homogenous and heterogeneous kinetics, collision cross-sections, gas breakdown physics and fundamental swarm parameters. The GEC community decided early in the evolution of gas-phase lasers to include papers on this topic and the result was many years of contributions to the evolution of and improvement in our understanding of this important class of lasers. Many of the ground-breaking results in gas laser technology were presented at the GEC over the last 3 decades as the traditional rare-gas atomic physics and low-temperature plasma groups turned their attention to parameters of interest to the laser modelers and experimenters. This paper will trace the development of this field, especially as it pertained to the GEC. Some of the key results will be highlighted, together with some of the unpublished trivia and anecdotal incidents in order to capture the flavor of the rapid developments in the early days. The talk will include speculation as to the direction this field is taking, and some suggestions as to opportunities. This work supported by the United States Department of Energy under Contract DE-AC04-94AL85000. Sandia is a multiprogram laboratory operated by Sandia Corporation, a Lockheed-Martin Company, for the United States Department of Energy.

**10:00****FT 4 Comments on the Kinetics of Swarms and Discharges from Models of Experiments.**A.V. PHELPS, *JILA, U. of Colorado and NIST*

These comments include a brief outline of the systematics of the theory of electron kinetics in swarm experiments and gas discharge experiments. Emphasis is on the early papers and their relationship to recent work. In the area of ion and fast-atom kinetics we discuss data needs and the shortage of such data for models. We cite the necessity for testing electron, ion, and fast-atom transport and reaction models against simple experiments and argue for maintaining easily accessible collections of cross sections and other basic data with accompanying documentation of tests.<sup>1</sup> I will also present some recollections regarding early contributors to the field who were my teachers and mentors and later contributors who were and are my colleagues during the 50 years of the Gaseous Electronics Conference.

<sup>1</sup>As an example see [ftp://jila.colorado.edu/electron\\_cross/](ftp://jila.colorado.edu/electron_cross/)

**SESSION GT: FOUNDATIONS OF GASEOUS ELECTRONICS**

Tuesday morning, 7 October 1997; Music Hall, University of Wisconsin campus at 11:00; Mark Kushner, University of Illinois, presiding

11:00

**GT 1 Physics and Chemistry of Amorphous Silicon Deposition Discharges.**

ALAN GALLAGHER, *JILA, NIST and University of Colorado, Boulder, CO 80309-0440*

Due to the technological importance of rf silane discharges for the production of thin film semiconductors, an enormous body of literature exists regarding their properties. Of necessity, I will only outline current understanding and note important gaps therein; detailed reviews are available<sup>1,2</sup>. I will describe the electron energetics, then the dissociation products of electron molecule collisions; these initiate the plasma and deposition chemistry. Radical-molecule and radical-surface reactions play a major role in establishing the film electronic properties; these and the film-growth model will next be discussed. Ions and ion-molecule chemistry will then be noted, but only briefly as they are believed to play a minor role in establishing film properties. Electron-silane collisions also form copious amounts of negative ions, and some of these grow into negatively charged silicon particles that are trapped in the plasma by the sheath fields. The particle charge density can approach the positive ion charge density in some regions, so this has a significant effect on the plasma. More significantly for devices, a large number of small particles deposit into the growing film, and larger particles can deposit onto the surface after discharge termination. Due to these deleterious effects on films, as well as a close connection to particle behavior in wafer-etching plasmas, considerable work is underway to elucidate the growth and behavior of silicon particles in plasmas. Current understanding, and gaps therein, will be outlined.

<sup>1</sup>M.J.Kushner, *J.Appl.Phys.*71,4173(1992)

<sup>2</sup>J.Perrin, O.Leroy and M.C.Bordage, *Contrib.Plasma Phys.*36,3(1996)

**SESSION IT1: SURFACE PROCESSES**

Tuesday afternoon, 7 October 1997

Class of '24 Reception Room, Memorial Union at 13:30

Mark Sobolewski, NIST, presiding

*Contributed Papers*

13:30

**IT1 1 Mass Spectrometry of Plasma/Surface Interactions in High Density Plasma Etching of HgCdTe and ZnSe** C.R. EDDY JR., D. LEONHARDT, V.A. SHAMAMIAN, J.E. BUTLER, *U.S. Naval Research Laboratory* Methyl-based high density plasma etching is important to the development of II-VI semiconductor devices, but remain empirically developed. Here, mass spectrometry is employed to characterize the incident plasma flux in CH<sub>4</sub>/H<sub>2</sub>/Ar ECR plasmas as process conditions are varied. Also, the changes in etch products evolving from the surface are examined under these conditions with additional variation in substrate temperature. This permits different regimes of ion-assisted surface chemistry to be defined. For HgCdTe, Cd and Te are removed as hydrides or dimethyl molecules while Hg removal transitions from elemental at low methane fractions to dimethylmercury at high fractions. The formation activation energy of etch products falls from 20 kJ/mol at 20 eV ion energies to 5 kJ/mol at 120 eV and

remains there for ion energies to 220 eV. For ZnSe, monitored product peaks include elemental, hydride, and dimethyl molecules. In this material, ion-assisted surface chemistry extends to a much higher ion energy range (> 300 eV), consistent with the higher bond energy of ZnSe.

13:45

**IT1 2 Secondary Electron and Negative Ion Emission from Oxygen Covered Molybdenum and Stainless Steel** SCOTT G. WALTON, JACK C. TUCEK, ROY L. CHAMPION, *College of William and Mary, Williamsburg VA 23187* Absolute Yields and kinetic energy distributions of secondary electrons and negative ions resulting from the collisions of positive sodium ions with the metal surfaces have been determined as a function of oxygen coverage. Experiments have been performed on polycrystalline Mo, single crystal Mo (100), and stainless steel surfaces with controlled oxygen exposures for impact energies below 500 eV. The negative ion and secondary electron yields are increased due to the presence of oxygen. The kinetic energy distributions of the negative ions and secondary electrons peak at energies of a few eV and are roughly independent of oxygen coverage. The results are discussed in terms of a model in which an excited state of a molecular negative ion (e.g., MoO<sup>-</sup>) is responsible for both the secondary electrons and the majority of the negative ions. This work was supported in part by the Division of Chemical Sciences, Office of Basic Energy science of the U.S. Department of Energy.

*Invited Paper*

14:00

**IT1 3 In-situ IR study of chemical processes on Si surfaces.**

MICHIO NIWANO, *Research Institute of Electrical Communication, Tohoku University, Japan*

Hydrogen plays an important role in the crystal growth, oxidation and reactive ion etching processes on Si surfaces. Numerical efforts have been directed towards understanding the adsorption and desorption kinetics of hydrogen on Si. To

this end, many experimental techniques have been employed, including photoemission and electron-energy loss spectroscopy, temperature-programmed desorption (TPD) spectroscopy, and scanning tunneling microscopy (STM). These techniques, however, do not permit an easy identification of bonding configurations of hydrogen. Thus, to obtain a detailed understanding of surface chemical processes in which a variety of hydride species are involved, it is important to employ spectroscopic techniques that are sensitive to the atomic bonding configuration of hydrogen in the vicinity of the surface. Infrared absorption spectroscopy in the multiple internal reflection (MIR) geometry, with its high surface sensitivity and energy resolution, is particularly suitable for this task. It allows the differentiation of hydrogen atoms in different chemical bonding environments. In this work we present a MIR-IR spectroscopy study of the adsorption of water and atomic hydrogen on the Si(100)(2x1) surface at room temperature (R.T.) and hydrogen desorption at elevated temperatures. To follow chemical changes of the surface during adsorption and desorption, we collected IR absorption spectra in the Si-H stretch vibration region. It is well known that water adsorbs dissociatively onto the Si(100)(2x1) surface, leading to the generation of the monohydride Si (Si-H) and Si-OH on the dimer. As the temperature is raised from R.T. to 800 K, the dimer bond is cleaved to produce the dihydride Si (SiH<sub>2</sub>), and the Si-Si bonds (dimer bonds and backbonds) are attacked by oxygen atoms released from the surface Si-OH bonds to produce intermediate oxidation species such as SiH<sub>2</sub>(SiO). We show that intermediate oxidation species SiH(O<sub>3</sub>) persists up to 900 K. At the initial stages of hydrogen adsorption, Si-H and SiH<sub>2</sub> are generated with Si-H being dominant. The formation of Si-H is due to the adsorption of hydrogen onto the dangling bonds of the dimer, and the generation of SiH<sub>2</sub> indicates that the dimer bond is cleaved by hydrogen. With increase of hydrogen exposure the trihydride Si (SiH<sub>3</sub>) is increasingly populated, suggesting the etching of the Si surface by atomic hydrogen. With annealing up to 700 K the SiH<sub>3</sub> surface concentration significantly diminishes. The monohydride Si remains up to about 800 K. MIR-IR is also a powerful tool for the investigation of chemical processes on Si surfaces in plasma.

### Contributed Papers

14:30

#### IT1 4 Investigation of the relation between arc spot ignition and surface properties of cold cathodes

M. SCHUMANN, D. NANDELSTÄDT, A. KORBEL, J. MENTEL, *Ruhr-Universität Bochum, Germany* J. SCHEIN, *University of Minnesota, Minneapolis, MN, USA* The magnetic blowing of an arc against a third so called commutation electrode CE positioned perpendicularly to the discharge axis allowed a reproducible interaction of the plasma with the electrode to be achieved. For a local definition of arc spot ignition an aperture (diameter 2 mm) in the center of a diaphragm in a distance of 1 mm in front of the CE is used. The moment of arc spot ignition indicated by a steep current increase in the CE is taken to define a commutation time  $t_c$ . Measurements of  $t_c$  and of the precurent characterized by the two parameters maximum precurent  $i_v$  and precurent flow time  $t_v$  in air and pure argon at atmospheric and reduced pressure using electrodes with different bulk properties and surface treatments showed that the latter is the dominant factor. High speed photography has disclosed a correlation between  $i_v$  and the mode of arc spot ignition. If arc spot ignition is initiated by an  $i_v$  of at least several milliamps the first step is that a luminous layer spreads over the CE. In a second step a bright channel is formed between the luminous layer and the bulk plasma. If  $i_v$  is very low the formation of a bright, small plasma ball in front of the CE is connected with a steep current

increase. Depending on the surface treatment very different arc traces are produced by arc spot ignition.

14:45

#### IT1 5 Wall Relaxation Measurements of the N<sub>2</sub> Ground Vibration States at Low Pressure\*

JOHN PARISH, PERRY YANEY, *UDayton* Relaxation probabilities,  $\gamma$ , for N<sub>2</sub>(X<sup>1</sup>Σ<sub>g</sub><sup>+</sup>, v) of v=1 to v=4 or 5 were determined at various pressures between 0.5 and 23 Torr and temperatures within 300 - 360K on pyrex and gold. 50collisions. V=1  $\gamma$  is on the order of 4x10<sup>-4</sup> on pyrex and 5x10<sup>-4</sup> for gold,  $\gamma$  is linear with v. Delta  $\gamma$  between v=1 and 2 is about 3 to 6 x10<sup>-4</sup> on pyrex, 4 to 8 x10<sup>-4</sup> on gold.  $\gamma$  decreases with temperature indicating no activation energy. This can be explained by interaction between gas and adsorbed molecules. Pyrex conditioned in active nitrogen can increase v=1  $\gamma$  by 60% over that of a neat surface and increase or decrease delta  $\gamma$  by 25%. Experiments are dependent on the exposure history. XPS showed about 10% coverage of nitrogen on pyrex. A dc discharge created vibrational populations and data was obtained with CARS spectroscopy corrected for saturation.<sup>1</sup> The master equation approach was used to extract  $\gamma$ . Stainless steel, aluminum and titanium data will be presented.

\*Supported by USAF contract F33615-93-C-2303

<sup>1</sup>P. P. Yaney and J.W. Parish, *Applied Optics*, 35, 2659-2664, (1996)

### Invited Paper

15:00

#### IT1 6 Sub-micron retarding field energy analyzer for plasma analysis.\*

MATTHEW BLAIN, *Sandia National Laboratories*

A retarding field energy analyzer with sub-micron apertures for measurement of ion energy distributions in processing plasmas has been built. The analyzer was fabricated using standard Si integrated circuit materials and processing techniques and consists of a shielding grid, an electron repeller grid, and a collector plate, all made of 400 nm thick polycrystalline silicon thin films. The grids are supported and insulated from each other by 1 μm and 2 μm of SiO<sub>2</sub>. The apertures in the grids are nominally 0.8 μm in diameter and are self-aligned, thereby minimizing field leakage and optimizing energy resolution. Ion trajectory modeling using SIMION predicts analyzer dispersion to be less than 0.1 eV for 20 eV incident ions. The analyzer can be operated on the wafer on which it was fabricated or can be separated into 1.6 x 1.2 cm<sup>2</sup> die for use as a discrete probe. The basic functionality of the analyzer has been demonstrated in inductively

coupled argon plasmas and measurements show energy spreads of 3-5 eV which are consistent with the expected presheath voltage drops and agree well with measurements made with differentially pumped, macroscopic ion energy analyzers. Changes in mean ion energy as a function of power and pressure agree with the expected scaling trends. Efforts to passivate the Si surfaces with Ni to allow for operation of the analyzer in reactive gas plasmas are also reported.

\*This work was supported by the United States Department of Energy under Contract DE-AC04-94AL85000 and by Sematech. Sandia is a multiprogram laboratory operated by Sandia Corporation, a Lockheed Martin Company, for the United States Department of Energy.

### Contributed Papers

15:30

**IT1 7 Issues in the Application of Mass Spectroscopic Techniques for In Situ Surface Chemistry Monitoring in High Density Plasma Etching** D. LEONHARDT, *U. S. Naval Research Laboratory, Washington, DC 20375* C. R. EDDY, JR., V. A. SHAMAMIAN, J. E. BUTLER, Mass spectrometry is a powerful diagnostic tool used to monitor gas phase species in semiconductor processing environments, thereby discerning etch product formation. We have studied various mass spectrometer sampling arrangements while etching GaAs substrates in our high density plasma source. By sampling through an aperture in the substrate's electrode, we find that the subsequent plasma reactions with the etch products are minimized, thereby giving the most accurate picture of the actual in situ surface chemistry. Conventional positioning of the mass spectrometer in front of the substrate requires the etch products to traverse a non-negligible portion of plasma, undergoing additional gas phase reactions before being detected. Through exemplary spectra, the implication and ramifications of etch product collisions with plasma species prior to detection will be shown. Determination of activation energies for etch product formation by sampling through the substrate electrode will also be discussed.

15:45

**IT1 8 Photorefectance Studies of the Electronic Properties of Etched GaAs Surfaces** O.J. GLEMBOCKI, *Naval Research Laboratory* R.T. HOLM, C.R. EDDY, D. LEONHARDT, D.S. KATZER, *Naval Research Laboratory* Because of its contactless and noninvasive nature, the optical technique of photorefectance (PR) has routinely been used to the study of the optical and electronic properties of bulk and thin film semiconductors. We show that PR can be used both in-situ and ex-situ to study etch induced surface damage of GaAs that is processed in a chlorine/Ar plasma generated by an electron resonance cyclotron source. We use special test layers consisting of 150nm of undoped GaAs were grown epitaxially on n+ and p+ GaAs to enhance the optical sensitivity to the electronic properties of the surfaces. We show that etch induced surface damage occurs at DC biases, as low as 100V. In-situ measurements allow us not only to characterize the etch damage in terms of Ga vacancies but also to explore damage healing procedures. We find that a low energy, chlorine plasma eliminates etch induced damage. Ex-situ measurements allow us to determine the behavior of the etched surfaces when exposed to ambient conditions, that are typical of semiconductor processing. We find that the two defects are responsible for the electronic properties of processed GaAs: Ga vacancies during etching and excess As during subsequent exposure to the ambient. Our results will be discussed in terms of a model utilizing these two surface defects and their interaction with light and chlorine.

---

## SESSION IT2: INDUCTIVELY COUPLED PLASMAS I

Tuesday afternoon, 7 October 1997; Tripp Commons, Memorial Union at 13:30; Moshe Sarfaty, Univ. of Wisconsin, presiding

### Invited Paper

13:30

#### IT2 1 Advantages of Using A High Density Plasma Source for FPD Plasma.

JOHN P. HOLLAND, *Lam Research, Fremont, CA*

The current trend in flat panel display (FPD) manufacturing is towards producing larger and higher quality displays. This trend has resulted in the increase in the size of the glass substrates used as the basis of the displays and the requirement for improvements in the performance for the processing steps used to deposit and etch films on the glass. Typically, either wet chemistry or low density, reactive ion etch (RIE) plasma sources have been used for these process steps. Both of these methods are largely adequate for small display sizes, however, as the dimensions of the of the glass substrates are increased to greater than 500 mm, these methods may be limited by their lower processing rates and poorer process uniformities. An alternative to the these techniques which have till recently been unavailable commercially is the use of a high density plasma source for plasma processing of the large area panels. High density plasma sources have become common place for wafer-based manufacturing, however, not all of the high density plasma sources proved to be scaleable for the large area applications. One exception to this problem of scalability of high density sources is the planar, inductively coupled plasma source. Operation of this source on substrate with dimensions greater than 600 mm have been recently demonstrated. Issues with processing rates can be overcome when using these high efficiency sources and process uniformities can be much lower than are achieved with either wet chemistry or RIE etching. Results etching of a variety of films which are involved in the plasma processing for both AMLCD and FED applications will be discussed.



14:00

**IT2 2 Thomson Scattering Measurements of Electron Temperature and Density in Low Density Discharges** M. D. BOWDEN, Y. GOTO, H. KUDO, K. UCHINO, K. MURAOKA, *Kyushu University, Japan* The laser diagnostic method of Thomson scattering has been used in recent years to measure electron properties in high density plasma sources such as ECR and ICP discharges. In order to measure electron properties in lower density discharges, several significant changes have been made to our existing Thomson scattering system. The new scattering system uses a photon counting ICCD camera to obtain the whole scattered spectrum simultaneously and a multipass cell for the laser beam to allow the laser beam to pass repeatedly through the discharge. In addition, some measurements were made using a low energy, very high repetition rate YAG laser as the laser source. Results of scattering measurements with the new system will be presented and the appropriateness of multipass cells for scattering experiments will be discussed. The final aim of the improvements is to construct a system capable of measuring densities of the order of  $10_{15}m^{-3}$  in plasma processing conditions.

## Invited Paper

14:30

**IT2 4 Effects of discharge frequency and UHF plasma source for precise ULSI patterning.**  
SEIJI SAMUKAWA, *Microelectronics research laboratories, NEC Corporation*

Ultrahigh-frequency (UHF) plasmas have drawn attention in fabrication of ultra-large-scale-integration (ULSI) devices in terms of precise patterning capability of fine-line features and high selectivity. Recently, it has also been found that the UHF plasmas possess a wide process window for highly selective etching of poly-Si, which is attributable to pressure-independent ion saturation current in the UHF plasmas. Since discharge frequency (500 MHz) is even higher than electron collision frequency in the UHF plasmas, electron energy distribution function (EEDF) is expected to be insensitive to pressure. Monte Carlo simulation of EEDF's in homogeneous infinite plasmas through Ar and Cl<sub>2</sub> confirms the pressure-independent feature of the EEDF's in the plasmas produced by 500-MHz UHF power. In contrast, the high energy tails of the EEDF's in RF (13.56 MHz) plasmas diminish significantly with an increase in pressure. The simulation also shows that the high electric field strength is needed to sustain the UHF plasmas. Electrons oscillate by the high field and gradually gain energy through elastic collisions after a number of UHF periods. Thus, the electrons which cause ionization are expected to spend a long time where the field strength is high. This suggests that UHF power deposition takes place in the high field region which is believed to appear off the symmetry axis of the plasma source, judging from the antenna used for UHF power introduction. Laser-induced fluorescence measurement indicates that metastable chlorine ion density becomes higher off axis than in the center of the source. Since production of the metastable ions from the ground-state ions requires higher energy than ionization potential of chlorine, the radial density distribution of the metastable ions indicates that the power deposition has a strong correlation with the UHF field distribution and occurs more off axis for the plasma source used in this work.

## Contributed Papers

15:00

**IT2 5 Measurements of Relative BCl Density in BCl<sub>3</sub>-containing Inductively-Coupled rf Plasmas** \* C. B. FLEDDERMANN, † G.A. HEBNER, *Sandia National Laboratories* The relative density of BCl radicals in inductively-coupled plasmas has been studied using laser induced fluorescence and plasma induced emission. Measurements were made as a function of input power, reactor pressure, position in the reactor, and as a function of gas ratio for metal etch gas mixtures containing BCl<sub>3</sub>, Cl<sub>2</sub>, Ar, and N<sub>2</sub>. The LIF and PIE intensities varied differently as the plasma parameters were changed. Between 150 and 400 W

14:15

**IT2 3 Determination of Electron Temperature, Plasma Density and Cl<sub>2</sub> Percent Dissociation by Optical Emission Spectroscopy** M.V. MALYSHEV, V.M. DONNELLY, *Bell Laboratories, Lucent Technologies* A new method, Trace Rare Gases-Optical Emission Spectroscopy (TRG-OES), was developed to determine electron temperature ( $T_e$ ) and density ( $n_e$ ) and was applied to Cl<sub>2</sub> and Ar inductively coupled plasmas. Emission intensities are calculated, assuming population of emitting levels by electron impact excitation from both the ground state, and from metastable levels that are formed and destroyed by electron impact. Assuming a Maxwellian EEDF,  $T_e$  is determined from a comparison of observed and calculated emission, and  $n_e$  is estimated from the relative contributions by metastables. The role of metastables was evaluated by pulsing the plasma (10 kHz) and observing the emission rise and decay times. TRG-OES provides better relative values of  $T_e$  than does the Langmuir probe. TRG-OES was also used to determine the percent dissociation in Cl<sub>2</sub> plasmas by actinometry, using 306 nm emission from Cl<sub>2</sub>. Using several rare-gas lines and taking metastables and variations of  $T_e$  into account, the accuracy of this actinometry method was improved.<sup>1</sup>

<sup>1</sup>M.V.Malyshev is also at Princeton University, Princeton Plasma Physics Laboratory

input power, there was no variation in BCl density, indicating that the dissociation fraction for BCl<sub>3</sub> to BCl was constant with power. No significant interactions between BCl<sub>3</sub> and Cl<sub>2</sub> or Ar were evident in the LIF measurements. However, the BCl density decreased with addition of nitrogen. The BCl density was radially uniform for all gas mixtures. After running the reactor with a BCl<sub>3</sub>/N<sub>2</sub> mixture, BCl was observable for up to an hour after the discharge was switched to Cl<sub>2</sub>, attributed to buildup of BN films on reactor surfaces.

\*This work was supported by the USDOE (DE-AC04-94AL85000) and Sematech.

†Permanent address: Dept. of Elec. and Comp. Eng., Univ. of New Mexico



15:15

**IT2 6 Relative atomic chlorine density in chlorine and boron trichloride containing inductively coupled plasmas** G. A. HEBNER, *Sandia National Laboratories* C. B. FLEDDERMANN, *Sandia National Laboratories* \* Two photon laser induced fluorescence (LIF) has been used to measure the relative atomic chlorine density in inductively driven radio frequency discharges containing mixtures of chlorine, boron trichloride, argon and nitrogen in a GEC reference cell. Relative density of the chlorine ground state was determined by exciting the  $3p^2P^0_{3/2} - 4p^4S^0_{3/2}$  transition with two photons at 233.3 nm and observing LIF from the  $4p^4S^0_{3/2} - 4s^1P^0_{3/2}$  transition at 725.6 nm. In contrast with previous measurements in pure chlorine, the atomic chlorine density increased with rf power in pure  $BCl_3$  discharges. In mixtures of  $Cl_2$  and  $BCl_3$ , the Cl density was constant with rf power and increased with pressure, similar to pure  $Cl_2$  discharges. In  $Cl_2 / BCl_3$  mixtures, the Cl density varied linearly with ratio, and was a factor of three higher in  $Cl_2$  than  $BCl_3$ . The addition of argon or nitrogen to  $BCl_3 / Cl_2$  mixtures had no effect on the relative Cl density. Finally, measurements of the Cl density as a function of radial position showed that the Cl density was constant with radius.

\*CBF, Permanent address: Dept. of Elec. and Comp. Eng., University of New Mexico, Albuquerque NM, 87131.

15:30

**IT2 7 Non-local Electrodynamics in Weakly Collisional Inductively Coupled Plasmas.** V.I. KOLOBOV, *University of Houston* V.A. GODYAK, *Osrsm Sylvania* D.J. ECONOMOU, *University of Houston* \* Most of the current models of Inductively Coupled Plasmas (ICPs) use local relation between rf current density and the electric field in the form of Ohm's law  $\mathbf{j} = \sigma \mathbf{E}$ . However, in the weakly collisional regime, when the effective mean free path of electrons is comparable to or exceeds the characteristic scale of the rf electric field decay, the plasma conductivity  $\sigma$  is a nonlocal integral operator. In a simple case, this situation corresponds to the conditions of anomalous skin effect. In the general case,  $\sigma$  is determined by the geometry of the system, the nature of electron trajectories, and the configuration of the external fields. We revived classical works on the anomalous skin effect to analyse peculiarities of electromagnetic phenomena in weakly collisional ICPs and extended the models to two-dimensional systems. The coupled set of Maxwell's equations for the electromagnetic fields and Boltzmann's equation for electrons was solved using Fourier method. The electromagnetic fields and rf current density were measured in a planar ICP in argon with a specially designed magnetic probe. The experimentally observed nonmonotonic distributions of the rf fields and current density, the phase bifurcations, the negative power absorption and other phenomena found in the experiments are in plausible agreement with calculation results.

\*Work at the University of Houston was supported by NSF

15:45

**IT2 8 Capacitive Bias Power Coupling in High Density Systems** M. M. TURNER, \* C. K. BIRDSALL, *EECS Department, UC Berkeley, Berkeley, CA 94720* V. VAHEDI, *Lam Research Corporation, 4650 Cushing Parkway, Fremont, CA 94538* In almost all high density plasma processing systems, the energy and directionality of the ions arriving at the wafer is controlled by an RF bias source coupled to the lower electrode. The RF bias source capacitively couples to the plasma and produces an RF sheath which can heat both electrons and ions (the ions gain most of their energy in the RF sheath before arriving at the wafer). It is believed that most (if not all) of the delivered RF bias power to the lower electrode is deposited into the ions, however this has not been

completely verified over the typical range of operation. We will use a particle-in-cell simulation code to investigate a typical high density inductively coupled plasma with an applied RF bias source. The code includes a self-consistent inductive and capacitive coupling from an RF coil, as well as capacitive coupling from the RF bias source.

\*Usual address: Plasma Research Laboratory, Dublin City University, Ireland

---

---

**SESSION JTPI: POSTER SESSION:  
ELECTRON COLLISION CROSS SECTIONS**

**Tuesday afternoon, 7 October 1997**

**Great Hall, Memorial Union at 16:00**

**Nicholas Hitchon, University of Wisconsin-Madison, presiding**

**JTPI 1 Electron scattering from Carbon Dioxide** J.C. GIBSON, S.J. BUCKMAN, *Atomic and Molecular Physics Laboratories, Australian National University* M.A. GREEN, M.J. BRUNGER, *Physics Department, Flinders University of South Australia* We have measured a series of absolute differential cross sections (DCS) for elastic scattering from carbon dioxide in the energy region between 1 and 50 eV. The initial motivation for this work was a distinct lack of recent, absolute data in the region below, near, and just above the low energy shape resonance, centred at about 3.8 eV. Recently, Tanaka *et al.*<sup>1</sup> have measured absolute elastic DCS between 1.5 and 100 eV and, our initial comparisons with this data provide further reason for the present study as we find differences between the present DCS and these most recent measurements, particularly with regard to the absolute values. Comparisons with these data and other previous measurements and theory will be provided.

<sup>1</sup>Private Communication from L. Boesten

**JTPI 2 Leakage Field Corrections for Hemispherical Energy Selectors** T SAGARA, S NISHIDA, L BOESTEN, *Sophia U. Tokyo* M.A. DILLON, *ANL* Field distortions from real apertures attached to hemispherical energy selectors and other fringing field corrections ( $180^\circ$  Herzog-type<sup>1</sup> or Jost-type<sup>2</sup>) were investigated by exact, numerical tracing of the electron paths in spherical coordinates for gap  $G$  to mean radius  $R_0$  ratios of 0.2-0.5. Beam bundles (entrance angle  $\alpha$  within  $\pm 5^\circ$ ) may be strongly defocused and show a banana-shaped asymmetry with respect to  $R_0$ . Base-resolution,  $dR_{out}/R_0 = -dR_{in}/R_0 + 2dE/E_0 - 2\alpha^2$ , and the maximum bundle width,  $W = 2R_0 \sin \alpha$ , are not affected. The bundle edges deviate equally from the midbeam ( $\alpha=0$ ), and the midbeam deviates from  $R_0$  by  $dR_{mid} \approx +0.089 G$  (Herzog),  $\approx +0.21 G$  (real apt.), and  $\approx +0.01 G$  (Jost). Defocusing and asymmetry can easily be corrected to those of an ideal spherical selector by simply adding  $d\alpha \approx -4.6^\circ G/R_0$  (Herzog),  $d\alpha \approx -11.8^\circ G/R_0$  (real apt.), and  $d\alpha = 0$  (Jost) to all entrance beams.

<sup>1</sup>R. Herzog, *Zeitschr. f. Physik* 97, 596-602 (1935) and references

<sup>2</sup>K. Jost, *J. Phys. E: Sci. Instrum.* 12, 1001-1005 (1979)

**JTPI 3 Normalization of experimental electron cross sections** N. AVDONINA, *U. of Pittsburgh* Z. FELFLI, *CTSPS, Clark Atlanta U.* A.Z. MSEZANE, *CTSPS, Clark Atlanta U.* Absolute experimental electron-impact differential cross sections (DCSS) can be obtained through an extrapolation of the relative general-

ized oscillator strength (GOS) values at some given impact energy  $E$  to zero momentum transfer squared  $K^2$ , the optical oscillator strength (OOS) [1]. We propose to normalize the relative experimental DCS data to the corresponding OOS value by extrapolating the GOS to  $K^2=0$  without involving the nonphysical region. This is possible only by simultaneously increasing  $E$  and decreasing  $K^2$  so that  $K^2=0$  corresponds to  $E=\infty$ . Thus is avoided a divergence of  $d(GOS)/d(K^2)$  at  $K^2=0$  [2]. Another advantage of our method is that, over a wide range of small  $K^2$  values the contribution of higher order terms of the Born series to the GOS function is negligible, contrary to the constant  $E$  case in which even order  $K^2$  terms are non-Born [2]. Thus first Born approximation can be used to normalize relative experimental DCSs to the OOS. This method is applicable to both the excitation and ionization of atomic and molecular targets by electron impact. The latter case generalizes the method of Ref. [3]. \*Supported by AFOSR, NSF and DoE Div. of Chemical Sciences, OBES. <sup>1</sup> E. N. Lassetre *et al.*, *J. Chem. Phys.* 50, (1829) <sup>2</sup> W. M. Huo, *J. Chem. Phys.* 71, 1593 (1979) <sup>3</sup> A. Saenz, W. Weyrich and P. Froelich, *J. Phys. B* 29, 97 (1996)

**JTP1 4 Electron Impact Excitation of Noble Gases** VLADO ZEMAN, KLAUS BARTSCHAT, *Drake University*\* We have applied the Breit-Pauli R-matrix method [1] to model electron impact excitation of the  $[np^5(n+1)s]$  and  $[np^5(n+1)p]$  states in the noble gases Ne – Xe. Special attention is given to the near-threshold region which is dominated by negative-ion resonances. Total and differential cross sections, together with the polarization of the light emitted in optical decays, will be presented and compared with recent experimental data [2–6]. 1. K.A. Berrington, W.B. Eissner and P.H. Norrington, *Comp. Phys. Commun.* 92, 290 (1995) 2. S.J. Buckman and C.W. Clark, *Rev. Mod. Phys.* 66, 539 (1994) 3. C. Noren and J.W. McConkey, *Phys. Rev.* A53, 3253 (1996) 4. T.J. Gay *et al.* (1996), *Phys. Rev.* A53, 1623 (1996) 5. D.H. Yu, P.A. Hayes and J.F. Williams (1997), *Phys. Rev. Lett.* 78, 2724 (1997) 6. D.H. Yu *et al.* (1997), *J. Phys. B* 30, 1799 (1997)

\*This work is supported by the National Science Foundation.

**JTP1 5 Integral cross section measurements of ion excitation by electron impact** J.B. GREENWOOD, *Jet Propulsion Laboratory* Ion excitation by electron impact is a source of line emission in solar, planetary, stellar and fusion plasmas. Observations of these transitions can be used to determine plasma characteristics if reliable total cross sections are available. The JPL experiment utilizes a merged-beams approach to collide the electrons and ions. A uniform magnetic field along the merged-beams axis confines all the inelastically-scattered electrons. These are then trochoidally separated from the main beams, enabling total absolute cross sections to be measured [1]. We have recently installed an Electron Cyclotron Resonance (ECR) ion source which has enabled us to study multiply charged ions (MCIs). First ECR results for MCIs will be presented, along with excitation data on S II and Ar II. [1] S. J. Smith *et al.*, *Ap. J.* 463, 808 (1996).

**JTP1 6 Methods for producing metastable atom targets for electron excitation experiments\*** GARRETT PIECH, MARK F. GEHRKE, JOHN B. BOFFARD, L. W. ANDERSON, CHUN C. LIN, *University of Wisconsin-Madison* \* We have developed two different metastable atom sources used to study electron excitation out of the metastable states of the rare-gas atoms (He, Ar, ...) using the optical method. A hollow cathode discharge producing a thermal atomic beam is used for high signal to noise measurements. This apparatus is limited to incident electron energies be-

low ground state threshold due to a high ground state concentration. In the case of argon, this apparatus was also used to measure the relative contributions from the two different metastable levels ( $3p^5 4s$  J=0 and J=2) by using a laser to quench one of the two levels. A second source uses a near-resonant charge exchange reaction ( $Rg^+ + Cs \rightarrow Rg^* + Cs^+$ ) of a fast ion beam with a cesium vapor to produce a primarily fast-metastable beam. This fast beam apparatus is used for electron energies up to 1 keV. Both experiments produce absolute results using two separate calibration procedures. Representative results will be presented.

\*Supported by the National Science Foundation.

**JTP1 7 Absolute Electron Scattering Cross Section Measurements at Backward Angles** K.W. TRANTHAM, C.J. DEDMAN, J.C. GIBSON, S.J. BUCKMAN, *Atomic and Molecular Physics Laboratories, Australian National University* In the measurement of electron scattering cross sections, traditional experimental techniques, using crossed-beam geometries, usually suffer from the mechanical constraints imposed by an in-plane monochromator/analyser system which mitigate against measurements at angles larger than about 140deg. In the past two years, Read and co-workers<sup>1</sup> have demonstrated a novel technique for the measurement of differential scattering cross sections at large scattering angles. They employ localised, radially symmetric magnetic fields in the collision region in order to rotate the incident, and scattered electron directions by about 90deg. This renders the backward scattering region accessible for both elastic and inelastic scattering measurements. Given the collateral problems that may arise from the use of strong magnetic fields in low energy experiments, we have used a slightly modified design to that of Read *et al.* together with the relative flow technique, to measure the first absolute scattering cross sections at backward angles for carbon dioxide.

<sup>1</sup>M.Zubek *et al.* *J. Phys. B.* 29, L239 (1996); F.H. Read and J.M. Channing *Rev. Sci. Instrum.* 67, 2372 (1996)

**JTP1 8 Electron Collisional Excitation of S II** SWARAJ TAYAL, *Clark Atlanta University* Electron collisional excitation strengths for inelastic transitions are calculated using the R-matrix method in a 19-state ( $3s^2 3p^3$   $^4S^o$ ,  $^2D^o$ ,  $^2P^o$ ,  $3s 3p^4$   $^4P$ ,  $^2D$ ,  $^2S$ ,  $3s^2 3p^2 3d$   $^2P$ ,  $^4F$ ,  $^4D$ ,  $^2F$ ,  $^4P$ ,  $3s^2 3p^2 4s$   $^4P$ ,  $^2P$ ,  $3s^2 3p^2 4p$ ,  $^2S^o$ ,  $^4D^o$ ,  $^4P^o$ ,  $^2D^o$ ,  $^4S^o$ , and  $^2P^o$ ) close-coupling approximation. These target states are represented by extensive configuration-interaction wave functions that give excitation energies and oscillator strengths that are usually in good agreement with the experimental values and the available accurate calculations. Rydberg series of resonances converging to the excited state thresholds are explicitly included in the scattering calculation. The effective collision strengths are determined assuming a Maxwellian distribution of electron energies. The results for collision strengths will be compared with the recent merged beams energy loss measurements and other calculations.

**JTP1 9 100 eV Electron Impact Ionization of Atomic Oxygen: First Experimental Results\*** J. DOERING, J. YANG, *Johns Hopkins University* The study of the ionization of atomic oxygen is of interest both because of the open shell electronic structure of the atom and the importance of atomic oxygen in the atmospheres of planets and astrophysical objects. The (e,2e) method allows the triple differential cross section for production of each of the three final states of the OII ion to be determined. The ionization potentials of atomic oxygen are 13.55 eV ( $^4S$ ), 16.86 eV ( $^2D$ ), and

18.54 eV ( $^2P$ ). We have recently begun experiments in which a microwave discharge atomic oxygen source is coupled to the (e,2e) spectrometer which we have previously used to study asymmetric (e,2e) processes in  $N_2$  and  $O_2$ . We are currently using an incident energy of 100 eV and detecting ejected secondary electrons at energies 2.5 - 12.5 eV, and ejection angles 30-120°. The typical primary electron scattering angle is 4 deg. All three final states of OII are detected in the coincidence energy loss spectrum. Improvements to the apparatus which will allow the absolute triple differential cross sections for ionization of atomic oxygen to be measured by comparing relative cross sections for all three states to the well-measured ionization cross section of argon will be discussed.

\*Supported by NSF grant ATM-9705115

**JTP1 10 Elastic Electron Scattering by Ground and Laser-Excited Sodium** C. H. YING, H. WEI, Y. WANG, L. VUŠKOVIĆ, *Old Dominion University* The importance of electron collision processes involving excited species for plasma diagnostics was recognized recently.<sup>1,2</sup> For the alignment of the excited particles and relation with linear polarization of subsequently emitted radiation, the electron distribution function has to be retained in the expansion. We will present experimental results of low energy electron elastic scattering with ground and laser-excited sodium. From these studies, we extracted differential scattering cross sections and parameters for elastic scattering by excited sodium prepared with circularly and linearly polarized laser light. Measurements were carried out at electron impact energies 1 to 10 eV and scattering angles up to 50°. Our previous superelastic measurements<sup>3</sup> were used in evaluation of the present work. Data will be compared with convergent-close-coupling<sup>4</sup> and R-matrix-based close-coupling<sup>5</sup> calculations.

<sup>1</sup>T. Fujimoto, *et al.*, National Institute for Fusion Science Report NIFS-Data-16, Nagoya, Japan, April 1992.

<sup>2</sup>S. A. Kazantsev, *Sov. Phys. Usp.* **26**, 328 (1983).

<sup>3</sup>T. Y. Jiang, Z. Shi, C. H. Ying, L. Vušković, and B. Bedreson, *Phys. Rev. A* **51**, 3773 (1995).

<sup>4</sup>I. Bray, D. V. Fursa, and I. E. McCarthy, *Phys. Rev. A* **49**, 2667 (1994).

<sup>5</sup>B. L. Whitten, *et al.*, *Bull. Am. Phys. Soc.* **39**, 1073 (1994).

---

**SESSION JTP2: POSTER SESSION:  
PHOTOABSORPTION**

Tuesday afternoon, 7 October 1997

Great Hall, Memorial Union at 16:00

Nicholas Hitchon, University of Wisconsin-Madison,  
presiding

**JTP2 1 Generalized Oscillator Strengths for Electron Scattering from  $CO_2$**  M KIMURA, *Yamaguchi University, Yamaguchi 755, Japan* J.P. GU, G HIRSCH, R.J. BUENKER, *Universitaet Wuppertal, Wuppertal, Germany* H TANAKA, *Department of Physics, Sophia University, Tokyo, Japan* I ITIKAWA, *Institute of Space and Astronautical Science, Sagami-hara, Kanagawa 229, Japan* M. A. DILLON, *Argonne National Laboratory* This work resolves the discrepancies among reported values of the Generalized Oscillator Strengths (GOS) obtained experimentally and theoretically for electron impact excitation of the  $^1\Sigma_{g,u}$  and  $^1\Pi_u$

states in  $CO_2$ . The present theoretical results employing molecular electronic wavefunctions obtained from the multireference single- and double-excitation configuration interaction (MRD-CI) method reduce the discrepancy with experiment to 30-40%. Inclusion of the vibrational motion in the calculation is found to further reduce this discrepancy to the range of 20%. Therefore a more rigorous study based on a full consideration of vibrational motion and hence, mixings of various electronic and vibrational states, is expected further improve agreement with experiment.

**JTP2 2 Temperature Dependent Photoabsorption Cross Section Measurements of  $O_2$**  L. W. BEEGLE, C. D. NOREN, I KANIK, *Jet Propulsion Laboratory, California Institute of Technology, Pasadena, CA 91109, USA* The analysis and interpretation of terrestrial ultraviolet (UV) airglow and auroral emissions require an accurate knowledge of absorption of the emission lines by the dominate atmospheric gases. In the terrestrial thermosphere, the only significant absorbing species at wavelengths longer than 1000 Å is  $O_2$ . Link *et al.*<sup>1</sup> pointed out that in the 100 -200 km altitude region where absorption by  $O_2$  is significant, the atmospheric temperature increases from 200 K to about 1000 K, suggesting the need for temperature-dependent measurements for the important absorbing gases. In this poster we present temperature-dependent measurements (at 295, 373, 473, and 573 K) of the  $O_2$  photoabsorption cross sections at the aeronomically-important Lyman- $\alpha$  (1215 Å) OI (1304, 1356 and 1641 Å) and NI (1200, 1492, and 1742 Å) emission lines. While the temperature range measured here does not reach the highest temperature encountered in the thermosphere, absorption by  $O_2$  is most important at the lower altitudes and temperatures. The measurements were carried out at a spectral resolution of 0.3 Å (FWHM). Direct application of the Beer-Lambert absorption equation yielded the absolute photoabsorption cross sections for  $O_2$ . [1] R. Link, J. S. Evans, G. R. Gladstone, *J. Geophys. Res.* **99** (1994) 2121.

**JTP2 3 Calculations of line broadening effects in a lithium vapor**\* J.F. BABB, R. CÔTÉ, A. DALGARNO, *ITAMP, Harvard-Smithsonian* Various types of broadening phenomena play important roles in high pressure discharges for lighting. Experimental and theoretical studies of cold atom collisions and long-range photoassociation spectroscopy have led to improvements in the description of alkali-metal dimer interaction potentials and radiative properties. The implications of these improvements for calculations of resonance line broadening widths and shifts and absorption coefficients determining line opacity in the wings at various temperatures are investigated for a lithium vapor.

\*Supported in part by the NSF.

**JTP2 4 Radiative Lifetimes and Atomic Transition Probabilities for Rare-Earth Elements**\* E.A. DEN HARTOG, J.J. CURRY, HEIDI M. ANDERSON, M.E. WICKLIFFE, J.E. LAWLER, *Department of Physics, University of Wisconsin* Interest in rare-earth elements has been on the rise in recent years in both the lighting and astrophysics communities. The lighting industry is increasingly using rare-earths in high-intensity discharge (HID) lamps and require comprehensive sets of accurate oscillator strengths for the modelling of these lamps. Spectroscopic data on rare-earths is also needed in astrophysical studies such as those dealing with the evolution of chemically-peculiar stars. The present work is addressing this need with extensive radiative life-



time and branching fraction measurements, which when combined will yield a large database of absolute transition probabilities of the elements thulium, dysprosium, and holmium. Radiative lifetimes are measured using laser-induced fluorescence of a slow atomic/ionic beam. Branching fractions are determined from spectra recorded using the 1.0 meter Fourier-transform spectrometer at the National Solar Observatory. Lifetimes for 298 levels of Tm I and Tm II and 440 levels of Dy I and Dy II are complete. Branching fractions have been measured for 522 transitions of Tm I and Tm II. Work is underway on lifetimes of Ho and branching fractions of Dy. Representative lifetime and branching fraction data will be presented and discussed.

\*Supported by the National Science Foundation and Osram-Sylvania.

### JTP2 5 High Sensitivity Absorption Spectroscopy on Co II using Synchrotron Radiation\*

K. L. MULLMAN, J. E. LAWLER, *University of Wisconsin-Madison* VUV oscillator strengths for Co II are being measured with the High Sensitivity Absorption Spectroscopy Experiment at the University of Wisconsin. This experiment uses a hollow cathode discharge as an absorbing sample, the Aladdin storage ring at the Synchrotron Radiation Center as a continuum source, and a 3 m focal length vacuum echelle spectrometer equipped with a CCD detector array. The experiment achieves spectral resolving powers of 350,000 and sensitivities to fractional absorptions much smaller than 1% at deep UV and VUV wavelengths. Column densities of sputtered metal atoms and ions as small as  $3 \times 10^8 \text{ cm}^{-2}$  can be detected. This experiment is applicable to essentially every element of the periodic table and could also be used as a plasma diagnostic by replacing the hollow cathode discharge with another plasma source such as a High Intensity Discharge lamp.

\*This research supported by NASA and NSF.

---

## SESSION JTP3: POSTER SESSION:

### RF GLOW DISCHARGES

Tuesday afternoon, 7 October 1997

Great Hall, Memorial Union at 16:00

Nicholas Hitchon, University of Wisconsin-Madison, presiding

### JTP3 1 Simulation of Gas Mixtures in RF Discharges for Nitride Deposition

HELEN HWANG, *Thermosciences Institute\** M. MEYYAPPAN, *NASA Ames Research Center* Tungsten and titanium nitride films have long been grown by chemical vapor deposition (CVD) methods. However, there has been recent interest in low temperature growth using plasma enhanced CVD. For this present work, we focus on the radio frequency (RF) discharge characteristics of gas mixtures used in nitride deposition (for example,  $\text{WF}_6$  and ammonia). Because the radial variations for a standard 200 mm, parallel plate reactor are limited to a small zone near the edges of the electrodes, a 1-D analysis is considered. This model consists of a self-consistent, 3-D moment fluid simulation that solves the continuity, momentum, and energy equations for neutral and charged species.<sup>1</sup> The results in terms of plasma structure, radical concentrations, and local deposition rate will be presented. We will also compare the 1-D results with those obtained

from a 2-D hybrid plasma equipment model (HPEM) developed at the University of Illinois.

\*This work is funded by NASA contract NAS2-14031 to Eloret.

<sup>1</sup>M. Meyyappan and T. R. Govindan, *J. Appl. Phys.* **74**, 2250 (1993).

### JTP3 2 Growth and Characterization of Boron Carbon Alloys Using Plasma Enhanced Chemical Vapor Deposition

ALI BADAQSHAN, VU ANH VU, FAISAL AHSAN, *Dept. of Physics, U. of Northern Iowa, Cedar Falls, Iowa 50614* DAQING ZHANG, DAVID MCILROY, *Dept. of Physics, University of Idaho, Moscow, Idaho 83844-0903* We report on the growth and characterization of boron carbon alloys, B5C, which were produced by plasma enhanced chemical vapor deposition. The growth temperature of our samples was 300C. All of the samples were grown on silicon and were approximately 1um thick. In order to determine the bandgap and the quality of our samples, we studied them by photoreflectance spectroscopy. Our efforts have concentrated on the first direct optical transition in the alloys. The strength of the transition provides a measure of the quality of the BC alloys. We also performed electroabsorption on selected samples to identify additional transitions. We observed that for samples with very good crystalline structure that there was a noticeable electroabsorption response. The results of photoreflectance and electroabsorption are in good agreement for most samples that we studied. These measurements will also be used to examine the potential formation of defect bands with high levels of metal doping. We have also studied the temperature dependence of the optical transitions of these BC alloys. These measurements will help to determine the optimal growth conditions which yield device quality B5C films for applications in high temperature semiconductors.

### JTP3 3 Study on growth processes of particles in $\text{GeH}_4$ rf discharges using laser light scattering method

H. KAWASAKI, J. KIDA, K. SAKAMOTO, T. FUKUZAWA, M. SHIRATANI, Y. WATANABE, *Graduate School of Information Science and Electrical Engineering, Kyushu University, Japan* Growth processes of particles in  $\text{GeH}_4$  rf parallel plate discharges are studied using a laser light scattering (LLS) method. For  $\text{GeH}_4(5\%)+\text{He}$ , 30sccm, 80Pa and 40W, particles begin to be observed from a very early time of  $\sim 0.1\text{s}$  after the discharge initiation around the plasma/sheath boundary near the powered electrode, where emission intensity of Ge atoms is high. This appearance time of particles is extremely fast compared to that ( $\sim 0.8\text{s}$ ) for a  $\text{SiH}_4$  rf discharge reported previously.<sup>1</sup> This suggests short-lifetime radicals may contribute to the particle nucleation for  $\text{GeH}_4$ , while no data concerning reaction rates for  $\text{GeH}_x$  radicals is available. After nucleation and subsequent initial growth of particles, they coagulate quickly with one another, which brings about a growth rate considerably high compared to that for  $\text{SiH}_4$ . Some Ge particles become sub-micron in size at an early time of  $\sim 0.3\text{s}$  and fall down to the plasma/sheath boundary near the lower grounded electrode because of their heavier weight than Si particles.

<sup>1</sup>Y. Watanabe *et al.*, *J. Vac. Sci. & Technol. A* Vol.14, 540 (1996).

### JTP3 4 Nonlinear Propagation of Helicon Waves\*

J. A. TATARONIS, *University of Wisconsin, Madison, WI, USA* V. PETRŽILKA, *Institute of Plasma Physics, Prague, Czech Republic* G. G. BORG, I. V. KAMENSKI, *Australian National University, Canberra, Australia* Poloidal ponderomotive forces exerted by large-amplitude helicon waves can modify the plasma density



profile and thereby alter the helicon wave fields, both in helicon plasma sources and in fusion devices, such as the heliac H-1. In this study, nonlinear changes in the helicon wave fields, self-consistently resulting from the nonlinear plasma density profile changes, are estimated. The computations proceed in iterations. For each computed inhomogeneous density profile, the radial and axial profiles of the wave electric fields and ponderomotive forces are computed using the coupling code FEM. For waves launched with negative helicity antennae, the helicon wave electric fields are very low in the plasma interior, where the nonlinearly modified plasma density has a strong maximum. This means that such discharges are difficult to sustain. On the other hand, the electric field profiles of helicon waves launched by positive helicity antennae broaden by nonlinear effects. Our results may provide the explanation why it is difficult to excite  $m = -1$  modes in helicon wave plasmas. \*Supported by the Czech grant GA CR 202/96/1355 and the U.S. DOE under grant No. DE-FG02-97ER54398.

**JTP3 5 A Radio Frequency Plasma Source for Plasma Lifetime Studies\*** M.H. BETTENHAUSEN, J.E. SCHARER, Y. MOUZOURI, *University of Wisconsin-Madison* The design of a radio-frequency plasma source for plasma lifetime studies is discussed. The aim of this work is to investigate radiofrequency excitation as an efficient means of increasing the lifetime of a laser-produced plasma. Such a plasma has a precise spatial profile but a short lifetime. Initial experiments will investigate operation in the 1–35 MHz range with Argon at 1–100 mTorr pressures and magnetic fields of 50–300 Gauss. Later experiments will investigate the use of low ionization seed gases in buffer gases since such gases can be ionized with an excimer laser. During these experiments, recombination and plasma chemistry processes will be studied to determine methods for increasing the plasma lifetime. Antenna modeling results obtained with our ANTENA2 code<sup>1</sup> for the device parameters above and plasma densities in the range  $10^{11}$ – $10^{13}$   $\text{cm}^{-3}$  are discussed. These modeling results are used to guide the design of the antenna for the radiofrequency source. The excitation frequency for the source and its effect on both the radiofrequency source operation and the lifetime of a laser produced plasma is considered.

\*This work is supported by AFOSR grant No. F49620-97-1-0262 and NSF grant No. ECS-9632377.

<sup>1</sup>Y. Mouzouris and J. Scharer, *IEEE Trans. on Plasma Science*, **24**(1), (1996)

**JTP3 6 Characterisation of the Heating Mechanisms in a Capacitively-Coupled RF Discharge** C.M. DEEGAN, M.B. HOPKINS, *Dublin City University* Capacitively coupled rf discharges are sustained via three heating mechanisms. Transitions from one heating mechanism to another are effected by external control parameters such as gas pressure, rf voltage, current density and the discharge geometry. In low pressure discharges, a heating mode unique to rf discharges has been reported. The plasma electrons are heated in the oscillating space charge sheaths. Increasing the gas pressure effects a transition to a collisional heating mode known as the alpha-mode. The third mechanism is called the gamma-mode as it is due mainly to secondary electron emission from the powered electrode. We describe studies of these heating mechanisms in an asymmetrically powered, capacitively coupled discharge, with argon as the working gas. Particular attention was paid to the alpha-gamma mode transition. Experiments were carried out at several electrode gaps over a wide range of input powers and pressures. Two electrical diagnostics, Langmuir probes and a current-voltage monitor were used to measure plasma param-

eters and store the relevant control parameters (i.e. current density and applied voltage). Voltage information was analysed for its harmonic content. Transition from the alpha to the gamma mode was characterised by a marked change in the plasma parameters, EEDF and harmonic content of the voltage waveform.

**JTP3 7 Measurements of the complex impedance of radio frequency excited CO<sub>2</sub> slab lasers and discharge chambers\*** C. LUECKING, *Ruhr-University Bochum, Germany* U. BERKERMANN, J. MENTEL, G. SCHIFFNER, *Ruhr-University Bochum* Matching design requires knowledge of the discharge impedance and its dependence on the input rf power, gas pressure and operation modes. Moreover measurements of the discharge impedance are important to achieve a model for the rf slab laser by a determination of the plasma impedance. Two independent methods are applied to measure the complex impedances of rf excited CO<sub>2</sub> slab lasers and of a discharge test chamber. The rf feedthroughs are chosen as reference ports for the measurements. One method using an adjusted matching network and a network analyser is compared with another method measuring two signals representing current and voltage with a digital oscilloscope and processing them numerically. Comparison of the results of the real and the imaginary parts of both methods have shown a full agreement. The true plasma impedance is calculated measuring additionally the impedance without a discharge at the ports of the discharge vessel.

\*supported by the German Ministry for Education and Science (BMBF) under the project number 13N6571

**JTP3 8 Plasma Characteristics of Two-Frequency-Operated Plasma in Ar by Two-Dimensional Modeling\*** N. NAKANO, T. MAKABE, *Keio University Yokohama, Japan* Two frequency operated plasma is used for various plasma processes, such as sputter deposition and etching. This type of reactor has an advantage of new function to control the processes, even though it has a simple geometrical structure with conventional parallel plate electrodes. Nonequilibrium plasma contains the very wide range processes of time scale. Therefore it is important that choosing the suitable frequency to control the target particles. In this work, the characteristics and the functions of two frequency-operated-plasma are discussed by two dimensional modeling. The relaxation continuum model is used for the analysis. The reactor consists of cylindrical chamber and two electrodes. The upper electrode is connected to VHF power supply for high density plasma source, and lower electrode is connected to LF bias power supply for ion acceleration. Voltage amplitude of LF is required to be higher than that of VHF to make the sheath for the acceleration of ions. In order to control the ion energy and the flux, low frequency with period longer than an ion transit time, is effective. In the present results, higher bias voltage than VHF affects to the plasma structure with increasing the high energy ion flux to the wafer.

\*The work was partly supported by Keio university Grant for ICRP.

**JTP3 9 Accuracy of the Unified Sheath Model\*** MERLE E. RILEY, *Sandia National Laboratories* The Unified Sheath Model<sup>1</sup> is designed to bridge the intermediate region of ion response between the high frequency Lieberman model and the low frequency Metzger, Ernie, and Oskam model. In order to make a quantitative check of the effective ion response time (inverse ion plasma radian frequency at the presheath boundary), I have compared the semi-analytic Unified Model predictions to time- and space-dependent numerical solutions of the ion fluid equations in an rf-biased

plasma sheath. In so doing, one is testing the most crucial of the physical approximations made in the model. The comparisons are good and lend confidence to use of the sheath model in the simulation of rf-biased plasmas in processing applications.

\*This work was supported by United States Department of Energy under contract DE-AC04-94AL85000. Sandia is a multiprogram laboratory operated by Sandia Corporation, a Lockheed Martin Company, for the United States Department of Energy.

<sup>1</sup>M. E. Riley, Sandia Labs Tech Reports SAND95-0775 UC-401 (May, 1995) and SAND96-1948 UC-401 (August, 1996)

**JTP3 10 A Study of the Characteristics of an RF and DC Driven Hydrogen Discharge** D BOILSON, N CURRAN, P MCNEELY, M.B. HOPKINS, *Dublin City University* The Deuterium Negative Ion Source Experiment, DENISE is being recommissioned as a test-bed for the production and extraction of H-/D- and is currently being modified to provide easier access for diagnostic purposes. Initial studies are being carried out on the characteristics of a Hydrogen Plasma in this new multicusp volume ion source. An RF (13.56MHz) power supply provides either the generation of a pulsed or a continuous inductively coupled hydrogen plasma. The plasma parameters are measured using a tuned Langmuir Probe, it is proposed that the concentration of hydrogen negative ions be quantified using a modified Laser photodetachment technique. Studies are carried out on the effect of pressure, power and the effect of an external cusp shaped magnetic field. It is expected that the use of a pulsed RF driver will increase D- production in the afterglow discharge. Replacing the RF antenna coil with 1.00mm tungsten filaments will allow the same source chamber to be used in studies to compare these two different methods of plasma generation.

**JTP3 11 Downflow Plasma-Enhanced Chemical Vapor Deposition Using Hexamethyldisiloxane for Preparation of Low Dielectric Constant Interlayer Dielectrics** T. FUJII, M. HIRAMATSU, M. NAWATA, *Meijo University, Nagoya, Japan* M. HORI, T. GOTO, *Nagoya University, Nagoya, Japan* S. HATTORI, *Nagoya Industrial Science Research Institute, Nagoya, Japan* Low dielectric constant interlayer dielectrics are required to realize high-performance in the future integrated circuit devices. Silicon-oxide based siloxane materials are known as low dielectric constant dielectrics. In this work, we propose a 13.56 MHz radio-frequency (rf) inductively coupled plasma-enhanced chemical vapor deposition system for preparation of insulating films with low dielectric constant. Hexamethyldisiloxane (HMDSO) was used as feed gas. Oxygen radicals generated by rf oxygen plasma were introduced into the reaction chamber for the polymerization of HMDSO. The monomer gas was injected in the downflow region of oxygen plasma. The effects of deposition conditions on film properties were investigated. From chemical analysis, polysiloxane films retaining Si-O and Si-CH<sub>3</sub> structures were formed at room temperature. Dielectric constant of the films showed a tendency to increase with increase of substrate temperature and rf power. The films with dielectric constant lower than 3.0 were obtained by using this system.

**JTP3 12 Deposition of high purity copper thin films using plasma CVD reactor with H radical source** H. KAWASAKI, H. J. JIN, T. KAWASAKI, T. FUKUZAWA, T. KINOSHITA, M. SHIRATANI, Y. WATANABE, *Graduate School of Information Science and Electrical Engineering, Kyushu University, Japan* \* M. TOYOFUKU, \* *Department of Electrical Engineering, Fukuoka Institute of Technology, Japan* We have demonstrated that high quality Cu films are deposited for a high H<sub>2</sub> dilution rate above about 90% in a plasma CVD using metal organic (MO) material Cu(hfa)<sub>2</sub>.<sup>1</sup> Recently, we develop a plasma CVD reactor with a H radical source to deposit high quality Cu thin films at a low H<sub>2</sub> dilution rate. High purity (almost 100%) Cu films of a low resistivity of 2μΩcm can be deposited for a H<sub>2</sub> dilution rate of 50-67% by using this reactor. To identify the role of H radicals in the Cu deposition, Cu films are exposed to H<sub>2</sub> rf discharges and concentrations of impurities such as F, C, O in the films are measured by in-situ FT-IR method. The concentrations can be greatly reduced by the H<sub>2</sub> plasma treatment and its effect is enhanced at the film temperature above about 70°C, while Ar plasma treatment is much less effective for impurity reduction. These results indicate that H radicals significantly contribute to purify the Cu films.

<sup>1</sup>M. Shiratani *et al.*, J. Phys. D: Appl. Phys., Vol.29, 2754 (1996).

**JTP3 13 Simulations of Downstream Processing Systems Sustained by Azimuthal Microwave TE(0,n) Mode Fields** \* RON KINDER, MARK J. KUSHNER, *University of Illinois-Urbana/Champaign* Moderate pressure (100s mTorr to a few Torr) microwave discharge sources are being used for downstream etching and deposition, and production of radicals for surface treatment. The spatial coupling of microwave radiation to the plasma in these systems is a concern due to issues related to gas utilization, heating and dissociation fraction. To investigate these issues, we have developed a finite-difference-time-domain (FDTD) simulation for microwave injection and propagation. The FDTD has been incorporated as module in the 2-dimensional Hybrid Plasma Equipment Model (HPEM). The system of interest uses TE(0,n) microwaves injected along the axis of a cylindrically symmetric downstream reactor. The model has been applied to the analysis of production of oxygen radicals and excited states from O<sub>2</sub> and other oxygen donors (CO<sub>2</sub>, N<sub>2</sub>O). Consequences of gas flow rate and pressure on radical production will be discussed.

\*Research supported by ARPA/NCSU, SRC and NSF (ECS94-04133, CTS 94-12565).

**JTP3 14 Nonvolatile Particle Transport from Etched Surface in 2-D CCP Modeling** M. HASEBE, N. NAKANO, T. MAKABE, *Keio Univ, Yokohama, Japan* Byproducts in etching processes are strongly linked to the incident ion flux on a wafer. We first discuss the radial uniformity of the ion flux incident on a substrate of the powered electrode as a function of reactor geometry. Nonvolatile particles ejected by etching (physical sputtering) from the substrate will be the origin of an absorbed layer on the etched surface as well as the particle growth in the plasma. We investigate the nonvolatile particle transport in a 2-D capacitively coupled plasma (CCP) under gas flow by using the relaxation continuum (RCT) model. We use a diffusion equation to analyze the nonvolatile particle transport with the gas flow. CCP is mainly maintained at 13.56 MHz with amplitude of 300 V at 100 mTorr in

Ar. We also show a series of 2-D space distributions of CCP in various reactor geometry and the nonvolatile particle transport.

### JTP3 15 Tailoring of Particle Energy Distributions in Low Temperature Plasmas\*

A. GOODYEAR, N.ST.J. BRAITHWAITE, *Open University* The efficiency and effectiveness of plasma processing benefits from a greater degree of control over the physical and chemical interactions in the plasma, especially those at and near surfaces. The electron energy (distribution eedf) influences directly the gas phase processes and indirectly the ion energy distribution (iedf). This work investigates the electrical tailoring of the eedf so that more effective use can be made of particular plasma sources. This is achieved by injecting extra electrons into the plasma; injection flux and energy are important new control parameters. In particular we have shown that injecting electrons changes potential structure and the balance of the energy exchange processes responsible for sustaining of the steady eedf; as a result the eedf and iedf are altered. The ionization balance is also disturbed and higher plasma densities can be achieved. These changes are reflected in an altered impedance of the plasma. Results are presented for 13.56 MHz plasmas in argon and other gases at 1-100 Pa.

\*Work supported by the EPSRC, Grant No. GR/K58067

### JTP3 16 Planar Plasma Producers on the Surface Wave Discharge with External Magnetic Field\*

N.A. AZARENKO, A. I. SMOLYAKOV, A. HIROSE, *Department of Physics and Engineering Physics, University of Saskatchewan, Saskatoon S7N 5E2 Canada* V.O. GIRKA, I.B. DENISENKO, K.N. OSTRIKOV, *Department of Physics and Technology, Kharkiv State University, 310077 Kharkiv, Ukraine* Radio-frequency and microwave discharges produced by surface waves are attractive candidates for large-area plasma sources. We study magnetically enhanced surface waves in the configuration of two parallel metal electrodes with dielectric coatings. The structure of the plasma discharge is studied for three (a,b, and c) different types of surface waves and different orientation of the external magnetic field. In (a) and (b), the external magnetic field is parallel to the electrodes. In (a), the magnetoplasma surface wave propagates along the magnetic field, and in (b), the discharge is sustained by the surface wave at harmonics of the electron cyclotron frequency propagating across the magnetic field. In (c), the external magnetic field is normal to the electrodes, and the discharge is produced by the surface cyclotron wave propagating along the interface. The spatial distributions of plasma density, electromagnet fields, energy flow, phase velocity and skin depth are obtained both analytically and numerically for all three configurations. Detailed comparison of obtained parameters with experimental data is given.

\*Supported by the Science and Technology Center of Ukraine and NSERC of Canada

### JTP3 17 Fast modelling of low pressure radio-frequency capacitively coupled discharge and investigation of non-Maxwellian electron distribution function

S.V. BEREZHNOI, I.D. KAGANOVICH, L.D. TSENDIN, *St.Petersburg Technical State University, Russia* The principles of fast-modeling of low-pressure radio-frequency capacitively coupled discharge are presented. They are based on averaging over electron and ion motions and eliminating small spatial scale - Debye radius. As a result the solution of the self-consistent system of electron kinetic equation, Poisson, and ion continuity equations takes approximately 10min on a 486PC. The calculation of discharge parameters has been performed for a wide range of current and pressure. The compari-

son with full-scale Monte-Carlo calculations and experimental data have been done. It has been demonstrated that the form of electron distribution function (EDF) is very sensitive to details of its description, e.g. small corrections in cross-sections result in considerable change in EDF. The mechanisms of the formation of non-Maxwellian EDF have been analyzed.

### JTP3 18 Kinetic Theory of a Collisionless RF Sheath at $\omega\tau \sim 1$ \*

V.I. KOLOBOV, D.J. ECONOMOU, *University of Houston* Novel high density plasma sources offer independent control of ion flux and energy by applying a RF bias to the substrate electrode. A collisionless sheath of thickness  $\delta$  is formed in front of the biased electrode. The characteristics of the sheath depend on the product,  $\omega\tau$ , of the driving frequency  $\omega$  and the mean ion transit time through the sheath  $\tau = \delta/v_0$ . Although the high and low frequency regimes of the sheath are well understood, the intermediate frequency regime  $\omega\tau \sim 1$  requires further study. The energy distribution of ions bombarding a biased electrode becomes wide in the case  $\omega\tau \sim 1$  because ions entering the sheath at different field phases acquire different kinetic energy in the sheath. We shall present a kinetic theory of the sheath in the regime  $\omega\tau \sim 1$  and compare this theory with a fluid model which treats ions as a fluid with mean velocity,  $v_0$ . The ion velocity distribution function is obtained as a solution of the collisionless Boltzmann equation for different values of the parameter  $\omega\tau$ .

\*Supported by NSF grant # CTS-9216023

### JTP3 19 Ions in RF-Discharges with Si-Organic Admixtures\*

R. FOEST, R. BASNER, M. SCHMIDT, *INP Greifswald, Germany* V. TARNOVSKY, K. BECKER, *Stevens Institute of Technology, USA* Results of mass spectrometric measurements in capacitively coupled asymmetric Ar rf discharges with small admixtures of the Si-organic compounds TMS, TEOS, and HMDSO are presented. The relative ion currents to the wall were determined using a plasma monitor and integrating the measured kinetic energy distribution of the ions over the energy range. The contribution of the fragment ions of the parent molecules to the total current is small, whereas hydrogen and light hydrocarbon ions are dominant. We also present partial and total electron-impact ionization cross sections of the parent molecules measured in a high resolution double-focussing mass spectrometer. The measured ion spectra are compared to the calculated ion populations derived from the rate coefficients for electron-impact ionization using various electron temperatures. The observed dominance of lighter fragment ions in the plasma indicates the important role of decomposition processes and secondary reactions in the plasma.

\*Work supported in part by the U.S. NSF

### JTP3 20 Studies on High Pressure RF Glow Discharges

JAEYOUNG PARK, I. HENINS, G.S. SELWYN, *Los Alamos National Laboratory* Experimental Studies on RF discharges at (13.56 MHz) in helium and helium + oxygen have been performed in very high gas pressures between 1 torr to 600 torr. Plasma parameters, comparable to the low pressure discharges, are observed in He discharges by optical emission spectroscopy and a Langmuir probe measurement. The observed electron density of  $1-5 \times 10^{11} \text{ cm}^{-3}$  and electron temperature of (1-2 eV) indicate that the discharge can be characterized by a normal glow. An absence of emission lines from Rydberg states shows that the dominant mechanism for the charged particle loss is due to the diffusion to the wall. By increasing the gas pressure, a decrease in He line emission is observed, consistent with the cooling of the electrons



by electron-neutral elastic collision. The plasma conditions change substantially as oxygen is introduced in the discharges. A decrease in electron density is observed due to the electronegativity of oxygen. A further increase in the oxygen flow results in the extinction of the discharge. A detailed analysis of optical emission spectroscopy and the probe measurement will be given as a function of gas pressure and composition.

**JTP3 21 Determination of Electron Density and Temperature from the External Voltages and Sheath Thickness in a rf-Discharge\*** M. SCHMIDT, F. HEMPEL, M. HANNEMANN, R. FOEST, *INP Greifswald, Germany* Results are presented for the relation between the electron density  $n_e$ , the electron temperature  $T_e$ , the external voltages (operating, self-bias), and the sheath thickness in front of the powered electrode of an asymmetric capacitively coupled rf discharge (Ar, 0.03 - 0.5 mbar, 0.2 - 0.5 W/cm<sup>2</sup>, 4 cm electrode spacing). A relationship between the sheath capacities and the rf and bias voltages in a sheath-determined rf discharge has been given by Koehler *et al.* (J. Appl. Phys. 57 (1985) 59). The capacity of the sheath near the powered electrode is determined by the electrode surface and the sheath thickness. Using the scaling law for the bias voltage in relation to the electrode surfaces, the Langmuir-Child law for the current density and the Bohm velocity of the ions in the pre-sheath, a balance equation for the particles is obtained as a function of  $T_e$ .  $T_e$  and  $n_e$  can be obtained assuming direct impact ionization of the Ar atoms in the discharge. The results are compared with data obtained from Langmuir probe measurements.

**JTP3 22 Hydrodynamics of Dusty Plasmas** AMITAVA BHAT-TACHARJEE, study the properties of strongly coupled dusty plasmas. For a dusty plasma linearly departing from a local thermodynamic equilibrium, the hydrodynamic limit is a good approximation. We have found the dispersion relations in this limit with three thermal diffusion modes and three dusty plasma waves (the Langmuir wave, the ion acoustic wave and the dusty acoustic wave (DAW)). The dusty lattice wave has not been found in the hydrodynamics limit. From the dispersion relation and linear response theory, the structure factors (so the correlation functions) can be calculated. It is found that the motion of the dust grains is too slow to respond to those fast modes such as Langmuir waves. Therefore, in that case, only do plasma particles contribute to the Debye shielding. However, the dust grains do shield each other in the DAW limit when the mode is slow enough to "feel" the shielding. This is in agreement with our previous kinetic theory and the particle simulation.

**JTP3 23 Ionization waves in a dusty plasma** D. SAMSONOV, J. GOREE, *The University of Iowa* Previously Praburam<sup>1</sup> showed the presence of a periodically rotating formation or "great void mode" in a particulate cloud grown in a parallel plate RF sputtering discharge. We attribute this mode to a dust-assisted ionization wave. The internal structure of the ionization wave was revealed by 2D optical emission spectroscopy and laser light scattering. Dust number density was measured by laser light extinction in the Mie regime. Electron micrographs revealed the size and shape of dust particles at each phase of the growth cycle. The ionization instability is believed to be caused by a change in local balance of forces acting on dust particles. As the particles grow, ion drag pushes them away from a region of enhanced ionization, thereby reducing electron depletion and further enhancing ionization.

<sup>1</sup>G. Praburam and J. Goree, Phys. Plasmas 3, 1212 (1996).

**JTP3 24 Study on growth processes of clusters formed in SiH<sub>4</sub> rf discharge using threshold photoemission method** T. FUKUZAWA, H. MIYAHARA, S. KUSHIMA, H. KAWASAKI, M. SHIRATANI, Y. WATANABE, *Graduate School of Information Science and Electrical Engineering, Kyushu University, Japan* We have proposed a threshold photoemission method for studying growth processes of Si<sub>n</sub>H<sub>x</sub> clusters formed in rf SiH<sub>4</sub> discharges. The experiments have shown that short lifetime radicals mainly contribute to the cluster formation, at least, for a high discharge power density ( $\geq 0.25$  W/cm<sup>2</sup>) and some clusters are neutral.<sup>1</sup> However, it has been difficult to obtain information on size growth of clusters in the size range in which their electron affinity and ionization potential become higher than a photon energy  $h\nu$  ( $=3.48$  eV) and lower than  $2 \times h\nu$  ( $=6.96$  eV), respectively. Utilizing a feature that the density decay of neutral clusters depends on their size, we can study time evolution of their size by measuring the characteristic density decay-time  $\tau$  after rf-power-off. Under experimental conditions of He+SiH<sub>4</sub>(3%), 10 sccm, 80 Pa, 60 W, the decay-time  $\tau$  increased from 0.8 ms for a discharging period  $T_{on}=50$  ms to 16 ms for  $T_{on}=200$  ms. Cluster sizes corresponding to  $T_{on}=50$  ms and 200 ms are estimated to be  $\sim 0.65$  and  $\sim 3.7$  nm, respectively, and hence the growth rate of neutral clusters is  $\sim 20$  nm/s. This growth rate is almost the same as that for  $T_{on} \leq 20$  ms reported before.<sup>1</sup>

<sup>1</sup>T. Fukuzawa *et al.*, J. Appl. Phys. Vol.80, 3202 (1996).

**JTP3 25 Langmuir probe measurements of very low frequency fluctuations in a dusty rf discharge in a GEC Reference Cell\*** RICK QUINN, JOHN GOREE, *The University of Iowa* A Langmuir probe was used to measure very low frequency electrostatic fluctuations in a GEC reference cell. We sought to identify any fluctuations that could heat highly charged dust particles in what is commonly called a plasma crystal. The probe drew an ion saturation current of a few  $\mu A$  when biased negatively, using batteries to reduce 60 Hz pickup. Power spectrums of the fluctuating current were obtained for various Kr gas pressures. We found a large portion of the fluctuation power to be deposited at 60 Hz due to ripple in the rf generator. We also observed large resonances in the power spectrum between 1 and 3 KHz which depended sensitively on the rf voltage applied to the electrode. Additionally a strong 18 Hz peak was observed for all rf discharge conditions, and its origin has not yet been identified. Using digital filtering to exclude the 60 Hz contribution, the power spectrum of the fluctuations was integrated over frequency. This integrated power did not vary significantly with pressure, suggesting that the heating and disorder observed in a plasma crystal are not due to these very low frequency electrostatic fluctuations.

\*Funded by NASA GSRP program

**JTP3 26 Initial Particle Growth Rates in a Pure Silane Plasma** M. A. CHILDS, ALAN GALLAGHER, *JILA, NIST and University of Colorado - Boulder* Silicon particles form and are suspended in silane plasmas, and small (less than 15 nm diameter) particles contaminate the growing films. We study these particles in a parallel plate rf discharge of pure silane designed to closely approximate reactors used to make hydrogenated amorphous silicon thin film transistors and photovoltaics. We determine the size and density of the particles in the plasma during the initial growth stages by a novel method. The particles are detected by light scat-



tering and the particle size is inferred from the diffusion of the particles shortly after the plasma is turned off. Since the scattered light intensity is proportional to the product of the density and the sixth power of the particle radius, the density is found from the scattered intensity. The scattered light intensity for particles less than 20 nm in diameter initially increases as the sixth to seventh power of the time after the discharge is started, which is consistent with our growth model. This model is based on growth primarily due to collisions with  $\text{SiH}_3$  radicals. (We would like to thank A. V. Phelps for helpful discussions. Supported in part by the National Renewable Energy Laboratory of the Department of Energy.)

**JTP3 27 On transition of spatial density profile of particles formed in  $\text{SiH}_4$  rf discharges** Y. WATANABE, H. KAWASAKI, T. FUKUZAWA, M. SHIRATANI, *Graduate School of Information Science and Electrical Engineering, Kyushu University, Japan* Spatial density profiles of particles in  $\text{SiH}_4$  rf discharges are examined as parameters of pressure and  $\text{SiH}_4$  concentration for an rf power ( $\geq 0.26 \text{ W/cm}^2$ ). When a diffusion time ( $\tau_d$ ) of  $\text{SiH}_2$  radicals (key species for fast particle nucleation<sup>1</sup>) through their generation region is longer than their reaction time with  $\text{SiH}_4$  ( $\tau_r$ ), particles grow at a fast growth rate of  $\geq 10^7 \text{ s nm/s}$  and are localized only around the plasma/sheath (P/S) boundary near the rf electrode. Under this condition, neutral clusters react many times before they diffuse out of the radical generation region. Since the diffusion time of clusters increases with their size, larger clusters tend to be localized and grow further to nm in size. For  $\tau_r > \tau_d$ , particles grow at a slow growth rate of  $\leq 1^7 \text{ s nm/s}$  and exist in the plasma bulk as well as around the P/S boundary. This broad existence of particles suggests that negatively charged clusters are indispensable for particle growth for  $\tau_r > \tau_d$ . The results also suggest that particle growth around the P/S boundary can be realized when  $\text{SiH}_2$  radicals are supplied sufficiently there, that is, when the rf power is high.

<sup>1</sup>Y. Watanabe *et al.*, *J. Vac. Sci. & Technol. A* Vol.14, 995 (1996).

**JTP3 28 Experimental Studies of Ar/O<sub>2</sub> Plasma in a Planar Inductive Discharge** JON TOMAS GUDMUNDSSON, TAKASHI KIMURA, MICHAEL A. LIEBERMAN, *Plasma Assisted Materials Processing Laboratory, Department of Electrical Engineering and Computer Sciences, University of California, Berkeley, CA 94720* A Langmuir probe was used to determine the electron density, electron temperature, plasma potential and the electron energy probability function (EPPF) in Ar, O<sub>2</sub> and Ar/O<sub>2</sub> plasma in a planar inductive discharge for pressure range 2 – 50 mTorr. The electron energy distribution function is found to be Maxwellian at low electron energy with a depletion at high electron energy over the power, pressure and fractional argon flowrate investigated. The electron density increases with increased argon content. At fractional argon flowrate around 66 % the electron density increases abruptly by a factor 2 – 4 and continues to increase slightly as argon content is increased further. The plasma potential and the average electron energy gradually decrease with increased argon content. Mass spectrometry indicates that the dominant ion is O<sub>2</sub><sup>+</sup> for fractional argon flowrate below roughly 66% but abruptly changes to Ar<sup>+</sup> ions if the fractional argon flowrate is increased.

## SESSION JTP4: POSTER SESSION: PROPULSION AND SPACE PLASMAS

Tuesday afternoon, 7 October 1997

Great Hall, Memorial Union at 16:00

Nicholas Hitchon, University of Wisconsin-Madison, presiding

**JTP4 1 Radio-Frequency Discharge in Martian Atmosphere<sup>1</sup>** L. VUŠKOVIĆ, R. L. ASH, S. POPOVIĆ, T. DINH, A. VAN ORDEN, *Old Dominion University* We investigated a capacitive radio-frequency discharge in a gas mixture containing 95.7% carbon dioxide, 2.7% nitrogen, and 1.6% argon in the pressure range from 5 to 10 Torr, which is a realistic representation of the Mars atmosphere. The main objective is to study carbon dioxide decomposition in the vicinity of silver electrodes and the atomic oxygen production process.<sup>2</sup> We designed the discharge region as a scaled-down version of the GEC Reference Cell.<sup>3</sup> One of the silver electrodes is heated and used as a membrane to extract atomic oxygen from the discharge. We will show the results of variation of carbon dioxide dissociation efficiency with gas pressure, electrode gap, and electrode temperature. The relation between carbon dioxide dissociation and atomic oxygen diffusion for various thickness of silver membrane will be established. The influence of several different silver membrane production and sealing techniques to oxygen extraction efficiency will be analyzed. The possibility of particulate confinement and extraction will be discussed.

<sup>1</sup>Supported by NASA Langley Research Center.

<sup>2</sup>L. Vušković, R. L. Ash, Z. Shi, S. Popović, and T. Dinh, 27th International Conference on Environmental Systems, Reno, Nevada, SAE Paper 972499 (1997).

<sup>3</sup>J. R. Hargis, Jr., *et al.*, *Rev. Sci. Instr.* **65**, 140 (1994).

### JTP4 2 Radiative emission from metastable multiply charged ions of importance in space plasmas

J.B. GREENWOOD, *Jet Propulsion Laboratory* With the launch of satellites capable of observing in the ultra-violet region, emission from a number of forbidden transitions in multiply charged ions has been observed [1]. The radiative rates for metastable states of these ions in diffuse interstellar, stellar, solar and planetary plasmas are comparable to the collisional rates. These emissions can be used to determine the electron temperature and density, if accurate values for the metastable radiative rates are available. We will be presenting preliminary results of metastable lifetimes of astrophysically important ions measured in a Kingdon ion trap. The experiment generates metastable multiply charged ions in an electron cyclotron resonance ion source. The ions are directed into the cylindrical electrostatic ion trap where confinement is achieved by a fast kilovolt pulse on the central wire of the trap. The photons emitted from the metastable state of interest are selected by a narrow bandpass filter and detected by a photomultiplier. From the time decay of the photon signal one determines the lifetime of the state. [1] K. R. Sembach *et al.*, *Ap. J.* **480**, 216 (1997).

### JTP4 3 Modelling of the Stationary Plasma Thruster

A. FRUCHTMAN, *Center for Technological Education Holon, P.O. Box 305, Holon 58102, Israel* N. J. FISCH, *Princeton Plasma Physics Laboratory, P.O. Box 451, Princeton, NJ 08543* \* The Stationary Plasma Thruster (the Hall thruster) is analyzed using kinetic and fluid models. In both pictures we derive analytical solutions for particular classes of plasma source functions, and show how, by specifying the electron mobility profile, one can

optimize the efficiency for the given source function. The more general equations are solved numerically for large domains in the parameter space. The thruster performance is explored for various values of the accelerating voltage, the mass flow rate and the thruster dimensions. We also examine how the efficiency can be improved by a modification of the magnetic field profile. The theoretical results are compared to the experimental results of the Soreq Hall thruster.

\*This research has been partially supported by AFOSR

**JTP4 4 Modeling the Stationary Plasma Thruster\*** J.P. BOEUF, L. GARRIGUES, L.C. PITCHFORD, *CPAT, Universit  Paul Sabatier, Toulouse, France* Stationary plasma thrusters (SPT) or closed drift thrusters are electrostatic propulsion devices whose properties are suitable for applications such as satellite station-keeping and orbit transfer. These devices are characterized by an ExB configuration where the externally applied magnetic field is radial and perpendicular to the axial, self-consistent electric field which accelerates the ions to the exhaust. Due to the complexity of electron transport in these devices, the properties of the stationary plasma thrusters are not well understood. We have developed quasi-neutral hybrid model which predicts reasonably well the discharge properties when some parameters (electron mobility, electron energy loss coefficient) are adequately adjusted. A transient version of this quasineutral model can reproduce well the low frequency, large amplitude oscillations observed in the SPT. The current oscillations are associated with a small oscillation of the location of the neutral density gradient and ionization source region. More work is however needed to confirm that the model provides the good physical interpretation of the oscillations.

\*supported in part by CNES through the "Groupement De Recherche Propulsion Plasma pour Vols Spatiaux"

---

## SESSION JTP5: POSTER SESSION: FLAT PANEL AND LARGE AREA PLASMAS

Tuesday afternoon, 7 October 1997

Great Hall, Memorial Union at 16:00

Nicholas Hitchon, University of Wisconsin-Madison, presiding

**JTP5 1 Surface Wave Discharge Between Large-Area Metal Electrodes in the External Magnetic Field\*** N.A. AZARENKOV, A. I. SMOLYAKOV, *Department of Physics and Engineering Physics, University of Saskatchewan, Saskatoon S7N 5E2 Canada* A.V. GAPON, I.B. DENISENKO, *Department of Physics and Technology, Kharkiv State University, 310077 Kharkiv, Ukraine* A theoretical model of a large-area surface wave discharge between two parallel electrodes is considered. Surface wave that produces and sustains the microwave discharge propagates along the external magnetic field with the frequency between the electron cyclotron and electron plasma frequencies. The symmetric and antisymmetric surface wave are considered. The spatial distribution of the produced plasma and the electromagnetic fields are obtained analytically and numerically taking into account the finite distance between the electrodes. Two mechanisms of electron losses (diffusion and volume recombination) are considered. Scaling of the characteristic electron temperature and plasma den-

sity are obtained as functions of the external magnetic field and geometrical characteristics.

\*Supported by the Science and Technology Center of Ukraine and NSERC of Canada

**JTP5 2 Modeling of micro-discharges** G.J.M. HAGELAAR, T. HBID, F.J. DE HOOG, *Eindhoven University of Technology, Dept. of Appl. Phys., The Netherlands* Micro-discharges are gas discharges on a scale of hundreds of microns and they are used in several flat panel display technologies. In order to learn more about the mechanisms underlying the behavior of these discharges, a one dimensional fluid model has been developed. The computer code of this model self-consistently solves a system of equations consisting of moments of the Boltzmann equation and the Poisson equation, using an explicit method. An exponential scheme is used for the solution of the moments of the Boltzmann equation. We concentrate on DC micro-discharges and afterglows in pure helium and helium-nitrogen mixtures. We study the influence of several discharge parameters like gas pressure, applied voltage, and secondary emission coefficients on steady state particle densities, electron energy and reaction rates, as well as density decay times in the afterglow. The results support classical ideas about DC discharges and agree with experimental measurements on a display panel. Currently we are working on the extension of the model into two dimension.

**JTP5 3 Design of a Large-Area, Transformer Coupled Plasma Source** Y.S. HWANG, *Dept. of Nuclear Engineering, KAIST, Taejon, Korea* H.J. KIM, K.H. HAN, *Dept. of Nuclear Engineering, KAIST, Taejon, Korea* N.S. YOON, *KBSI, Taejon, Korea* Single wafer plasma processing requires high-density plasmas with good uniformity in large area to achieve high throughput. A large-area transformer coupled plasma (TCP) source has been designed and constructed. The large-area TCP chamber needs very thick dielectric windows to resist mechanical stresses, which makes radio frequency (RF) power coupling difficult. In our design, a plasma generation chamber and an RF antenna chamber have been separated with dielectric material, and differentially pumped to accommodate large-area, relatively-thin dielectric window against mechanical pressures. Both chambers are made of stainless steel, and the size of the plasma chamber is 78 cm in diameter and 37cm in height. 4MHz, 10KW RF power source was used to generate plasmas via a single-turn copper tube antenna and an impedance matching network. Based on two-dimensional heating theory and zero-dimensional plasma transport theory, plasma parameters are studied as functions of external operational parameters and geometrical parameters of the chamber. From this model, the diameter of a single-turn copper coil antenna was optimized to provide high-density plasmas in large area. Also, minimum threshold input power for inductive coupling was calculated from this model and compared with experimental results. In this large-area TCP source, efficient RF power couplings into plasmas are crucial. Initial experimental results of this source will be presented.

**JTP5 4 A Two-dimensional Simulation of Pulsed Discharge for a Color DC Plasma Display Panel** Y. MURAKAMI, *NHK Sci. Tech. Res. Labs.* K. TACHIBANA, *Kyoto Univ.* Plasma display panels (PDPs) are considered to be the most promising candidate for use in wall-mounted HDTV (high-definition TV) receivers. In order, however, to realize a practical PDP, it is essential to improve their luminance and luminous efficiency. We have been developing a CAD tool for calculating the spatio-temporal densities of particles as well as the VUV emission intensities in a pulsed discharge

cell filled with a mixture of He and Xe gas. In this study we employed a two-dimensional fluid model with local field approximation for electrons, four types of ions, and seven excited species. The model took the imprisonment of resonant radiation and secondary electron emissions with ions, metastable atoms and photons into consideration. Twelve simultaneous continuity equations were solved together with Poisson's equation and a circuit equation. The results for the density of the resonance state of Xe( $1s_4$ ), which emits effective VUV for the phosphors, and the discharge current waveforms agreed qualitatively with the experimental results<sup>1</sup>.

<sup>1</sup>K.Tachibana, *et al.*, Appl. Phys. Lett., Vol.65, No.8, p935(1994).

**JTP5 5 Breakdown and plasma formation in coplanar plasma displays** C. PUNSET, J.P. BOEUF, L.C. PITCHFORD, *CPAT, Universite Paul Sabatier, Toulouse, France* Our previously developed, 2-D discharge model<sup>1</sup> has been used to study the discharge initiation and plasma formation in AC plasma display panels a coplanar (single substrate) geometry. Results from this model show that the voltage required to initiate the discharge is strongly dependent, not only on pd, the product of the gas pressure and the distance between the electrodes, but also on the distance, h, between the coplanar electrodes and the addressing electrode. The minimum breakdown voltage is in qualitative agreement with experiment; the minimum voltages moves to larger pd values when d is increased. During one current pulse in steady-state conditions, the maximum light emission occurs at the sheath edge, but in the coplanar geometry, the sheath is never parallel to the dielectric surface. Wereported previously in Ref. 1 for matrix geometries (electrodes on opposite substrates) the radial spreading of the plasma along the dielectric surfaces, due to the accumulation of wall charges. This also occurs in the coplanar geometry, and, as a result, a secondary maximum in the light emission appears near the anode.

<sup>1</sup>J.P. Boeuf and L.C. Pitchford, IEEE Trans Plasma Science, vol 24, pp. 95-96 (1996).

**JTP5 6 1-D Model of a Helium AC Discharge in PDP** A. SH-VYDKY, J.R. GOTTSCHALK, S. AMBALANATH, J.M. TRUXON, A.D. COMPAAN, C.E. THEODOSIOU, W. WILLIAMSON, JR., *Department of Physics and Astronomy, University of Toledo* A self-consistent 1D model of a helium (100%) ac discharge in a plasma display panel cell is developed. The model is based on a two-moments fluid description of electron and ion transport, coupled with Poisson's equation, and a set of kinetic equations characterizing the evolution of the population of excited states. Results are presented for a gap length of 0.1 mm and a gas pressure of 400 Torr at ambient temperature. The discharge current as a function of time will be discussed for typical sustained voltages. The visible light output as well as relative intensities of major spectral lines, the voltage transfer curves and the sustained voltage margins will also be analyzed. Results of our calculations which have been compared with experiment carried out at the University of Toledo will be presented. Theory and experiment are in reasonably good agreement.

**JTP5 7 Modeling of a 3-Electrode AC Plasma Display Panel\*** P. J. CHRISTENSON, Y. IKEDA, <sup>†</sup> J. P. VERBONCOEUR, K.L. CARTWRIGHT, *Dept. EECS, University of California, Berkeley, CA 94720-1770* A global model of a 3 electrode type, AC Plasma Display Panel (PDP) is developed and used to identify the most significant reactions in a near atmospheric pressure, Ne/Xe gas

mixture. Particle in Cell codes with Monte Carlo Collisions (PIC-MCC) in both one (XPDP1<sup>1</sup>) and two (XOOPIC<sup>2</sup>) dimensions are used to model breakdown of a Ne/Xe gas in one and two cell systems. Changes in the geometry of a single PDP cell are examined, and the effects of those variations on discharge delay are analyzed for various discharge gaps. The effects of asymmetry, and perturbations in electrode voltages in a two dimensional, two celled system are studied. Such variations may enhance or reduce the development of neighbor discharges in between the two cells.

\*This work supported in part by Hitachi Ltd., and the Miller Institute for Basic Research in Science.

<sup>†</sup>Hitachi Research Laboratory

<sup>1</sup>Vahedi and Surendra, Comp. Phys. Com., 104 (1993)

<sup>2</sup>Verboncoeur, *et. al.*, Comp. Phys. Com., 87 (1995)

**JTP5 8 A Global Reactor Model for Pure Argon Microwave Discharges** YUNLONG LI, *University of Arkansas* UMESH KELKAR, MATTHEW GORDON, LARRY ROE, *University of Arkansas* A two-dimensional axisymmetric model is developed for analyzing plasma heat transfer characteristics in a microwave reactor by using FLUENT. The boundary conditions, such as the reactor cavity and belljar temperatures, are obtained from the experimental data. The microwave energy is assumed to be absorbed by the plasma uniformly. It is found that it is impossible to remove 680 W, the input power measured experimentally, from the plasma, through the belljar, to the cavity walls which are water-cooled. For accurate electron energy and electron density predictions, a numerical model is developed by coupling the non-Maxwellian electron energy distribution function (EEDF) from a Boltzmann solver with a 25-level collisional-radiative model (CRM). It is found that the nonequilibrium effects are very important for the predicted excited state number densities, as well as for the predicted power absorbed by the plasma. The experimental data for the excited state number densities are obtained by optical emission spectroscopic (OES) measurements. For those solutions which match the excited state number densities within a factor of 2, the predicted absorbed power (25-100 W) is much lower than the indicated input power (680 W). Thus, it is concluded that only 5-15/microwave power is absorbed by the plasma.

**JTP5 9 On the Afterglow Decay of the Diffusion Determined Positive Column Plasma in Neon** DETLEF LOFFHAGEN, ROLF WINKLER, *Institut für Niedertemperatur-Plasmaphysik, 17489 Greifswald, Germany* SIGISMUND PFAU, *Institut für Physik, Universität Greifswald, 17489 Greifswald, Germany* Theoretical studies of the temporal decay of the diffusion determined afterglow plasma up to the ms-range are presented. The model for the positive column plasma of the neon discharge consists of the time-dependent electron Boltzmann equation, the rate equations for the two lowest excited neon states, and an appropriate description of the decaying electric field. A radially averaged treatment of the cylindrical, axially homogeneous plasma has been employed. Results for a plasma column with a tube radius of 1.7 cm at a pressure of 75 Pa, starting from steady state of a dc glow discharge at currents around 20 mA, are given. The electron velocity distribution is subject to large structural changes in about the first 40  $\mu$ s of the decay and undergoes slower changes at later times. Then, the velocity distribution has a nearly Maxwellian form in its low energy range and two distinct plateaus are established at higher energies. The analysis shows that the structure of the velocity distribution is substantially influenced by the chemo-ionization of excited atoms. The decay behaviour of the excited atoms and of



the main processes in the time-dependent particle and energy balance of the electrons are comprehensively discussed.

**JTP5 10 Ion Chemistry in Trimethylsilane** CHARLES Q. JIAO, ALAN GARSCADDEN, PETER D. HAALAND, *Wright Laboratory, Wright-Patterson AFB, OH* The cross sections of electron impact ionization of trimethylsilane,  $(CH_3)_3SiH$ , have been measured using Fourier-transform mass spectrometry from threshold to 70 eV. High resolution mass spectra prove that the parent ion,  $(CH_3)_3SiH^+$ , is not formed by electron impact, in contrast to findings from some previous studies. The total ionization cross section is  $5.1 \pm 0.5 \times 10^{16} cm^2$  at 70 eV. While electron impact ionization produces  $(CH_3)_2SiH^+$  and  $(CH_3)_3Si^+$  as the most and second most abundant ions, respectively, ion-molecule reactions simplify this composition by converting  $(CH_3)_2SiH^+$  and other minor fragment ions from dissociative ionization to  $(CH_3)_3Si^+$  at near-Langevin rates. The absence of the parent ion, the partitioning among dissociative ionization channels, and the thermodynamic bottleneck at trimethylsilyl cation are described by *ab initio* quantum electronic structure calculations at the MP2/6-31g\* level of theory.

**JTP5 11 Photoresist etching with dielectric barrier discharges in oxygen** ZORAN FALKENSTEIN, *Los Alamos National Laboratory* This paper presents results on the surface etching of a photoresist (Shipley, SPR2) on Si wafers using dielectric barrier discharges in oxygen at room temperature. The etching depth is measured by mechanical profilometry as function of the gap spacing and gas pressure and is given, for comparison to conventional plasma surface treatment, as etch rate per power density coupled onto the specimen surface (nm J-1 cm<sup>2</sup>), as well as etch rate per energy density coupled into the discharged gas volume (nm J-1 cm<sup>3</sup>). Both etch rates (nm J-1 cm<sup>2</sup> and nm J-1 cm<sup>3</sup>) are shown as a function of the gap spacing (d) and the total oxygen gas pressure (p), as well as a function of the product of pd. At a constant gap spacing and gas pressure, the removal rate is a linear function of the applied power density. Variation of the gas pressure in the range 50 to 1500 mbar and of the gap spacing in the range 1 to 20 mm leads to the highest achieved etching rate per power density on the sample surface, 2.2 nm J-1 cm<sup>2</sup> at 730 mbar and 1 mm (corresponding to 0.2 nm J-1 cm<sup>3</sup>) and to the highest etching rate per energy density coupled into the discharged gas volume, 0.85 nm J-1 cm<sup>3</sup> at 290 mbar and 7 mm (corresponding to 0.87 nm J-1 cm<sup>2</sup>). The surface of the etched photoresist is characterized by SEM and mechanical profilometry.



**SESSION LW1: POSITRON AND ELECTRON SCATTERING**

Wednesday morning, 8 October 1997; Class of '24 Reception Room, Memorial Union at 8:00; Klaus Bartschat, Drake University, presiding

*Invited Papers***8:00****LW1 1 Investigations in Gaseous Positronics: Positron - Atom, Molecule Scattering.\***

WALTER E. KAUPPILA, *Wayne State University, Detroit, MI 48202*

At various locations in our universe positrons are known to interact with neutral and ionized gases. In addition to participating in the same scattering processes as electrons in a gas, positrons can also undergo annihilation (generally important only at thermal energies) and positronium (Ps) formation. Total, Ps formation, and differential elastic cross section measurements for many gases (e.g., H, He, Ar, Na, K, H<sub>2</sub>, CO<sub>2</sub>, SF<sub>6</sub>) have revealed that at intermediate energies (within a few tens of eV above the Ps formation threshold) Ps formation can be one of the principal contributors to positron scattering and that coupling effects between different scattering channels can be significant. Comparisons with electron-gas scattering show that elastic scattering is more prominent for electrons, while inelastic scattering processes are larger for positrons. Evidence is being found in Ps formation studies that inner shell electrons of the target gases play a role.

\*This research performed in collaboration with T.S. Stein and C.K. Kwan in the positron scattering group at Wayne State University and is supported by NSF Grant PHY 94-22271.

**8:30****LW1 2 Recent Progress in the Calculation of Positron Interaction with Gases.\***

ALLAN D. STAUFFER, *York University, Toronto, Canada*

Although the positron is an antiparticle of the electron, the cross section (probability) for direct annihilation is much smaller than that for elastic or inelastic scattering. For these latter processes, calculations can be carried out by treating the positron as a positive electron and using the usual theoretical methods developed for electron scattering from atoms. There are several important differences between electron and positron scattering, however. Since the positron is a distinct particle from the electron, exchange interactions with the bound atomic electrons do not occur. More interestingly, the formation of positronium (the bound state of an electron and a positron) can and does occur in positron-atom scattering. In addition, the fact that the sign of the interaction between the positron and the atom is the opposite of that for electrons leads to rather different behavior of the cross sections. We will give an overview of the current methods used for calculating positron-atom scattering and illustrate this with examples highlighting the differences between the behavior of electrons and positrons in gases.

\*Work supported by the Natural Sciences and Engineering Research Council of Canada

*Contributed Papers***9:00**

**LW1 3 A Rubidium Spin Filter for Electrons** \* B.A. HITT, H. BATELAAN, A.S. GREEN, T.J. GAY, *University of Nebraska-Lincoln* We report on experiments testing a novel way to create polarized electrons through collisions with optically pumped Rb. A swarm of electrons is created in a well defined DC discharge at a nitrogen pressure of 30 Torr. The nitrogen conveniently quenches the Rb, limiting depolarization of the Rb due to radiation trapping<sup>1</sup>. The electron swarm will be passed through the dense polarized Rb vapor and should acquire a net polarization due to exchange collisions. Presently, unpolarized electron currents of 30 nA have been extracted through a 1 mm aperture at 30 Torr. One possible advantage of this setup would be its use as a "turn-key" source of polarized electrons.

\*Supported by NSF grant #9504520

<sup>1</sup>M.E. Wagshul and T.E. Chupp, *Phys. Rev. A*, 49, 3854 (1994).

**9:15**

**LW1 4 Ionization Cross Sections Of Cl<sub>2</sub> by Electron Impact**  
S.K. SRIVASTAVA, R. BOIVIN, *Jet Propulsion Laboratory, California Institute of Technology, Pasadena, CA 91109, USA*

Ionization properties of Cl<sub>2</sub> are of interest for modeling plasmas used for material processing. By utilizing a crossed electron beam and molecular beam collision geometry we recently studied these properties in the single collision conditions. Our data differ from previously published data<sup>1-3</sup>. The ionization efficiency curve shows structures which are interpreted as due to opening of new ionization channels in Cl<sub>2</sub><sup>+</sup> ion. The work is under progress at the present time. These data along with new data to be collected before the time of the meeting will be presented at the conference. References: 1. R. E. Center and A. Mandl, *J. Chem. Phys.* 57, 4104 (1972). 2. M. V. Kurepa and D. S. Belic, *J. Phys.* B11, 3712 (1978). 3. F. A. Stevie and M. J. Vasile, *J. Chem Phys.* 74, 5106 (1981).

**9:30**

**LW1 5 Theoretical Support for a Ramsauer-Townsend Minimum in e<sup>-</sup>-CF<sub>4</sub> scattering** \* W. A. ISAACS, C. W. McCURDY, *LBNL* T. N. RESCIGNO, *LLNL* We have recently conducted large-scale ab initio calculations on low energy electron scattering from CF<sub>4</sub> using the complex Kohn method. It is well known that the details of the Ramsauer-Townsend effect are critically dependent on the accurate representation of electron-electron correlation. The only previous theoretical work on CF<sub>4</sub> beyond the static-exchange (SE) approximation is that of Giant-

urco *et. al.*,<sup>1</sup> who used a DFT-inspired model correlation-polarization potential. Their results showed marked improvement over SE calculations, but quantitative differences with experimental data remain at the lowest energies. We account for correlation by employing a set of polarized virtual orbitals in the target basis, which allows for a compact representation of closed channels in the Kohn trial functional. Our calculations indicate a Ramsauer-Townsend minimum below 0.3 eV, and we find excellent agreement with recent measurements of integrated and differential cross sections.

\*Work performed under the auspices of the USDOE by LBNL under contract DE-AC03-76SF00098 and LLNL under contract W-7405-Eng-48, using the computational resources of NERSC.

<sup>1</sup>J. Chem. Phys. **100**, 6464 (1994), J. Chem. Phys. **104**, 6482 (1996)

9:45

**LW1 6 Interactions of Slow Electrons with C<sub>2</sub>F<sub>6</sub>** L. G. CHRISTOPHOROU, J. K. OLTHOFF, *NIST* The results of a review and an assessment<sup>1</sup> of the cross sections and coefficients for the interactions of slow electrons (mostly below 100 eV) with C<sub>2</sub>F<sub>6</sub> will be presented. The following cross sections and their intercomparison will be discussed: total electron scattering, momentum transfer, elastic integral, differential elastic, differential vibrational, vibrational inelastic, total ionization, partial ionization, total dissociation, and electron attachment. Information will be presented also on the coefficients for electron impact ionization, effective ionization, electron attachment, and electron transport (lateral diffusion and drift velocity), as well as on the rate constant for electron attachment as a function of the mean electron energy and gas temperature. Measurements are especially needed on the cross sections for electron scattering, momentum transfer, and dissociation of C<sub>2</sub>F<sub>6</sub> into neutral fragments. The coefficients are generally better known than the cross sections although further measurements on electron diffusion coefficients and electron attachment at high E/N values are indicated.

<sup>1</sup>L. G. Christophorou, J. K. Olthoff, and M. V. V. S. Rao, J. Phys. Chem. Ref. Data, **25**, 1341 (1996)

---

## SESSION LW2: PROPULSION AND SPACE PLASMAS/ MICRODISCHARGES AND PLASMA DISPLAY PANELS

Wednesday morning, 8 October 1997

Great Hall, Memorial Union at 8:00

Erich Kunhardt, Stevens Institute of Technology, presiding

### Contributed Papers

8:00

**LW2 1 Microdischarge Devices** D. J. WHEELER, *University of Illinois at Urbana-Champaign* J. W. FRAME, T. A. DETEMPLE, J. G. EDEN, *University of Illinois at Urbana-Champaign* Cylindrical microdischarge cavities 200–400 μm in diameter and 0.5–5 mm in depth have been fabricated in silicon and operated at room temperature with neon or nitrogen at specific power loadings beyond 10 kW/cm<sup>3</sup>. The discharges are azimuthally uniform and stable operation at N<sub>2</sub> and Ne pressures exceeding 1 atm and ≈600 Torr, respectively, has been realized for 400 μm diameter devices. Spectroscopic measurements on neon discharges demonstrate that the device behaves as a hollow cathode discharge for pressures > 50 Torr. As evidenced by emission from Ne and Ne<sup>+</sup> (2P, 2F) states as well as N<sub>2</sub> (C → B) fluorescence (316–492 nm), these discharge devices are intense sources of ultraviolet and visible radiation and are suitable for fabrication as arrays.

### Invited Papers

8:45

**LW2 4 Spectroscopy of Astrophysical Plasmas.**

J. E. LAWLER, *University of Wisconsin-Madison*

It is through (atomic) spectroscopy that we learn many details of the physics and chemistry of the universe beyond the solar system. Most of the observable matter in the universe is in the plasma state. New technologies are vastly increasing

drical microdischarge cavities 200–400 μm in diameter and 0.5–5 mm in depth have been fabricated in silicon and operated at room temperature with neon or nitrogen at specific power loadings beyond 10 kW/cm<sup>3</sup>. The discharges are azimuthally uniform and stable operation at N<sub>2</sub> and Ne pressures exceeding 1 atm and ≈600 Torr, respectively, has been realized for 400 μm diameter devices. Spectroscopic measurements on neon discharges demonstrate that the device behaves as a hollow cathode discharge for pressures > 50 Torr. As evidenced by emission from Ne and Ne<sup>+</sup> (2P, 2F) states as well as N<sub>2</sub> (C → B) fluorescence (316–492 nm), these discharge devices are intense sources of ultraviolet and visible radiation and are suitable for fabrication as arrays.

8:15

**LW2 2 Time Resolved Current Waveform and Light Emission in a PDP** J.R. GOTTSCHALK, S. AMBALANATH, A. SHIVIDKY, J.M. TRUXON, A.D. COMPAAN, W WILLIAMSON, JR., *Department of Physics and Astronomy, University of Toledo* \*

We have used a He filled monochrome plasma display panel to study current waveforms and optical emission as a function of the applied ac voltage. The voltage source has a quick risetime (20 ns), which allows resolution of the displacement current and the discharge current. The separation of the displacement and discharge current is dependent on the voltage. For voltage just above threshold (=B1110V) the delay was 100 ns, and at higher voltages this delay decreases to 30 ns at =B1150V. We can measure the range of bistability in the panel by measuring the current waveform and optical emission as the applied voltage is increased from well below threshold to well above threshold and then decreased to well below threshold.

\*We would like to thank B. Byrum of Electro Plasma Inc. for supplying the test PDP.

8:30

**LW2 3 Breakdown in a 3-Electrode AC Plasma Display Panel Cell** \* J. P. VERBONCOEUR, P. J. CHRISTENSON, K. L. CARTWRIGHT, *Dept. EECS, University of California, Berkeley, CA 94720-1770* Y. IKEDA, *Hitachi Research Laboratory* Breakdown in an AC Plasma Display Panel (PDP) cell depends upon the electrode geometry and voltages, the initial wall charge, secondary emission coefficient, and the gas pressure and composition. Secondary electrons, ejected by ion impact on a dielectric-coated cathode, accelerate in the strong fields of the cathode fall, generating an avalanche of ionization events. The ions generated accelerate toward the cathode, sustaining the secondary current. When the electric field gradient is large over an electron scattering mean free path, electrons are not tied to the field lines, resulting in a spatial distribution of ions returning to the cathode. In this work, we consider a simple 3 electrode structure with argon and neon-xenon gas mixtures. Using a Monte Carlo technique, the electron energy distribution function is mapped for the initial fields. An amplification factor can be defined along the secondary emitting surface. Coupled with the spatial distribution of the ion flux, this technique provides a description of the initiation of the breakdown.

\*This work supported in part by Hitachi Ltd., and the Miller Institute for Basic Research and Science.

our capabilities to make observations on these plasmas. Quantitative observations of astrophysical plasmas require accurate spectroscopic data, especially  $f$ -values, from laboratory work. The laboratory astrophysics effort at the University of Wisconsin will be briefly reviewed. Some representative applications of the laboratory data from this program in cosmology and in studies of stellar evolution, chemically peculiar stars, and the interstellar medium will be described.

9:15

**LW2 5 Qualification and On-Orbit Use of Xenon Ion Propulsion.**

J.R. BEATTIE, *Hughes Telecommunications and Space Co.*

Following a development effort that spanned nearly four decades, Hughes Space and Communications Company is scheduled to launch its first geosynchronous communications satellite equipped with ion propulsion in August 1997. The 500-W Xenon Ion Propulsion Subsystem (XIPS) will be used for North-South stationkeeping and momentum-wheel dumping on Hughes' HS601HP three-axis-stabilized satellite, saving approximately 400 kg of chemical propellant mass over a 15-year period. In this paper, the principles of operation and performance characteristics of the XIPS thruster are discussed, and the qualification and lifetest programs that certified it for space application are described. On-orbit performance of the thruster is presented and compared with ground test data. Finally, the next Hughes application of this technology is described, in which a 4.5-kW XIPS propulsion system will be used not only for stationkeeping and attitude control, but also for orbit raising on Hughes' new HS702 high-power satellite.

---

**SESSION MW1: COLD COLLISIONS AND RECOMBINATION**

Wednesday morning, 8 October 1997; Class of '24 Reception Room, Memorial Union at 10:15; Stephen J. Buckman, Australian National University, presiding

*Invited Papers*

10:15

**MW1 1 Collisions Between Laser-Cooled Atoms.\***

THAD WALKER, *University of Wisconsin-Madison*

Collisions between laser-cooled atoms have a number of remarkable features. The exceptionally low temperature in laser-cooled clouds ( $< 100 \mu\text{K}$ ) means that the collision dynamics are not only sensitive to very long-range interatomic forces (even as modified by tiny hyperfine interactions), but also strongly depend on multiple light emission and absorption processes during the course of the collision. The light-induced collision dynamics have been extensively studied over the past few years. In this talk I will present a series of such experiments that elucidate the collision dynamics. The interplay with theory along the way will be emphasized. The experiments, beginning with the discovery of the hyperfine sensitivity and demonstration of means to avoid excessive complications of hyperfine interactions, proceed to study the mechanism of light absorption, optical suppression of collision processes, and finally to a detailed study of two-photon collisions. The two-photon experiment is sensitive to all the effects that were studied before, but is sufficiently robust to allow the relationships between the various effects to be understood. Very low saturation intensities are observed for the two individual laser frequencies, but, surprisingly, result from vastly different mechanisms. Measurements of energy-pooling branching ratios will also be presented.

\*Research supported by the NSF and the Packard Foundation

10:45

**MW1 2 Quantitative Collision Rates of ultracold Collisions.**

PAUL JULIENNE, *National Institute of Standards and Technology, Gaithersburg, MD 20899* \*

Quantitative calculations of collision rates for elastic and inelastic collision processes at ultralow collision energies are now becoming possible due to the precise determination of threshold scattering lengths by high resolution photoassociation spectroscopy of cooled and trapped atoms. This spectroscopy also determines very precise atomic lifetimes of the trapped species. Progress in quantitative determination of collision rates will be described. For example, the relaxation rates of  $^{23}\text{Na}$  and  $^{87}\text{Rb}$  due to spin-exchange collisions are now known to be very different because of accidental similarity of singlet and triplet scattering lengths for the latter species, which has unusually low relaxation rates.

\*Partial Support provided by ARO and ONR

11:15

**MW1 3 Recombination at thermal and ultracold energies.**M. R. FLANNERY, *Georgia Institute of Technology*\*

The interesting differences between the thermolecular recombination processes,  $A + B + M \rightarrow AB + M$ , at the thermal (300K) and at ultracold (nK) temperature will be discussed. In Bose-Einstein Condensation (BEC) the kinetic energy acquired ( $\sim 1-2$  mK) by the third body  $M$  generally exceeds the barrier energy (nK) of the trap. Collisional redissociation of  $AB$  cannot then occur and the atom loss via the dimer formation therefore can limit densities obtainable in BEC. At ultracold energies, recombination proceeds only into a few bound levels and is reduced to its most elemental character so that full quantal approaches - rather than semiclassical flux methods - must be considered. Various methods will be explored.

\*Research supported by AFOSR: F49620-96-0142

**Contributed Papers**

11:45

**MW1 4 Observation of Final Product States from the Dissociative Recombination of  $N_2^+$**  KENNETH A. HARDY, SEBASTIAN ODDONE, *Florida International University, Miami, FL 33199* J. PETERSON, *SRI International, Menlo Park, Ca. 94025*\* We have observed the final product states of the Dissociative Recombination (DR) reaction of  $N_2^+$  by Time-of-Flight spectroscopy. The DR reaction took place in a hot cathode discharge surrounded by a variable cylindrical magnetic field of up to 250 Gauss. We observed the following final state populations:  $^4S + ^2D$ ,  $^4S + ^2P$ , and  $^2D + ^2D$ .  $^4S$  is the ground state of N, and  $^2D$  and  $^2P$  are the lowest excited states and are metastable. These states are expected by theory<sup>1</sup> and have been observed in recent experiments on the ASTRID heavy ion storage ring<sup>2</sup> with which our results are compared. In addition, under conditions of very high discharge voltage (150-250 V), we have observed the DR of the  $N_2^+ \ ^2\pi_u$  A excited state in the  $V=1, J=0, 5-9$  rovibrational levels. The  $V=1, J=0, 5-9$  levels populate the  $^2P + ^2P$  final product states.

\*K. H. received partial support from NASA NAG-5-2583, NASA NAG-5-3862, and LLNL Research Collaborations HBCU and MI.

<sup>1</sup>S.L. Guberman, *Geophys. Res. Lett.*, 18, 1051(1991)

<sup>2</sup>D. Kella, P.J. Johnson, H.B. Pederson, L. Vejby-Christensen, and

L.H. Anderson, *Phys. Rev. Lett.*, 77, 2432(1996)

12:00

**MW1 5 A Kinematic Explanation for the Observation of Very Narrow Dissociative Recombination Final Product State Line Widths in Time of Flight Measurements** KENNETH A. HARDY, *Florida International University, Miami, FL 33199*\* Final product state line widths as narrow as 10 m/sec have been observed in measurements by Time of Flight spectroscopy of final product states from the Dissociative Recombination of  $Ar_2^+$ ,  $Ne_2^+$ , and  $N_2^+$ <sup>12</sup>. If the precursor molecular ions in a gas discharge have Maxwellian velocity distributions, line widths as great as 1000 m/sec. are expected.<sup>3</sup> A model is presented which shows that if these precursor ions are formed by the associative ionization process, extremely narrow line widths will be observed. Extensions of this model suggest sources of molecules that can be used for doppler free spectroscopy.

\*Partial Support from NASA NAG-5-2583 and LLNL collaboration for HBC and MI.

<sup>1</sup>G.B. Ramos, M. Schlamkowitz, J. Sheldon, K. Hardy and J. Peterson, *Phys. Rev. A*, 66 4556(1995)

<sup>2</sup>G.B. Ramos, J. Sheldon, K. Hardy and J. Peterson, Accepted for publication *Phys. Rev. A*, (1997)

<sup>3</sup>G.B. Ramos, M. Schlamkowitz, J. Sheldon, K. Hardy and J. Peterson, *Phys. Rev. A* 51 2945(1995)

**SESSION MW2: DIAGNOSTICS I**

Wednesday morning, 8 October 1997; Tripp Commons, Memorial Union at 10:15; D. Leonhardt, Naval Research Laboratory, presiding

**Invited Paper**

10:15

**MW2 1 Planar Laser-Induced Fluorescence Detection of Gas-Phase Intermediates in Plasmas.**KRISTEN L. STEFFENS, *National Institute of Standards and Technology*\*

Low-pressure radio-frequency (rf) fluorocarbon plasmas are extensively used for etching and chamber-cleaning during microelectronics device fabrication. For efficient optimization of etch rate, spatial uniformity and reproducibility, an understanding of the plasma physics and chemistry is desired. Models which are necessary to understand the complex plasma processes require experimental input and must be rigorously verified by comparison to experimental measurements. Planar laser-induced fluorescence (PLIF) is one of the most useful optical techniques for 2-D measurements of gas-phase species relative densities and distributions. Because the entire 2-D map of the species density is obtained simultaneously, the need for multiple point measurements is eliminated. Also, PLIF is highly sensitive for free-radical intermediates, which play crucial roles in plasma chemistry. In this work, PLIF measurements are made in the Gaseous



Electronics Conference (GEC) capacitively-coupled parallel-plate reference cell. This reference reactor facilitates comparison with models under current development and with other experimental results. The results to be discussed include PLIF of the  $CF_2$  radical, performed in various  $CH_xF_y/Ar$  plasmas to investigate the effect of precursor molecular structure versus precursor stoichiometry (C:H:F ratio) on the spatial distribution and density of  $CF_2$ . In addition,  $CF_2$  PLIF measurements were made in 8 plasmas. The PLIF results are correlated to discharge current and voltage measurements to help understand the chemical and electrical factors affecting the spatial uniformity, which is likely related to chamber-cleaning uniformity.

\*Special thanks to Michael R. Zachariah and Mark A. Sobolewski for their participation in this research.

### Contributed Papers

10:45

**MW2 2 Diagnostics of Diatomic Carbon in High-Density  $C_4F_8$  Plasmas** C. SUZUKI, K. SASAKI, K. KADOTA, *Department of Electronics, Nagoya University, Nagoya 464-01, Japan* Optical emission and laser-induced fluorescence (LIF) spectroscopy was applied to the diagnostics of diatomic carbon ( $C_2$ ) molecules in low-pressure ( $\approx 10$  mTorr) and high-density ( $n_e \approx 10^{12} \text{ cm}^{-3}$ )  $C_4F_8$  plasmas generated by helicon wave discharges. Strong greenish emission from  $C_2$  (Swan band) was observed in visible optical emission spectrum from the  $C_4F_8$  plasmas. After the chamber was sufficiently seasoned by the  $C_4F_8$  plasmas, this greenish emission was also observed even in  $CF_4$  plasmas, but was not observed in argon plasmas. However, after the chamber was cleaned by oxygen plasmas, the greenish emission was hardly observed in  $CF_4$  plasmas. These experimental results suggest that  $C_2$  molecules were produced by chemical reactions among carbon-containing species on the wall surface seasoned by the  $C_4F_8$  plasmas. This was supported by the fact that the hollow shape radial profiles of  $C_2$  ( $a^3\Pi_u$ ) density were observed by the LIF measurements. The production and loss processes of  $C_2$  molecules will be discussed in more detail based on the LIF measurements.

11:00

**MW2 3 Tow-D Emission profile of parallel plate RF plasma -Effect of driving frequency-** \* T. KITAJIMA, Y. TAKEO, N. NAKANO, T. MAKABE, *Keio University Yokohama, Japan* RF plasma is widely used for surface processing at various driving frequencies. In most processes, plasma uniformity is an important issue to be accomplished. In this work, two dimensional profiles of net excitation rate in parallel plate Ar RF plasma is investigated using a 2D-t optical emission spectroscopy analyzed by Abel inversion method and temporal deconvolution procedure.<sup>1</sup> The research is mainly focused on the effect of driving frequency (100kHz ~ 100MHz) on the plasma uniformity in radial direction. The radial profile of the net excitation rate has a peak at the center at 100kHz as the discharge is maintained by  $\gamma$  electrons from electrodes.<sup>2</sup> At frequency higher than 1MHz ( $\alpha$  regime), the radial profile ( $p=1$ Torr) shows a sharp peak around the edge of the RF electrode due to the electron heating by the local edge field. The effect of the edge field is enhanced further at VHF(40MHz< $f$ ) region. It has the advantage in radial uniformity at low pressure ( $p<100$ mTorr) where the radial diffusion of electrons is influential.

\*Work supported by KEIO Univ. under I.C.R.J.

<sup>1</sup>T. Kitajima, M. Izawa, R. Hashido, N. Nakano and T. Makabe, *Appl.Phys.Lett.* **69**, 758 (1996), *J.Phys.D* **30**, 1783(1997).

<sup>2</sup>S. Kakuta, T. Makabe and F. Tochikubo, *J.Appl.Phys* **74**, 4907 (1993).

11:15

**MW2 4 Measurement of Einstein's A Coefficient of Transition Line at 296.7 nm for Carbon Atom** H. ITO\*, M. ITO, M. HORI, A. KONO, T. TAKEO\*, H. HATTORI\*, T. GOTO, *Nagoya University, JAPAN* \**Nagoya Municipal Industrial Research Institute, JAPAN* In order to investigate the role of radicals such as  $CH_3$ ,  $CF_x$ ,  $SiH_x$  ( $x=1\sim 3$ ) in the plasma process, the absolute densities of radicals have been measured by using infrared diode laser absorption spectroscopy (IRLAS). Moreover, we have successfully measured the relative density of C atom in the inductive coupled radio frequency (13.56 MHz) CO plasma by using ultra-violet absorption spectroscopy (UVAS) with a carbon hollow cathode lamp. The transition line used for the measurement was  $2s2p^3 \ ^5S_2-2s^2p^2 \ ^3P_2$  at 296.7 nm for the C atom. However, the Einstein's A coefficient at 296.7 nm for C atom has never been measured experimentally. To develop the plasma process such as etching and chemical vapor deposition employing gases containing C atoms, quantitative analysis for C atoms in the plasma is indispensable. In this study, the Einstein's A coefficient at 296.7 nm for C atom was measured from the emission decay rate as a function of feed gas pressure in electron cyclotron resonance (ECR) CO plasma. The emission decay was almost constant with increasing feed CO gas pressure. The Einstein's A coefficient obtained was  $4.7 \times 10^4 \text{ s}^{-1}$  with the error in the range of  $\pm 30\%$ . This value is almost 2000 times larger than the theoretically calculated A coefficient reported previously. Using this Einstein's A coefficient, the absolute C atom density obtained in the CO and  $CH_4$  plasmas is discussed.

11:30

**MW2 5 Spectroscopic Determination of  $[C_2]$  in  $Ar/H_2/CH_4$  and  $Ar/H_2/C_{60}$  Microwave Plasmas for Nanocrystalline Diamond Synthesis** \* A.N. GOYETTE, J.E. LAWLER, L.W. ANDERSON, *Department of Physics, University of Wisconsin, Madison, WI 53706* D.M. GRUEN, T.G. MCCAULEY, D. ZHOU, A.R. KRAUSS, *Chemistry and Materials Science Divisions, Argonne National Laboratory, Argonne, IL 60439* In contrast with conventional methods of diamond chemical vapor deposition (CVD), nanocrystalline diamond films may be grown in environments where hydrogen comprises a small percentage of the feed gas mixture. Methyl, which is thought to be critical to diamond formation in conventional hydrogen-rich CVD environments is produced in only small quantities under these novel chemistries and alternative mechanisms for diamond growth must be considered. The carbon dimer,  $C_2$ , is believed to be an important species in these growth chemistries. We have measured the concentration of gas phase  $C_2$  in  $Ar/H_2/CH_4$  and  $Ar/H_2/C_{60}$  microwave plasmas used in the deposition of nanocrystalline diamond films. High sensitivity white light absorption spectroscopy is used to monitor  $C_2$  concentration using the  $a^3\Pi \rightarrow d^3\Pi$  (0,0) vibrational band of  $C_2$  as chamber pressure, microwave power,

substrate temperature and feed gas mixtures are varied in both chemistries. We present the results of these experiments.

\*Work supported by the U.S. Army Research Office under grant DAAH-04-96-1-0413 and the U.S. Department of Energy, BES-Materials Sciences, under contract W-109-ENG-38.

11:45

**MW2 6 Investigation of rf excited CO<sub>2</sub> slab laser discharges by mass spectrometry and optical spectroscopy of CO and N<sub>2</sub> emission bands\*** U. BERKERMANN, *Ruhr-University Bochum, Germany* A. LIFFERS, C. LÜCKING, J. MENDEL, G. SCHIFFNER, *Ruhr-University Bochum* A problem associated with sealed off CO<sub>2</sub> lasers is the partial dissociation of CO<sub>2</sub> in an electrical discharge. To achieve a long operation lifetime in a sealed off rf excited slab laser system it is necessary to know the main discharge parameters, the discharge behaviour and the plasma chemistry as a function of different gas compositions, gas contaminations and electrode surface layers. For this purpose we measure with high spatial resolution the emission of CO and N<sub>2</sub> molecular bands and He lines emitted in the visible and UV spectral range from slab discharges operated at 80 MHz. Measurements are made in a test chamber and CO<sub>2</sub> slab laser modules with 100 W and 2 kW output power for different defined contaminations of water vapor. The gas temperature profiles and spatial distribution of the power input across the discharge gap are determined. The time resolved development of the gas composition is recorded by mass spectrometry. For the first time, the influence of controlled water vapor contaminations is measured quantitatively for different electrode coatings and different mixtures of the filling gas.

\*supported by the German Ministry for Education and Science (BMBF) under the project number 13N6571

12:00

**MW2 7 The influence of an injected electron beam on the ion population of an RF plasma** ALAN REES, TERENCE WHITMORE, DAVID SEYMOUR, THOMAS RUSSELL, *Hidden Analytical Limited* The nature and energy distribution of ions in a

parallel plate RF discharge have been studied using a Hiden EQP instrument to monitor the ions arriving at the grounded electrode. The ion energies are dependent on the plasma potential and on ion/molecule collisions in the sheath region formed in front of the grounded electrode. Low current beams of electrons with mean energies of up to 200 eV have been used to interact with the plasma. The energy distribution of the electron beam was measured using a retarding field energy analyser and the effects of the auxiliary ionisation produced on the ion population and their energies examined. The results confirm the pronounced effects to be as expected when modulating processing plasmas with weak electron beams of appropriate energy in this way.

12:15

**MW2 8 Experimental and modeling studies of fluorocarbon plasmas.** H. SINGH, A. FIALA, J.W. COBURN, M. LI, D.B. GRAVES, *UCB* The comparison of experimental results with model predictions is the key to developing and validating plasma chemistry models. We report the comparison of experimental results with the predictions of a hybrid model for a cylindrical ICP over a range of powers and pressures. Mass resolved ion energy distributions are measured by an electrostatic energy analyzer and a mass spectrometer. Modulated beam mass spectrometry is used to measure the concentration of the neutrals in the plasma. Simultaneously, optical emission spectroscopy and argon actinometry are performed to measure the concentration of selected neutrals. A Langmuir probe is used to measure the plasma density and plasma potential. The 2-D hybrid plasma model includes equations of continuity, momentum and energy of ions and neutrals. The inhomogeneous Boltzmann equation is solved for the electron energy distribution in the reactor. In order to explain experimental results, the simulations suggest that F<sup>+</sup>/CF<sub>4</sub> ion-molecule chemistry significantly influences the plasma positive ion composition. Wall reactions involving both neutrals and ions, including the simultaneous deposition and etching of fluorocarbon films, play a significant role in determining neutral and ionic composition in the plasma.

---

## SESSION NW1: MODELING

Wednesday afternoon, 8 October 1997; Class of '24 Reception Room, Memorial Union at 13:30; Dimitris Lymberopolous, Applied Materials, presiding

### *Invited Papers*

13:30

**NW1 1 High Density Plasma Modeling for Laser and Pulsed-Power Systems.**  
MICHAEL E. JONES, *Los Alamos National Laboratory*\*

In the Plasma Physics Applications Group at Los Alamos, we have developed a variety of plasma models to study both laser plasma interactions and magnetically driven "plasmas" in pulsed-power systems. The parameters for the plasmas range from the collisionless regime of highly ionized, relatively low density ( $10^{19} \text{cm}^{-3}$ ) plasma of laser fusion targets to solid metal liners driven by multi-megaAmpere currents. The wide range of parameters, as well as disparate temporal and spatial scales make the modeling these plasmas particularly challenging. For collisionless plasmas, novel Particle-in-Cell methods have been developed. For pulsed-power systems, sophisticated magnetohydrodynamic methods that include material strength and radiation transport are needed. An overview of the various methods and approximations that are used will be given, along with a discussion of methods for modeling the intermediate or semi-collisional regime.

Comparison of the models with experiments performed on a number of facilities including the Livermore NOVA laser, the Los Alamos TRIDENT laser, the Sandia PBFA-Z pulsed power facility, and the Los Alamos PEGASUS pulsed-power facility will be given.

\*In collaboration with Plasma Physics Applications Group of Los Alamos National Laboratory This work was performed under the auspices of the U.S. Department of Energy

14:00

**NW1 2 Parallel Monte Carlo Computations of a Plasma Etch Reactor.**

IAN D. BOYD, *Mechanical & Aerospace Engineering, Cornell University, Ithaca, NY 14853*

Accurate computer simulations of plasma etch reactors offer the possibility of improved design in terms of efficient operation, process control, and decreased feature size. Unfortunately, simulation of plasma etch reactors presents a major challenge. The creation of energetic electrons using radio wave sources needs to be understood at the level of the electron energy distribution function. The interaction of the plasma with the supply gas flow leads to a variety of collision phenomena including vibrational excitation, molecular dissociation, and ionization of both atoms and molecules. The modeling of all these physical mechanisms points to the need for use of advanced numerical simulation techniques. In this paper, the direct simulation Monte Carlo method (DSMC) is used to model the transport processes in a low-pressure, chlorine plasma etch reactor. A massively parallel implementation of the DSMC technique is described [Dietrich & Boyd, *J. Comp. Phys.*, Vol. 126, 1996, p. 328] that is targeted primarily for the IBM SP-2 architecture. The DSMC technique is coupled to the Particle In Cell method (PIC) to simulate plasma effects. Results are presented for a commercial helicon wave reactor [Font & Boyd, *J. Vac. Sci. Techn. A*, Vol. 15, 1997, p. 313]. Comparisons are made with experimental measurements of atom density and ion current. The future role of parallel computing in plasma processing is discussed in terms of decreased solution times and more detailed physical modeling.

**Contributed Papers**

14:30

**NW1 3 Plasma sheath transition and Bohm criterion for finite**

$\lambda_D$  K.-U. RIEMANN, *Theoretische Physik 1, Ruhr-Universität Bochum, D-44780 Bochum, Germany* In the asymptotic limit  $\lambda_D/L \rightarrow 0$  (where  $\lambda_D$  is the electron Debye length and  $L$  represents the smallest competing ion length scale, the plasma boundary layer is split up in a collision free planar sheath (scale  $\lambda_D$ ) and a quasi-neutral presheath (scale  $L$ ). The "sheath edge" separating the presheath and the sheath is defined by a singularity which is closely related to the Bohm criterion. For (small but) finite  $\lambda_D$  the validity of the Bohm criterion and the plasma sheath concept become questionable and were discussed controversially. To answer this question an asymptotic theory on an "intermediate scale" (scale length  $L^\alpha \lambda_D^{1-\alpha}$ ,  $0 < \alpha < 1$ ) is presented. This theory is suitable to account for finite ratios  $\lambda_D/L$  and to match the plasma and sheath solutions smoothly without singularity. The intermediate scale again is closely related to the asymptotic Bohm criterion. It is shown that there is no place to "generalize" the Bohm criterion for finite  $\lambda_D/L$ .

14:45

**NW1 4 Attempts to make Particle Codes Approach Fluid Code Speeds Applied to RF Plasma Discharges**

E. KAWAMURA, C. K. BIRDSALL, *University of California at Berkeley* V. VAHEDI, *Lam Research Corp., Fremont CA* \* Particle codes, such as PIC-MCC<sup>1</sup>, provide detailed descriptions of plasma behavior but run much slower than fluid codes. We demonstrate, on argon and oxygen RF discharges, means for speeding up particle codes, by up to 30 times, with some run times under one hour. We used: implicit coding (longer time steps); subcycling of electrons (many electron steps per ion step); lighter mass ions for acceleration to intermediate equilibrium, then return to full mass; different weights for electrons and ions; improved initial density profiles. Tables are provided showing the gains achieved by each method, and six global cautions (e.g., a particle should not travel more than one grid spacing in one timestep), used to determine the time step

and grid spacing for each simulation. Explanations are also provided for any observed gains being less than simple expectations.

\*We are grateful to our supporters AFOSR under contract number F49620-94-1-0387, ONR under contract number N00014-97-1-0241 and the Institute for Scientific Computing Research (ISCR) at LLNL.

<sup>1</sup>V. Vahedi and M. Surendra, *Comp. Phys. Comm.* **87**, 170-198, 1995

15:00

**NW1 5 Advantages and disadvantages of the nonlocal approach**

D. UHRLANDT, M. SCHMIDT, R. WINKLER, *Institute for Nonthermal-Plasmaphysics Greifswald, Germany* The method of the nonlocal approach is used to study the radial structure of the electron kinetics under the radial electric field action in the cylindrical positive column plasma of glow discharges. A new extension of the nonlocal approach has been developed to determine beside the isotropic part also the anisotropic part of the electron velocity distribution function. The results are illustrated and critically discussed by means of the comparison with the strict solution of the appropriate inhomogeneous kinetic equation. The applicability and accuracy of the nonlocal approach for the description of the radial alteration of the distribution function and of related macroscopic quantities of electrons in the column plasma for low and intermediate pressures are evaluated. The abilities of the conventional and extended nonlocal approach to analyse the electron particle and energy fluxes and the spatially resolved electron particle and energy budget in the column plasma are critically discussed.

15:15

**NW1 6 Pressure dependence of EEDF in low pressure Ar and Cl<sub>2</sub> UHF plasmas**

H. AKASHI, *National Defense Academy, Dept. Appl. Phys.* S. SAMUKAWA, *NEC, Corp.* N. TAKAHASHI, T. SASAKI, *National Defense Academy, Dept. Appl. Phys.* Electron energy distribution functions (EEDF), ionization rate co-



efficient  $k_i$  and mean electron energy  $\bar{\epsilon}$  in low pressure high frequency discharges have been examined using Monte Carlo method. Pressure dependence of EEDF,  $k_i$  and  $\bar{\epsilon}$  under applying frequency of UHF (500MHz) and RF (13.56MHz) is investigated for actual etching pressures (5mTorr~30mTorr). It is obtained that the EEDF,  $k_i$  and  $\bar{\epsilon}$  in the UHF plasma do not depend on the pressure, whereas those in the RF plasma are strongly influenced

by the pressure in both Ar and Cl<sub>2</sub> gases. These results support the experimental results of which ion current density in UHF plasma does not depend on the pressure<sup>1</sup>. In the UHF plasma, driving frequency of electric field is rather higher than the electron collision frequency. This is why the EEDF and  $k_i$ , etc. do not depend on the pressure.

<sup>1</sup>S.Samukawa and T.Tsukada, J.Phys.Lett., to be submitted

#### Invited Paper

15:30

#### NW1 7 A Highly Flexible Simulation Tool for Applied Physics.

NICHOLAS HITCHON, *ERC for Plasma-Aided Manufacturing; University of Wisconsin, Madison* \*

A highly flexible simulation tool has been developed, which automates most of the laborious steps involved in setting up computational solutions of PDEs. The technique is suitable for a general system of coupled, nonlinear PDEs and their associated boundary conditions, on an arbitrary triangular/rectangular mesh. Both the system of equations and the mesh information are given in input files. A simple mesh labeling scheme is used in the equation specification. The mesh is divided into named regions, so that the equation specification can state by name where the equation applies. The software reads the mesh information; refines the mesh; reads the equations; symbolically generates all needed functions; writes code to solve the equations; calls Numerical Algorithm Modules to solve the equations; solves the equations; and plots the results.

\*K. M. Kramer

---

#### SESSION NW2: ETCHING

Wednesday afternoon, 8 October 1997

Tripp Commons, Memorial Union at 13:30

Peter Ventzek, Hokkaido University, presiding

13:30

**NW2 1 An Experimental and Computational Investigation of Design Issues in Atmospheric Pressure RF Glow Discharge Reactors** KEI SAKAI, *Hokkaido University* P.L.G. VENTZEK, Y. SAKAI, *Hokkaido University* H. MIYAJIMA, *Seiko-Epson* H. TAGASHIRA, *Hokkaido Institute of Technology* Recently, atmospheric pressure glow discharges have been re-investigated as a plasma source for cleaning, wettability, chemical etch and plasma chemical process applications because of through-put and cost considerations and recently developed stabilization techniques. Problems still remain. Two open issues are the mitigation of dust generation and developing an accurate understanding of the stable operating regimes of the discharge. We will present results of experimental investigations of these issues and present the results of a simulation study of an oxygen/nitrogen discharge at 1 atmosphere. In particular, the relationship between different discharge parameters, electrode properties and particle count will be presented.

13:45

**NW2 2 Molecular Dynamics (MD) simulations of Reactive Ion Etching (RIE) of a silicon surface by Cl ions.** DAVID E. HANSON, JOEL D. KRESS, ARTHUR F. VOTER, *Theoretical Division, Los Alamos National Laboratory, Los Alamos, NM 87545* Plasma etching of Si surfaces is an important material processing technique widely employed by the semiconductor industry. The interaction between the plasma and the wafer surface is one of the least understood aspects of the process. We report recent MD simulations of RIE of a silicon surface by Cl ions with impact energies between 15 and 200 eV. Results from the following investigations and comparisons with experiments are presented: (1) the Si yield as a function of ion energy, (2) the dependence of Si

yield as a function of the angle of incidence of the impact ion, (3) the stoichiometry of the desorbed material as a function of ion energy, (4) the effect of a background or thermal flux of Cl atoms on the Si yield, (5) the equilibrium Cl content of the surface layer during RIE, (6) the relative etching efficiency of Cl<sub>2</sub> vs. Cl ions, and (7) the development of surface roughening.

14:00

**NW2 3 Electron Transport to a Substrate in an rf Capacitively Coupled Plasma by the Boltzmann Equation** J. MATSUI, M. SHIBATA, N. NAKANO, MAKABE, *Keio University Yokohama, Japan* Anomalous etching, caused by the local charging on a patterned wafer surface immersed in a plasma, is one of the urgent subject to be overcome in plasma processing. We have developed a quantitative argument for the potential control of both the fluxes and the velocity components of charged particles on the wafer in a pulsed rf plasma in SF<sub>6</sub> using the RCT/Boltzmann equation model. The plasma reactor consists of infinite parallel plate electrodes with distance of 20 mm. Powered-electrode is driven by the sinusoidal wave at 13.56 MHz and the amplitude of 250V. The other bias electrode is operated in a pulsed mode. When the bias is applied during the CW operation in the powered electrode, the sheath electric field does not collapse and electrons are still decelerated in front of the bias electrode, as forming an isotropic velocity distribution. When the bias pulse is driven after the powered electrode is switched off, an acceleration mode of electrons is achieved to the bias electrode due to the collapse of the field as a function of time. The fundamental knowledge of the bias pulse operation has been obtained by RCT/Boltzmann equation model, and the results will be valuable to model the surface charging transient.

14:15

**NW2 4 RIE Glow Discharge Tomography** STEVEN SHANNON, JAMES PAUL HOLLOWAY, M.L. BRAKE, *The University of Michigan* A glow discharge tomography sensor for reactive ion etch process monitoring has been built and successfully tested. Sputter etch processes of silicon oxide have yielded identical macroscopic etch rate profiles to the radial emission profiles obtained



in-situ by the sensor in a GEC reference cell at pressures from 25 mTorr to 125 mTorr and powers ranging from 75 W to 175 W. The sensor combines a rotating sensor capable of accommodating the confining geometries of industrial etching machines with an advanced reconstruction algorithm using an optimized Tikonov regularization algorithm. Sensor design considerations, the reconstruction process, and direct correlation between emission profiles and RIE etch profiles will be presented. Supported by SRC contract 96-FC-085, NSF grant ECS-9358344 and SEMITECH project ETCH001

14:30

**NW2 5 Real-time Control and Modeling of Plasma Etching** M. SARFATY, *ERC for Plasm-Aided Manufacturing, University of Wisconsin-Madison* C. BAUM, M. HARPER, N. HERSHKOWITZ, J.L. SHOHET, *ERC for Plasm-Aided Manufacturing, University of Wisconsin-Madison* The relatively high process rates in high density plasma tools as well as the shrinking thickness of the films, require fast estimate of the process state in order to implement real-time advanced process control. The fast etch rate estimate, within one second, in a single spot size of 1-2 mm and the time averaged rates across the wafer are obtained by a combined use of an in-situ two-color laser interferometer and a full wafer image interferometer, respectively. The gas phase state is monitored by optical emission spectroscopy and a residual gas analyzer. The magnetically confined ICP tool state, including gas flow, pressure, and RF power to the antenna and the electrostatic chuck, is computer controlled and monitored. The absolute thickness of the film is determined during the process, thus providing an end-point prediction. The advantages of two-color laser interferometry for real-time process monitoring, development and control will be described. Langmuir kinetics modeling of the measured etch rates of polysilicon and SiO<sub>2</sub> films in Cl<sub>2</sub> and CF<sub>4</sub> discharges using tool state parameters will be described. The etch rate model enabled us to develop a model-based real-time control algorithm. The achieved real-time control of plasma etch rates of un-patterned SiO<sub>2</sub> and polysilicon films will be described. This work is funded by NSF grant No. EEC-8721545.

14:45

**NW2 6 The Applications of Plasma Diagnostic and Simulation in the Development of 300mm Etch Tool** TOM Q. NI, *Lam Research Corp.* WENLI Z. COLLISON, *Lam Research Corp.* MICHAEL S. BARNES, *Lam Research Corp.* Plasma uniformity and reactant delivery in plasma etch chamber have become challenging issues as wafer size increased to 300mm. In order to design a process chamber capable of performing uniform etch across large area wafer substrate in an inductive-coupled high density plasma etch chamber, the generation and transport of charged and neutral species in the chamber need to be understood and characterized. In this work, extensive plasma diagnostic techniques including ion flux patternator, Langmuir probe, 2-D optic emission spectroscopy (OES) and self optic absorption together with plasma simulation have been employed to investigate the plasma physics and chemistry. The information from the plasma simulation and diagnostic were used to assist the design and optimization of the high density plasma etch tools capable of processing 300mm wafers. The ion flux patternator, which measures the local ion current flux to wafer surface in plasma chamber, consists of 61 surface probes mounted on the 300mm electrode. A high voltage isolated multiplexer allows a computer to scan through all the surface probes in two second, and subsequently updates the plasma uniformity information. The experimental results from ion flux patternator confirmed that the plasma chamber designed from plasma simulation can generate uniform plasma in a wide process window

for all applications including poly silicon, silicon nitride, silicon oxide and metal etching. In addition to uniform plasma on top of the wafer surface, an uniform delivery of reactants is required to produce uniform etch rate across the wafer. 2-D OES and self optic absorption measurements indicated that reactants deplete rapidly during Al wafer etch. This depletion effect, which significantly slows down the etch rate in the center of the wafer, was accurately simulated with FLUID code. Based on the simulation results, a novel process gas injector has been designed to assure uniform etch across 300mm wafers.

15:00

**NW2 7 Correlation between Etch Selectivity and Neutral Radical Composition in High-Density Fluorocarbon Plasmas** K. NAKAMURA, N. HIRAKATA, K. SEGI, H. KOKURA, H. SUGAI, *Department of Electrical Engineering, Nagoya University*

In etching processes based on high-density fluorocarbon plasmas, high etch selectivity of SiO<sub>2</sub> to Si is required to achieve high quality LSI fabrication. The selectivity has been believed to be governed by the ratio of fluorocarbon radical (CF<sub>x</sub>) density to fluorine (F) atom density in the plasma, since the CF<sub>x</sub> radical may interrupt the etching by depositing polymer on the Si layer. Thus, the radical composition measurement is crucial for the etch selectivity control. We report absolute density measurements of F atom and CF<sub>x</sub> (x=1-3) radicals based on appearance mass spectrometry (AMS) as well as a correlation between the etch selectivity and a radical density ratio of CF<sub>x</sub>/F in CF<sub>4</sub> or C<sub>4</sub>F<sub>8</sub> fluorocarbon plasma produced by a 13.56 MHz inductive discharge. The F density reaches ~10<sup>19</sup> m<sup>-3</sup> in the 100 % CF<sub>4</sub> or C<sub>4</sub>F<sub>8</sub> plasmas while addition of 50 % hydrogen decreases the F density by one order of magnitude. A conventional actinometry technique results in a factor of ~4 greater reduction of F density in comparison with the AMS result. High etch selectivity of SiO<sub>2</sub> to Si is achieved for the radical density ratio CF<sub>x</sub>/F larger than 5 (x=1-3), and is observed to be correlated in particular with the ratio of CF/F. Further experiments in other sources such as a surface-wave-plasma etcher are in progress.

15:15

**NW2 8 Etch Process Sensitivity To An Inductively Coupled Plasma Etcher Treated With Fluorine-Based Plasma** SONG-LIN XU, *Applied Materials Inc* ZHIWEN SUN, *Applied Materials Inc* XUEYU QIAN, *Applied Materials Inc* GERALD YIN, *Applied Materials Inc* Significant etch rate drop after the treatment of an etch chamber with Fluorine-based plasma has been found for some silicon etch processes on an inductively coupled plasma reactor, which might cause problems in IC production line once the etch chamber runs alternative processes with F-based and F-free chemistry, or needs frequent cleaning with F-plasma. In this work, a systematic study of the root cause of process sensitivity to the etch chamber treated with F-plasma has been conducted. The experimental results show that pressure is a key factor to affect the etch rate drop. Processes at high pressure are more sensitive than those at low pressure because the quenching of neutral reactive species becomes more severe after the F-treatment. O<sub>2</sub> addition also increases the etch rate sensitivity, basically due to higher O<sub>2</sub>(subscript:)concentration after F-treatment which enhances the oxidation of silicon. The EDX and XPS elemental analysis of the chamber interior wall reveals a significant composition change after the interaction with F-plasma, the altered surface might accelerate the recombination of free radical species.

15:30

**NW2 9 Reactive Ion Etching in a VHF Parallel Plate Reactor**

H. DAHI, D. E. MURNICK, *Rutgers University, Newark NJ* M. MEYYAPPAN, *NASA Ames Research Center, Moffett Field CA* VHF capacitive plasma reactors may allow development of new RIE systems with high etch rates, excellent uniformity and anisotropy and low damage.<sup>1</sup> High ion and radical fluxes can be obtained by raising the rf frequency which increases plasma density dramatically at a fixed voltage. The effects of variation in frequency (25-120 MHz), pressure (10-250 mTorr), and flow rate (1-100 sccm) in a  $CF_4$  discharge have been investigated. The RF current versus voltage characteristics and spatially resolved optical emission are used as diagnostics. Experiments on etch rates, etch uniformity and anisotropy in silicon, silicon dioxide and silicon nitride will be discussed. Results of fluid model simulations are used to interpret the experimental data.

<sup>1</sup>M. J. Colgan, M. Meyyapan in "High Density Plasma Sources" ed. by Oleg A Popov, Noyes Pub. Park Ridge NJ (1995) p 149-190

15:45

**NW2 10 High Density Plasma Etching of GaAs with  $SiCl_4$**

MARK JARNYK, *Australian Scientific Instruments* ROD BOSWELL, *Australian National University* It has been found that etching GaAs in a helicon reactor with  $SiCl_4$  arises from a combination of the flux of Cl neutrals and the flux of ions, being sensitive to the ratio of these quantities,  $CI/J_+$ . At low values of  $CI/J_+$ , the etch rate is limited by the flux of Cl atoms and is independent of the ion flux, whereas at high values of this ratio, the etch rate is limited by the ion flux and independent of the Cl flux. This is well described by the model:

$$r = \frac{k_i \Gamma_i k_{Cl} \Gamma_{Cl}}{k_i \Gamma_i + k_{Cl} \Gamma_{Cl}}$$

We believe this is the first time an analytical model based on simple physical mechanisms of GaAs etching in  $SiCl_4$  has been reported in the literature.

---

**SESSION OWP1: POSTER SESSION: IONIZATION**

Wednesday afternoon, 8 October 1997

Great Hall, Memorial Union at 16:00

L. Wilmer Anderson, Univ. of Wisconsin, presiding

**OWP1 1 Multiple ionization of lead by electron impact** J. GED-

DES, *Department of Pure and Applied Physics, The Queen's University of Belfast, Belfast, United Kingdom*. P. McCARTNEY, M.B.S. SHAH, H.B. GILBODY, *Department of Pure and Applied Physics, The Queen's University of Belfast, Belfast, United Kingdom* A pulsed crossed beam technique incorporating time-of-flight spectroscopy is being used to study the multiple ionization of heavy metal atoms, a detailed understanding of which is important in the context of both high and low temperature plasmas. There are many gaps and serious discrepancies in the available experimental data. In the present measurements, cross sections for n fold ionization where  $n = 1$  to 6 have been determined for electron energies ranging from near threshold to 3 keV. The results are discussed in terms of the few previous experimental measurements available and current theoretical models of multiple ionization.

**OWP1 2 Electron-Impact Double Ionization of Magnesium\***

M.J. FORD, *University of Maryland* J.H. MOORE, M.A. COPLAN, *University of Maryland* B. EL MARJI, J.P. DOERING, *Johns Hopkins University* We have measured the differential cross-section for electron-impact double ionization of magnesium. Two electrons ejected from the double ionization event are detected, in coincidence, at energies of 100-eV. We observe the angular distribution of the electrons at a number of discrete points in three dimensions. The third electron is undetected. We have performed measurements in two distinct incident energy regimes, 1-keV and 422-eV. The cross-sections are clearly largest when the momentum vectors of the two outgoing electrons are co-planar with the incident vector, and show a weaker dependence on the included angle between the two electrons, 90 degree included angle being preferred. At high incident energy the electron pair are ejected into the forward direction, whereas at 422-eV they are found anywhere in a plane containing the incident electron vector regardless of the actual direction they are ejected into.

\*Funded by NSF grant PHY-95-15516

**OWP1 3 Kinetic-Energy Distributions of Positive and Negative Ions in DC Townsend Discharges of Carbon Dioxide** M. V.

V. S. RAO, R. J. VAN BRUNT, J. K. OLTHOFF, *NIST* Ion kinetic-energy distributions (IEDs), mean energies, and relative abundances are measured for  $CO_2^+$ ,  $CO^+$ ,  $O_2^+$ ,  $O^+$ ,  $C^+$ , and  $O^-$  ions produced in dc Townsend discharges in pure carbon dioxide. The discharges are generated at electric field-to-gas density ratios (E/N) ranging from  $3.5 \times 10^{-18} \text{ Vm}^2$  to  $20 \times 10^{-18} \text{ Vm}^2$  (3.5 to 20 kTd). Ions sampled from the discharge through a small orifice in the center of the grounded electrode were energy and mass analyzed by an electrostatic energy analyzer attached to a quadrupole mass spectrometer.<sup>1</sup> In the present experiments,  $CO_2^+$  was determined to be the dominant positive ion (greater than 85%) at all E/N. The IEDs of  $CO_2^+$ ,  $O_2^+$ , and  $O^+$  are Maxwellian at all E/N, with  $CO^+$  exhibiting non-Maxwellian behavior above 10 kTd, and  $C^+$  exhibiting non-Maxwellian behavior at all E/N. Negative ion fluxes were substantially lower than positive ion fluxes, with  $O^-$  being the only detectable negative ion. The IEDs for  $O^-$  are Maxwellian at 6 kTd and below. The fact that  $O^-$  is the only negative ion indicates that no asymmetric charge transfer exists for  $O^-$  in  $CO_2$ .

<sup>1</sup>M. V. S. Rao, R. J. Van Brunt, and J. K. Olthoff, *Phys. Rev. E* 54, 5641 (1996)

**OWP1 4 Kinetic-Energy Distributions of Positive and Negative Ions in DC Townsend Discharges of  $CHF_3$  at High E/N** M.

V. S. RAO, R. J. VAN BRUNT, J. K. OLTHOFF, *NIST* In this paper we present ion kinetic-energy distributions (IEDs), mean energies, and relative abundances of  $CF_3^+$ ,  $CF_2^+$ ,  $CF^+$ ,  $CHF_2^+$ ,  $CHF^+$ ,  $CH^+$ ,  $C^+$ ,  $H^+$ , and  $F^-$  ions produced in dc Townsend discharges in pure  $CHF_3$ . The discharges are generated at electric field-to-gas density ratios (E/N) ranging from  $5 \times 10^{-18} \text{ Vm}^2$  to  $25 \times 10^{-18} \text{ Vm}^2$  (5 to 25 kTd). Ions sampled from the discharge through a small orifice in the center of the grounded electrode were energy and mass analyzed by an electrostatic energy analyzer attached to a quadrupole mass spectrometer.<sup>1</sup> In the present experiments,  $CHF_2^+$  was determined to be the dominant positive ion at all E/N, followed by  $CF^+$ . The negative ion fluxes were substantially lower than the positive ion fluxes, with  $F^-$  being the only negative ion with significant intensity. At 5 kTd, the IEDs of all positive ions exhibit Maxwellian behavior. However, at higher E/N the role of collisional dissociation processes increases and the

IEDs of the positive ions deviate from those predicted by simple collisional charge-transfer models. The IEDs for  $F^-$  are non-maxwellian at all  $E/N$ .

<sup>1</sup>M. V. V. S. Rao, R. J. Van Brunt, and J. K. Olthoff, *Phys. Rev. E* **54**, 5641 (1996)

**OWP1 5 Time-resolved measurement of the effective ionization coefficient and ion drift in  $CH_4$ -Ar mixtures** \* JAIME DE URQUIJO, CARLOS ARRIAGA, EDUARDO BASURTO, † CARMEN CISNEROS, IGNACIO ALVAREZ, *Instituto de Física, UNAM, México* A pulsed Townsend technique has been used to measure the electron effective ionization coefficient,  $\alpha_e/N$ , and the drift velocity of positive ions for methane-argon mixtures over the density-normalized electric field intensity,  $E/N$ , between 100 and 1000 Td. The  $CH_4$ -Ar mixing ratios were varied between 100:0% and 25:75%. The ionic avalanche pulshapes were obtained without integration, thereby representing a direct measurement of the displacement current within the interelectrode gap. For  $E/N < 300$  Td, the trend of  $\alpha_e/N$  as a function of  $E/N$  displays a systematic increase with the argon share in the mixture. Moreover, the  $\alpha_e/N$  values for pure argon from Kruithoff<sup>1</sup> represent the upper bound. Above  $E/N = 500$  Td, no clear variation is observed on the  $\alpha_e/N$  values for different mixing ratios. Also, a well defined parametric dependence with the mixing ratio for the average mobility of the positive ions is observed.

\*Work supported by DGAPA, Project IN104795

†Also at ESM-IPN

<sup>1</sup>A.A. Kruithoff, *Physica* **7** (1940) 519

**OWP1 6 A Penning discharge as a dc source for multiply ionized atoms** KLING RAINER, KOCK MANFRED, *Institute of Atomic and Molecular Physics, University of Hannover, Callinstrasse 38, D-30167 Hannover, Germany* We report upon a specially designed Penning discharge which has been further developed from a source published by Finley *et al.*<sup>1</sup> towards a radiation standard for the XUV.<sup>2</sup> The discharge stands out for low buffer gas pressure, high electric power input and a strong superimposed magnetic field. That leads to intense sputtering of the cathodes which can be made of nearly any material. The efficient excitation and ionization of the sputtered atoms permit spectroscopy on multiply ionized species. W III and Fe III spectra will be given as examples. We also will present kinetic temperatures of the non-thermal plasma showing that the ionic component is decoupled from the cold neutral gas component.

<sup>1</sup>Finley, D. S., Bowyer, S., Paresce, F., Malina, R. F.: *Appl. Opt.* **18** (1979) 649

<sup>2</sup>Heise, C., Hollandt, J., Kling, R., Kock, M., Kuehne, M.: *Appl. Opt.* **33** (1994) 5111

**OWP1 7 Electron-Impact Total Ionization Cross Sections of Fluorine Compounds** Y.-K. KIM, NIST M. A. ALI, *Howard Univ.* M. E. RUDD, *Univ. Nebraska-Lincoln* \* A theoretical method called the Binary-Encounter-Bethe (BEB) model<sup>1</sup> that combines the Mott cross section at low incident energies  $T$  and the Bethe cross section at high  $T$  was applied to fluorine compounds of interest to plasma processing of semiconductors ( $CF_4$ ,  $CHF_3$ ,  $C_2F_6$ ,  $C_4F_8$ , etc.). The theory provides total ionization cross sections in an analytic form from the threshold to a few keV in  $T$ , making it convenient to use the theory for modeling. The theory is

particularly effective for closed-shell molecules. The theoretical cross sections are compared to available experimental data.

\*Work at NIST was supported in part by the Office of Fusion Energy, US DOE, and work at the Univ. of Nebraska by NSF Grant No. PHY-9119818.

<sup>1</sup>M. A. Ali, Y.-K. Kim, H. Hwang, N. M. Weinberger, and M. E. Rudd, *J. Chem. Phys.* **106**, 9602 (1997), and references therein.

**OWP1 8 Chemionization Cross Sections for Various Rare Gas Metastable Pairs** DAVID F. HUDSON, *GERA* We present the chemionization cross sections for several pairs of rare gas metastables using the semiempirical approach of Miller<sup>1</sup>. A new model potential is used to describe the interactions between the pairs of metastables. Numerical cross sections will be presented for  $He^* + He^*$ ,  $Ar^* + Ar^*$  and  $Xe^*$ .

<sup>1</sup>Miller *J. Chem. Phys.* **52**, 3563 (1970)

**OWP1 9 Photoionization of the Neon isoelectronic sequence using RRP** NASREEN HAQUE, *Department of Physics, Morehouse College, Atlanta, Ga 30314* ALFRED MSEZANE, *CTSPS, Clark Atlanta University, Atlanta, Ga 30314* STEVEN T. MANSON, *Dept. Of Physics and Astronomy, Georgia State University, Atlanta, Ga 30303* PRANAWA DESHMUKH, *Dept. of Physics, Indian Institute of Technology, Madras, India* Calculations of photoionization cross section using Relativistic Random Phase Approximation (RRPA) of Neon atom and ions isoelectronic to it are presented. In this isoelectronic sequence we investigated the first eleven members of the sequence, from the neutral neon to Ca+10. The calculations included coupling of channels obtained by dipole excitations of the 2p and 2s subshells. There are seven such jj-coupled channels. The 2p and 2s cross sections are plotted against photon energy. The cross sections appear to shift to the right with increasing stage of ionization. Also with increasing Z in an isoelectronic sequence the photoionization becomes more hydrogenic. We see that the cross sections decrease fairly rapidly with increasing stage of photoionization.

---

## SESSION OWP2: POSTER SESSION: HIGH DENSITY PLASMAS FOR PROCESSING

Wednesday afternoon, 8 October 1997

Great Hall, Memorial Union at 16:00

L. Wilmer Anderson, *Univ. of Wisconsin*, presiding

**OWP2 1 Silicon and Silicon Oxide Etching with a Novel Microwave ECR Plasma Source** REX ANDERSON, AARON WILSON, W. D. GETTY, M.L. BRAKE, *Center for Display Technology and Manufacturing, University of Michigan* We are running etch experiments on a-Si and SiO<sub>2</sub> with a novel ECR microwave plasma. A 1 kW, 2.45 GHz microwave source<sup>1</sup> is connected to a microwave horn which expands the microwave aperture to a 15 cm x 20 cm rectangle. The horn is attached to the top plate of the 28-cm diameter vacuum chamber which holds a 15 cm x 20 cm aluminum 6-slot grill containing 5 rows of permanent magnets. The resulting ECR surface of 875 G is approximately 1 cm from the grill. Measured etch rates of SiO<sub>2</sub> in CF<sub>4</sub>/H<sub>2</sub> plasmas vary due to polymer buildup on the wafer resulting from the use of H<sub>2</sub> and the low energies of the ions produced by the ECR plasma. The effect of self DC bias applied to the wafer with 13 MHz power



toaid the etching process is being studied. Using the exposure time and the film thickness change, the etch rate is calculated for various percentages of H<sub>2</sub> and compared with the known etch rates for SiO<sub>2</sub>. Similar tests with a-Si will be performed. The goal of these measurements is to explore the differences in CF<sub>4</sub>/H<sub>2</sub> etching between the present source and standard ECR reactive-ion etching tools.

<sup>1</sup>W. Getty and J. Geddes, *J. Vac. Sci. Technol. B* 12(1), 408-415 (1994)

#### **OWP2 2 Kinetic Model of a O<sub>2</sub>-N<sub>2</sub> Low Pressure Microwave Discharge**

V. GUERRA, J. LOUREIRO, *CEL-IST, Lisbon Tech. Univ., PORTUGAL* A self-consistent model governing the kinetics of electrons, ions and neutral heavy-particles in a O<sub>2</sub>-N<sub>2</sub> low pressure (p=1 Torr) microwave discharge (433 MHz, 2.45 GHz) was developed by coupling the homogeneous electron Boltzmann equation, under the effective field approximation, to a system of rate balance equations for the populations of charged and neutral species. Both volume and surface processes were considered in the model. The former ones include the V-V and V-T energy exchange processes, along with a large number of other collisional processes, whereas a statistical Monte Carlo simulation of a sequence of elementary surface processes has been used to describe the wall recombination of O(<sup>3</sup>P) atoms on pyrex glass. The maintenance reduced electric field has been determined from the solution of the continuity and transport equations for the charged particles with the inclusion of O<sup>-</sup> ions, by considering an appropriate theory for discharges in electronegative gases. This model also predicts the mean absorbed power per length unit required to sustain the discharge, as well as the concentrations of the neutral an ionic species created for the complete range of O<sub>2</sub>:N<sub>2</sub> mixture composition.

#### **OWP2 3 Negative Ion Measurements in Electron Cyclotron Resonance Etching Plasmas\***

BON-WOONG KOO, NOAH HERSHKOWITZ, *University of Wisconsin-Madison* Negative ions are known to be the precursor for particle formation in processing plasmas. Significant concentrations of negative ions have previously been identified in capacitively-coupled low pressure fluorocarbon and silane plasmas, low pressure multi-dipole hydrogen plasmas, etc. Negative ions can also change the plasma potential, spatial plasma profiles and plasma density in processing plasmas. Since electronegative gases are often used in plasma etching, it is interesting to know what negative ion species are present. Here we report measurements of negative ions in an electron cyclotron resonance (ECR) etching tool. An omegatron mass analyzer, which took advantage of the dc magnetic field in the etching tool, was used to make measurements at pressures of 0.1-5.0mTorr. The omegatron mass analyzer was geometrically modified to detect both positive and negative ions by changing the polarity and magnitude of the bias voltage of the electrodes inside the omegatron chamber. The geometry also provides differential pumping with pressure inside the omegatron below the 0.05 mTorr range, reducing collisional effects and insulating film deposition. The main goals of this study are (1) to understand omegatron physics and (2) to measure the negative ion species in ECR etching plasmas. Positive ions were also measured mainly to calibrate the ion mass in negative ion measurements. Preliminary results show H(+), H<sub>2</sub>(+), H<sub>3</sub>(+) and He(+) ions in an H<sub>2</sub> + He plasmas, H(-) and H<sub>2</sub>(-) in hydrogen plasmas, N(+), N<sub>2</sub>(+) in nitrogen plasmas, F(-), F<sub>2</sub>(-) in fluorocarbon ECR plasmas. Recent experiments will be presented.

\*Work supported by the National Science Foundation grant no. EEC-8721545

#### **OWP2 4**

WITHDRAWN

#### **OWP2 5 Plasma Production Using Waves in a Lower Hybrid Frequency Range**

Y YASAKA, K OHNISHI, K TACHIBANA, Kyoto University T ITOH, *Plasma System Corp.* Plasma production using waves in a lower hybrid frequency range is investigated numerically and experimentally. A two-dimensional fluid simulation code is employed to predict plasma production properties in a designed plasma source. In contrast to the helicon wave case, the radial region of wave propagation of the lower hybrid wave can be changed, leading to a control of power deposition profile. The measured ion saturation current profile varies from hill to hollow shape with increased magnetic field strength in accordance with the calculation. By choosing the radial region of wave propagation, the plasma is mainly produced in outer radii and diffuses to form a radially uniform profile in downstream region.

#### **OWP2 6 A Two-Coupled-Sheath Simulation of RF Chuck Bias\***

S. K. KANAKASABAPATHY, L. J. OVERZET, *The University of Texas at Dallas* Current flow induced charge build-up causes several types of etch related damage. There are claims<sup>1</sup> that appropriate chuck biases provide alternate irradiation by positive and negative ions and decrease this charge build up. A 1-D, two-coupled-sheath, fluid model has been developed to study such a bias. Whereas most ICP simulations focus on the bulk plasma using analytic sheath models, our code focuses on the ion and electron dynamics of two sheaths bounding a plasma bulk, modeled as an infinite source/sink of species. Ion momentum conservation and continuity equations are solved, closed by Poisson's equation for each sheath and the Bohm criterion arises self-consistently. The two sheaths are coupled by current continuity and a common bulk potential. High electronegativity, electrode asymmetry, bias amplitude and low frequency, as well as transverse coupling tend to favor sheath inversion and subsequent



negative ion extraction. Spatio-temporal variation of sheath properties, vindicates a time dynamic approach.

\*This material is based in part upon work supported by the Texas Advanced Research Program under Grant No. 009741-043 and by the National Science Foundation Young Investigator Award No. ECS-9257383.

<sup>1</sup>Shibayama et. al. *Plasma Sources Sci. Technol.* 5, 254 (1996).

**OWP2 7 Measurements of an Inductively Coupled Plasma Source for Microelectronics Processing\*** MARWAN H. KHATER, L. J. OVERZET, B. E. CHERRINGTON, *The University of Texas at Dallas* Inductively coupled plasma (ICP) sources produce high plasma densities at low pressures, thus achieving high etch rates and uniformities. We have designed a new ICP source operating at 13.56 MHz and measured the spatial profiles of the magnetic fields using a B-dot probe. The fields have better azimuthal symmetry than a simple planar spiral coil. We also measured the spatial profiles of plasma density, plasma and floating potentials, electron temperature and ion saturation current density in Ar and SF<sub>6</sub> glows near the wafer surface. The new source produced high plasma densities ( $\sim 10^{12}$  cm<sup>-3</sup>), and low electron energies, plasma and floating potentials ( $\sim 3$  eV, 14 V and 1 V) in an Ar glow at 20 mTorr and 1 kW. The  $I_{sat}$  profiles were measured at a variety of powers and pressures. The best plasma uniformity occurred at high power and low pressure for the new source design and was slightly better than that of a planar spiral coil. The new source produced 1  $\mu$ m/min etch rates of polysilicon in an SF<sub>6</sub>/Ar discharge.

\*This material is based upon work supported by Beta Squared, Inc., Allen, Texas.

**OWP2 8 Experimental Test of Models of High-Density, Radio-Frequency Plasma Sheaths** M. A. SOBOLEWSKI, Y. WANG, J. K. OLTHOFF, *NIST* Particle dynamics in the narrow sheaths of high-density plasmas, especially in sheaths biased by radio-frequency (rf) voltages, are complicated and nonlinear. Models of such high-density, rf sheaths are needed to predict ion bombardment energies in simulations of high-density plasma etching. Several treatments based on simplifying assumptions have been proposed, but they have not been sufficiently tested by experiment. To provide data to test these models, we have measured sheath voltages, sheath currents, ion currents, and ion kinetic energies in a high-density, inductively-coupled GEC Reference Cell, for argon discharges at 1.3 Pa and rf biases of 1-300 V and 0.1-30 MHz. The sheath at the powered electrode as well as the opposing sheath at grounded surfaces were investigated. The rf voltage across each sheath was determined from an external voltage probe on the powered electrode and a capacitive probe immersed in the plasma. The rf current and dc ion saturation current were measured at the powered electrode; kinetic energy distributions were measured for ions crossing the ground sheath. For either sheath, the measurements extended from rf periods much less than ion transit times to rf periods much greater than ion transit times. Thus they provide a test of sheath models over this entire range.

**OWP2 9 Two Dimensional Modeling of Ar RF ICP by RCT Model,** K. IYANAGI, N. NAKANO, T. MAKABE, *Keio University, Yokohama Japan* An inductively coupled plasma (ICP) excited by a radio frequency has been applied as sources in semiconductor processing. We have developed 2D ICP model for use in high density plasma, considering the electron transport under both time varying electric and magnetic fields. We investigate the spatiem-

poral structure of ICP in Ar. The discharge model consists of the electromagnetic module and Relaxation Continuum (RCT) module<sup>1</sup> with electrons, positive ions and Ar metastables(<sup>3</sup>P<sub>0</sub>). The results in a collision dominated region for pressures 0.1-0.3 Torr at 13.56MHz are shown. In particular, the influence of the plasma density and metastables on ICP maintenance are discussed. The additional small peaks due to the effect of  $E(t) \times B(t)$  drift in the net ionization rate appears close to the wall prior to the main signal at higher pressure. The direct net ionization rate has two peaks during one period, while the stepwise ionization is almost independent of time.

<sup>1</sup>K. Kamimura, T. Makabe, K. Iyanagi and N. Nakano, *J. Phys. D* (submitted)

**OWP2 10 Hysteresis on the E to H mode transition in radio frequency discharges** M. M. TURNER, J. GOSS, *Plasma Research Laboratory, Dublin City University, Ireland* I. M. EL-FAYOUMI, I. R. JONES, *School of Physical Sciences, Flinders University, Adelaide, Australia* There is a (now) familiar and spectacular transition between the E (or capacitive) and H (or inductive) modes of a radio frequency discharge—the increase in plasma density and power dissipated can be more than an order of magnitude going from the E mode to the H mode. This mode transition exhibits hysteresis<sup>1</sup> in the sense that the antenna current at the E-H transition is not the same as the current at the H-E transition. In this paper we show that this can sometimes be a large effect (difference of more than a factor of two between the two transition currents) and that the effect can be reproduced by self-consistent simulations. We offer an interpretation of these data in terms of power and particle balance arguments, and we will relate the results to certain instabilities that sometimes occur in inductive radio frequency discharges.

<sup>1</sup>e.g., U. Kortshagen, N. D. Gibson and J. E. Lawler, *J. Phys. D* 29, 1224 (1996)

**OWP2 11 Laser Scattering Diagnostics of a Magnetic Neutral Loop Discharge Plasma** K. UCHINO, T. SAKODA, K. MURAOKA, *Kyushu University, Japan* M. ITOH, T. UCHIDA, *UL-VAC Japan Ltd* A magnetic neutral loop discharge (NLD) has been proposed as a new plasma source for plasma processing<sup>1</sup>. In order to characterize the production and the transport processes in the NLD plasma, laser Thomson scattering was applied to diagnose the plasma<sup>2</sup>. Also, laser-induced fluorescence measurements were performed to measure atomic densities at excited states and metastable states. By using these data, the excitation processes in the plasma were analyzed quantitatively. The result clearly showed the essential role of the neutral loop for the production of the NLD plasma.

<sup>1</sup>T. Uchida, *Jpn. J. Appl. Phys.* 33, L43 (1994).

<sup>2</sup>T. Sakoda, et al., *Jpn. J. Appl. Phys.* 36, L67 (1997)

**OWP2 12 Space- and Time- Resolved Measurements of F<sup>-</sup> Density in High-Density Fluorocarbon Plasmas by Laser Photodetachment** D. HAYASHI, N. TAKADA, K. SASAKI, K. KADOTA, *Department of Electronics, Nagoya University, Nagoya 464-01, Japan* The importance of F<sup>-</sup> has been pointed out in ion-enhanced plasma etching of SiO<sub>2</sub>/Si with fluorocarbon plasmas. However, the difficulty in negative ion diagnostics in the fluorocarbon plasmas has led us to the paucity of the knowledge of the production and loss mechanisms of F<sup>-</sup>. This is partly because that conventional Langmuir probes do not work in the fluorocarbon plasmas due to the deposition of films with insulation property on

the probe surface. In the present work, we developed a Langmuir probe with a heated tip to evaporate the insulated films. The heated probe was combined with a laser photodetachment technique to measure the  $F^-$  density in high-density ( $n_e > 10^{12} \text{ cm}^{-3}$ ) and low-pressure ( $< 20 \text{ mTorr}$ )  $CF_4$  and  $C_4F_8$  plasmas produced by helicon wave excitation. In the  $CF_4$  plasmas with a pressure of 2.5 mTorr, the concentration in  $F^-$  in negatively charged particles was  $\sim 30\%$  during the active discharge phase. In the afterglow, a rapid decrease in the electron density with a decay time constant of  $10 \mu\text{s}$  was observed. This can be attributed to the production of  $F^-$  due to dissociative attachment to neutral species under the low-electron temperature of 1 eV. The decay time constant of  $F^-$  was similar with that of positive ions. Hence mutual neutralization with the positive ions is probably the major loss process of  $F^-$  in the high-density plasmas.

**OWP2 13 Density and Kinetics of Fluorine Atoms in Helicon-Wave  $C_4F_8$  Plasmas** K. SASAKI, C. SUZUKI, K. KADOTA, *Department of Electronics, Nagoya University, Nagoya 464-01, Japan*  $C_4F_8$  plasmas are increasingly used for selective dry etching of  $SiO_2$  over Si in place of conventional  $CF_4$  plasmas. In the present work, the absolute F atom density in high-density  $C_4F_8$  plasmas was measured by vacuum ultraviolet absorption spectroscopy. The reaction kinetics of F atoms was investigated by the lifetime measurements in the afterglow. The experiments were carried out in a helicon-wave plasma source which can produce high electron densities of  $n_e = 4 \times 10^{10} \sim 1 \times 10^{13} \text{ cm}^{-3}$  for rf powers of 0.2~1.5 kW and  $C_4F_8$  gas pressures of 2~7 mTorr. The resultant F atom densities were  $n_F = 1 \times 10^{12} \sim 5 \times 10^{13} \text{ cm}^{-3}$ . In the high-power region, the F atom density in the  $C_4F_8$  plasma was approximately two times higher than that in the  $CF_4$  plasma for the similar discharge conditions. When the  $C_4F_8$  pressure was low ( $\leq 3 \text{ mTorr}$ ), the F atom density decreased exponentially in the afterglow. On the other hand, a linear decrease in the F atom density was observed when the  $C_4F_8$  pressure was higher than 5 mTorr. The decay time constant of the F atom density was shorter for the higher gas pressure. The reaction kinetics of F atoms especially on the wall surface will be discussed by referring to the experimental observations.

**OWP2 14 Wave Propagation and Absorption in a Helicon Plasma Source** \* Y. MOUZOURIS, J. E. SCHARER, M. H. BETTENHAUSEN, *University of Wisconsin-Madison* The MAX\_EB computer code<sup>1</sup> is used to study and model helicon sources. MAX\_EB, a two-dimensional (r,z) simulation code, calculates the electromagnetic wave fields and power absorption in an inhomogeneous cold plasma immersed in a non-uniform magnetic field. The current distribution of the launching antenna which provides the full antenna spectra is included in the model. We have modified the code to include collisionless warm plasma thermal effects. We benchmarked the modified MAX\_EB code with our ANTENA2 code<sup>2</sup> for an axially uniform plasma in a uniform axial magnetic field. The effect of an applied magnetic field 2-D (r,z) profile on the wave properties and power absorption is investigated. We present studies of the wave fields and electron heating profile due to collisional and collisionless (Landau damping) wave absorption mechanisms in a non-uniform plasma. Our helicon simulations will be directly compared with selected experimental data.

\*This work is supported by NSF grant No. ECS-9632377

<sup>1</sup>L. A. Berry and J. C. Whitson, private communication (1996)

<sup>2</sup>Y. Mouzouris and J. Scharer, IEEE Trans. on Plasma Science, 24(1), (1996)

**OWP2 15 Surface and helicon wave propagation in an inductively coupled plasma at low magnetic field** T. LHO, N. HER-SHKOWITZ, W. STEER, *Nuclear Engineering and Engineering Physics, University of Wisconsin, 1500 Engineering Dr., Madison, WI 53705, U.S.A.* J. MILLER, *Twinstar Semiconductor Inc., 500 west Renner Rd., Richardson, TX 75080, U.S.A.* G.H. KIM, *Department of Physics, University of Hanyang, Gyunggi-Do, Annsi, Korea* Azimuthally symmetric ( $m=0$  mode) surface and helicon wave propagation in an inductively coupled Ar plasma ( $P=1-2 \text{ mTorr}$ ) at low B-field (0-28G) have been measured. The plasma mode transition from the E-mode to H-mode has also been observed by applying an axially uniform low B-field. Plasma is generated by a planar four turn spiral coil antenna, whose axis is parallel to the B-field, mounted on the outside the chamber end window. There is no Faraday shield to prevent electrostatic field coupling. A T-shaped glass chamber whose dimensions are  $D=10 \text{ cm}$ ,  $L=35 \text{ cm}$  is used. Applied rf is 13.56 MHz and many harmonic components of the fundamental frequency are observed in each mode. The dominant frequencies extend to the 5<sup>th</sup> harmonic. Surface waves with frequencies  $f=13.56$  and  $27.12 \text{ MHz}$  propagate at low densities ( $n < 10^{11} \text{ cm}^{-3}$ ) as the B-field is varied. At high densities ( $n > 10^{11} \text{ cm}^{-3}$ ) and relatively high B-field ( $\omega_c/\omega > 2.5$ ), helicon waves with  $f=13.56 \text{ MHz}$  are observed. Otherwise, surface waves with  $f=27.12 \text{ MHz}$  are measured at relatively low B-field ( $\omega_c/\omega < 2.5$ ).

**OWP2 16 Spectroscopic Observations of Helicon Discharge Evolution** JAMES GILLAND, NOAH HERSHKOWITZ, *University of Wisconsin-Madison* Helicon waves are capable of producing high density ( $10^{13} \text{ cm}^{-3}$ ), low temperature (3-5 eV) plasmas using rf powers of less than 1 kW. At high electron densities, the helicon discharge becomes an efficient neutral pump, ionizing essentially all the neutrals in the high density region. Previous measurements of this effect on plasma and neutral densities along the length of the discharge have been augmented with spectroscopic measurements of ion and neutral line radiation intensities. An argon plasma was created using helicon waves in a 1.2 m long, 10 cm diameter chamber. A uniform applied axial magnetic field of 1000 Gauss was imposed in the chamber. Centerline electron temperatures and densities were measured in the high density region of the discharge and near the end, using an rf compensated Langmuir probe. Line averaged argon ion (480.6 nm) and neutral (763.5 nm) line radiation intensities were measured at several axial locations within the discharge for rf powers from 100 to 700 W. The experiment was performed using cusped and uncusped magnetic fields at the ends of the discharge. These measurements show a change in discharge composition at a power of approximately 300 W. The neutral intensity achieves a maximum near this power level, while the ion intensities increase monotonically with power, with a sharp increase near the 300 W level. The impact of these observations on theories of helicon plasma power loss mechanisms will be discussed. This work is funded by NSF grant No. ECS-9529565.

**OWP2 17 Large-area, low-field, multi-tube helicon plasma sources** J.D. EVANS, F.F. CHEN, *UCLA* G.R. TYNAN, *Trikon Technologies, Inc.* Multi-source helicon plasma production has been observed for the first time using a 7-tube array of small ( $r = 2.5 \text{ cm}$ ) helicon plasma sources coupled to a larger ( $R = 20 \text{ cm}$ ) bulk plasma chamber. Plasma densities in excess of  $10^{12} \text{ cm}^{-3}$  are obtained with 2kW of RF power at  $f = 13.56 \text{ MHz}$  in Ar and Cl gases at pressures of 10mT and  $B \leq 250 \text{ G}$ . Excitation of an

$m = +1$  helicon wave leads to an enhancement of the bulk plasma density by a factor of 5. A low-field peak in plasma density vs magnetic field is clearly observed in both single-tube and multi-tube experiments, using both  $m=0$  and  $m=1$  helicon antenna designs. Short solenoidal magnetic field coils surrounding each individual antenna are inadequate for producing a helicon-enhanced plasma, producing instead an inductively coupled plasma (ICP) with a maximum density occurring for  $B = 0$ . Large magnetic field coils that surround the entire source array and produce fields that penetrate into the bulk plasma chamber are suitable for helicon-enhanced plasma production, with density maxima at B 100G. Density, electron temperature and plasma potential radial profiles are obtained using a pneumatically-driven, rapid-scanning probe (FastProbe<sup>R</sup>), while a rotatable Langmuir probe array ("lazy susan" probe) is used to measure azimuthal symmetry of the discharge. Dependence of plasma parameters on RF frequency, antenna geometry, neutral pressure, proximity of conducting surfaces (image currents), and quality of impedance matching will be presented.

**OWP2 18 Electron Beam Biasing of Substrates during Plasma Etching** \* A. K. QUICK, N. HERSHKOWITZ, *Engineering Research Center for Plasma-Aided Manufacturing, University of Wisconsin-Madison*

Electron beam biasing of substrates is being studied as an alternative to the usual method of using a capacitively coupled, rf-powered wafer chuck. The advantage of biasing with an electron beam is that the electrons which arrive at the wafer do so with an anisotropic velocity distribution similar to the plasma sheath-accelerated ions. This becomes important when etching large aspect ratio features. Isotropic plasma electrons can't follow the ions to the bottom of deep wells and they adhere to and charge up the feature sidewalls. This differential charging creates electric fields which deflect incoming ions and causes sidewall profile defects such as bowing, notching, and microtrenching and contributes to RIE(Reactive Ion Etch) lag<sup>1</sup>. The effects of etching sub-half micron nested poly-Silicon lines in Cl<sub>2</sub> plasmas in the presence of an electron beam will be presented particularly in regard to notch suppression. The effects that the electron beam has on RIE lag suppression in SiO<sub>2</sub> etching in fluorocarbon plasmas will also be discussed.

\*Work supported by the National Science Foundation grant no. EEC-8721545

<sup>1</sup>R. A. Gottscho, C. W. Jurgensen, and D. J. Vitkavage, *J. Vac. Sci. Technol. B* 10(5), Sep/Oct 1992, 2133.

**OWP2 19 Characterisation of an SF<sub>6</sub> Helicon Discharge** R.W.

BOSWELL, *RSPHysSE, Australian National University, Canberra, ACT 0200, Australia* P. CHABERT, *Laboratoire PRIAMONERA, F-91761, CEDEX, France* J. SAVY, T.E. SHERIDAN, *RSPHysSE, Australian National University, Canberra, ACT 0200, Australia* A continuous helicon discharge made using the processing gas SF<sub>6</sub> has been characterized as a function of neutral pressure, flow rate and rf power with a number of diagnostic techniques. Two modes of operation are found—at low pressures the electron mean free path is long and plasma is created throughout the vacuum chamber, while for higher pressures plasma creation is localized in the helicon source and plasma diffuses into the chamber. In the first case, a sizeable electron drift from the source to the substrate is inferred using a planar Langmuir probe. The mass spectrum of positive ions was measured, and it is found that for low rf powers SF<sub>3</sub><sup>+</sup> and SF<sub>5</sub><sup>+</sup> dominate, while for high powers

S<sup>+</sup> and F<sup>+</sup> are the main ions. The concentration of atomic F was determined by optical emission actinometry, and saturated with increasing rf power. Paradoxically, for increasing rf power the ion saturation current collected by a Langmuir probe increased while the Ar optical emission decreased. Probe measurements suggest that this discrepancy may be due to an increase in the negative ion density with a concomitant decrease in the electron density.

**OWP2 20 Pure Silicon Plasma in a Helicon Plasma Deposition System** R.W. BOSWELL, *RSPHysSE, Australian National University, Canberra, ACT 0200, Australia* A. DURANDET, C.A.

DAVIS, *RSPHysSE, Australian National University, Canberra, ACT 0200 Australia* A plasma containing only silicon atoms and ions has been obtained by electron-beam evaporation of solid silicon through a helicon rf plasma source. The density of the silicon plasma in the diffusion chamber is  $3 - 5 \times 10^{10} \text{ cm}^{-3}$ , and the electron temperature 12 eV. These plasma conditions correspond to a predicted deposition rate from silicon ions of 230 =B1 60 nm/minute, comparable to the deposition rate of 250 nm/minute obtained using the same evaporation conditions, without generating a plasma. The large contribution of silicon ions, the high deposition rate and the absence of other species such as hydrogen or argon, leads to novel conditions for plasma assisted deposition.

**OWP2 21 Determination of Metal Vapor Ion Concentration in an Ar/Cu Plasma For Ionized Physical Vapor Deposition** J.E.

FOSTER, W. WANG, A.E. WENDT, J. BOOSKE, *The University of Wisconsin Plasma ERC* Determination of the metal vapor ionization fraction is an important aspect of characterizing ionized physical vapor deposition (IPVD) systems. In such systems, metal ions formed by passing sputtered metal vapor through a high density plasma are used for ion plating applications. Here, a fairly straightforward Langmuir probe technique which takes advantage of changes in the ratio of the electron saturation current to the ion saturation current to determine the variations in both the copper and the argon ion concentration is utilized. Variations in ion concentration as a function of sputter power and pressure at a number of different rf powers are presented. The data suggests that at fixed rf power the copper ion concentration increases rapidly with increasing sputter rate. In addition to this diagnostic, absorption spectroscopy is used to infer the degree of change in copper ionization by measuring how the copper neutral concentration varies as a function of rf power. It is shown that modest increases in rf power can give rise to significant reductions in the copper neutral concentration.

**OWP2 22 Time-Resolved Langmuir Probe Measurements in an Ionized PVD System** D. R. JULIANO, D. B. HAYDEN, D. N.

RUZIC, *University of Illinois-Urbana* The experimental apparatus consists of a commercial-scale magnetron<sup>1</sup> with an RF coil between the target and substrate holder. This coil creates a secondary inductive plasma that ionizes a significant portion of the sputter flux en route from target to substrate. Ionization of the metal atoms that make up the sputter flux is highly sensitive to the high energy tail of the electron energy distribution, which in turn is highly dependent on the background gas mixture. Since there is some capacitive coupling from the coil this high energy population could change through the RF cycle. Time-averaged Langmuir probe measurements would not reveal either the extent of this high energy population or its time dependence. Further, if the probe



voltage were held constant for such time-resolved measurements, they would yield incorrect results. At probe voltages above the plasma potential minimum the sheath is disrupted so that at points in the phase for which the probe voltage is below plasma potential the data is invalid. Therefore in order to take valid measurements at all phase points, it is necessary for the probe voltage to follow the RF variation in plasma potential. Using such a system, we have made time-resolved Langmuir probe measurements. Current-voltage traces as a function of phase then reveal plasma parameters as a function of time over the RF cycle for various background gases and operating parameters.

<sup>1</sup>Donated by Materials Research Corporation

**OWP2 23 Measurement of Absolute Densities of SiF<sub>x</sub> in Electron Cyclotron Resonance SiF<sub>4</sub> Plasma** MASAYUKI NAKAMURA, HIROYOSHI ARAI, KOJI MIYATA, MASAFUMI ITO, MASARU HORI, TOSHIO GOTO, *Information Electronics, Nagoya University, JAPAN* Fluorine-doped silicon oxide (SiOF) films have been studied intensively as interlayer low dielectric films in ULSI. The SiOF films are deposited by using a plasma CVD method with a mixture of SiF<sub>4</sub>/SiH<sub>4</sub> gases. It is indispensable to know the behaviors of feed gas and reactive species in the plasma to develop the films with good quality. In this study, we used a large-scale-compact ECR plasma system employing SiF<sub>4</sub> gas. The ECR plasma source is 30 cm in diameter and 8.6 cm in height using rings of permanent magnets. SiF<sub>4</sub> flow rate and pressure were fixed at 30 sccm and 2.0 Pa, respectively, and microwave power was changed from 0 W to 900 W. We have measured successfully the absolute density of SiF<sub>4</sub> molecule in ECR-SiF<sub>4</sub> plasma using infrared diode laser absorption spectroscopy (IRLAS) measurement for the first time. Two spectra near 1008 cm<sup>-1</sup> for the measurement of SiF<sub>4</sub> molecule were used. As a result, the absolute density of SiF<sub>4</sub> was decreased with increase of microwave power. In particular, the absolute density of SiF<sub>4</sub> was  $2.5 \times 10^{14}$  /cm<sup>3</sup> when microwave power was 900 W and was about a half of that without discharge. The behaviors of SiF<sub>x</sub> radical densities in ECR plasma are also discussed.

**OWP2 24 Measurement of Si atom density in ultra high frequency discharge silane plasma** YASUO YAMAMOTO, RYOHEI YOSHIDA, MASAFUMI ITO, MASARU HORI, TOSHIO GOTO, *Dept. of Quantum Eng., Nagoya Univ., JAPAN* SEIJI SAMUKAWA, *NEC Co., JAPAN* TSUTOMU TSUKADA, *ANELVA Co., JAPAN* Recently, in order to solve problems in etching process, ultra high frequency (UHF) plasma source has been developed as the plasma source which can produce high density and low temperature plasma in a large area. Applying this plasma source for deposition process, it is expected that neutral radicals are efficiently produced by low energy electrons because the electron temperature in UHF plasma is lower than that in other high density plasmas. In this work, we have measured Si atom density in a UHF silane plasma using ultraviolet absorption spectroscopy. Si atom density at  $3p^2 \ ^3P_2$  level is about  $1 \times 10^9$  cm<sup>-3</sup> at a UHF power of 400 W, a pressure of 30 mTorr and a silane flow rate of 20 sccm. This value is the same order of that in the ECR silane plasma at a microwave power of 400 W and a pressure of 10 mTorr. Si atom density increases with increasing pressure from 20 to 100 mTorr at a UHF power of 400 W. This behavior is quite different from that in the ECR silane plasma where Si atom density decreases with increasing the pressure. The behavior of Si atom density in the UHF silane plasma will be discussed.

**OWP2 25 Ionized PVD with an Inductively Coupled Plasma Source** D. B. HAYDEN, D. R. JULIANO, D. N. RUZIC, *University of Illinois at Urbana-Champaign* Ionized physical vapor deposition (iPVD) is used to enhance the directionality of metal deposition. This is a potential solution to depositing into higher aspect-ratio trenches and vias for metal interconnects. A dc magnetron<sup>1</sup> is coupled with an inductively coupled plasma (ICP) coil to increase the ionization of the sputtered metal atoms. This allows metal ions to be accelerated across the plasma sheath to a biased substrate and deposited normally. One coil design has a wider diameter than the substrate to reduce shadowing and flaking effects. Argon and neon working gases and aluminum and copper targets are investigated at varying pressures and power levels. Deposition rates and metal flux ionization fractions are measured with a quartz crystal microbalance and a multi-grid analyzer.

<sup>1</sup>Donated by Materials Research Corporation

**OWP2 26 Diamond Film Formation Using a Low Pressure Radio Frequency Inductively Coupled Plasma** H. NODA, H. NAGAI, M. HIRAMATSU, M. NAWATA, *Meijo University, Nagoya, Japan* M. HORI, T. GOTO, *Nagoya University, Nagoya, Japan* Diamond film formation using radio frequency (rf) inductively coupled plasma (ICP) has been reported by several researchers. Diamond films using ICPs are generally formed at high pressures above 1 Torr and high rf powers. In this work, we utilized a low pressure (a few 100s mTorr) rf (13.56 MHz) ICP to deposit diamond films. A mixture of CH<sub>3</sub>OH and H<sub>2</sub> was introduced into a reaction chamber through a quartz tube of 12 mm inner diameter. 7-turn rf coil was mounted on the tube. The Si substrate was located in a downstream region. Film formation was carried out with varying mixture ratio between CH<sub>3</sub>OH and H<sub>2</sub> at rf powers of 500-800 W, substrate temperatures of 600-700 °C, and a substrate bias of +30 V. Diamond films were successfully synthesized using rf ICP at the total pressure of 100 mTorr. Films were evaluated by scanning electron microscopy and Raman spectroscopy.

**OWP2 27 Self-Consistent Particle Simulation of Axisymmetrical Magnetron Discharge** S. KONDO, K. NANBU, *Tohoku University* Magnetron sputtering is widely used in fabricating thin films in microelectronics industries. In magnetron discharge charged particles move in the electric field that is governed by their distribution. In a self-consistent discharge simulation the equations of motion for the particles and Poisson's equation for the field should be solved simultaneously. Coupling of motion and field is the essential difficulty in numerical simulation. Since the pressure is a few mTorr, we should have recourse to the particle simulation although the computational load is intensive. In this work the structure of an axisymmetrical dc planar magnetron discharge is clarified by the use of the PIC/MC method. The magnetron has two concentric cylindrical magnets behind the cathode which form axisymmetrical magnetic field. Here we examined the effect of magnetic field on the discharge structure. Spatial distributions of electric field and number densities of charged particles are shown for  $M=0.50$  T, 0.75 T and so on,  $M$  being the magnetization. It is found that the axial component of electric field varies greatly in the cathode sheath between the two magnets. The plasma density profile shows a peak. As  $M$  increases in strength, the sheath thickness decreases and the position of the peak comes nearer to the sheath edge.



**SESSION OWP3: POSTER SESSION:  
EXTREME SUBMICRON PROCESSING**

**Wednesday afternoon, 8 October 1997**

**Great Hall, Memorial Union at 16:00**

**L. Wilmer Anderson, Univ. of Wisconsin, presiding**

**OWP3 1 Plasma Etching of Semiconductor Trenches by Three Processes** CHUNG DAR DANIEL WANG, BARBARA ABRAHAM-SHRAUNER, *Department of Electrical Engineering Washington University, St. Louis, MO, 63130* \* Model plasma etch profiles in semiconductor wafer processing include the superposition of etch rates of ions and shadowed and isotropic neutrals. The etch rates are given by analytical expressions. The etch profiles for a long trench are calculated numerically from trajectory equations for the evolution equation of the profile surface. The etch rate for the ions is assumed proportional to the ion energy flux where the ions are represented by a drifted Maxwellian distribution function. The etch rate for the shadowed neutrals is proportional to the neutral flux where these neutrals are represented by a Maxwellian distribution function. To model the scattering of neutrals off the trench surface the etch rate of isotropic neutrals which is constant on the etch surface is added to the etch rate of the shadowed neutrals.

\*Research supported by the National Science Foundation under Grant No. ECS-9310408

**OWP3 2 Modification of Plasma Etching of Trenches by Sputtering** \* B. ABRAHAM-SHRAUNER, N. JAGANNATHAN, *Washington University* The effect of sputtering on trench etch profiles is modeled by a modification of the analytical etch rate expression for the incident ions. The ion etch rate has been assumed proportional to the ion energy flux in the absence of sputtering.<sup>1</sup> Measured etch rates for ion beam etching by sputtering show a peak in the etch rate for ions incident at angles between 40 and 70° with respect to the normal direction to the surface of some etched materials.<sup>2</sup> The off normal angular peak of the etch rates due to sputtering is more pronounced at lower pressures. In high density low pressure reactors the pressures are in the range where sputtering may affect the etch rates. The ion beam etch rate data are fit by polynomials in the cosine of the angle that the ion velocities make with the surface normal. These polynomials replace the cosine factor in the ion energy flux integral and give a modified yield with angle. Trench profiles are computed and compared with those for which sputtering is ignored.

\*Research supported by the National Science Foundation under Grant No. ECS-9310408.

<sup>1</sup>B. Abraham-Shrauner and C. D. Wang, *J. Appl. Phys.* 77, 3445 (1995).

<sup>2</sup>R. E. Lee, *J. Vac. Sci. Technol.* 16, 164 (1979).

**OWP3 3 Model Etch Profiles for Ion Energy Distribution Functions in ICP and Helicon Plasma** \* WENJING CHEN, BARBARA ABRAHAM-SHRAUNER, C. DANIEL WANG, *Department of Electrical Engineering, Washington University, St. Louis, MO 63130* † Measured argon ion axial energy distribution functions in a helicon plasma and angular distribution functions in an inductively coupled plasma are fitted to theoretical ion energy distribution functions derived from one and two-temperature drifted Maxwellian velocity functions by a simulated annealing procedure. We assume that an etching plasma has these ion energy

distributions and that the etch rate is proportional to the ion energy flux in the ion flux-limited regime. Etch profiles are calculated and compared for a trench where the etch rates are given by the approximate expressions derived for one<sup>1</sup> and two-temperature drifted Maxwellian velocity distribution functions.

\*Research supported by the National Science Foundation under Grants No. ECS-9310408 and ECS-9500251.

†Special thanks to Hong-Young Chang of Korea Advanced Institute Science and Technology and Joseph R. Woodworth of Sandia National Laboratory for supplying measured data.

<sup>1</sup>W. Chen and B. Abraham-Shrauner, *J. Appl. Phys.* 81, 2547 (1996).

<sup>2</sup>B. Abraham-Shrauner and C. D. Wang, *J. Appl. Phys.* 77, 3445 (1995).

**OWP3 4 Experimental study of the charging of structures on wafers** GURPRIT CHANDHOKE, BRIAN HEIL, UWE KORTSHAGEN, *University of Minnesota, Dept. of Mech. Engineering* In recent years, it has been observed that the charging of high aspect ratio structures in semiconductor devices causes a deterioration in the etching characteristics. This tends to limit attempts to further reduce the smallest feature size in current microelectronic devices. We present first experimental results on the charging of structures on a test wafer. On top of a conducting silicon wafer a 5 micron silicon-dioxide layer was grown. Test structures consisting of arrays of holes with various diameters in the micron range have been etched into the silicon-dioxide. We discuss measurements of the charging of these structures performed in a low pressure capacitive discharge. We present the effects of gas pressure and of the power dissipated in the discharge.

**OWP3 5 Sub-0.5mm Polysilicon Gate Etching with Cl<sub>2</sub>/O<sub>2</sub> Plasma in An Inductively Coupled Plasma Etcher** SONGLIN XU, XUEYU QIAN, GERALD YIN, *Applied Materials Inc* An extensive process characterization and development has been carried out on sub-0.5mm polysilicon gate etching with Cl<sub>2</sub>/O<sub>2</sub> chemistry on an inductively coupled plasma reactor. By evaluating etch performance such as etch rate, selectivity and profile against different process parameters, including source power, bias power, pressure, flow rate, additive concentration and cathode temperature, critical process trends have been determined. These trends were further correlated with plasma properties such as ion flux and ion energy to provide better understanding on etch mechanism and approaches for process control. Based on the trend study, the optimum process region has been identified to be at low pressure, low source power and appropriate O<sub>2</sub> concentration. A baseline process with highly anisotropic and selective polysilicon gate etching has been developed.

**OWP3 6 Characteristics of Dry Etched GaN Using Ar/SF<sub>6</sub> and He/SF<sub>6</sub> in an Assymmetric RF Parallel Plate Discharge** J SCOFIELD, P. BLETZINGER, B.N. GANGULY, *Air Force Research Laboratory* GaN has attracted considerable attention for utilization in visible and near UV light emitting diodes, semiconductor lasers, and devices for high power, frequency, and temperature applications. However, considerable development is still required in the area of device fabrication and processing. Due to the large cohesive energy of atoms in the GaN lattice dry etching is the only practical method to achieve reliable pattern definition in GaN. We will present results of our investigation of the etch rates and corresponding surface region damage associated with Ar/SF<sub>6</sub> and He/SF<sub>6</sub> plasma etch conditions. Using the SF<sub>6</sub> chemistry in ratios of 5-20% it has been determined that the resulting etch rate

of MOCVD grown a-GaN/Al<sub>2</sub>O<sub>3</sub> is independent of the inert buffer gas used, indicating that the sputter etch mechanism is minimal in comparison to the fluorine ion and radical etch mechanism. This inert gas independence has been observed for d.c. self bias conditions ranging from -200 to -350 volts and for 13.56 MHz r.f. power inputs in the 60 watt range. GaN etch rates of 30 to 50 angstroms/min has been demonstrated for these parametric conditions at operating pressures of between 50 and 250 mTorr. GaN crystal damage resulting from contamination, sputtering, or energetic-ion kinetic mechanisms induced during plasma etching has also been evaluated in terms of the same rf discharge characteristics. Initial results indicate that under these conditions, He may be a more attractive buffer gas to use in processing GaN devices due to potentially reduced sputtering damage.

**OWP3 7 Charging of Substrates Irradiated by Particle Beams**  
P. N. GUZDAR, A. S. SHARMA, S. K. GUHARAY, *Institute for Plasma Research, University of Maryland, College Park, MD 20742* Charging of a substrate due to irradiation by charged particle beams is a major problem in many applications of current interest, namely, ion implantation, etching, lithography etc. A simple model of a beam propagating and interacting with a solid substrate is modelled. The self-consistent field associated with the beam is included, as well as the loss of secondary electrons at the substrate is accounted for using a simple distribution function. The beams used in the present study are positive ions as well as negative ions. We find that the charging voltage is very small for the negative ion case. Typical charging voltages of a few volts for a beam with energy of tens of KVs are obtained. On the other for positive ion beams, the charging voltage is comparable to the ion beam energy. Thus negative ion beams are an attractive option for the above-mentioned applications. Quantitative comparison for the charging voltage with observations by Ishikawa [Rev. Sci. Instrum. **67**, 1410, 1995] will be presented.

---

**SESSION OWP4: POSTER SESSION:  
DIAGNOSTICS AND SENSORS**

**Wednesday afternoon, 8 October 1997**

**Great Hall, Memorial Union at 16:00**

**L. Wilmer Anderson, Univ. of Wisconsin, presiding**

**OWP4 1 UV and VUV spectra of Metal-Etch Plasma Processing Discharges** JOSEPH WOODWORTH, RAMANA VEERASINGAM, *Sandia National Laboratories* We are investigating the emission spectra of metal-etch processing discharges containing mixtures of chlorine and boron trichloride in the spectral region from 115 to 300 nm. Our measurements are being carried out in an inductively-driven GEC reference cell. Our goals are to identify spectral features which can be isolated inexpensively with photomultiplier-plus-filter detectors and used as process or endpoint monitors. Initial measurements, made with a 0.3 meter monochromator with 0.1 nm resolution show a rich spectrum, containing many atomic and molecular features. Promising emission features observed to date include atomic chlorine lines between 135 and 140 nm, boron lines at 167, 209, and 250 nm, silicon lines near 221 and 251 nm and narrow emission bands of BCl and AlCl at 272 and 261 nm respectively. This work was supported by the United States Department of Energy under Contract DEAC04-94-AL85000. Sandia is a multiprogram laboratory

operated by the Sandia Corporation, a Lockheed Martin Company, for the United States Government.

**OWP4 2 Simultaneous electric field measurements in a dc discharge by fluorescence and optogalvanic Stark spectroscopies** D.A. DOLSON, *Wright State University, Dayton, OH* B.N. GANGLY, *Wright Laboratory, WPAFB, OH* The electric field in the cathode fall region of a 2.2 Torr helium dc discharge with 1 mA/cm<sup>2</sup> current density has been measured from the Stark splittings of 11 <sup>1</sup>P helium Rydberg state by simultaneous optogalvanic and fluorescence techniques. The 2s <sup>1</sup>S to 11 <sup>1</sup>P transition was excited by a collimated (0.05 cm diameter) tunable pulsed uv laser beam. The fluorescence at 447.1 nm (4d<sup>3</sup>D to 2p<sup>3</sup>P) was collected from a small volume while the optogalvanic signals were obtained from a line-of-sight average over the entire discharge cord length. The Stark spectra exhibited narrower linewidths for fluorescence compared to the optogalvanic spectra. However, the electric field values obtained from the two methods were in agreement within three percent for all the measured locations in the sheath. Also, the spatial variation of the fluorescence intensities from 4d<sup>3</sup>D and 3d <sup>3</sup>D states, in the discharge volume, show that the collisional intensity transfer from the singlet Rydberg state to the lower triplet states is dominated by electron collision.

**OWP4 3 C<sub>2</sub> Swan Band Emission Intensity as a Function of [C<sub>2</sub>]** \* A.N. GOYETTE, J.E. LAWLER, L.W. ANDERSON, *Department of Physics, University of Wisconsin, Madison, WI 53706* D.M. GRUEN, T.G. MCCAULEY, D. ZHOU, A.R. KRAUSS, *Chemistry and Materials Science Divisions, Argonne National Laboratory, Argonne, IL 60439* We report the systematic comparison of the optical emission intensity of the d<sup>3</sup>Π → a<sup>3</sup>Π (0,0) vibrational band of the C<sub>2</sub> Swan system with the absolute C<sub>2</sub> concentration in Ar/H<sub>2</sub>/CH<sub>4</sub> and Ar/H<sub>2</sub>/C<sub>60</sub> microwave plasmas used in the deposition of nanocrystalline diamond. The absolute C<sub>2</sub> concentration is obtained using white light absorption spectroscopy. Emission intensity correlates linearly with C<sub>2</sub> density for a variation of several plasma parameters and across two decades of species concentration. Although optical emission intensity generally is not a highly quantitative diagnostic for gas phase species concentrations, these results confirm the reliability of the (0,0) Swan band for relative determination of [C<sub>2</sub>] with high sensitivity under conditions used for hydrogen deficient plasma-enhanced chemical vapor deposition of diamond.

\*Work supported by the U.S. Army Research Office under grant DAAH-04-96-1-0413 and the U.S. Department of Energy, BES-Materials Sciences, under contract W-109-ENG-38.

**OWP4 4 H<sup>-</sup> Diagnostics by CW-Laser Absorption Spectroscopy** E. QUANDT, H.-F. DÖBELE, *Institut für Laser- und Plasmaphysik, Universität GH Essen, D-45117 Essen, Germany* W.G. GRAHAM, *The Queen's University Belfast/ Northern Ireland* \* A novel diagnostic technique for the measurement of negative ions is presented. Negative hydrogen ions are detected by measuring the absorption of a CW-laser beam with a wavelength close the maximum of the photodetachment cross section for the negative ion. In our case a He-Ne laser at λ = 632.8 nm is used. The present measurements were made in a filament-driven, multi-cusp source operated in a hybrid configuration to optimise negative ion production. The discharge is periodically pulsed and the absorption of the negative ions is detected with a photomultiplier followed by a lock-in amplifier. The laser beam undergoes multiple reflections through the discharge volume using either a Herriott or a White arrangement, so that approximately 100 passes can take place. H<sup>-</sup>

density measured by this method is in agreement with published data both with respect to the absolute value and the dependence of the various discharge parameters.

\*Supported in part by the UK-German ARC programme and by the DFG in the frame of the SFB 191

**OWP4 5 Laser Detection of Methylene Radicals in CH<sub>4</sub>-H<sub>2</sub> dc Discharges** G. SULTAN, G. BARAVIAN, *LPGP, CNRS, U. of Paris-Sud, F-91405 Orsay* C. HAYAUD, *Innovatique, F-69386 Chassieu* J. AMORIM, *ITA, Sao Jose dos Campos, Brazil* The CH<sub>2</sub> radical, which is usually difficult to detect in plasmas, is identified in a CH<sub>4</sub>-H<sub>2</sub> discharge by LIF measurement of the H atom. A 205 nm laser photon photodissociates the CH<sub>2</sub> radical in CH + H species and the resulting fast H atom is excited by two photons during the same laser pulse and emits the H-alpha radiation. The obtained Doppler profile of the H atoms leads to the determination of a dissociation energy of the hydrocarbon photofragment equal to 4.2 eV which corresponds to the detection of CH<sub>2</sub> radicals. At a pressure of 2 Torr and a discharge current of 10 mA, we show that the CH<sub>2</sub> radical density increases almost linearly with the percentage - until 15% of CH<sub>4</sub> in the gas mixture, while the population density of the H atoms created in the plasma remains quasi-constant, except in the cathode sheath.<sup>1</sup>

<sup>1</sup>work supported in part by an EDF contract

**OWP4 6 Laser-Induced Fluorescence Measurement of SiH<sub>2</sub> in Silane Plasmas Using a CW Ring Dye Laser** A. KONO, S. HIROSE, T. GOTO, *Nagoya University, Nagoya, Japan* K. KINOSHITA, *ASET, Yokohama, Japan* Low density SiH<sub>2</sub> in silane plasmas was detected using a laser-induced fluorescence (LIF) technique with a cw ring dye laser. The method enabled us to study the translational temperature and also to obtain a higher S/N ratio in measuring the dynamic behavior of the radical as compared with measurements by use of a pulsed dye laser.<sup>1</sup> The translational temperature of SiH<sub>2</sub> was measured in a 40-mTorr rf SiH<sub>4</sub>/Ar plasma with varying mixing ratio. The temperature was ~300 K and no dependence on the mixing ratio was detected; the result makes a marked contrast to the case of Si, whose temperature was high in a pure SiH<sub>4</sub> plasma and decreased with increasing Ar dilution. The behavior of SiH<sub>2</sub> in a 40-mTorr SiH<sub>4</sub>/SiH<sub>2</sub>Cl<sub>2</sub> plasma was also studied. The use of a cw laser was essential to study the transient behavior of the SiH<sub>2</sub> density in the afterglow because high repetition-rate signal averaging was necessary to eliminate the effect of relatively strong interfering emission from long-life SiCl<sub>2</sub>( $\tilde{a}^3B_1$ ). It was found that SiH<sub>2</sub>Cl<sub>2</sub> plays a minor role both in production and destruction of SiH<sub>2</sub> in the SiH<sub>4</sub>/SiH<sub>2</sub>Cl<sub>2</sub> plasma. (A part of this work was supported by NEDO.)

<sup>1</sup>A. Kono *et al.* Jpn. J. Appl. Phys. 34 (1995) 307.

**OWP4 7 Measurement of quenching rates of the argon 750.4 nm actinometer line by various gases** A. FRANCIS, U. CZARNETZKI, H.-F. DOBELE, *Institut für Laser- and Plasmaphysik, Universität GH Essen, D-45117 Essen, Germany* N. SADEGHI, *Université Joseph Fourier, Bp 87, 38402 Saint Martin d'Hères, France* \* Argon is a frequently used gas for actinometry, in particular in connection with thin film diamond deposition in e.g. methane/hydrogen discharges. Here H densities are deduced from the ratio of the intensity of hydrogen Balmer lines to the Argon 750.4 nm (4p'[1/2] - 4s'[1/2]) line. Although this method is experimentally simple, care has to be taken concerning the quenching of the 4p' [1/2] state. At elevated pressures quenching can substantially change the relationship between the line intensity and

the population of the state from which it arises. For hydrogen, especially for the Balmer- $\alpha$  transition, quenching rates with some important gases are known but there has been a lack of data for argon. In our experiment we used two-photon excitation of argon by short laser pulses (FWHM = 3D 4 ns) at 184 nm, to selectively populate the 4p'[1/2] state. The resulting fluorescence is observed with a fast photomultiplier and the quenching rates are deduced from the variation of the decay time vs reagent partial pressure. Among the various gases investigated are several diatomic and polyatomic molecules of plasma interest e.g. H<sub>2</sub>, O<sub>2</sub>, CH<sub>4</sub>, C<sub>2</sub>H<sub>2</sub>, F<sub>2</sub>, and SF<sub>6</sub>.

\*Support by the DAAD/CNRS PROCOPE program is gratefully acknowledged.

**OWP4 8 A novel four-wave mixing scheme for atomic hydrogen detection: First results** M. THOMSON, U. CZARNETZKI, H.-F. DOBELE, *Institut für Laser- and Plasmaphysik, Universität GH Essen, D-45117 Essen, Germany* \* The measurement of atomic hydrogen concentration in plasma discharges is usually based on the emission of fluorescence light after excitation by one- or two-photon absorption from a laser beam. Although these schemes are very sensitive background radiation from the plasma can be a serious problem under certain conditions. Four-wave mixing schemes like CARS have been proven to be quite insensitive to background radiation. The reason for this is the emission of the signal beam in a small cone comparable to the incoming laser beam which allows efficient suppression of the background by spatial filtering. Unfortunately CARS can only be applied in practice to molecules but not to atoms. Here, we present an alternative scheme for atomic hydrogen also based on four-wave mixing: Two parallel laser beams at 205 nm and 656 nm are in resonance with the two-photon transition to n=3D3 and close to resonance with the Balmer- $\alpha$  transition, respectively. The signal beam is generated in the VUV close to Lyman- $\alpha$ . First experimental results showing the dependence on various parameters like density, energy, and frequency are presented.

\*Support by the DFG is gratefully acknowledged.

**OWP4 9 UV absorption spectroscopy diagnostics of etching plasmas** JEAN-PAUL BOOTH, GILLES CUNGE, NADER SADEGHI, *Laboratoire de Spectrometrie Physique, Grenoble, France* PASCAL CHABERT, *Thomson CSF-LCR, Orsay, France* FRANCOIS NEUILLY, *SGS Thomson, Crolles, France* Broadband UV absorption spectroscopy is a simple but powerful diagnostic for the measurement of absolute concentrations of reactive radicals in etching plasmas. Using a Xe arc lamp and a 25 cm monochromator equipped with a UV-enhanced CCD array detector allows absorptions lower than 10<sup>-3</sup> to be detected easily in the spectral range 210 - 300 nm. We have used this technique to detect CF<sub>2</sub> radicals in CF<sub>4</sub> and C<sub>2</sub>F<sub>6</sub> capacitively coupled 13.56 MHz plasmas. CF<sub>2</sub> concentrations as low as 10<sup>12</sup> cm<sup>-3</sup> are readily detected. Previous studies in our laboratory have shown that this species is intimately involved in polymerisation, selectivity and wall passivation mechanisms in oxide etching processes. Therefore, monitoring of [CF<sub>2</sub>] by this simple technique has potential for real-time process control. The technique also allows the CF<sub>2</sub> vibrational and (with a larger spectrograph) rotational temperature to be determined: this temperature is expected to be in equilibrium with the gas translational temperature in the reactor under these conditions. The S<sub>2</sub> molecule was also detected during Si etching by an SF<sub>6</sub> plasma.



**OWP4 10 Density Measurements of Metastable He in a Parallel Plate Discharge Using a Diode Laser** MICHAEL W. MILLARD, PERRY P. YANEY, *Univeristy of Dayton, Dayton, Ohio* BISWA N. GANGULY, *Wright Laboratories, Wright-Patterson AFB, Dayton, OH.* A diode laser has been used to measure the spatial profile of the absolute number density of He metastables using the  $2^3S \rightarrow 2^3P$  transition in steady state, parallel plate dc and pulsed discharges. These measurements were carried out at a pressure of 2 Torr and current density of  $4.4 \times 10^{-5} A/cm^2$ . The measured density path length product ranged from  $3.7 \times 10^{10} cm^{-2}$  near the anode surface to  $4.3 \times 10^{11} cm^{-2}$  in the sheath region. The laser used was a distributed feedback diode laser with a 3MHz average linewidth with an instantaneous linewidth of less than 250kHz while the Doppler width of the He lines was approximately 2GHz. By selectively choosing different J levels of the  $2^3S \rightarrow 2^3P$  to observe in the triplet, we show that due to the narrow linewidth of the laser and the 5:3:1 ratio of statistical weights of the lines, this technique has sufficient sensitivity for absolute density measurements over nearly five orders of magnitude. A technique for measuring the diffusion rate and the surface sticking probabilities of the metastable He in the active and afterglow regions of the discharge will also be presented showing one possible application.

**OWP4 11 A Study of Electron Energy Distribution Functions in Inductively Coupled Plasmas by Laser Thomson Scattering** M. D. BOWDEN, T. HORI, M. KOGANO, K. UCHINO, K. MURAKA, *Kyushu University, Japan* The electron energy distribution function (eedf) in an inductively coupled plasma was studied using the method of laser Thomson scattering. In order to completely characterize the eedf, measurements were made for various plasma conditions, spatial and temporal dependencies were measured, and the eedf in the afterglow part of a pulsed discharge was measured. In high electron density plasmas, the eedf was observed to be Maxwellian while in low density discharges, a non-Maxwellian eedf was observed. The transition between Maxwellian and non-Maxwellian eedfs was attributed to the thermalization of the electron population in higher density plasmas. The results were compared with recent models and simulations of electron motion in the inductive rf field in an ICP discharge. The electron behaviour and the shape of the eedf are explained in terms of ICP heating mechanisms and the effect of the rf magnetic field.

**OWP4 12 A Technique for Observing Infrared Emissions from Thermal Electron-Ion Plasmas** B.K. DECKER, T.L. WILLIAMS, J.M. BUTLER, N.G. ADAMS, *Univ. of Georgia, Athens, GA* \* A technique has been developed to observe infrared emissions (1.8-3.5 microns) from the products of gas-phase reactions such as binary neutral-neutral and ion-molecule reactions and electron-ion dissociative recombination. This involves the use of a flow tube in which one of the reactive components is modulated by pulsing either the microwave cavity ionization source or one of the reactant gases (to effect the concentration of that gas or to modulate the electron density using a rapidly attaching gas). The modulation is used as a reference signal for a digital lock-in amplifier. The radiations from the reactions are spectrally dispersed in a monochromator. Sufficient signals have been obtained to permit a resolution of 1 nm, which gives rotational resolution of vibrational bands. The technique has been tested on the well-known reaction  $H + NO_2 \rightarrow OH(v^*) + NO$  and on recombining electron-ion plasmas. Data from these systems will be presented.

\*Funding by NSF AST-9415485; contributions by Peter W. Harland are gratefully acknowledged.

**OWP4 13 Laser and Spectroscopic Studies of  $^4S$  Atomic Nitrogen Production in  $N_2-H_2$  Gas Mixtures in a Microwave Discharge** STEVEN F. ADAMS, BISWA GANGULY, *Wright Laboratory, WPAFB, OH* TERRY A. MILLER, *The Ohio State University* The production of ground state ( $^4S$ ) N-atoms by microwave discharge has been investigated for the addition of small fractions of  $H_2$  in  $N_2$  at constant microwave power. Two-photon absorption LIF has been used to obtain concentration measurements of ( $^4S$ ) N-atoms just downstream of the flowing discharge at pressures of 1-5 Torr. The results show that with a very small addition of  $H_2$  in  $N_2$  (approx. 0.2 percent), the concentration of ( $^4S$ ) atomic nitrogen is enhanced beyond that of a pure  $N_2$  discharge by up to 15 percent. Higher fractions of  $H_2/N_2$  lead to a decay in ( $^4S$ ) N-atom concentration. LIF and emission measurements of several other discharge products have also been used to determine the relative behavior of  $N_2^+$ ,  $N_2(X,v)$ ,  $N_2(A,B,C)$ ,  $N(^2D)$ , H, and NH as function of  $H_2/N_2$ . These measurements help us formulate a model for N atom production as a function of  $H_2$  addition which takes into account several factors including changing electron energy distribution, variation of  $N_2(X,v)$  high v states, and changing  $N_2$  metastable states.

**OWP4 14 Comparison of Electron-Density Measurements using the Plasma Oscillation Method and a Langmuir Probe in an Inductively Coupled GEC Reference Cell** A. SCHWABEDISSEN, E.C. BENCK, J.R. ROBERTS, *NIST* \* The absolute electron density in planar inductively coupled plasmas has been measured by two different plasma diagnostic techniques, the plasma oscillation method and a Langmuir probe. The plasma oscillation method uses the effect that a weak electron beam injected into the plasma excites electrostatic electron waves oscillating at the electron plasma frequency, which is proportional to the square root of the electron density. The plasma source is a modification of the GEC RF Reference Cell with the upper electrode replaced by a planar spiral coil and a quartz vacuum interface. The results for both methods in electropositive, pure rare gas discharges (Ar, Kr) and in electronegative gases and gas mixtures like  $O_2$ ,  $Cl_2$ ,  $Ar/Cl_2$ ,  $Ar/SF_6$ ,  $Ar/BCl_3$  and  $Ar/CF_4$  are presented and analyzed for a variety of plasma parameters.

\*A.S. was sponsored by a Lynen Fellowship of the Humboldt Foundation

**OWP4 15 Langmuir probe characterization of capacitively driven discharges in different gases** J. MCFARLAND, *Dept. of Physics, The Queens University of Belfast, Northern Ireland* C.M.O. MAHONY, *Dept. of Physics, The Queens University of Belfast, Northern Ireland* P.G. STEEN, *Dept. of Physics, The Queens University of Belfast, Northern Ireland* W.G. GRAHAM, *Dept. of Physics, The Queens University of Belfast, Northern Ireland*. \* A compensated Langmuir probe technique has been used to study and contrast the plasma parameters of 13.56 MHz capacitively driven discharges operating in  $H_2$ ,  $D_2$ , He and Ar. The discharge was created in a GEC reference reactor configured in the asymmetric capacitive mode. Standard GEC I(V) measurement techniques were used to characterize the energy input. In all gases the form of the electron energy distribution function (EEDF) was found to be dependent on the operating power and pressure and in a manner which was consistent with those previously reported in other capacitively coupled systems<sup>1</sup>. In Ar the electron densities, mean energies and plasma potentials were gratifyingly close to those measured in the University of Texas GEC reference reactor<sup>2</sup>. For input powers between 10 and 100 watts and pressures in the range 75 mTorr to 1000 mTorr the electron densities were between  $5 \times 10^8$  and  $9 \times 10^{10} cm^{-3}$  with the highest density in Ar and the



lowest in  $D_2$ . Mean electron energies were between 2-4 eV. A detailed discussion of the variation between the different gases will be presented.

\*This work was funded by the Engineering and Physical Sciences Research Council

<sup>1</sup>V.A. Godyak, R.B. Piejak and B.M. Alexandrovich, *Plasma Sources Sci. Technol.*, 1 p 36-58 (1992)

<sup>2</sup>L.J. Overzet and F.Y. Leong-Rousey, Private communication

**OWP4 16 Development of new analysis algorithm based on wavelet transform for Langmuir probe traces from an ECR plasma** \* G.-H. KIM, *Physics* D.-G. KIM, *Mathematics* W.-H. JUNG, *Mathematics, Hanyang University*

The Langmuir probe has been used widely as an important plasma diagnostic because of its simplicity and ability to operate over a wide range of plasmas. However, it is difficult to interpret the data. The manual approaches often lose accuracy and reproducibility, especially, in the noisy magnetized plasmas. Due to ECI (electron cyclotron instability) noise, it was extremely difficult to choose the plasma potential from raw trace data. Thus, some of the common analysis algorithms use the averaging technique with statistical treatments, but they easily lose important information if care is not taken in interpreting the data, especially, the bi-maxwellian ECR plasma data. In this work, a new algorithm for automating the analysis of Langmuir probe traces from ECR plasmas was developed. In order to obtain de-noised data without loss of important information when the plasma parameters were determined, the wavelet shrinkage method proposed by Donoho and Johnston<sup>1</sup> was adapted. Differentiation of the processed data gave clear inflection points so that the plasma potential could be easily determined. The electrons were modeled by bi-maxwellian with hot and bulk temperatures. The plasma parameters could be obtained accurately.

\*Work supported by HANBIT-97 user program.

<sup>1</sup>Donoho and Johnson, *Biometrika*, 81, 425-455 (1994).

**OWP4 17 Fast Langmuir Probe Measurements in a Laser Produced Plasma** \* G. DING, J. E. SCHARER, K. L. KELLY, *University of Wisconsin-Madison*

Sheath motion has been found to be an important influence on Langmuir probe measurements for a rapidly decaying plasma. The plasma is created when an organic molecule, tetrakis(dimethyl-amino)ethylene (TMAE), is ionized by a 193 nm pulsed excimer laser. The laser beam is expanded by a series of lenses to produce a plasma sheet with dimensions 0.7 - 1.5 cm × 9.0 cm. The sheath motion effect is investigated after a 20 ns laser pulse produces plasma with a high initial plasma density ( $n_e > 10^{13} \text{cm}^{-3}$ ). The electron temperature decays from 0.9 to 0.6 eV during the period 100 - 1000 ns after the laser pulse. An expression to account for this effects on plasma density measurements is derived. Microwave reflection measurements from this plasma sheet are carried out, and the results are compared with a model incorporating plasma spatial and temporal profiles measured by this fast Langmuir probe method.

\*This work is supported by AFOSR grant No. F49620-97-1-0262

**OWP4 18 On the Probe Measurements of Ion Distribution Function in Electronegative Gas Plasmas** N.A. KHROMOV, S.A. GUTSEV, A.A. KUDRYAVTSEV, *Institute of Physics, St. Petersburg State University, Russia*

Since Langmuir probe measures the total current  $i$  or its derivatives, in practice a problem to extract ion contributions is arisen. For example it should be pointed out that even at weak discharge currents temperatures  $T_n^*$

evaluated from the slope of semi-logarithmic graph of  $i''(V)$  far exceed a gas temperature  $T(T < T_n^* = (0.08 - 0.6)eV)$ <sup>1</sup>. In order to clear up the cause of this paradox we carried out probe *CVC* and  $i''(V)$  measurements in a ion-ion (electronless) plasma. This plasma was observed in pauses of oxygen pulse discharge current at low pressure as a result of fast electrons escaping from volume effect<sup>2</sup>. As far as probe *CVC* is practically symmetric, the problem on the second derivative current selection is more simple. It has been established that temperatures  $T_{n,p}^* = 600 - 1600K$  measured with plot of  $i''$  against  $V$  are significantly greater than  $T = 300K$ . However values of  $T_{n,p}$  measured following OML theory from intersection of the  $V$  axis and curve  $i(V)$ <sup>2</sup> were close to 300K. This results uniquely indicate that paradox is due to  $i''$  as DF identification.

<sup>1</sup>H.Amemiya, *IGPIG-21 Proc.3(1993)88*.

<sup>2</sup>S.A.Gutsev *et al.*, *Zh.Tekh.Fiz.65(1995)77*

**OWP4 19 Modification of Ion Species by Gas Addition in an Inductive Metal Etch Reactor** PETER K. LOEWENHARDT, *Applied Materials, Santa Clara, CA 95054* DIANA X. MA, HIROJI HANAWA, YAN YE, TIMOTHY R. WEBB, ALAN ZHAO, JAY SHIAU, STEVE MAK, JAMES PAPANU, GERALD Z. YIN, *Applied Materials, Santa Clara, CA 95054*

Interconnect etching requires the complete removal of aluminum from predetermined zones. Since present day interconnect is usually an alloy (typically aluminum with 0.5 to 1.0% Cu), the complete removal of copper residue from areas being etched is paramount to produce an operational device. This is a significant issue since copper etches much more slowly than aluminum under standard conditions. Any remaining residue can short circuit the interconnect lines, resulting in device failure. It was found that the addition of certain inert gases to the etching process would enhance residue removal. Measurements of wafer ion flux, wafer-surface ion energy and voltage bias, and ion species were made to determine any changes made in the plasma that may have facilitated this enhancement. It will be shown that although the ion energy and flux were changed only a small amount by the gas addition, the composition of the ions were significantly altered.

**OWP4 20 Feedforward-Enhanced PID Control for Fast Response and Disturbance Rejection in Plasma Etching** C. BAUM, M. SARFATY, M. HARPER, J. L. SHOHET, N. HERSHKOWITZ, \*Advanced process control is becoming increasingly important in semiconductor manufacturing, especially for devices with small critical dimensions. Short process times require rapid feedback of important process state variables. Real-time measurements of unpatterned thin films are obtained using an in-situ, two-color laser reflectance interferometer (LRI) in a magnetically contained ICP device. A Kalman Filter is used to determine accurate measurements of the etch rate from each laser color using the LRI signals, following rescaling to model predictions (using real-time peak detection) and linearization using a novel transform. Real-time linear feedback control of SiO<sub>2</sub> and polysilicon etch rates is achieved using Proportional-Integral-Derivative (PID) control of chuck power. Response is improved by augmenting the PID algorithm with a feedforward model of etch rate response to ramp changes in chuck power. Rejection of unmeasured disturbances in other process inputs is also demonstrated. This work is funded by NSF grant No. EEC-8721545.

\*ERC for Plasma-Aided Manufacturing University of Wisconsin-Madison

\*ERC for Plasma-Aided Manufacturing University of Wisconsin-Madison

**OWP4 21 Ion Distributions in Metal-Etch Plasma Processing Discharges** CHRISTOPHER NICHOLS, JOSEPH WOODWORTH, *Sandia National Laboratories* THOMAS HAMILTON, *Applied Physics International* We are using a mass spectrometer and gridded energy analyzers to determine positive ion species, fluxes and energy distributions in discharge mixtures of Cl<sub>2</sub>, BCl<sub>3</sub> and Ar. Our experiments are being carried out in an inductively coupled GEC Ref cell using a variety of electrode materials. In most of the discharges studied, the ion energy distribution formed a single peak, well speateted from zero energy. In Cl<sub>2</sub>/BCl<sub>3</sub> discharges, ion flux and energy were not affected when a Si wafer was placed on the stainless lower electrode, but increased significantly when the electrode was changed to anodized aluminum. Positive ion species were dominated by BCl<sub>2</sub><sup>+</sup>, Cl<sub>2</sub><sup>+</sup> and Cl<sup>+</sup>. This work was supported by the United States Department of Energy under Contract DEAC0R-94-AL85000 and by SEMATECH. Sandia is a multiprogram laboratory operated by the Sandia Corporation, a Lockheed Martin Company, for the United States Government.

**OWP4 22 Oxide Etch Endpoint Detection by Downstream FTIR On An AMAT 5300 ION** C. ABRAHAM, *UW-Madison Plasma ERC* ENLIAN LU, QINGYUN YANG, *SEMATECH* HAROLD M. ANDERSON, *University of New Mexico* R. CLAUDE WOODS, *UW-Madison Plasma ERC* A method for detecting the endpoint in oxide etching of contact holes in an AMAT 5300 HDP etch tool by downstream FTIR was explored. A multi-pass cell sampled the flow stream between the turbomolecular and roughing pumps. The C<sub>2</sub>F<sub>6</sub> chemistry was the standard Applied Materials recipe. Patterned wafers at 2% and 0.4% open oxide area, and varying oxide layer thickness were processed. Dummy wafers (1% open area, patterned, but with no expected endpoint), and blanket photoresist wafers were also processed. The 2% open area wafers required only monitoring the slight change in absorption intensity of the C<sub>2</sub>F<sub>4</sub> line for endpoint detection. The sensitivity of detection for the 0.4% open area wafers was greatly improved by evolving window principal component analysis, a potentially real-time technique for systematically monitoring the variation of all spectral features. An apparent endpoint signature was obtained for both the 2% and 0.4% oxide wafers. The time of arrival of the endpoint signature increased for the thicker oxide layer wafers, as expected. No substantial signature was observed for the dummy and resist wafers.

**OWP4 23 Two dimensional imaging of electron temperature in GEC reference cell** J. GOREE, D. SAMSONOV, *The University of Iowa* Using two video cameras fitted with bandpass interference filters for two different ArI spectral lines, we computed images of the line intensity ratio, which corresponds to the effective electron temperature in the energetic tail of the electron distribution. The two upper energy levels that are probed by this method are at 13.1 and 15.3 eV. In a capacitively coupled Ar discharge with 400 V self bias at 400 mtorr in a sputtering reactor similar to a GEC reference cell, we find an energetic tail localized within 1 mm of the powered electrode and a lower temperature region in the next 5 mm. This experiment will be repeated using a GEC reference cell.

**OWP4 24 Diagnosis of System Condition using System Parameter Data** CARL ALMGREN, GEORGE COLLINS, *Colorado State University* Parameter data collected during the processing of films during the production of semiconductors can give critical information relating to both the stability of the processing tool, and the incoming wafer condition. In a plasma processing tool, the

system parameters are dependent upon a number of factors, which include both the system hardware, and the chamber conditions. The chamber conditions are affected the amount of sidewall polymer present, the gases present, and the impedance of the plasma, for example. By using the system parameters, and correlating previously-diagnosed problems with data trace signatures, fast and predictive system diagnoses can be made, while the system is running production wafers, and therefore at no cost of running additional tests which consume system time.

**OWP4 25 Induction Probe Studies of an Electrostatic Shield Around an Inductively Coupled Plasma** \* V.A. SHAMAMIAN, J.L. GIULIANI, *Naval Research Laboratory* A.E. ROBSON, *Berkeley Scholars, Inc.* R.E. CAMPBELL, *Geo-Centers, Inc.* An electrostatic shield comprised of a hollow metal cylinder is often placed between the drive coil and the discharge tube of an inductively coupled plasma. It is generally not realized that the electrostatic shield can also lead to a significant reduction of the RF magnetic field inside the tube as well as altering its axial distribution. This effect must be considered in detailed modeling of inductively coupled plasmas, and is of practical importance in determining the impedance the plasma presents to the RF generator. We have employed calibrated and capacitively shielded induction probes to measure the RF magnetic field inside and outside metal cylinders with different slot configurations (non-plasma). We have interrogated the degree to which the plasma screens the field as a function of pressure and coupled power in argon and hydrogen discharges. We also determined, using optical emission spectroscopy, the axial dependence of the electron temperature and plasma spatial extent. Finally, we have developed electromagnetic models for thin and thick shields which are in good agreement with the non-plasma induction probe observations. The thick shield results are relevant to high power systems in which the discharge tube itself is a thick-walled, water cooled, slotted metal cylinder. Plasma coupling in this system is compared to coupling of an unshielded dielectric tube and the predictions of the model will be discussed.

\*Supported by DARPA, BMDO/IST, and the 3M Corporation

**OWP4 26 The Influence of Different Coil Geometries on the Spatial Distribution of the Plasma Density in an Inductively Coupled GEC Reference Cell** A. SCHWABEDISSEN, E.C. BENCK, J.R. ROBERTS, *NIST* \* The radial distributions of the electron density and the relative atomic argon excited state densities have been investigated by means of Langmuir probes and optical emission spectroscopy in planar inductively coupled plasmas in pure argon. The plasma source is a modification of the GEC RF Reference Cell with the upper electrode replaced by a planar coil and a quartz vacuum interface. Two different planar coil geometries, a five-turn spiral coil and a one-turn circular coil, were investigated for a variety of plasma parameters. Additionally, we investigated the effect of different powering configurations of the spiral coil and an electrostatic shield between the coil and the plasma. We found that the coil geometry and power configuration of the coil influences the radial distribution of the electron density in the region close to the coil only, while in the region close to the lower electrode the radial distribution is dominated by diffusion.

\*A.S. was sponsored by a Feodor Lynen Fellowship of the Humboldt Foundation

**OWP4 27 Characterisation of Plasmoids in an RF Inductively Coupled Plasma** D VENDER, B CROWLEY, *Dublin City University* A radio frequency (13.56 MHz) inductively coupled

plasma with internal antenna is studied. The diagnostics include a Langmuir probe, rf current and voltage monitors and an optical emission sensor. In an argon discharge at pressures above 250 mTorr and at certain input powers the plasma changes from a diffuse glow to one in which the discharge is concentrated in two or more spherical lobes around the antenna tube. Gross inhomogeneities of this kind are known as plasmoids and in the present experiment their behaviour is characterised in Ar and mixtures of Ar with He by *in situ* measurements of the plasma parameters, the number and size of lobes, and the rotation frequency. Depending on external parameters values, the plasmoids are stationary or rotate in either direction with a maximum rate of about 50 revolutions per second. The effect of an external magnetic field on the rotation rate and direction is described. Langmuir probe measurements are used to determine the plasmoid structure at pressures between 250 mTorr and 1.5 Torr. A map of the discharge behaviour in the power range of 5 W to 150 W and pressures from 10 mTorr to 1.5 Torr is presented.

#### OWP4 28 Detection of atomic oxygen in a GEC-Reference Cell

by TALIF A. GOEHLICH, T. KAWETZKI, H.-F. DÖBELE, *Institut für Laser- und Plasmaphysik, Universität GH Essen, D-45117 Essen, Germany* \* Atomic oxygen is detected in a GEC parallel plate Reference reactor (13.56 MHz) by two photon excited laser induced fluorescence spectroscopy ( $2 \times \lambda = 226 \text{ nm}$ ). For the determination of the degree of dissociation a calibration is performed using xenon and taking advantage of the spectrally neighbouring two photon transition ( $\lambda = 226 \text{ nm}$ ;  $5p^6 \ ^1S^0 \rightarrow 5p^5 \ 7p \ [3/2]_2$ ). In the small signal regime where both the oxygen and xenon fluorescence scale as the square of the irradiated intensity the ratio of the oxygen density to the xenon density can be obtained from the spectrally integrated fluorescence signal. For this calibration the knowledge of the two photon excitation cross section of xenon is necessary. This cross section is not available from the literature. It was determined therefore in a second experiment using a flow tube reactor in which a quantitatively known concentration of oxygen atoms is established. The two photon cross section for xenon can then be inferred from the corresponding cross section for oxygen. Besides the determination of the degree of dissociation spatially resolved concentration profiles were determined. The temperature of the oxygen atoms is found from the Doppler width of the absorption line.

\*Supported by the DFG in the frame of the SFB 191

#### OWP4 29 Improved diagnostics for neutral species generated in processing plasmas

ALAN REES, PAUL READ, DAVID SEYMOUR, *Hidden Analytical Limited* Modification of the surfaces of target materials in both deposition and etching systems involves incident neutral species as well as charged particles. Studies of the neutral species have been carried out by previous authors using mass spectrometer systems to monitor the relative abundance of given species arriving at the target surface as a function of the plasma conditions. Information on the energy state of a given species can be obtained by examining its ionisation efficiency as a function of the electron energy used in the mass spectrometer source. In the present work the advantages of examining the formation of negative ions, through electron attachment or pair production, from the sampled neutral species are discussed. The technique is illustrated by examples of data obtained using a commercially available instrument for RF plasmas in methane and sulphur hexafluoride. The technique is applicable to a wide range of processing plasmas involving electronegative gases.

**OWP4 30 Oxygen radical increase with the addition of helium in a discharge excited by a ring-shaped cathode** SHANE LLOYD, D. VONA, D. M. SHAW, Z. YU, G. J. COLLINS, *Dept. of Electrical Eng., Colo. St. Univ., Ft. Collins, CO 80523* The oxygen radical flux from a 10-inch disc-shaped oxygen plasma is measured using a silver coated quartz-crystal microbalance (QCM) and actinometry. The plasma source may be excited using either dc or rf (13.56 MHz) at powers up to 150 W, and is operated primarily at 300 mTorr total pressure. With dc excitation, the QCM shows a linear increase in oxygen radical flux at a fixed power when up to 70 percent helium is added to the oxygen feedstock gas. The measurements taken by the QCM agree with actinometry measurements using up to 50 percent helium. Above 50 percent helium, the QCM and actinometry results diverge. When the divergence occurs, the QCM and actinometry measurements are compared to provide details on the production mechanisms of the oxygen radicals. The oxygen radical flux using rf excitation is also examined. While actinometry shows a slight increase in oxygen radical concentration with the addition of helium to the oxygen feedstock gas when using rf excitation, the QCM shows no increase in oxygen radical flux. As in the dc case, the differences in the QCM and actinometry techniques are compared to investigate the oxygen radical production mechanisms when using rf excitation.

#### OWP4 31 Radical Column Density Measurements During the Flame Deposition of Diamond

\* S. J. FIRCHOW, K. L. MENNINGEN, *University of Wisconsin - Whitewater* Highly sensitive absorption spectroscopy is used to measure column densities of various flame radicals during the growth of diamond by means of an atmospheric pressure oxyacetylene torch. Column densities of  $C_2$ , CH, CN, and OH are measured under optimum diamond growth conditions. The relative densities of singlet and triplet  $C_2$  are determined, and upper limits of the  $CH_3$  and  $C_3$  column densities are presented. Finally, the measured column densities are correlated to growth quality and are compared with other theoretical and experimental values. This work demonstrates the applicability of absorption spectroscopy using multielement detector arrays under conditions where there exists significant atomic or molecular emission from the flame or plasma sample.

\*Work supported by the Research Corporation and by the Petroleum Research Fund.

#### OWP4 32 Electron Beam Ablation of Metal and Fused Silica

\* R.M. GILGENBACH, S.D. KOVALESKI, *Intense Energy Beam Interaction Laboratory, Nuclear Engineering and Radiological Sciences Department, University of Michigan, Ann Arbor, MI 48109-2104* We present results of experiments in which a 15-20 kV, 1.5 kA, 200 ns channel spark electron beam is utilized for ablation of Fe and fused silica. Optical emission spectroscopy diagnosis is performed by means of a 0.3 m imaging spectrograph and gated, intensified, CCD detector. Ablation plume optical emission consists mainly of singly ionized and doubly ionized target ion lines. Argon fill gas ion-focuses the e-beam; emission spectra show argon ionization states up to triply-ionized. The temporal evolution of plume ion emission spectra are presented. Comparisons are made to excimer laser ablation plumes of Fe. Effects of space charge buildup and arcing on fused silica are being studied.

\*Research supported by National Science Foundation Grant CTS-9522282



**OWP4 33 Limits in Detection of UV Induced Damage Using SPV Surface Charge Measurements** KENTON STILES, PATRICK GONZALEZ, GEORGE COLLINS, *Colorado State University, Ft. Collins, CO 80521* The limits of using Surface Photovoltage (SPV) under high excitation levels as a method of detecting high energy radiation to the gate oxide is presented. We show SPV as a fast, non-destructive way of assessing UV assisted damage as well as post anneal efficiency for healing the weakened oxide. Short loop monitors as well as product wafers are shown to be very sensitive indicators of varying plasma conditions.

**OWP4 34 Parametric X-ray Radiation** ALEXANDER SHCHAGIN, *Kharkov Institute of Physics and Technology, Kharkov 310108, Ukraine* The main PXR properties [1,2] are considered in the paper: energy, width, smooth tuning of monochromatic PXR spectral line; fine structure and absolute differential yields of PXR in the vicinity of and at angular distances from Bragg directions; angular spread of the PXR beam; the influence of incident electron energy and of the density effect on the PXR properties; linear polarization of PXR; background in PXR spectra. Experimental setups for linacs and the results of measurements are discussed. Experimental data are compared to theoretical calculations at PXR energies between 5 and 400 keV for incident electron energies ranging from 15 to 1200 MeV. Possible applications of PXR as a new source of a bright, tunable X-ray beam in science and industry are discussed.[1] A.V. Shchagin and N.A. Khizhnyak, NIM B119, 115-122 (1996). [2] A.V. Shchagin and X.K. Maruyama, "Para-

metric X-rays," a chapter in the book "Accelerator-based Atomic Physics Techniques and Applications," edited by S.M. Shafroth and J.C. Austin, AIP Press, 1997, pp 279-307.

**OWP4 35 Experimental Measurement of the Band Structure of Solids by Electron Momentum Spectroscopy** VLADIMIR SASHIN, *Flinders University of South Australia* SHANE CANNEY, ZIWEI FANG, MICHAEL FORD, *Flinders University of South Australia* Electron momentum spectroscopy, or (e,2e), has been used to great success for determining directly the electronic wavefunction of atoms and molecules<sup>1</sup>. At Flinders University we have applied the technique to thin solid samples<sup>2</sup>. For high impact energy and momentum transfer the (e,2e) cross-section is proportional to the square of the momentum-space wavefunction of the target electrons, and the energy-momentum dispersion of the solid target can be determined directly. The geometry of our spectrometer means the measurements are relatively surface sensitive and the apparatus is ideally suited to investigating interfaces, for example Cu deposited onto Si. In this poster we present the results of recent work to illustrate the detailed information that is available using EMS.

<sup>1</sup>M.A. Coplan, J.H. Moore, and J.P. Doering, Rev. Mod. Phys. 66 985 (1994)

<sup>2</sup>P. Storer, R.S. Caprari, S.A.C. Clark, M. Vos, and E. Weigold Rev. Sci. Instrum. 65, 2214 (1994)



**SESSION PR1: ELECTRON-ATOM COLLISIONS**

Thursday morning, 9 October 1997; Class of '24 Reception Room, Memorial Union at 8:00; Yong Ki Kim, National Institute for Standards and Technology, presiding

*Invited Paper*

8:00

**PR1 1 New Results in Electron-Atom Ionization.\***DON MADISON, *University of Missouri-Rolla*

A deeper insight into atomic ionization by electron impact is gained by studying electron-electron correlation in a model-independent approach for calculating  $(e,2e)$  triply-differential cross sections using correlated (three-body) wave functions of arbitrary complexity. Results will be presented from the continuum distorted wave (CDW) model, three Coulomb-wave (3C) model, three-body distorted-wave Born approximation (3DWBA), Alt and Mukhamedzhanov (AM) model, dynamic-screening three Coulomb-wave (DS3C) model, and the eikonal approximation (EA). The successes and failures of the above models can be used to gain a better understanding of ionization processes.

\*Work supported by the NSF.

*Contributed Paper*

8:30

**PR1 2 Electron Impact Mass Spectrometric Study of Li vapor**

S.K. SRIVASTAVA, IONE IGA, *Jet Propulsion Laboratory, California Institute of Technology, Pasadena, CA 91109, USA* In our work Li vapor was generated by heating Li in a crucible with small orifice. The Li vapor was found to consist of clusters of Li

ranging from monomer to  $(Li)_8$ . The vapor was studied by electron impact ionization. Mass spectra revealed that the ratios of various clusters were highly dependent on the temperature of the crucible. The ionization efficiency curves for  $Li^+$ ,  $Li_2^+$ ,  $Li_4^+$  and  $Li_6^+$  were obtained for electron impact energy range of 0 to 70 eV. From these curves ionization cross sections were determined. The measurements and data analysis are in progress at the present time. Final results will be presented at the time of the conference.

*Invited Paper*

8:45

**PR1 3 Differential Electron Scattering from Metastable Helium.**STEPHEN J. BUCKMAN, *Atomic and Molecular Physics Laboratories, Australian National University*

There has been an increasing amount of experimental activity regarding the measurement of cross sections for scattering from metastable excited states, given that the long lifetimes and large amounts of internal energy involved can result in their interactions having a significant effect on the behaviour of a discharge or plasma environment. To date the overwhelming majority of measurements have been of integral cross sections. At the ANU we have implemented a program to study differential (in angle) electron scattering cross sections from metastable helium. These studies (to date superelastic and inelastic scattering) have suffered from the same problems that appear to plague most measurements in this field - low target number density and bad signal to noise ratios. To counteract these problems we have constructed a slow, "bright" beam of metastable He ( $2^3S$ ) using laser cooling techniques. The bright beam will provide an increase in number density of several orders of magnitude over present state-of-the-art sources. This talk will summarise our differential scattering results to date, using conventional atomic beam sources, give a brief update of the bright beam source and indicate future directions that the use of this source will offer.

*Contributed Papers*

9:15

**PR1 4 Measurement of electron impact excitation cross sections out of the metastable levels of argon**

JOHN B. BOFFARD, *University of Wisconsin-Madison* \* Few experimental results for excitation of metastable atoms are available due to the difficulty in producing targets of sufficient density. We have measured cross sections for electron-impact excitation out of the  $3p^5 4s$   $J=0$  and  $J=2$  metastable levels of argon ( $1s_3$  and  $1s_5$  in Pachén's notation) into levels of the  $3p^5 4p$  manifold using the optical method. Both a hollow cathode discharge and a fast atom-beam formed via charge exchange were used as sources of metastable atoms. A limit on the cascade contribution to the apparent

cross section was found by using a type of time-resolved excitation on the fast beam experiment. The peak values of the cross sections are two to three orders of magnitude larger than the cross sections for excitation out of the ground state. The largest cross section measured is for excitation into the  $3p^5 4p$   $J=3$  level ( $2p_9$ ).<sup>1</sup> In general, the cross sections have a broad shape as a function of electron energy, characteristic of excitation into the first dipole-allowed level. The exceptions being the two  $J=0$  levels ( $2p_1$  and  $2p_5$ ) which have sharply peaked excitation functions.

\*Supported by the National Science Foundation.

<sup>1</sup>J B Boffard, G A Piech, M F Gehrke, M E Lagus, L W Anderson, and C C Lin, *J Phys. B* **29**, L795 (1996).

9:30

**PR1 5 Electron-Impact Excitation Cross Sections of Argon and Xenon: A Detailed Investigation of the Pressure Dependence**<sup>1</sup>

JOHN T. FONS, J. ETHAN CHILTON, PAUL RUGHEIMER, CHUN C. LIN, *University of Wisconsin-Madison* We have investigated the optical emission cross sections for electron-impact excitation of the  $2p$  levels (Paschen's notation) of argon and xenon. These levels are populated through two different processes: the direct excitation out of the ground state into the  $2p$  manifold and the cascade from higher lying  $nd$  and  $ns$  levels that radiate into the  $2p$  levels. Previous investigations of Ar and Xe have shown that some of the measured  $2p \rightarrow 1s$  emission cross sections appear to show significant dependence on pressure. We have confirmed this pressure dependence, and through the use of a Fourier Transform Infrared Spectrometer have found that many of the  $3d \rightarrow 2p$  and  $2s \rightarrow 2p$  infrared transitions have a similar dependence on pressure, attributed to reabsorption of resonant radiation. By subtracting the cascade cross sections from the apparent cross sections at various energies (10 - 300 eV) and pressures (0.05 - 4 mTorr) to obtain the direct excitation cross sections, we show that the pressure dependence is due mainly to the contribution from cascade.

<sup>1</sup>Supported by the Air Force Office of Scientific Research and by the U.S. Dept. of Commerce, NIST.

9:45

**PR1 6 Long-Time Stability of Superexcited High Rydberg Molecular States** YIFEI ZHU, LAL PINNADUWAGE, *Oak Ridge National Laboratory and University of Tennessee, Knoxville*

Using a time-resolved, mass analyzed, pulsed field ionization technique we have observed that molecules laser-excited to energies within several electron volts above their ionization thresholds can survive for microseconds. These observations are consistent with our recent observations (see <sup>1</sup> footnote P. G. Datskos, L.A. Pinnaduwege, and J.F. Kielkopf, *Phys. Rev. A* 55(1997)4131., and references therein) of efficient dissociative electron attachment to molecules excited to energies above their ionization thresholds.

\*Research supported by the EMSP Program of the U.S. DOE and the National Science Foundation. The Oak Ridge National Laboratory is managed by Lockheed Martin Energy Research Corp. for the U. S. DOE under contract No. DE-AC05-96OR22464.

<sup>1</sup>L.A. Pinnaduwege and P.G. Datskos, *J. Appl. Phys.* (June 15, 1997 issue)

**SESSION PR2: MAGNETIZED PLASMAS**

Thursday morning, 9 October 1997

Tripp Commons, Memorial Union at 8:00

Chip Eddy, Naval Research Laboratory, presiding

8:00

**PR2 1 Modeling the Transitions from Capacitive to Inductive to Helicon RF Discharges** M. A. LIEBERMAN, *University of California, Berkeley*

R.W. BOSWELL, *The Australian National University, Canberra* Radio frequency (rf) plasma sources used in the processing of thin films can be divided into three categories: capacitive (E), inductive (H), and wave (W) -sustained (e.g., helicon) discharges. As the excitation power or voltage is increased, transitions from capacitive to inductive to helicon discharges are often observed, in some cases exhibiting hysteresis. A model is developed to determine these transitions based on the electron energy balance in the discharge and the coupling between capaci-

tive, inductive, and helicon electron energy deposition. The excitation is represented as an axisymmetric ( $m=0$  mode) sheet antenna coupling both inductively (electric field  $E_{\theta}$ ) and capacitively ( $E_r$  and  $E_z$ ) to a uniform, magnetized, collisional plasma-filled waveguide across a dielectric gap. The elements of a circuit theory representation are determined from the waveguide model. For an inductive discharge, a finite capacitive sheath thickness reduces the inductive power deposition and can lead to hysteresis in the density versus voltage discharge characteristics. For a helicon discharge (non-zero axial magnetic field), resonances can exist when the plasma length is an integral number of helicon half-wavelengths, leading to strong hysteresis in the discharge characteristics.

8:15

**PR2 2 Ion Fluxes and Velocity Distributions in an ECR Discharge Plasma**<sup>\*</sup> GLENN JOYCE, MARTIN LAMPE, W. M. MANHEIMER, STEVEN P. SLINKER, *Naval Research Laboratory*

Experiments in ECR plasmas have typically observed a rather large thermal spread of ion velocities, in the direction perpendicular to the ion flow, as well as in the direction parallel to the flow. The perpendicular ion temperature, which has significant implications in regard to etch anisotropy, cannot be explained by any of the ion-neutral scattering processes that are typically included in numerical models. We report on simulations of an ECR discharge in argon at 1 mT, in an insulating vessel, based on the NRL axisymmetric particle simulation code QUASI-rz. The code represents all charged species as particles in a formulation which determines the electrostatic field from the requirement of quasineutrality and avoids small time and space scales. The code includes collisions of charged particles with neutral species and with each other. We determine the ion flux pattern and velocity distribution throughout the system. We find that the ion flux forms large scale eddies, which are nearly field aligned downstream, but involve cross-field return flows upstream. The ion parallel temperature is due primarily to charge exchange collisions, while the ion transverse temperature is due primarily to ion-ion collisions.

<sup>\*</sup>Supported by the Office of Naval Research

8:30

**PR2 3 Absolute density measurement of FCN in CHF<sub>3</sub> ECR plasma etching of Si<sub>3</sub>N<sub>4</sub>**<sup>\*</sup> KOJI MIYATA, HIROYOSHI ARAI, MASAFUMI ITO, MASARU HORI, TOSHIO GOTO, *Department of Quantum Engineering, Nagoya University, Japan*

Si<sub>3</sub>N<sub>4</sub> has been widely used as masks in the local oxidation and etch-stop layers in self-aligned contact fabrication. As the devices are developed, the Si<sub>3</sub>N<sub>4</sub> etching requires higher controllability to achieve ideal etch characteristics. However, it is difficult to develop the Si<sub>3</sub>N<sub>4</sub> etching without knowledge of etching mechanisms. To study the etching mechanism, it is very helpful to know absolute densities of etch products. In this study, the absolute density of cyanogen fluoride (FCN), which is one of etch products of the Si<sub>3</sub>N<sub>4</sub>, was measured for the first time in a CHF<sub>3</sub> ECR plasma using infrared diode laser absorption spectroscopy (IRLAS). The typical FCN density during Si<sub>3</sub>N<sub>4</sub> etching was derived to be  $4 \times 10^{11} \text{ cm}^{-3}$  in the CHF<sub>3</sub> plasma at an etch rate of 48 Å/s. Substrates of 25 cm<sup>2</sup> were used in this experiment. The FCN density during Si<sub>3</sub>N<sub>4</sub> etching is so large that the FCN is considered to be a major etch product of the Si<sub>3</sub>N<sub>4</sub>. Moreover, disappearance processes of the FCN will be discussed on the basis of FCN decay rates after discharge termination in CHF<sub>3</sub>/N<sub>2</sub> mixtures.

<sup>\*</sup>This presentation is partly supported by Nishiaki Scholarship Foundation.

8:45

**PR2 4 Langmuir probe measurements in the Hollow Cathode Magnetron** MIRKO VUKOVIC, KWOK-FAI LAI, *Novellus*  
The Hollow Cathode Magnetron (HCM) is a new kind of a high density plasma device which has been proposed as an ionized physical vapor deposition source for semiconductor device fabrication<sup>1</sup>. The target is of high purity metal machined to resemble a hollow cathode (id. 4cm, depth 6cm). It resides in a cooled metal housing. The magnetic field (several hundred Gauss) is generated by permanent magnets stacked on the outside of the metal housing, aligned parallel to the HCM axis. At the mouth of the HCM, a magnetic cusp traps a high density plasma. Beyond the cusp, a slowly diverging magnetic field produces a low temperature ( $T_e \sim 2-3\text{eV}$ ), high density ( $n_e \sim 10^{12}-10^{13}\text{cm}^{-3} \propto P_{DC}$ ) plume. The HCM serves to both sputter and ionize metal atoms from the target. These ions may deposit onto a silicon device wafer, enabling metal deposition into the bottom of very small ( $<0.5\mu\text{m}$ ) high aspect ratio ( $\geq 6:1$ ) features. The unique properties of the films deposited using the HCM will be presented and related to the plasma parameters obtained from Langmuir probe data and magnetic field modeling.

<sup>1</sup>John C. Helmer, Kwok F. Lai, Robert L. Anderson US Patent 5,482,661, Jan. 9, 1996

9:00

**PR2 5 Development of a surface-wave magnetoplasma sputtering source for the elemental analysis of solid samples** LOUIS-PHILIPPE MASSE, JOELLE MARGOT, *Dept de Physique, Universite de Montreal, Montreal, Quebec, Canada* JOSEPH HUBERT, *Dept de Chimie, Universite de Montreal, Montreal, Quebec, Canada* Over the last few years, the use of DC or RF discharges operating below 10 mtorr for the elemental analysis of solid materials has regained popularity. Nonetheless, operation at further reduced pressure is preferable since it provides a cleaner environment, results in larger sputtering yields and finally is much easier to interface with a mass spectrometer. This has led us to design a plasma source which can be efficiently operated down to the sub- mtorr domain. This source is based on the propagation of surface- waves in the presence of a magnetic field. It is operated in argon at microwave frequency (2.45 GHz) with a magnetic field intensity close to ECR conditions. The samples are biased either in DC or RF mode thus allowing the analysis of conducting and isolating materials. In this presentation, we use emission spectroscopy to characterize the sputtering of Cu. Our measurements show that the Cu emission peaks at about 1 mtorr. In addition, there is some experimental evidence that the presence of metallic vapors may decrease electron temperature and plasma density in the vicinity of the samples. From theoretical considerations, we provide some semi- quantitative explanation for these observations.

9:15

**PR2 6 Study of Ar and Cu Plasma in a Magnetic Field Enhanced rf Argon Plasma for Ionized Sputtering of Cu** W WANG, *UW-Madison* J FOSTER, A WENDT, J.H BOOSKE, S.S GEARHART, N HERSHKOWITZ, *UW-Madison* One of the challenges for the manufacturing of ULSI integrated circuits is to deposit metal and alloy films into trenches with a high aspect ratio for vertical contact and interconnect purposes. As the device sizes are reduced to sub-0.25 micron regime, conventional sputtering deposition becomes insufficient. Recently, ionized sputtering has been studied to solve the aforementioned issues. In ionized sput-

tering, a high density RF argon plasma (density  $10^{11}$  to  $10^{12}$  ions per  $\text{cm}^3$ ) is generated between the sputtering source and the substrate. The sputtered metal atoms become ionized when they travel through the high density RF plasma region. When a negative bias is applied to the stage, the positive metal ions will be attracted toward the wafer stage and become deposited on the substrate with good directionality. In this way, trenches with a high aspect ratio can be uniformly filled with metals. In this presentation, we will describe a prototype ionized sputtering system that utilizes a multipole magnetic field to enhance an inductively coupled rf argon plasma for ionization of Cu vapor. We will also report the Ar and Cu plasma properties as a function of Cu sputtering power by using Langmuir probe measurements in different argon pressures, as well as ionization trends for the sputtered Cu vapor in the argon plasma from optical emission spectroscopy.

9:30

**PR2 7 Dynamics of Three-Dimensional DC Magnetron Discharge Plasma** K. NANBU, S. KONDO, *Tohoku University* Magnets like a racetrack are often used in sputter deposition of large wafers and liquid crystal displays. In self-consistent discharge simulation the equations of motion for the particles and Poisson's equation for the field should be solved simultaneously. For such magnets not only the magnetic field but also the electric field is fully three-dimensional. Also, since the pressure in a discharge space is of the order of mTorr, the fluid (continuum) model is not applicable as it stands; the particle simulation is most reliable although it is computationally intensive. Except for our previous report [Jpn. J. Appl. Phys. (in press)] no work has been published on the three-dimensional particle simulation of the magnetron discharge. In that work we found a strange irregularity in a spatial distribution of plasma density for certain discharge conditions. The objective of the present work is to clarify physical characteristics of that phenomenon. The dynamic structure of three-dimensional dc magnetron discharge has been found by the use of the Particle-in-Cell/Monte Carlo method. The plasma is essentially dynamic; its density chaotically changes with time even for a steady boundary condition.

9:45

**PR2 8 Spatially Resolved DC Bias Over A High-Powered M.E.R.I.E. Cathode** R.A. LINDLEY, *Applied Materials, Inc.* K.-H. KE, *Applied Materials, Inc.* K. DOAN, *Applied Materials, Inc.* H.C. SHAN, *Applied Materials, Inc.* Non-uniform plasmas produce non-uniform potentials across a wafer, thus stressing the gate-oxide layers in device structures. A tool has been developed to measure the DC bias uniformity across the wafer pedestal in a high-power, dielectric M.E.R.I.E. chamber in order to provide a zeroth- order estimation of the chamber's damage performance. Using blanket oxide wafers, it was determined that a gradient magnetic field (B) improved the plasma uniformity several fold over the use of the standard saddle shaped B by reducing the B strength on the electron surplus side of the wafer. Using the new tool, the range of DC bias across the wafer was measured in a full factor DOE (L108) as a function of pressure (50mT- 250mT), B strength (10G-90G), and B shape (saddle to steep gradient). The computer acquired data was analyzed to separate the ave. DC bias-, hardware-, time- and B-components. It was found that the optimum B shape for uniform plasma was strongly dependent on the pressure and the B strength. In addition, slightly different B gradients produce nearly the same DC bias range, therefore defining a process window that narrows with increasing B strength.



**SESSION QRI: ELECTRON-MOLECULE COLLISIONS**

Thursday morning, 9 October 1997; Class of '24 Reception Room, Memorial Union at 10:15; Russ Bonham, Illinois Institute of Technology, presiding

*Invited Papers***10:15****QR1 1 Dissociation of Highly Excited Molecules.**YOSHIHIKO HATANO, *Tokyo Institute of Technology, Japan*

A survey of the spectroscopy and dynamics of the dissociation of highly excited molecules is presented with emphasis on superexcited molecules by electron- and photon-impact.<sup>1</sup> Topics will include newly developed experimental methods covering two-dimensional spectroscopy of photodissociation<sup>2,3,4</sup>, and coincident electron-energy-loss spectroscopy of the dissociation dynamics of highly excited molecules.<sup>5,6</sup> The measurement of absolute photoionization quantum yields will also be discussed.<sup>7</sup> Comparative studies of electron- and photon-impact dissociative excitation of molecules will be summarized. The molecules studied are H<sub>2</sub>, N<sub>2</sub>, O<sub>2</sub>, CO, CO<sub>2</sub>, N<sub>2</sub>O, hydrocarbons, and some Si-containing compounds.

<sup>1</sup>See review articles: a) Y. Hatano, *The Physics of Electronic and Atomic Collisions*, eds., L. J. Dube *et al.*, AIP Press, New York (1995) pp.67-88; b) N.Kouchi *et al.*, *J. Phys. B*, 30, 2319 (1997); c) Y. Hatano, *Dynamics of Excited Molecules*, ed., K. Kuchitsu, Elsevier, Amsterdam (1994) Chapter 6.

<sup>2</sup>M. Ukai *et al.*, *Phys. Rev. Lett.*, 74, 239 (1995).

<sup>3</sup>S. Machida *et al.*, *J. Phys. Chem. A*, 101, 656 (1997).

<sup>4</sup>A. Ehresmann *et al.*, *J. Phys. B*, 29, 3629 (1996).

<sup>5</sup>T. Odagiri *et al.*, *J. Phys. B*, 28, L465 (1995).

<sup>6</sup>T. Odagiri *et al.*, *J. Phys. B*,

<sup>7</sup>K. Kameta *et al.*, *J. Chem. Phys.*, 99, 2487 (1993).

**10:45****QR1 2 Computational Study of Electron-Molecule Collisions Related to Low-Temperature Plasmas.**WINIFRED M. HUO, *NASA Ames Research Center*

Computational study of electron-molecule collisions not only complements experimental measurements, but can also be used to investigate processes not readily accessible experimentally. A number of *ab initio* computational methods are available for this type of calculations. Here we describe a recently developed technique, the finite element Z-matrix method. Analogous to the R-matrix method, it partitions the space into regions and employs real matrix elements. However, unlike the implementation of the R-matrix method commonly used in atomic and molecular physics,<sup>1</sup> the Z-matrix method is fully variational.<sup>2</sup> In the present implementation, a mixed basis of finite elements and Gaussians is used to represent the continuum electron, thus offering full flexibility without imposing fixed boundary conditions. Numerical examples include the electron-impact dissociation of N<sub>2</sub> via the metastable  $A^3\Sigma_u^+$  state, a process which may be important in the lower thermosphere, and the dissociation of the CF radical, a process of interest to plasma etching. To understand the dissociation pathways, large scale quantum chemical calculations have been carried out for all target states which dissociate to the lowest five limits in the case of N<sub>2</sub>, and to the lowest two limits in the case of CF. For N<sub>2</sub>, the structural calculations clearly show the preference for predissociation if the initial state is the ground  $X^1\Sigma_g^+$  state, but direct dissociation appears to be preferable if the initial state is the  $A^3\Sigma_u^+$  state. Multi-configuration SCF target functions are used in the collisional calculation.

<sup>1</sup>C. J. Gillan, J. Tennyson, and P. G. Burke, Chapter 10 in *Computational Methods for Electron-Molecule Collisions*, W. M. Huo and F. A. Gianturco, Editors, Plenum, New York (1995), p. 239.

<sup>2</sup>D. Brown and J. C. Light, *J. Chem. Phys.* **101**, 3723 (1994).

**11:15****QR1 3 Progress in Computational Electron-Molecule Collisions.\***TN RESCIGNO, *LLNL*

The past few years have witnessed tremendous progress in the development of sophisticated *ab initio* methods for treating collisions of slow electrons with isolated small molecules. Researchers in this area have benefited greatly from advances in computer technology; indeed, the advent of parallel computers has made it possible to carry out calculations at a level of sophistication inconceivable a decade ago. But bigger and faster computers are only part of the picture. Even with today's computers, the practical need to study electron collisions with the kinds of complex molecules and fragments encountered in real-world plasma processing environments is taxing present methods beyond their current capabilities. Since extrapolation of existing methods to handle increasingly larger targets will ultimately fail as it would require computational resources beyond any imagined, continued progress must also be linked to new theoretical developments. Some of the techniques recently introduced to address these problems will be discussed and illustrated with examples of electron-molecule collision calculations we have carried out on some fairly complex target gases encountered in pro-

cessing plasmas. Electron-molecule scattering continues to pose many formidable theoretical and computational challenges. I will touch on some of the outstanding open questions.

\*This work was performed under the auspices of the U.S. Department of Energy by the Lawrence Livermore National Laboratory under contract W-7405-Eng-48. The use of computational resources of the National Energy Research Scientific Computing Center is also acknowledged.

### Contributed Papers

11:45

**QR1 4 Semiempirical Theory of Dissociative Electron Attachment to  $\text{CH}_3\text{Cl}$  and  $\text{CF}_3\text{Cl}$  Molecules** \* R.S. WILDE, I.I. FABRIKANT, *Univ. of Nebraska* We use the resonant  $R$ -matrix theory<sup>1</sup> for calculation of the dissociative electron attachment to the  $\text{CH}_3\text{Cl}$  and  $\text{CF}_3\text{Cl}$  molecules. The  $R$ -matrix parameters are fitted to reproduce experimental data on vibrational excitation. The dissociative attachment cross sections for both molecules demonstrate similar behavior with respect to the electron energy and the gas temperature. At room temperature they exhibit a peak whose position is lower than the vertical attachment energy. An additional zero-energy peak due to contribution of excited vibrational states appears at higher temperatures. However, due to a higher vertical attachment energy, the dissociative attachment cross section for  $\text{CH}_3\text{Cl}$  at room temperature is substantially lower (by at least five orders of magnitude) than that for  $\text{CF}_3\text{Cl}$ . We compare our results with available experimental data and the classical theory<sup>2</sup> for  $\text{CF}_3\text{Cl}$ .

\*Supported by the National Science Foundation

<sup>1</sup>I.I. Fabrikant, *Phys. Rev. A* **43**, 3478 (1991).

<sup>2</sup>L. Lehr and W.H. Miller, *Chem. Phys. Lett.* **250**, 515 (1996).

12:00

**QR1 5 Electron Attachment to Radicals and Highly-Excited States in Laser-Irradiated  $\text{CCl}_2\text{F}_2^*$**  LAL PINNADUWAGE, PANOS DATSKOS, *University of Tennessee, Knoxville, and Oak Ridge National Laboratory* We have measured electron attachment rate constants for two species produced via ArF-excimer-laser irradiated  $\text{CF}_2\text{Cl}_2$ , i.e., the  $\text{CF}_2\text{Cl}$  radical and the highly-excited electronically-excited states of  $\text{CF}_2\text{Cl}_2$ . These measurements show that while electron attachment to the fragment radical has a rate constants about an order of magnitude higher compared to the ground states of  $\text{CF}_2\text{Cl}_2$ , electron attachment to the highly-excited states have many orders of magnitude larger rate constants. To our knowledge, only one other electron attachment measurement has been conducted on molecular fragments up to now. Implications of these measurements for plasma processing discharges will be discussed. \*Research supported by the National Science Foundation under contract No. ECS-9626217 with the University of Tennessee, Knoxville. The Oak Ridge National Laboratory is managed by Lockheed Martin Energy Research Corp. for the U. S. DOE under contract No. DE-AC05-96OR22464.

12:15

**QR1 6 Electron Attachment to Laser-Excited  $\text{Cl}_2$  molecules**\* PANOS DATSKOS, *Oak Ridge National Laboratory and University of Tennessee, Knoxville* LAL PINNADUWAGE, *Oak Ridge National Laboratory and University of Tennessee, Knoxville* We studied the electron attachment to ArF (=193 nm) excimer-laser irradiated chlorine molecules. We present evidence that laser-excited electronic states of  $\text{Cl}_2$  molecules attach electrons more efficiently compared to  $\text{Cl}_2$  molecules in their ground state. At low laser intensities only electron attachment to ground electronic state  $\text{Cl}_2$  molecules is observed. However, at higher laser intensities electron attachment to laser-excited  $\text{Cl}_2$  molecules dominates. We

estimate that the electron attachment rate constant to laser-excited  $\text{Cl}_2$  molecules is more than three orders of magnitude higher than the ground state electron attachment rate constant. The possible significance of this process for plasma processing discharges using  $\text{Cl}_2$  mixtures is indicated. \*Research supported by the the NSF under contract No. ECS-9626217 with the University of Tennessee. The Oak Ridge National Laboratory is managed by Lockheed Martin Energy Research Corp. for the U. S. DOE under contract number DE-AC05-96OR22464

---

### SESSION QR2: HELICON AND SURFACE WAVE PLASMAS

Thursday morning, 9 October 1997

Tripp Commons, Memorial Union at 10:15

Nobuhiko Nakano, Keio University, presiding

### Contributed Papers

10:15

**QR2 1 Helicons, the Early Years** R.W. BOSWELL, *RSPHysSE, The Australian National University, Canberra, ACT 0200, Australia* F.F. CHEN, *University of California, Los Angeles, California 90095-1594, USA* Helicon waves are right hand polarised (RHP) waves which propagate in radially confined magnetised plasmas for frequencies  $\omega_{ci} \ll \omega \ll \omega_{ce}$  where  $\omega_{ci}$  is the ion cyclotron frequency and  $\omega_{ce}$  is the electron cyclotron frequency. They are part of a much larger family of waves which can propagate down to zero frequency and constitute a very rich field for studying complex propagation characteristics and wave-particle interactions. This talk gives a historical perspective of the waves and their relationship to plasma source development up to the mid 1980's, presents a simple description of their propagation characteristics in free and bounded plasmas, and finishes with their first reported use in plasma processing experiments.

10:30

**QR2 2 Helicons, the Past Decade** F.F. CHEN, *Electrical Engineering Department, University of California, Los Angeles, California* R.W. BOSWELL, *RSPHysSE, The Australian National University, Canberra, ACT 0200, Australia* First observed in gaseous plasmas in the early 1960s, helicon discharges lay like a sleeping giant until they emerged in the 1980s, when their usefulness as efficient plasma sources for processing microelectronic circuits for the burgeoning semiconductor industry became recognised. Research on helicons spread to many countries; new, challenging, unexpected problems arose; and these have spawned solutions and novel insights into the physical mechanisms in magnetised radiofrequency discharges. Among the most baffling puzzles were the reason for the high ionization efficiency of helicon discharges and the dominance of the right-hand polarized mode over the left-hand one. The most recent results indicate that a non-obvious resolution of these problems is at hand.

10:45

**QR2 3 Very High Density Helicon Mode Operation in WOMBAT** A.W. DEGELING, *RSPHysSE, The Australian National University, Canberra, ACT 0200, Australia* A Helicon Wave mode which exhibits a peak downstream density of greater than  $10^{12}$  cm<sup>-3</sup> in argon (called the "blue mode" because of bright ArII emission along the axis) has been observed. The experimental conditions are: argon gas pressure of 3 mtorr, dc magnetic field of 100G and rf power input of 2 to 3 kW at 13.56MHz into a source region of 18 cm radius and 50 cm length using a double half - turn antenna. The nominal plasma density is about  $10^{11}$  cm<sup>-3</sup> when tuned for the normal Helicon wave mode under these conditions, and the blue mode appears sporadically for intervals of about 2 ms every few seconds. By pulsing the rf power for a duration of a few milliseconds it was found that a correct tuning for the blue mode could be found, however the duration of the mode never exceeded a few milliseconds until the power level was increased above 4kW (where the blue mode operated continuously). B-dot probe measurements indicate that the wave phase velocity before the blue mode is  $6 \times 10^6$  m/s while the blue mode operates is about  $3 \times 10^6$  m/s, which has been shown previously to be the optimum velocity for resonant wave heating of plasma electrons to increase the ionisation rate. Investigations of the plasma wavefield and the unstable nature of the mode are presented.

11:00

**QR2 4 Characteristics of M=0 Helicon Wave Plasmas in Reactive Gas Environment** S. MIYAKE, Y. SETSUHARA, Y. SAKAWA, T. SHOJI, *JWRI, Osaka University, Osaka Japan* \**Nagoya University, Nagoya Japan* Plasma production in various reactive gases are more important in the actual plasma processing of materials than those in rare gas environment. Characteristics of high density plasmas produced by the m=0 azimuthal mode helicon wave in reactive gases in a nonuniform magnetic field is studied experimentally. Loop antennas of several turns are wound on a quartz tube of 38mm diameter to excite the m=0 helicon wave with a 3kW rf oscillator of 13.56MHz. Plasma production is

performed in various dissociative gases (H<sub>2</sub>, N<sub>2</sub>, O<sub>2</sub> and/or CF<sub>4</sub>) in the pressure range around 0.1Pa and the rf wave fields are measured to know the excitation of the helicon wave in these gases. The plasma density jump from the range of  $10^{11}$  cm<sup>-3</sup> to  $10^{12-13}$  cm<sup>-3</sup> is observed for each gas at a critical rf power, after which the excitation of helicon wave is verified to propagate. The optical emission measurements indicate an efficient dissociation of molecules after the density jump. As an example of application of this type of discharge, the DC discharge characteristics in N<sub>2</sub>+Ar gas on the cylindrical carbon target set for the sputtering process in the down stream region is studied in correlation with the properties of the helicon wave plasmas.

11:15

**QR2 5 Maximum density plasma production with helicon wave excitation** D.G. MILJAK, \* F.F. CHEN, *UCLA* An attempt was made to produce a very high density plasma column suitable for use in generation of light or particle beams. It is well known that helicon discharges can create peak densities of order  $10^{14}$  cm<sup>-3</sup> with  $\leq 2$  kW of RF power, and the hope was to extend this to around  $10^{15}$  cm<sup>-3</sup>. The attempt was made in a 5-cm diam system with two helical antennas, each driven with its own 2-kW, 27.12-MHz power supply and matching circuit. The antenna helicities were such as to launch m = +1 waves toward the mid-plane. Since the density was found in previous work to peak about 50 cm downstream from an antenna, the antennas were spaced so that the peaks overlapped. This spacing changed with pressure. A cusp magnetic field was used behind each antenna to reduce energy loss in the backward direction. With this arrangement, the best result obtained was at 1200 G and 63 mTorr of argon, when a density on axis of  $8 \times 10^{13}$  cm<sup>-3</sup> was achieved, uniform to 7% over an axial length of 60 cm. We expect that this can be improved with a larger diameter gas plenum. Electron-ion collisions at these high densities are probably the limiting factor.

\*Present address: ANU, Canberra ACT 0200, Australia

#### Invited Paper

11:30

#### QR2 6 Surface waves: A tool for producing plasmas from sub-millitorr to atmosphere.

JOELLE MARGOT, *Groupe de Physique des Plasmas, Département de Physique, Université de Montréal, Montréal, Québec, Canada*

Since the first experimental evidence of plasma generation by surface waves in the early 1970's, the use of these plasma sources has rapidly grown both for the fundamental study of HF plasmas and for applications. The main interest of these discharges is their wide range of experimental conditions which allows operation from sub-mtorr to atmosphere pressure regime, opening the way to quite diversified applications. The versatility of these sources in terms of frequency range is also a major asset which allows to link the characteristics of many other plasmas. Recently the demonstration that surface wave plasmas could be operated at extremely low pressure in the presence of a magnetic field has made these sources to compete with more conventional high density plasma sources. Finally, recent work by Japanese researchers has shown that the traditional cylindrical geometry of these plasmas could be revisited to generate planar sources of interest for applications, for example, to flat pannel displays. In this presentation, we review some of the achievements of our group in terms of plasma characterization and understanding as well as some selected applications covering a wide range of pressures.

#### Contributed Papers

12:00

**QR2 7 High- and Low-Density Modes in a Large-Area Surface-Wave Sustained Plasma Source** I. GHANASHEV, M. NAGATSU, S. MORITA, H. SUGAI, *Department of Electrical Engineering, Nagoya University* Recently we reported<sup>1</sup> a new

high ( $\sim 10^{12}$  cm<sup>-3</sup>) density large-area (diameter 22 cm) plasma source without external DC magnetic field operating at 2.45 GHz. The plasma was produced in a cylindrical metal chamber below a 17 mm thick quartz plate. We identified<sup>2</sup> the electromagnetic modes (launched by slots in the chamber top wall just above the quartz plate), which sustained the plasma in Ar at relatively high pressures (about 80 Pa), as surface waves propagating azimuthally



and radially along the plasma-dielectric interface. Dry etching applications, however, require lower gas pressures and other, reactive gases with larger electron-impact cross-sections. Both decreasing the pressure down to about 10 mTorr and/or applying a non-noble reactive gas (e.g.  $\text{CF}_4$ ) resulted at the same generator power (0.5–2 kW) in a lower plasma density ( $\sim 10^{11} \text{ cm}^{-3}$ ), which is still enough for dry etching, but is close to the cut-off density  $7.4 \times 10^{10} \text{ cm}^{-3}$ . Similar densities are expected also in the about two times larger source being developed now even if the input power is increased up to 4 kW. Microwave propagation at these conditions is quite different from that in strongly overdense plasmas.<sup>1,2</sup> Therefore, in this contribution we compare theoretically and experimentally the high- and low-density regimes.

<sup>1</sup>M. Nagatsu *et al.*, *Jpn. J. Appl. Phys.* **35** (1996) L341.

<sup>2</sup>I. Ghanashev *et al.*, *Jpn. J. Appl. Phys.* **36** (1997) 337.

12:15

**QR2 8 High-Density Plasma Generation by Surface Waves Excited on Metal-Plasma Interface** HIDEO SUGAI, IVAN

GHANASHEV, MASAOKI NAGATSU, *Department of Electrical Engineering, Nagoya University* Recent studies on microwave discharges without magnetic field showed a new possibility of production of large-diameter (40 cm) high-density ( $10^{12} \text{ cm}^{-3}$ ) plasmas at low pressures (10 mTorr). In the overdense condition ( $\omega_p > \omega$ ), surface waves are excited along the interface between dielectric wall and the adjacent plasma and they play an essential role in power transfer to plasma. When the plasma diameter is as large as 1 m, however, a very thick and expensive dielectric disk is required to withstand a huge force against the atmospheric pressure. To overcome this difficulty, a full metal vessel is used and microwaves are launched through small slots on the metal wall: this type of excitation successfully gives dense plasmas as high as the conventional dielectric wall excitation. Furthermore, to optimize the antenna structure, small-amplitude test waves are launched from the slot antenna into an independently produced rf plasma and surface waves are measured together with microwave power reflection from the antenna.

## SESSION RR1: DIAGNOSTICS II

Thursday afternoon, 9 October 1997; Class of '24 Reception Room, Memorial Union at 13:30; Kristen L Steffens, NIST, presiding

### Contributed Papers

13:30

**RR1 1 Simulations of Control Schemes for Inductively Coupled Plasma Sources** P.L.G. VENTZEK, *Hokkaido University* A. ODA, *Hokkaido University* J.W. SHON, P. VITELLO, *Lawrence Livermore National Laboratory* Process control issues are becoming increasingly important in plasma etching. Numerical experiments are an excellent test-bench for evaluating a proposed control system. Models are generally reliable enough to provide information about controller robustness, fitness of diagnostics. We will present results from a two dimensional plasma transport code with a multi-species plasma chemistry obtained from a global model. [1-2] We will show a correlation of external etch parameters (e.g. input power) with internal plasma parameters (e.g. species fluxes) which in turn are correlated with etch results (etch rate, uniformity, and selectivity) either by comparison to experiment or by using a phenomenological etch model. After process characterization, a control scheme can be evaluated since the relationship between the variable to be controlled (e.g. uniformity) is related to the measurable variable (e.g. a density) and external parameter (e.g. coil current). We will present an evaluation using the HBr-Cl<sub>2</sub> system as an example. [1] E. Meeks and J. W. Shon, *IEEE Trans. on Plasma Sci.*, **23**, 539, 1995. [2] P. Vitello, *et al.*, *IEEE Trans. on Plasma Sci.*, **24**, 123, 1996.

13:45

**RR1 2 A General Circuit Model for rf Plasma Processing Equipment\*** SHAHID RAUF, MARK J. KUSHNER, *University of Illinois-Urbana/Champaign* To model plasma equipment accurately, one must concurrently simulate the plasma dynamics and external circuitry. This is, however, often difficult since the time in which the external circuit of rf discharges attains the steady-state is several orders of magnitude longer than typical plasma simulation times. To address these issues, a general circuit model has been developed and incorporated into the Hybrid Plasma Equipment Model (HPEM), a comprehensive plasma equipment simulator. The circuit model approximates the plasma chamber by a simple circuit consisting of interconnected nonlinear sheaths (using plasma properties obtained from the HPEM) which also allows external elements to be included. The circuit model produces rf voltage and current amplitudes and phases (fundamental and harmonics) and dc biases, which are then used in the HPEM. This process is iterated to convergence. Comparisons are made of predicted dc bias and harmonic amplitudes with experimental data in the Gaseous Electronics Conference Reference Cell over a wide range of gas pressure and applied voltage. Results are also presented for rf biased inductively coupled plasmas.

\*Research supported by AFOSR/ARPA (F49620-95-1-0524), NIST, SRC and NSF (ECS94-04133).

### Invited Paper

14:00

**RR1 3 Time Resolved Studies of Radio Frequency Driven Plasmas.**

BILL GRAHAM, *Physics Department, The Queen's University of Belfast, Northern Ireland\**

The physics of technological plasmas is of both great intrinsic and industrial interest. The challenge of trying to understand the complex interplay of electrodynamic, atomic, molecular, surface and chemical processes, inherent in the

study of such plasmas, is matched by their exciting applications. The ability to obtain a fuller understanding of such complex systems has been facilitated by recent developments in computing power and techniques, advances in data acquisition and processing rates and developments in diagnostics. Here the use of a number of different experimental techniques to characterise rf driven plasmas will be discussed. The primary focus will be on the simultaneous application of fast gated ICCD's and accurate electrode and plasma potential measurements. ICCDs with time resolution of about 2ns can now allow rapid spatial and temporal resolution of the light emission at different phases of the 13.56 MHz rf driving frequency. An insight into sheath dynamics can be obtained by synchronising these measurements with the driving frequency and with the measured ac component of the electrode and plasma potentials. This work is supported by the UK Engineering and Physical Sciences Research Division.

\*in collaboration with Charlie Mahony

### Contributed Papers

14:30

**RR1 4 Problems of Radio-Frequency Capacitive Discharge Plasma Parameters Control** NIKOLAI YATSENKO, *Head Scientist, Professor, Institute for Problems in Mechanics, Russian Academy of Sciences* Applications which call for the use of a gas discharge quite often make use of the positive column of a low pressure discharge. However, the parameters of such a plasma are determined by the conditions of the local ionization balance. These plasma parameters are not always optimal for the majority of applications. This research has studied alternative methods of controlling the plasma parameters in a transverse RF capacitive discharge at frequency range of 0.1 - 100 MHz. The main attention in this report is paid to the regions which are influenced by the proximity of the electrodes. These regions include the near electrode sheaths of space charge (sheath region) which dimension  $s$  and the transition region with dimension  $t$ . Research has been conducted with inter-electrode gap height  $h = 2s + t$ . It is shown that with this spacing, the ionization balance in the plasma of the transition region is determined not only by the value of the local electric field, but also by the processes in the sheath region of

14:45

**RR1 5 Sheath dynamics of a helium discharge in the GEC reference cell investigated by Rydberg-Stark spectroscopy** U. CZARNETZKI, D. LUGGENHÖLSCHER, H.-F. DÖBELE, *Institut für Laser- und Plasmaphysik, Universität GH Essen, D-45117 Essen, Germany* \* The dynamics of the sheath formed in front of the electrodes in an asymmetric 13.56 MHz RF-discharge in the GEC reference cell is studied by means of time and spatially resolved electric field measurements. The electric field distributions are measured by laser induced fluorescence spectroscopy in helium. Metastable helium atoms ( $2s$ ) are excited to a Rydberg-state ( $n=3D11$ ) and the resulting integral fluorescence light is observed perpendicular to the laser beam with an intensified CCD-camera. The time evolution of the voltage drop over the sheath regions at the powered and the grounded electrode, the ion density within the sheath, the dynamics of the sheath edge, and the displacement current in the sheath are deduced from these measurements.

\*Support by the BMBF is gratefully acknowledged.

15:00

**RR1 6 Positive Potential Formation in a Collisionless Negative Ion Plasma** ZAHEDUL HASSAN, NOBUYA HAYASHI, YASUNORI OHTSU, HIROHARU FUJITA, *Department of Electrical Engineering, Saga University, Japan* The ion sheath near a substrate has been widely studied also, in negative ions plasmas. In rf discharges, however, the potential at the crest in the oscillating field would become positive or equal to the plasma potential at the rf electrode. Negative ions would be attracted to the electrode

at the crest potential. So, the study on the positive potential formation in the electronegative plasma becomes an interesting topic. In this work, positive potential formation in the electronegative plasma was experimentally studied by detecting the potential profile around the positive biased substrate. The Ar plasma with introducing SF<sub>6</sub> gas was produced at a pressure of  $2 \times 10^{-4}$  Torr, to achieve a low electron temperature ( $\approx 0.4eV$ ) in order to obtain an efficient electron attachment. This was realized by the plasma diffusion through the magnetic filter and before which the plasma was produced by filament dc discharge ( $n_e \approx 10^{10} cm^{-3}$  and  $T_e \approx 2eV$ ). The results revealed that a potential dip with electron temperature depth was observed in the spatial potential profile for the positive bias in electropositive plasma. While in electronegative plasma a conventional big negative charge sheath was formed. An rf potential oscillation in a wide range of frequency superimposed to the positive dc bias was also investigated.

15:15

**RR1 7 First Experimental Test of the Godyak and Sternberg Sheath Model For Collisional Plasma** NOAH HERSHKOWITZ, *UW-Madison* HUSAIN KAMAL, *Kuwait University* An emissive probe is used to measure sheath potential profiles in an argon dc glow discharge operated at 0.1 or 1.0 Torr. The emissive probe is operated in the limit of zero electron emission [yan]. Experimental data are found to be in good agreement with the collisional sheath model given by Godyak and Sternberg<sup>1</sup>. For example, the ion velocity at the sheath edge (inferred from the measured electric field) is found to be much smaller than the ion sound speed. Ion velocities much less than the Bohm velocity are a consequence of ion collision mean-free-paths that are compatible to or smaller than the electron Debye length as first described by Persson<sup>2</sup>. A fluid equation based analysis is presented to demonstrate the transition from Bohm-like behavior at low collisionality to Persson-like behavior at high collisionality making clear the role of electric fields at the sheath boundary.

<sup>1</sup>V. A. Godyak and N. Sternberg, IEEE Trans. Plasma Sci. 18, 159 (1990)

<sup>2</sup>K.-B. Persson, Phys. Fluids 5, 1625 (1962)

15:30

**RR1 8 A Novel Electro-optical Probe to Diagnose Plasma Uniformity** M. SARFATY, *ERC for Plasm-Aided Manufacturing, University of Wisconsin-Madison* M. HARPER, N. HERSHKOWITZ, *ERC for Plasm-Aided Manufacturing, University of Wisconsin-Madison* A major concern in plasma processing of materials is the spatial uniformity of the process, which is strongly dependent on the spatial distribution of both charged and neutral particles. A novel electro-optical probe has been designed to provide information on the plasma uniformity. The electro-optical probe combines a double sided Langmuir probe (Mach probe) to measure the local plasma parameters and spatially resolved optical emission. The low cost electro-optical probe is relatively easy to

operate, it requires a small access port, and it provides spatial information that is much more difficult to obtain by other methods. The plasma density, the electron energy distribution function, as well as the plasma and the floating potentials, are all determined by the Mach probe. The ion velocity field, perpendicular to the probe surface, is determined by the ratio of the ion saturation currents of the two counter facing probe surfaces. The collimated optical emission is collected by an optical fiber recessed inside a ceramic tube facing the Mach probe surface. The spectrally resolved light emission, which can be induced either by the plasma electrons or by an external light source, is measured by an optical-multi-channel analyzer. The spatial distribution of chlorine and fluorine radicals obtained by actinometry is analyzed with the locally measured electron energy distribution function. Probe results of  $\text{Cl}_2$ ,  $\text{CF}_4$ , and  $\text{SF}_6$  discharges in helicon and magnetically confined inductively coupled plasma sources will be discussed. This work is funded by NSF grant No. EEC-8721545.

15:45

**RR1 9 Studies of Ion and Electron Beams in a Spherical IEC Device** G. H. MILEY, *UIUC* JOHN M. DEMORA, *UIUC* The

spherical inertial electrostatic confinement (IEC) device is a unique apparatus that focuses and confines plasma ions without magnetic fields. The IEC consists of a spherical vacuum vessel (anode), a centrally located spherical wire cathode grid, and low pressure fill gas. When a large negative voltage is applied to the grid, positive ions are attracted to the cathode, but many pass completely through the holes of the grid in narrow beams called ion microchannels. The microchannels always pass through the center of the IEC in symmetric patterns and pass through the grid where the electric potential is smallest, which occurs at the centers of the largest grid openings. Electrons also are important to the IEC discharge. At higher pressures, a single electron cloud and jet are visible inside the cathode grid. The jet always passes through the largest hole of the cathode. The formation of the electron jet appears to be related to the ion microchannels. Experiments in progress measure the current of the ion and electron beams to determine the density and energy of charged particles in the beams. Also, experiments with various cathode grids show the effects of grid design on beam size and location. These experiments provide a better understanding of both the plasma physics and fusion capabilities of the spherical IEC device.

---

## SESSION RR2: INDUCTIVELY COUPLED PLASMAS II

Thursday afternoon, 9 October 1997; Tripp Commons, Memorial Union at 13:30; Chris Nichols, Sandia National Lab, presiding

### *Invited Paper*

13:30

**RR2 1 Use of Sensors and RF System Models to Control Inductively Coupled Plasma Sources.\***

LEE A. BERRY, *Oak Ridge National Laboratory*

Research for the development of plasma sources and processes for new generations of feature and wafer sizes must meet requirements in many dimensions including performance, cost, schedule, and yield. This last requirement is becoming increasingly difficult to meet because the process for submicron features frequently have narrow windows and it is difficult to have the needed tool to tool and wafer to wafer repeatability to consistently hit the window. Data from sensors, in particular post-match rf sensors, can be used to measure and control some of the critical process parameters. This work, in many respects, parallels previous work by Paul Miller on capacitively coupled tools. Three examples utilizing post-match rf sensor data will be presented. First, a common approach to auto-matching is to (separately) use the phase and magnitude of the reflected rf power signal to control two capacitors in the match box. At a minimum, presets must be changed for new processes and auto-matches sometimes fail. By utilizing error signals derived from both pre-and post-match rf sensors, we have developed and tested a new matching algorithm that accommodates a wide range of power and plasma conditions without the need for presets. Second, the same rf data can be used to infer power input to the plasma. Losses in match boxes range from 10-50%, depending on the both the rf system and desired plasma conditions. In addition, because of small, but significant differences in particular tool installation or rf components, there can be differences between the efficiencies of nominally the same tool under identical conditions. Thus machine control based on net power is needed for optimum control. Post-match sensors provide the data needed to separate the losses in the matchbox from power coupled to the plasma. The third use of rf system data is the measurement parameters that can be used to both characterize the tool and to indicate and help diagnose or even predict equipment failures. The difference between generator output power and plasma input power is an indication of match box efficiency and antenna losses. Increased losses likely indicate component failure that requires attention even though process might be stable as a result of net power control. Similarly, changes in plasma load resistance would likely indicate variations in plasma parameters that could impact process results. This research was the result of contributions from many staff members at ORNL. I would especially like to acknowledge the work of John Caughman and Rick Goulding for rf diagnostics and analysis; Tony Moore for rf sensor electronics; and Paul Rathke and Mike Hileman for computer data acquisition and control. The first two individuals are from the Fusion Energy Division at ORNL and the last three from the Instruments and Controls Division.

\*Research sponsored by the Laboratory Directed Research and Development Program of Oak Ridge National Laboratory, managed by Lockheed Martin Energy Research Corp. for the U. S. Department of Energy under Contract No. DE-AC05-96OR22464.



14:00

**RR2 2 Transport of argon ions in the presheath of an ICP M.** VAN DE GRIFT, T. HBID, E.W.M. KNOLS, G.M.W. KROESEN, F.J. DE HOOG, *Eindhoven University of Technology, Dept. of Appl. Phys., The Netherlands* N. SADEGHI, *Lab. Spectrometry Phys. Grenoble, France* Doppler Shifted Laser Induced Fluorescence (DS-LIF) is used to measure the radial and axial velocity distributions of metastable ( $^2G_{9/2}$ ) argon ions on the axis of an ICP reactor<sup>1</sup>. The ICP is powered up to 500W at pressures of 2.5-80 mTorr in a volume of 700 cm<sup>3</sup>. Both the ion temperature and the ion acceleration in the presheath region can be deduced. The values of the ion velocity at the presheath edge are well in agreement with the Bohm theory. To investigate the relation between the groundstate ions and the measured metastable ions, the results are compared to the simulations of a 3D Monte Carlo model. This model calculates the velocity distribution of the ions using the electric field obtained from emission experiments. Metastable ions are supposed to be created from the ion groundstate level and to be quenched by collisions. The comparison shows that the relation between the two levels is not linear. In particular, the zero velocity component in the groundstate distribution is suppressed for the metastable distribution function. Langmuir probe measurements show the spatial, pressure and power dependence of the electron temperature and density. The results are in agreement with the calculations from a global model.

<sup>1</sup>Appl.Phys.Lett.70(7),pp.835-7

14:15

**RR2 3 Magnetic Probe Measurements in an Inductively Coupled Argon Discharge** ROBERT PIEJAK, *OSRAM SYLVANIA Products Inc.* VALERY GODYAK, *OSRAM SYLVANIA Products Inc.* BENJAMIN ALEXANDROVICH, *OSRAM SYLVANIA Products Inc.* Azimuthal components of the electric field (Eq) and the current density (Jq) in a low pressure inductively coupled argon discharge have been determined from B-dot (dB/dt) magnetic probe measurements. The radial component (Br) and the radial gradient of the axial component (dBz/dr) of the rf magnetic field were measured 4 cm (radially) from the discharge axis cor-

responding to the radius where the induced electric field is greatest. The magnitude and relative phase of Br and dBz/dr were measured at three frequencies: 3.4, 6.8 and 13.6 Mhz. Measurements at these three frequencies were made at: 1 mTorr and 10 mT with 100W discharge power and at 100 mT with 50 W discharge power. At each experimental condition, a series of magnetic measurements were made at 0.25 cm intervals along the axial direction. Assuming azimuthal symmetry about the axis of the cylindrical discharge chamber, Maxwell equations were used to determine the axial variation of the phase and magnitude of Eq and Jq from the magnetic probe data. Comparison of Eq and Jq for three frequencies will be presented and discussed.

14:30

**RR2 4 An Inductively Coupled Large Area Plasma Source for Flat Panel and Large Size Wafer Processing** YAOXI WU, M.A. LIEBERMAN, A.J. LICHTENBERG, *UC Berkeley*

When the dimension of the antenna coil of an RF-powered plasma is comparable to the RF wavelength, the non-uniformity of power distribution, due to a standing wave, may not be acceptable. This is especially true for inductive coupled systems used for flat panel processing. To overcome this difficulty, a novel high density plasma reactor, without the need of magnetic field confinement, is constructed and characterized. The plasma source is inductively driven by a planar coil embedded in the plasma. The coil consists of 8 parallel sections of copper tubes in series, covered with thin quartz tubes. This provides an efficient coupling between the RF power and plasma. A tuning network is adjusted to launch a pure traveling wave along the antenna to obtain a uniform field distribution over a large processing area. The reactor chamber, made of stainless steel and rectangular in processing cross section, provides a processing area of 73×61 cm<sup>2</sup>, and is designed for processing glass substrates for a flat panel display, yet suitable for large size wafer processing. The experiments are designed to study the electrical and plasma properties under various processing conditions. The traveling wave properties are examined by 8 voltage sensors equally spaced along the antenna coil, and the plasma density and uniformity are measured using Langmuir probes. The plasma source is also studied theoretically using a global model and the results are compared with those from experiments.

### Invited Paper

14:45

**RR2 5 Prediction of Etch Rate Distribution from the Flow Analysis of Radicals, Excited Molecules, Gas Molecules, and Reaction Products.**

K. NANBU, *Tohoku University* \*

Etch rate is governed by the flux of etchant on a wafer surface and the reaction probability at the surface. The latter is close to unity for ion-assisted etching. What governs the flux of etchant? It is the flow of feed gas, reaction product, and etchant itself. What governs the flow of these mixtures? They are the flow rate of feed gas, the pumping speed, the rate of production of reaction product on the wafer (which is governed by the etch rate), and the spatial distribution of production rate of etchant. The last is determined by electron-molecule dissociative collisions in discharge space. The discharge itself depends on the flow. Prediction of etch rate requires the analyses of the discharge, flow, and surface reaction, all of which are mutually coupled. The objective of this paper is to present a solution to this complicated problem. A total simulation method is developed for a parallel plate etcher with 300 mm aluminum wafer. Gas is chlorine. The input data are the mass flow rate from a shower head, pumping speed or gas pressure in discharge space, amplitude of applied rf voltage, and geometrical dimensions of the etcher. The output is the distribution of etch rate on the wafer. The simulation code consists of plasma module and flow module. The plasma module gives the positive ion current and the production rates of hot chlorine atoms and electronically excited molecules. In the flow module we calculate, (1) the motion and collision of atoms, excited molecules, reaction products, and gas molecules, (2) production of reaction

products and etch rate, and (3) gas feed from a shower head and gas pumping at the exit. The etch rate obtained is quite uniform except near the periphery of the wafer, where a sharp rise of etch rate occurs due to the diffusion of etchants from the outside to the inside of the wafer. We can explain the sharp rise by the density field of etchants in the etcher.

\*The author expresses his thanks to Mr. M. Suetani for programming and data processing.

### Contributed Papers

15:15

#### RR2 6 Modeling Study of Asymmetric Plasma Properties Produced by Pumping and Gas Injection in Inductively Coupled Plasmas\*

ERIC KEITER, MARK J. KUSHNER, *University of Illinois-Urbana/Champaign* The trend towards operating with lower gas pressures for plasma processing is partly motivated by the desire to operate in a "diffusive" environment with the goal of obtaining more uniform reactant fluxes to the substrate. Based on the premise that reactant transport is dominantly diffusive, low pressure, high plasma density reactors often use azimuthally asymmetric gas injection and pumping. In this paper, the consequences of asymmetric gas injection and pumping on the uniformity of

reactant fluxes in inductively coupled plasma reactors are computationally investigated using a 3-dimensional plasma equipment model.  $\text{Cl}_2$  and  $\text{Ar/SiH}_4$  gas mixtures are studied as examples of etching and deposition systems while injecting gas from discrete nozzles with side or symmetrical pumping. We found that under nominal operating conditions (10 mTorr, 400 W, 150 sccm) fluxes of ions to the wafer are little affected by asymmetric gas injection and pumping due to the dominance of ambipolar transport. Reactant fluxes to the substrate, such as  $\text{Cl}$ , can display significant asymmetries, which worsen with increasing pressure and increasing reactive sticking coefficient.

\*Research supported by ARPA/NCSU, SRC, NSF (ECS94-04133, CTS 94-12565) and the U of Wisconsin ERC.

### Invited Paper

15:30

#### RR2 7 Modeling and Diagnostics for an ICP in a Collision Dominated Region.

TOSHIAKI MAKABE, *Keio University, Yokohama Japan*

Inductively coupled plasmas (ICP) are one of the candidates in the next reactor generation of plasma processings for ULSI microelectronic devices as very reliable, high density sources that produce uniform treatment over large areas. The basic mechanisms of excitation in ICP have been studied by theoretical and experimental procedures. It has been established that in ICP the induced azimuthal electric field  $E_\theta$  gives to electrons the energy to sustain the discharge at lower pressure. The temporal profile of the field may be associated with the temporal profile of the current in the coil while the radial profile is determined mostly by the skin depth of the plasma. Recently, however, it has been predicted in a collision dominated region that there are additional mechanisms operating in ICP which may provide energy to electrons. One such mechanism is the drift due to the static, radial component of the field  $E_r$  and the time varying magnetic field which will result in an azimuthal motion of electrons. This mechanism will result in a different space- and time-dependence of the plasma emission and would be expected to occur with a phase difference of approximately  $\pi/4$  as compared to the excitation due to the basic mechanism of electron acceleration by the azimuthal field. The influence of the capacitive coupling may add an amount of power to electrons and can also be distinguished by the space- and time profile of the emission. Thus in order to obtain a detailed description of plasma excitation kinetics a comparison between the models and the experimental emission CT for the time resolved net excitation rates is discussed as well as the influence of the interaction between the external electromagnetic wave and the plasma density, and of the direct and stepwise ionizations in Ar and  $\text{O}_2$  at  $p \geq 15$  mTorr.

## Author Index

### A

Abraham, Ion C.  
CM2 1, **OWP4 22**  
Abraham-Shrauner, B.  
**OWP3 2**  
Abraham-Shrauner,  
Barbara OWP3 1,  
OWP3 3  
Abramzon, N. AM1 7  
Adams, N.G. OWP4 12  
Adams, Steven F.  
**OWP4 13**  
Aflatooni, K. **DMP1 4**  
Ahsan, Faisal JTP3 2  
Ajello, J.M. DMP1 10  
Akashi, H. **NW1 6**  
Akashi, Haruaki  
DMP5 3  
Alexandrovich, Ben-  
jamin RR2 3  
Ali, M.A. OWP1 7  
Almeida, R.M.S.  
BM1 4  
Almgren, Carl  
**OWP4 24**  
Alvarez, Ignacio  
OWP1 5  
Ambalanath, S. JTP5 6,  
LW2 2  
Amorim, J. OWP4 5  
Anderson, Harold M.  
**CM2 1**, OWP4 22  
Anderson, Heidi M.  
**BM1 5**, DMP4 25,  
JTP2 4  
Anderson, L.W. JTP1 6,  
MW2 5, OWP4 3  
Anderson, Rex  
DMP5 1, **OWP2 1**  
Anderson, Scott A.  
**DMP5 1**  
Andy, Jonhson AM2 1  
Arai, Hiroyoshi  
OWP2 23, PR2 3  
Armentrout, P.B.  
**AM1 1**  
Armorer, L. DMP4 16  
Arriaga, Carlos  
OWP1 5  
Ash, R.L. JTP4 1  
Avdonina, N. **JTP1 3**  
Azarenkov, N.A.  
**DMP4 18**, **JTP3 16**,  
**JTP5 1**

### B

Babaritski, A. AM2 5  
Babb, J.F. **JTP2 3**

Badakhshan, Ali  
**JTP3 2**  
Bailey, Wm.F.  
DMP4 15  
Baravian, G. OWP4 5  
Barnes, Michael S.  
NW2 6  
Barnes, Paul N.  
**DMP3 3**  
Bartschat, Klaus JTP1 4  
Basner, R. JTP3 19  
Basurto, Eduardo  
OWP1 5  
Batelaan, H. LW1 3  
Baum, C. NW2 5,  
**OWP4 20**  
Beattie, J.R. **LW2 5**  
Becker, K. AM1 7,  
DMP1 9, DMP4 16,  
JTP3 19  
Beegle, L.W. **JTP2 2**  
Behle, St. BM2 6,  
DMP3 2  
Belinger, A. DMP3 10  
Benck, E.C. OWP4 14,  
OWP4 26  
Benilov, M.S. **BM1 4**  
Bennett, E.J. **DMP4 15**  
Berezhnoi, S.V.  
**JTP3 17**  
Berkermann, U. JTP3 7,  
**MW2 6**  
Berry, Lee A. **RR2 1**  
Bettenhausen, M.H.  
**JTP3 5**, OWP2 14  
Bhattacharjee, Amitava  
**JTP3 22**  
Birdsall, C.K. IT2 8,  
NW1 4  
Bisyukov, A.A.  
MP4 18  
Blain, Matthew **IT1 6**  
Bletzinger, P. CM1 2,  
OWP3 6  
Boesten, L. JTP1 2  
Boeuf, J.P. **JTP4 4**,  
JTP5 5  
Boffard, John B.  
JTP1 6, **PR1 4**  
Boilson, D **JTP3 10**  
Boivin, R. LW1 4  
Booske, J.H. DMP3 8,  
OWP2 21, PR2 6  
Booth, Jean-Paul  
**OWP4 9**  
Borg, G.G. JTP3 4  
Boswell, Rod NW2 10

Boswell, R.W. **BM2 1**,  
**DMP3 10**, **OWP2 19**,  
**OWP2 20**, PR2 1,  
**QR2 1**  
Božin, J.V. DMP4 20  
Bowden, M.D. **IT2 2**,  
**OWP4 11**  
Boyd, Iain D. **NW1 2**  
Braithwaite, N.St.J.  
DMP4 14, JTP3 15  
Brake, M.L. DMP5 1,  
NW2 4, OWP2 1  
Brockhaus, A. **BM2 6**,  
**DMP3 2**  
Brooke, G. **DMP4 5**  
Brown, K. **DMP3 9**  
Brueck, S.R. J. **CM2 4**  
Brunger, M.J. JTP1 1  
Buckman, S.J. JTP1 1,  
JTP1 7  
Buckman, Stephen J.  
**PR1 3**  
Buenker, R.J. JTP2 1  
Burrow, P.D. DMP1 4  
Butler, J.E. IT1 1,  
IT1 7  
Butler, J.M. OWP4 12

### C

Campbell, R.E.  
OWP4 25  
Canney, Shane  
OWP4 35  
Cartwright, K.L.  
JTP5 7, LW2 3  
Cekic, M. **DMP5 5**  
Chabert, P. OWP2 19  
Chabert, Pascal  
OWP4 9  
Champion, Roy L.  
AM1 5, IT1 2  
Chandhoke, Gurprit  
DMP4 1, **OWP3 4**  
Charles, C. DMP3 10  
Chen, F.F. OWP2 17,  
**QR2 2**, **QR2 5**  
Chen, Wenjing  
**OWP3 3**  
Cherrington, B.E.  
DMP3 6, OWP2 7  
Cherrington, Blake E.  
**DMP3 5**  
Childs, M.A. **JTP3 26**  
Chilton, J. Ethan PR1 5  
Christenson, P.J.  
**JTP5 7**, LW2 3  
Christophorou, L.G.  
DMP1 8, **LW1 6**

Chung, H.K. **BM2 9**  
Cisneros, Carmen  
OWP1 5  
Clark, J.D. **DMP4 30**  
Clark, R.W. DMP2 3  
Coburn, J.W. MW2 8  
Cohen, D.H. BM2 9  
Collins, George  
OWP4 24, OWP4 33  
Collins, G.J. OWP4 30  
Collison, Wenli Z.  
NW2 6  
Compaan, A.D. JTP5 6,  
LW2 2  
Coplan, M.A. OWP1 2  
Côté, R. JTP2 3  
Counts, D. DMP2 3  
Crowley, B. OWP4 27  
Cunge, Gilles OWP4 9  
Curran, N. JTP3 10  
Curry, J.J. BM1 5,  
**DMP5 6**, JTP2 4  
Czarnetzki, U.  
OWP4 7, OWP4 8,  
**RR1 5**

### D

Dahi, H. BM1 6,  
**NW2 9**  
Dalgarno, A. **FT 2**,  
JTP2 3  
Dalvie, Manoj CM2 6  
Date, Hiroyuki **CM1 4**  
Datskos, Panos QR1 5,  
**QR1 6**  
Daube, Th. DMP3 1  
Dave, Silvetti AM2 1  
David, Cheung AM2 1  
Davis, C.A. OWP2 20  
de Hoog, F.J. JTP5 2,  
RR2 2  
de Urquijo, Jaime  
**OWP1 5**  
Decker, B.K. **OWP4 12**  
Dedman, C.J. JTP1 7  
Deegan, C.M. **JTP3 6**  
Degeling, A.W. **QR2 3**  
DeMora, John M.  
RR1 9  
Den Hartog, E.A.  
**JTP2 4**  
Denisenko, I.B.  
DMP4 18, JTP3 16,  
JTP5 1  
Derbyshire, Joseph  
**DMP1 1**  
Deshmukh, Pranawa  
OWP1 9



## Author Index

- DeTemple, T.A. LW2 1  
Dhali, Shirshak  
**DMP2 6**  
Dickson, B. DMP3 10  
Dillon, M.A. DMP1 12,  
JTP1 2, JTP2 1  
Ding, G. **OWP4 17**  
Dinh, T. JTP4 1  
Doan, K. PR2 8  
Döbele, H.-F. DMP2 2,  
OWP4 4, OWP4 7,  
OWP4 8, OWP4 28,  
RR1 5  
Doering, J.P. **JTP1 9**,  
OWP1 2  
Dolson, D.A. **OWP4 2**  
Donnelly, V.M. IT2 3  
Doughty, Douglas A.  
**BM1 2**  
Dubost, L. DMP3 10  
Durandet, A. OWP2 20  
Dyakov, Ilya V. AM1 5
- E**  
Economou, D.J. BM2 4,  
**BM2 8**, IT2 7,  
TP3 18  
Eddy, C.R. IT1 8  
Eddy Jr., C.R. **IT1 1**,  
IT1 7  
Eden, J.G. AM1 2,  
AM1 3, LW2 1  
El Marji, B. OWP1 2  
El-Fayoumi, I.M.  
OWP2 10  
El-Habachi, A. BM1 3  
Engemann, J. BM2 6,  
DMP3 2  
Etievant, C. AM2 5  
Evans, J.D. **OWP2 17**
- F**  
Fabrikant, I.I. **DMP1 3**,  
QR1 4  
Falkenstein, Zoran  
**JTP5 11**  
Fang, Ziwei OWP4 35  
Felfli, Z. JTP1 3  
Fiala, A. MW2 8  
Figen, Z.G. **AM1 2**,  
**AM1 3**  
Firchow, S.J. **OWP4 31**  
Fisch, N.J. JTP4 3  
Flannery, M.R. **MW1 3**  
Fleddermann, C.B.  
**IT2 5**, IT2 6  
Foest, R. **JTP3 19**,  
JTP3 21
- Fons, John T. **PR1 5**  
Ford, Michael  
OWP4 35  
Ford, M.J. **OWP1 2**  
Forrister, Ray CM2 1  
Foster, J.E. **OWP2 21**,  
PR2 6  
Frame, J.W. LW2 1  
Francis, A. **OWP4 7**  
Frank, J.D. DMP5 5  
Fridman, A. DMP4 2  
Fruchtman, A. **JTP4 3**  
Fujii, T. **JTP3 11**  
Fujita, Hiroharu RR1 6  
Fujita, K. **DMP2 4**  
Fukuzawa, T. JTP3 3,  
JTP3 12, **JTP3 24**,  
JTP3 27  
Furkal, E. **DMP4 6**,  
DMP4 24
- G**  
Gallagher, Alan **GT 1**,  
JTP3 26  
Gallup, G.A. DMP1 3,  
DMP1 4  
Ganguly, Biswa N.  
OWP4 10, OWP4 13  
Ganguly, B.N. **CM1 2**,  
OWP3 6, OWP4 2  
Gapon, A.V. DMP4 18,  
JTP5 1  
Garner, Richard C.  
DMP5 8  
Garrigues, L. JTP4 4  
Garscadden, Alan  
CM1 2, DMP4 30,  
JTP5 10  
Gay, T.J. LW1 3  
Gearhart, S.S. DMP3 8,  
PR2 6  
Geddes, J. **OWP1 1**  
Gehrke, Mark F. JTP1 6  
Georg, A. BM2 6,  
DMP3 2  
Getty, W.D. OWP2 1  
Ghanashev, I. **QR2 7**  
Ghanashev, Ivan QR2 8  
Gibson, J.C. **JTP1 1**,  
JTP1 7  
Gilbody, H.B. OWP1 1  
Gilgenbach, R.M.  
**OWP4 32**  
Gilland, James  
**OWP2 16**  
Girka, V.O. JTP3 16  
Giuliani, J.L. **DMP2 3**,  
OWP4 25
- Glembocki, O.J. **IT1 8**  
Godyak, V.A. IT2 7  
Godyak, Valery RR2 3  
Goehlich, A. **OWP4 28**  
Golde, M.F. AM1 6  
Gonzalez, Patrick  
OWP4 33  
Goodyear, A. **JTP3 15**  
Gordon, Matthew  
JTP5 8  
Goree, J. JTP3 23,  
**OWP4 23**  
Goree, John JTP3 25  
Goss, J. OWP2 10  
Goto, T. DMP2 4,  
JTP3 11, MW2 4,  
OWP2 26, OWP4 6  
Goto, Toshio OWP2 23,  
OWP2 24, PR2 3  
Goto, Y. IT2 2  
Gottschalk, J.R. JTP5 6,  
**LW2 2**  
Gougousi, T. AM1 6  
Goyette, A.N. **MW2 5**,  
**OWP4 3**  
Graham, Bill **RR1 3**  
Graham, W.G. DMP5 4,  
OWP4 4, OWP4 15  
Graves, D.B. MW2 8  
Green, A.S. LW1 3  
Green, David S. **AM2 4**  
Green, M.A. JTP1 1  
Greenwood, J.B.  
**JTP1 5**, **JTP4 2**  
Grill, V. **AM1 7**  
Gruen, D.M. MW2 5,  
OWP4 3  
Gu, J.P. JTP2 1  
Gudmundsson,  
Jon Tomas **JTP3 28**  
Guerra, V. **OWP2 2**  
Guharay, S.K. OWP3 7  
Gutsev, S.A. OWP4 18  
Guzdar, P.N. **OWP3 7**
- H**  
Haaland, P.D. CM1 2  
Haaland, Peter D.  
JTP5 10  
Haas, F.A. **DMP4 14**  
Hagelaar, G.J.M.  
**JTP5 2**  
Hall, Lindsay DMP1 11  
Hamilton, Thomas  
OWP4 21  
Han, K.H. JTP5 3  
Hanawa, Hiroji  
OWP4 19
- Hannemann, M.  
JTP3 21  
Hanson, David E.  
**NW2 2**  
Haque, Nasreen  
**OWP1 9**  
Harb, Tarek **DMP1 2**  
Hardy, Kenneth A.  
**MW1 4**  
Hardy, Kenneth A.  
**MW1 5**  
Hari, Ponnekanti  
AM2 1  
Harper, M. **BM2 5**,  
NW2 5, OWP4 20,  
RR1 8  
Hasebe, M. **JTP3 14**  
Hasegawa, H. CM1 4  
Hash, David **DMP4 32**  
Hassan, Zahedul **RR1 6**  
Hatano, Yoshihiko  
**QR1 1**  
Hattori, H. MW2 4  
Hattori, S. JTP3 11  
Hayashi, D. **OWP2 12**  
Hayashi, Nobuya  
RR1 6  
Hayaud, C. OWP4 5  
Hayden, D.B.  
OWP2 22, **OWP2 25**  
Hays, Gerry **FT 3**  
HBid, T. JTP5 2, RR2 2  
Hebner, G.A. IT2 5,  
**IT2 6**  
Heil, Brian CM1 6,  
OWP4 4  
Hempel, F. JTP3 21  
Henins, I. JTP3 20  
Hershkowitz, N.  
BM2 5, NW2 5,  
OWP2 15, OWP2 18,  
OWP4 20, PR2 6,  
RR1 8  
Hershkowitz, Noah  
OWP2 3, OWP2 16,  
**RR1 7**  
Hirakata, N. NW2 7  
Hiramatsu, M. JTP3 11,  
OWP2 26  
Hirose, A. DMP4 6,  
JTP3 16  
Hirose, S. OWP4 6  
Hirsch, G. JTP2 1  
Hitchon, Nicholas  
**NW1 7**  
Hitchon, W.N.G.  
CM1 8, DMP4 31  
Hiitt, B.A. **LW1 3**

- Hogan, M.J. **DMP4 22**  
Holland, John P. **IT2 1**  
Holloway, James Paul  
NW2 4  
Holm, R.T. **IT1 8**  
Hopkins, M.B. **JTP3 6,**  
**JTP3 10**  
Hori, M. **DMP2 4,**  
**JTP3 11, MW2 4,**  
**OWP2 26**  
Hori, Masaru  
**OWP2 23, OWP2 24,**  
**PR2 3**  
Hori, T. **OWP4 11**  
Horie, I. **DMP4 13**  
Hubert, Joseph **PR2 5**  
Hudson, David F.  
**OWP1 8**  
Huo, Winifred M.  
**QR1 2**  
Hutcherson, R. Kenneth  
**DMP5 8**  
Hwang, Helen **JTP3 1**  
Hwang, Y.S. **JTP5 3**
- I**  
Iga, Ione **PR1 2**  
Ikeda, Y. **JTP5 7,**  
**LW2 3**  
Ikegami, Naokatsu  
**CM2 2**  
Ikuta, N. **DMP4 26**  
Ikuta, Nobuaki  
**DMP4 21**  
Inayoshi, M. **DMP2 4**  
Ingold, J.H. **CM1 10,**  
**DMP4 27**  
Isaacs, W.A. **LW1 5**  
Itikawa, I **JTP2 1**  
Ito, H. **MW2 4**  
Ito, M. **DMP2 4,**  
**MW2 4**  
Ito, Masafumi  
**OWP2 23, OWP2 24,**  
**PR2 3**  
Itoh, H. **DMP4 26**  
Itoh, M. **OWP2 11**  
Itoh, T **OWP2 5**  
Iyanagi, K. **OWP2 9**
- J**  
Jagannathan, N.  
**OWP3 2**  
James, G.K. **DMP1 10**  
Jarnyk, Mark **NW2 10**  
Jelenković, B.M.  
**DMP4 20**
- Jiao, Charles Q.  
**JTP5 10**  
Jin, H.J. **JTP3 12**  
Jivotov, V. **AM2 5**  
Johnsen, R. **AM1 6**  
Jones, I.R. **OWP2 10**  
Jones, Michael E.  
**NW1 1**  
Joyce, Glenn **PR2 2**  
Juliano, D.R. **OWP2**  
**22, OWP2 25**  
Julienne, Paul **MW1 2**  
Jung, W.-H. **OWP4 16**
- K**  
Kadota, K. **MW2 2,**  
**OWP2 12, OWP2 13**  
Kaganovich, I.D.  
**CM1 7, JTP3 17**  
Kamal, Husain **RR1 7**  
Kamenski, I.V. **JTP3 4**  
Kanakasabapathy, S.K.  
**OWP2 6**  
Kanik, I **DMP1 10,**  
**JTP2 2**  
Kanzari, Z.S. **DMP4 7**  
Karasik, Max **DMP2 5**  
Katzer, D.S. **IT1 8**  
Kauppila, Walter E.  
**LW1 1**  
Kawamoto, Shinji  
**DMP4 10**  
Kawamura, E. **NW1 4**  
Kawasaki, H. **JTP3 3,**  
**JTP3 12, JTP3 24,**  
**JTP3 27**  
Kawasaki, T. **JTP3 12**  
Kawetzki, T. **OWP4 28**  
Ke, K.-H. **PR2 8**  
Kedzierski, Wladyslaw  
**DMP1 1, DMP1 2**  
Keiter, Eric R. **CM1 1,**  
**DMP4 31, RR2 6**  
kelkar, Umesh **JTP5 8**  
Kelly, K.L. **OWP4 17**  
Kepple, P. **DMP2 3**  
Kevin, Fairbairn **AM2 1**  
Khater, Marwan H.  
**OWP2 7**  
Khromov, N.A.  
**DMP3 4, OWP4 18**  
Kida, J. **JTP3 3**  
Kim, D.-G. **OWP4 16**  
Kim, G.H. **OWP2 15**  
Kim, G.-H. **OWP4 16**  
Kim, H.J. **JTP5 3**  
Kim, Y.-K. **OWP1 7**
- Kimura, M **DMP1 12,**  
**JTP2 1**  
Kimura, Takashi  
**JTP3 28**  
Kinder, Ron **CM2 7,**  
**JTP3 13**  
Kinoshita, K. **OWP4 6**  
Kinoshita, T. **JTP3 12**  
Kitajima, T. **MW2 3**  
Kitamori, K. **BM2 2,**  
**BM2 7, CM1 5,**  
**DMP4 13, DMP4 19**  
Knignik, A. **DMP4 2**  
Knols, E.W.M. **RR2 2**  
Kogano, M. **OWP4 11**  
Kokura, H. **NW2 7**  
Kolobov, V.I. **BM2 4,**  
**BM2 8, IT2 7,**  
**JTP3 18**  
Kondo, K. **CM1 4**  
Kondo, S. **OWP2 27,**  
**PR2 7**  
Kono, A. **MW2 4,**  
**OWP4 6**  
Koo, Bon-Woong  
**OWP2 3**  
Korbel, A. **IT1 4**  
Korbel, Adam **DMP4 9**  
Kortshagen, Uwe  
**CM1 6, DMP4 1,**  
**OWP3 4**  
Kovaleski, S.D.  
**OWP4 32**  
Krauss, A.R. **MW2 5,**  
**OWP4 3**  
Kress, Joel D. **NW2 2**  
Kroesen, G.M.W.  
**RR2 2**  
Kudo, H. **IT2 2**  
Kudryavtsev, A.A.  
**DMP3 4, OWP4 18**  
Kunhardt, E.E.  
**DMP4 16**  
Kurihara, M. **CM1 3**  
Kurunczi, P. **DMP1 9**  
Kushima, S. **JTP3 24**  
Kushner, Mark J.  
**CM1 1, CM2 6,**  
**CM2 7, DMP4 4,**  
**DMP4 31, JTP3 13,**  
**RR1 2, RR2 6**
- L**  
Lafrance, Denis  
**DMP3 7**  
Lai, Kwok-Fai **PR2 4**  
Lampe, Martin **PR2 2**
- Lawler, J.E. **BM1 5,**  
**DMP4 25, DMP5 6,**  
**JTP2 4, JTP2 5,**  
**LW2 4, MW2 5,**  
**OWP4 3**  
Lee, C.-H. **DMP1 5,**  
**DMP1 6**  
Lenef, A. **DMP5 7**  
Leonhardt, D. **IT1 1,**  
**IT1 7, IT1 8**  
Lho, T. **OWP2 15**  
Li, Jing **DMP2 6**  
Li, M. **MW2 8**  
Li, Yan-Ming **DMP5 2**  
Li, Yunlong **JTP5 8**  
Lichtenberg, A.J. **RR2 4**  
Lieberman, M.A.  
**PR2 1, RR2 4**  
Lieberman, Michael A.  
**JTP3 28**  
Liffers, A. **MW2 6**  
Lin, Chun C. **JTP1 6,**  
**PR1 5**  
Lindley, R.A. **PR2 8**  
Liu, H.L. **DMP3 8**  
Lloyd, Shane **OWP4 30**  
Loewenhardt, Peter K.  
**OWP4 19**  
Loffhagen, Detlef  
**JTP5 9**  
Loureiro, J. **OWP2 2**  
Lu, Enlian **CM2 1,**  
**OWP4 22**  
Lücking, C. **MW2 6**  
Luecking, C. **JTP3 7**  
Luggenhölscher, D.  
**DMP2 2, RR1 5**  
Lymberopoulos, D.P.  
**BM2 4**
- M**  
Ma, Cheng-Yu **DMP2 1**  
Ma, Diana X. **OWP4 19**  
MacDonagh-Dumler, J.  
**BM1 5**  
MacDonagh-Dumler,  
Jeff **DMP4 25**  
MacFarlane, J.J. **BM2 9**  
Madison, Don **PR1 1**  
Maerk, T.D. **AM1 7**  
Mahony, C.M.O.  
**DMP5 4, OWP4 15**  
Mak, Steve **OWP4 19**  
Makabe, NW2 3  
Makabe, T. **JTP3 14**  
Makabe, T. **CM1 3,**  
**JTP3 8, MW2 3,**  
**OWP2 9**

## Author Index

- Makabe, Toshiaki  
**RR2 7**
- Malik, Shamim **CM2 5**
- Malović, G.N.  
**DMP4 20**
- Malyshev, M.V. **IT2 3**
- Manfred, Kock  
OWP1 6
- Manheimer, W.M.  
PR2 2
- Manson, Steven T.  
OWP1 9
- Margot, Joelle PR2 5,  
**QR2 6**
- Martus, K.E. **DMP1 9**
- Masai, T. **DMP1 12**
- Masse, Louis-Philippe  
**PR2 5**
- Matsui, J. **NW2 3**
- McCartney, P. OWP1 1
- McCauley, T.G.  
MW2 5, OWP4 3
- McConkey, William  
**DMP1 1, DMP1 2**
- McCorkle, Dennis  
**DMP2 1**
- McCurdy, C.W. LW1 5
- McFarland, J. **DMP5 4,**  
**OWP4 15**
- McIlroy, David **JTP3 2**
- McKoy, V. **DMP1 5,**  
**DMP1 6**
- McNeely, P. **JTP3 10**
- McNevin, Susan  
**CM2 3**
- Menning, K.L.  
OWP4 31
- Mentel, J. **IT1 4,**  
**JTP3 7, MW2 6**
- Mentel, Juergen  
**DMP4 9**
- Meyer, P. **DMP3 1**
- Meyyappan, M. **BM2 2,**  
**DMP4 32, JTP3 1,**  
**NW2 9**
- Miley, G.H. **RR1 9**
- Miljak, D.G. **QR2 5**
- Millard, Michael W.  
**OWP4 10**
- Miller, J. **OWP2 15**
- Miller, Terry A.  
OWP4 13
- Miyahara, H. **JTP3 24**
- Miyajima, H. **NW2 1**
- Miyake, S. **QR2 4**
- Miyata, Koji **OWP2 23,**  
**PR2 3**
- Mohan, Bahn **AM2 1**
- Moore, J.H. **OWP1 2**
- Morgan, W.L. **DMP1 7,**  
**DMP4 29**
- Morita, S. **QR2 7**
- Moses, G.A. **BM2 9**
- Moskowitz, W. **DMP5 7**
- Mouzouri, Y. **JTP3 5**
- Mouzouris, Y.  
**OWP2 14**
- Msezane, Alfred  
OWP1 9
- Msezane, A.Z. **JTP1 3**
- Mukul, Kelkar **AM2 1**
- Mullman, K.L. **JTP2 5**
- Murakami, Y. **JTP5 4**
- Muraoka, K. **IT2 2,**  
**OWP2 11, OWP4 11**
- Murnick, D.E. **BM1 6,**  
**NW2 9**
- N**
- Nagai, H. **OWP2 26**
- Nagatsu, M. **QR2 7**
- Nagatsu, Masaaki  
**QR2 8**
- Nakamura, K. **NW2 7**
- Nakamura, Masayuki  
**OWP2 23**
- Nakamura, Satoru  
**DMP4 19**
- Nakano, N. **CM1 3,**  
**JTP3 8, JTP3 14,**  
**MW2 3, NW2 3,**  
**OWP2 9**
- Nanbu, K. **BM1 7,**  
**OWP2 27, PR2 7,**  
**RR2 5**
- Nanbu, Kenichi  
**DMP4 10**
- Nandelstädt, D. **IT1 4**
- Nandelstädt, Daniel  
**DMP4 9**
- Nawata, M. **JTP3 11,**  
**OWP2 26**
- Neiger, Manfred **BM1 1**
- Neuilly, Francois  
OWP4 9
- Ni, Tom Q. **NW2 6**
- Nichols, Christopher  
**OWP4 21**
- Nishida, S. **JTP1 2**
- Niwano, Michio **IT1 3**
- Noda, H. **OWP2 26**
- Noren, C. D. **DMP1 10**
- Noren, C.D. **JTP2 2**
- O**
- Oda, A. **RR1 1**
- Oda, Akinori **DMP5 3**
- Oddone, Sebastian  
MW1 4
- Ogawa, U. **DMP4 13**
- Ohnishi, K. **OWP2 5**
- Ohtsu, Yasunori **RR1 6**
- Olsen, J. **DMP5 7**
- Olthoff, J.K. **DMP1 8,**  
**LW1 6, OWP1 3,**  
**OWP1 4, OWP2 8**
- Ostrikov, K.N. **JTP3 16**
- Overzet, Lawrence J.  
**DMP3 5**
- Overzet, L.J. **DMP3 6,**  
**OWP2 6, OWP2 7**
- P**
- Palatini, L. **DMP4 16**
- Papanu, James  
OWP4 19
- Parish, John **IT1 5**
- Park, Jaeyoung  
**JTP3 20**
- Parker, G.J. **CM1 8**
- Peko, Brian L. **AM1 5**
- Pelletier, Yvan **DMP3 7**
- Peterson, J. MW1 4
- Petrović, Z.Lj.  
**DMP4 20**
- Petržilka, V. **JTP3 4**
- Pfau, Sigismund **JTP5 9**
- Phelps, A.V. **DMP4 8,**  
**FT 4**
- Piech, Garrett **JTP1 6**
- Piejak, Robert **RR2 3**
- Pinheiro, M.J.  
**DMP4 11**
- Pinnaduwege, Lal  
**DMP2 1, PR1 6,**  
**QR1 5, QR1 6**
- Pitchford, L.C. **JTP4 4,**  
**JTP5 5**
- Poll, H.U. **AM1 7**
- Popović, S. **DMP4 3,**  
**DMP4 5**
- Popovic, S. **DMP5 5**
- Popović, S. **JTP4 1**
- Potapkin, B. **AM2 5,**  
**DMP4 2**
- Potechin, S. **AM2 5**
- Punset, C. **JTP5 5**
- Q**
- Qian, Xueyu **NW2 8,**  
**OWP3 5**
- Quandt, E. **OWP4 4**
- Quick, A.K. **OWP2 18**
- Quinn, Rick **JTP3 25**
- R**
- Rainer, Kling **OWP1 6**
- Rao, M.V.V.S.  
**OWP1 3, OWP1 4**
- Rauf, Shahid **RR1 2**
- Read, Paul **OWP4 29**
- Rees, Alan **MW2 7,**  
**OWP4 29**
- Rescigno, T.N. **LW1 5**
- Rescigno, TN **QR1 3**
- Richley, Edward A.  
**CM1 9**
- Riemann, K.-U.  
**DMP3 1, NW1 3**
- Riley, Merle E. **JTP3 9**
- Rissman, P. **DMP3 9**
- Ritter, D. **AM1 4**
- Roberts, J.R. **OWP4 14,**  
**OWP4 26**
- Robson, A.E. **OWP4 25**
- Roe, Larry **JTP5 8**
- Rogerson, J.E. **DMP2 3**
- Roquemore, L. **DMP2 5**
- Rosocha, Louis A.  
**AM2 3**
- Rudd, M.E. **OWP1 7**
- Rugheimer, Paul **PR1 5**
- Rusanov, V. **AM2 5**
- Russell, Thomas  
**MW2 7**
- Ruzic, D.N. **OWP2 22,**  
**OWP2 25**
- S**
- Sadeghi, N. **OWP4 7,**  
**RR2 2**
- Sadeghi, Nader  
OWP4 9
- Sagara, T. **JTP1 2**
- Sakai, Kei **NW2 1**
- Sakai, M. **DMP5 6**
- Sakai, Y. **BM2 2,**  
**BM2 7, CM1 5,**  
**NW2 1**
- Sakai, Yosuke  
**DMP4 17, DMP5 3**
- Sakamoto, K. **JTP3 3**
- Sakawa, Y. **QR2 4**
- Sakoda, T. **OWP2 11**
- Samsonov, D. **JTP3 23,**  
**OWP4 23**
- Samukawa, S. **NW1 6**
- Samukawa, Seiji  
**IT2 4, OWP2 24**
- Sandstrom, P. **BM2 5**
- Sarfaty, M. **BM2 5,**  
**NW2 5, OWP4 20,**  
**RR1 8**



- Sarkissian, Andranik  
**DMP3 7**
- Sartwell, B. **DMP2 3**
- Sasaki, K. MW2 2,  
**OWP2 12, OWP2 13**
- Sasaki, T. NW1 6
- Sashin, Vladimir  
**OWP4 35**
- Savy, J. **DMP3 10,**  
**OWP2 19**
- Schappe, R. Scott  
**DMP1 11**
- Scharer, J.E. **JTP3 5,**  
**OWP2 14, OWP4 17**
- Schein, J. **IT1 4**
- Schein, Jochen **DMP4 9**
- Schiffner, G. **JTP3 7,**  
**MW2 6**
- Schmidt, M. **JTP3 19,**  
**JTP3 21, NW1 5**
- Schoenbach, K.H.  
**BM1 3**
- Schulz-von der Gathen,  
V. **DMP2 2**
- Schumann, M. **IT1 4**
- Schumann, Michael  
**DMP4 9**
- Schwabedissen, A.  
**OWP4 14, OWP4 26**
- Scofield, J **OWP3 6**
- Sebastien, Raoux  
**AM2 1**
- Segi, K. NW2 7
- Selwyn, G.S. **JTP3 20**
- Serikov, Vladimir  
**DMP4 10**
- Setsuhara, Y. **QR2 4**
- Seymour, David  
**MW2 7, OWP4 29**
- Shah, M.B.S. **OWP1 1**
- Shamamian, V. A.  
**DMP2 3**
- Shamamian, V.A. **IT1 1,**  
**IT1 7, OWP4 25**
- Shan, H.C. **PR2 8**
- Shannon, Steven  
**NW2 4**
- Sharma, A.S. **OWP3 7**
- Shaw, D.M. **OWP4 30**
- Shchagin, Alexander  
**OWP4 34**
- Sheridan, T.E.  
**OWP2 19**
- Shi, W. **BM1 3**
- Shiau, Jay **OWP4 19**
- Shibata, M. NW2 3
- Shimozuma, M. **CM1 4**
- Shiratani, M. **JTP3 3,**  
**JTP3 12, JTP3 24,**  
**JTP3 27**
- Shohet, J.L. **DMP3 9,**  
**NW2 5, OWP4 20**
- Shoji, T. **QR2 4**
- Shon, J.W. **RR1 1**
- Shott, J. **DMP3 9**
- Shvidky, A. **LW2 2**
- Shvydky, A. **JTP5 6**
- Siegel, R.B. **DMP1 8**
- Singh, H. **MW2 8**
- Skrzyzkowski, M.P.  
**AM1 6**
- Slinker, Steven P.  
**PR2 2**
- Smith, B.A. **DMP3 6**
- Smith, H.B. **DMP3 10**
- Smolyakov, A.I.  
**DMP4 6, DMP4 18,**  
**DMP4 24, JTP3 16,**  
**JTP5 1**
- Sobolewski, M.A.  
**OWP2 8**
- Spaan, M. **DMP2 2**
- Srivastava, S.K.  
**LW1 4, PR1 2**
- Stansfield, Barry  
**DMP3 7**
- Stark, R.H. **BM1 3**
- Stauffer, Allan D.  
**LW1 2**
- Steen, P.G. **DMP5 4,**  
**OWP4 15**
- Steer, W. **OWP2 15**
- Steffens, Kristen L.  
**MW2 1**
- Stiles, Kenton  
**OWP4 33**
- Sugai, H. NW2 7,  
**QR2 7**
- Sugai, Hideo **QR2 8**
- Sugawara, Hirotake  
**CM1 5, DMP4 17,**  
**DMP5 3**
- Sultan, G. **OWP4 5**
- Sun, Zhiwen NW2 8
- Suzuki, C. **MW2 2,**  
**OWP2 13**
- Suzuki, T **DMP1 12**
- T**
- Tachibana, K. **JTP5 4**
- Tachibana, K **OWP2 5**
- Tagashira, H. **BM2 2,**  
**BM2 7, CM1 4,**  
**CM1 5, DMP4 19,**  
**NW2 1**
- Takada, N. **OWP2 12**
- Takahashi, N. NW1 6
- Takeda, Akihide  
**DMP4 21**
- Takeo, T. MW2 4
- Takeo, Y. MW2 3
- Tanaka, H **DMP1 12,**  
**JTP2 1**
- Tanaka, Satoshi **BM2 7**
- Tarnovsky, V. **JTP3 19**
- Tataronis, J.A. **JTP3 4**
- Tayal, Swaraj **JTP1 8**
- Theodosiou, C.E.  
**JTP5 6**
- Thomson, M. **OWP4 8**
- Tomi, Tanaka **AM2 1**
- Toyofuku, M. **JTP3 12**
- Trail, W.K. **DMP4 29**
- Trantham, K.W. **JTP1 7**
- Truxon, J.M. **JTP5 6,**  
**LW2 2**
- Tsendin, L.D. **CM1 7,**  
**JTP3 17**
- Tsukada, Tsutomu  
**OWP2 24**
- Tucek, Jack C. **IT1 2**
- Turner, M.M. **IT2 8,**  
**OWP2 10**
- Tynan, G.R. **OWP2 17**
- U**
- Uchida, Satoshi **BM2 7,**  
**DMP4 17**
- Uchida, T. **OWP2 11**
- Uchino, K. **IT2 2,**  
**OWP2 11, OWP4 11**
- Uhrlandt, D. **DMP4 23,**  
**NW1 5**
- Ulrich, A. **BM1 6**
- V**
- Vahedi, V. **IT2 8,**  
**NW1 4**
- Van Brunt, R.J.  
**OWP1 3, OWP1 4**
- van de Grift, M. **RR2 2**
- Van Orden, A. **JTP4 1**
- Veerasingam, Ramana  
**OWP4 1**
- Vender, D **OWP4 27**
- Ventzek, P.L.G. **BM2 2,**  
**BM2 7, CM1 4,**  
**DMP4 13, DMP4 17,**  
**DMP4 19, DMP5 3,**  
**NW2 1, RR1 1**
- Verboncoeur, J.P.  
**JTP5 7, LW2 3**
- Vitello, P. **RR1 1**
- Vona, D. **OWP4 30**
- Voter, Arthur F. NW2 2
- Vu, Vu Anh **JTP3 2**
- Vukovic, Mirko **PR2 4**
- Vušković, L. **DMP4 3,**  
**DMP4 5, JTP1 10,**  
**JTP4 1**
- W**
- Walker, Thad **MW1 1**
- Walton, Scott G. **IT1 2**
- Wang, C. Daniel  
**OWP3 3**
- Wang, Chungdar Daniel  
**OWP3 1**
- Wang, W **DMP3 8,**  
**OWP2 21, PR2 6**
- Wang, Xiaogang  
**DMP4 28**
- Wang, Y. **JTP1 10,**  
**OWP2 8**
- Watanabe, Y. **JTP3 3,**  
**JTP3 12, JTP3 24,**  
**JTP3 27**
- Wawrzyniak, Mark  
**DMP1 11**
- Waymouth, John F.  
**FT 1**
- Webb, Timothy R.  
**OWP4 19**
- Wei, H. **JTP1 10**
- Wendt, A.E. **OWP2 21,**  
**PR2 6**
- Wheeler, D.J. **LW2 1**
- Whitmore, Terence  
**MW2 7**
- Wickliffe, M.E. **JTP2 4**
- Wieser, J. **BM1 6**
- Wilde, R.S. **QR1 4**
- Williams, T.L.  
**OWP4 12**
- Williamson Jr., W  
**JTP5 6, LW2 2**
- Wilson, Aaron **OWP2 1**
- Wingsch, V. **BM2 6,**  
**DMP3 2**
- Winkler, R. **DMP4 23,**  
**NW1 5**
- Winkler, Rolf **JTP5 9**
- Winstead, C. **DMP1 5,**  
**DMP1 6**
- Wood, C.H. **DMP5 5**
- Woods, R. Claude  
**CM2 1, OWP4 22**
- Woodworth, Joseph  
**OWP4 1, OWP4 21**
- Wrbanek, J.D.  
**DMP4 30**

## Author Index

Wright, B.W. DMP4 30  
Wu, Yaoxi RR2 4  
Wurden, G.A. DMP2 5

### X

Xu, Songlin NW2 8,  
OWP3 5  
Xu, Xudong DMP4 4  
Xu, Y. DMP1 3

### Y

Yamamoto, Yasuo  
OWP2 24

Yaney, Perry P. IT1 5,  
OWP4 10  
Yang, J. JTP1 9  
Yang, Jing BM2 2  
Yang, Qingyun CM2 1,  
OWP4 22  
Yasaka, Y OWP2 5  
Yatsenko, Nikolai  
RR1 4  
Ye, Yan OWP4 19  
Yin, Gerald Z. NW2 8,  
OWP3 5, OWP4 19  
Ying, C.H. JTP1 10

Yonemura, S. BM1 7  
Yoon, N.S. JTP5 3  
Yoshida, Ryohei  
OWP2 24  
Yousfi, M. AM2 2,  
DMP4 7  
Yu, Z. OWP4 30

### Z

Zeman, Vlado JTP1 4  
Zhang, Daqing JTP3 2  
Zhang, Da CM2 6

Zhao, Alan OWP4 19  
Zhou, D. MW2 5,  
OWP4 3  
Zhu, Yifei PR1 6  
Zuev, V.S. AM1 2  
Zweben, S.J. DMP2 5

---

THURSDAY MORNING  
9 OCTOBER

---

8:00

- PR1 **Electron-Atom Collisions**  
*Madison, Buckman*  
Class of '24 Reception Room
- PR2 **Magnetized Plasmas**  
Tripp Commons

---

THURSDAY MORNING  
9 OCTOBER

---

10:15

- QR1 **Electron-Molecule Collisions**  
*Hatano, Huo, Rescigno*  
Class of '24 Reception Room
- QR2 **Helicon and Surface Wave Plasmas**  
*Margot*  
Tripp Commons

---

THURSDAY AFTERNOON  
9 OCTOBER

---

13:30

- RR1 **Diagnostics II**  
*Graham*  
Class of '24 Reception Room
- RR2 **Inductively Coupled Plasmas II**  
*Samukawa, Nanbu, Makabe*  
Tripp Commons



# EPITOME OF THE 50th ANNUAL GASEOUS ELECTRONICS CONFERENCE

---

**MONDAY MORNING  
6 OCTOBER**

---

- 8:00
- AM1 **Heavy Particle Collisions**  
*Armentrout*  
Class of '24 Reception Room
- AM2 **Environmental Applications**  
*Yousfi, Rosocha, Green*  
Tripp Commons

---

**MONDAY MORNING  
6 OCTOBER**

---

- 10:15
- BM1 **Light Sources**  
*Neiger, Doughty*  
Class of '24 Reception Room
- BM2 **Pulsed Plasma**  
Tripp Commons

---

**MONDAY AFTERNOON  
6 OCTOBER**

---

- 13:30
- CM1 **Glows, Swarms and  
General Discharge Physics**  
Class of '24 Reception Room
- CM2 **Future Processing Trends**  
*Ikegami, McNevin, Brueck*  
Tripp Commons

---

**MONDAY AFTERNOON  
6 OCTOBER**

---

- 16:00
- DMP1 **Poster Session:  
Electron-Molecule Collisions**  
Great Hall
- DMP2 **Poster Session:  
Environmental Applications**  
Great Hall
- DMP3 **Poster Session:  
Pulsed Plasmas (Processing)**  
Great Hall
- DMP4 **Poster Session: Glows**  
Great Hall
- DMP5 **Poster Session: Lighting**  
Great Hall

---

**MONDAY EVENING  
6 OCTOBER**

---

- 19:30
- EM **Town Hall Meeting on  
Topical Group**  
Union Theater

---

**TUESDAY MORNING  
7 OCTOBER**

---

- 8:00
- FT **Plenary**  
*Waymouth, Dalgarno, Hays, Phelps*  
Music Hall

---

**TUESDAY MORNING  
7 OCTOBER**

---

- 11:00
- GT **Foundations of Gaseous  
Electronics**  
*Gallagher*  
Music Hall

---

**TUESDAY MORNING  
7 OCTOBER**

---

- 11:45
- HT **GEC Business Meeting**  
Music Hall

---

**TUESDAY AFTERNOON  
7 OCTOBER**

---

- 13:30
- IT1 **Surface Processes**  
*Niwano, Blain*  
Class of '24 Reception Room
- IT2 **Inductively Coupled Plasmas I**  
*Holland, Berry*  
Tripp Commons

---

**TUESDAY AFTERNOON  
7 OCTOBER**

---

- 16:00
- JTP1 **Poster Session: Electron Collision Cross  
Sections**  
Great Hall
- JTP2 **Poster Session: Photoabsorption**  
Great Hall
- JTP3 **Poster Session: RF Glow  
Discharges**  
Great Hall
- JTP4 **Poster Session: Propulsion and Space Plas-  
mas**  
Great Hall
- JTP5 **Poster Session: Flat Panel and Large Area  
Plasmas**  
Great Hall

---

**TUESDAY AFTERNOON  
7 OCTOBER**

---

- 18:30
- KT **Reception and Banquet**  
Lowell Hall

---

**WEDNESDAY MORNING  
8 OCTOBER**

---

- 8:00
- LW1 **Positron and Electron Scattering**  
*Kauppila, Stauffer*  
Class of '24 Reception Room
- LW2 **Propulsion and Space Plasmas/  
Microdischarges and Plasma  
Display Panels**  
*Lawler, Beattie*  
Great Hall

---

**WEDNESDAY MORNING  
8 OCTOBER**

---

- 10:15
- MW1 **Cold Collisions and  
Recombination.**  
*Walker, Julienne, Flannery.*  
Class of '24 Reception Room
- MW2 **Diagnostics I**  
*Steffens*  
Tripp Commons

---

**WEDNESDAY AFTERNOON  
8 OCTOBER**

---

- 13:30
- NW1 **Modeling**  
*Jones, Boyd, Hitchon*  
Class of '24 Reception Room
- NW2 **Etching**  
Tripp Commons

---

**WEDNESDAY AFTERNOON  
8 OCTOBER**

---

- 16:00
- OWP1 **Poster Session: Ionization**  
Great Hall
- OWP2 **Poster Session: High Density Plasmas for  
Processing**  
Great Hall
- OWP3 **Poster Session: Extreme  
Submicron Processing**  
Great Hall
- OWP4 **Poster Session: Diagnostics and Sensors**  
Great Hall



0003-0503(199710)42:8;1-Q